

WHOI-91-08

*Copy 2*

# **Woods Hole Oceanographic Institution**

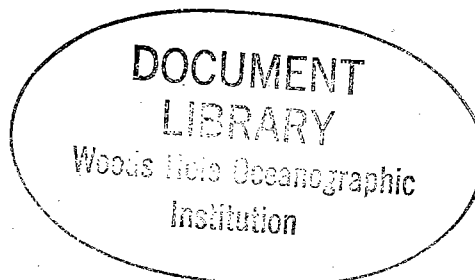


---

## **Abstracts of Manuscripts Submitted in 1990 for Publication**

---

**Technical Report WHOI-91-08**



**WHOI-91-08**

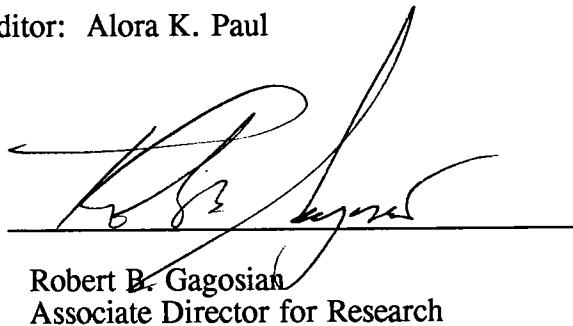
*Research In Progress*

**Abstracts of Manuscripts  
Submitted in 1990 for Publication**

Woods Hole Oceanographic Institution  
Woods Hole, Massachusetts

Editor: Alora K. Paul

Approved for Distribution:



Robert B. Gagosian  
Associate Director for Research

When citing this report, it should be referenced as:

Woods Hole Oceanographic Institution  
Technical Report No. WHOI-91-08





## **PREFACE**

This volume contains the abstracts of manuscripts submitted for publication during calendar year 1990 by the staff and students of the Woods Hole Oceanographic Institution. We identify the journal of those manuscripts which are in press or have been published. The volume is intended to be informative, but not a bibliography.

The abstracts are listed by title in the Table of Contents and are grouped into one of our five departments, marine policy center, coastal research center, or the student category. An author index is presented in the back to facilitate locating specific papers.

## **Acknowledgements**

Special thanks to Suzanne B. Volkmann, Research Associate; Staff Assistants Shirley Bowman, Applied Ocean Physics and Engineering; Peggy Dimmock, Biology; Molly Lump-  
ing, Chemistry; Pamela Foster, Geology & Geophysics; Lisa Wolfe, Physical Oceanography;  
Ellen Gately, Marine Policy Center; Olimpia McCall, Coastal Research Center; Pamela  
Goulart, Education; and Maureen O'Donnell, Library Assistant.





# TABLE OF CONTENTS

## DEPARTMENT OF APPLIED OCEAN PHYSICS AND ENGINEERING

|   |        |
|---|--------|
| Improved Meteorological Measurements from Ships and Buoys<br><i>Kenneth Prada, David Hosom and Alan Hinton</i>  | AOPE-1 |
| A Multi-Node Three Component Seismic System for Deep Sea Drilling Project (DSDP) Boreholes<br><i>Donald E. Koelsch, Robert G. Goldsborough, Henri O. Berteaux and Ralph Stephen</i>                 | AOPE-1 |
| Robust 5000 Bit Per Second Underwater Communication System for Remote Applications<br><i>Lee E. Freitag and J. Stevens Merriam</i>  | AOPE-1 |
| Drag Forces and Flow-Induced Vibrations of Long Vertical Tow Cables Part I: Steady State Towing Conditions<br><i>D. R. Yoerger, M. A. Grosenbaugh, M. S. Triantafyllou and J. J. Burgess</i>        | AOPE-2 |
| The Influence of Thruster dynamics on Underwater Vehicle Behavior and their Incorporation into Control System Design<br><i>Dana R. Yoerger, John G. Cooke and Jean-Jacques E. Slotine</i>           | AOPE-2 |
| A Wavetank Study of the Dependence of X-Band Cross Sections on Wind Speed and Water Temperature<br><i>Mary Ruth Keller, William C. Keller and William J. Plant</i>                                  | AOPE-2 |
| New Criteria for Blind Deconvolution of Nonminimum Phase Systems (Channels)<br><i>Ofir Shalvi and Ehud Weinstein</i>  | AOPE-3 |
| A Model-Based Approach to 3-D Imaging and Mapping Underwater<br><i>W. K. Stewart</i>  | AOPE-3 |
| Some Observational evidence on the effect of atmospheric forcing on Tidal Variability in the Upper Delaware Bay<br><i>Kuo-Chuin Wong and John H. Trowbridge</i>                                     | AOPE-3 |
| Wave Influences on Wind Profiles Over Water<br><i>William J. Plant</i>  | AOPE-3 |
| Specifications & Applications for an Advanced Acoustic Telemetry System<br><i>Josko Catipovic, Daniel Frye and Dave Porta</i>   | AOPE-4 |
| A Comparison of Broadband and Narrowband Modal Inversions for Bottom Geoacoustic Properties at a Site Near Corpus Christi, Texas<br><i>James F. Lynch, Subramaniam D. Rajan and George V. Frisk</i> | AOPE-4 |
| Basin-Scale Tomography: A New Tool for Studying Weather and Climate<br><i>John L. Spiesberger and Kurt Metzger</i>  | AOPE-5 |
| Measuring Wave Direction Using Upward-Looking Doppler Sonar<br><i>E. A. Terray, H. E. Krogstad, R. Cabrera, R. L. Gordon and A. Lohrmann</i>  | AOPE-6 |
| High Data Rate Acoustic Telemetry for moving ROVs in a fading Multipath Shallow Water Environment<br><i>Josko A. Catipovic and Lee E. Freitag</i>   | AOPE-6 |
| New Estimates of Sound-Speed in Water<br><i>John L. Spiesberger and Kurt Metzger</i>  | AOPE-6 |
| The Effect of Seasonal Temperature Fluctuations in the Water Column on Sediment Compressional Wave Speed Profiles in Shallow Water<br><i>Subramaniam D. Rajan and George V. Frisk</i>               | AOPE-6 |

|  |         |
|--|---------|
| Optical Disk Recorders in Arctic Instrumentation<br><i>Kenneth R. Peal and Kenneth E. Prada</i>  | AOPE-7  |
| Transient Eddy Formation around Headlands<br><i>Richard P. Signell and W. Rockwell Geyer</i>   | AOPE-7  |
| Forth Interrupt Handling<br><i>Barrie B. Walden</i>  | AOPE-7  |
| Development of the Arctic Remote Autonomous Measurement Platform<br><i>Kenneth R. Peal and Kenneth E. Prada</i>  | AOPE-7  |
| A Standardized Electronic Package for IMET Sensor Development<br><i>Geoff Allsup</i>   | AOPE-8  |
| Monitoring Fishbite Activities and Protecting Synthetic Fiber Ropes used in Deep Sea Moorings<br><i>H. O. Berteaux, Bryce Prindle and Susan S. Putman</i>        | AOPE-8  |
| Air and Sea Temperature Measurements for IMET<br><i>Alan Hinton</i>  | AOPE-8  |
| Estimates of Directional Spectra from the Surface Acoustic Shear Sensor (SASS)<br><i>Markku J. Santala and Albert J. Williams III</i>                            | AOPE-9  |
| The Effect of unsteady Motion on the Drag Forces and flow-induced Vibrations of a Long Vertical Tow Cable<br><i>M. A. Grosenbaugh</i>                            | AOPE-9  |
| Modelling the Dynamics of a Deeply-Towed Underwater Vehicle System<br><i>Franz S. Hover, Michael S. Triantafyllou and Mark A. Grosenbaugh</i>                    | AOPE-9  |
| Bandwidth-efficient trellis-coded Modulation for Phase Random Rayleigh Fading Channels<br><i>Josko A. Catipovic</i>  | AOPE-9  |
| Algorithms for Joint Channel Estimation and Data Recovery - Application to Equalization in Underwater Communications<br><i>Meir Feder and Josko A. Catipovic</i> | AOPE-10 |
| The Need for Global Ocean Wave Spectral Information<br><i>Hans C. Graber, Vincent J. Cardone and Mark A. Donelan</i>   | AOPE-10 |
| Sequential Algorithms for Parameter Estimation based on the Kullback-Leibler Information Measure<br><i>Ehud Weinstein, Meir Feder and Alan V. Oppenheim</i>      | AOPE-11 |
| Asymmetric Behavior of an Oceanic Boundary Layer above a Sloping Bottom<br><i>J. H. Trowbridge and S. J. Lentz</i>   | AOPE-11 |
| A Reassessment of the Role of Tidal Dispersion in Estuaries and Bays<br><i>W. Rockwell Geyer and Richard P. Signell</i>  | AOPE-11 |
| Sound scattering by Deformed Wedges of finite length<br><i>Dezhang Chu and Timothy K. Stanton</i>  | AOPE-12 |
| Three-Dimensional Stochastic Modeling using Sonar Sensing for Undersea Robotics<br><i>W. Kenneth Stewart</i>   | AOPE-12 |
| Hydrodynamic Facilitation of gregarious settlement of a Reef-Building Tube Worm<br><i>Joseph R. Pawlik, Cheryl Ann Butman, and Victoria R. Starczak</i>          | AOPE-12 |
| Basin-Scale Acoustic Tomography: Observations of Baroclinic Tides generated by Seamounts<br><i>Robert H. Headrick, John L. Spiesberger, and Paul J. Bushong</i>  | AOPE-13 |

|   |         |
|---|---------|
| A Chebychev type Inequality and its Applications<br><i>Meir Feder</i> . . . . .   | AOPE-13 |
| Drag Forces and Flow-Induced Vibrations of a long vertical Tow Cable - Part II: Unsteady Towing conditions<br><i>M. A. Grosenbaugh, D. R. Yoerger, F. S. Hover, and M. S. Triantafyllou</i> . . . . .                                 | AOPE-13 |
| Robust control of surface-positioned Tethered Underwater Vehicle<br><i>Michael S. Triantafyllou and Mark A. Grosenbaugh</i> . . . . .   | AOPE-14 |
| Sound Scattering by randomly Rough Elongated Objects. I. Means of Scattered Field<br><i>T. K. Stanton</i> . . . . .   | AOPE-14 |
| Acoustic Estimates of Antarctic Krill<br><i>Charles H. Greene, Timothy K. Stanton, Peter H. Wiebe, and Sam McClatchie</i> . . . . .   | AOPE-14 |
| Fresnel Zone Effects in the Scattering of Sound by intermediate Length Cylinders<br><i>Daniel T. DiPerna and Timothy K. Stanton</i> . . . . .   | AOPE-15 |
| In Situ Evaluation of Ocean Profiling Sensors<br><i>Marinna A. Martini, James D. Irish, Albert M. Bradley, and Alan R. Duester</i> . . . . .  | AOPE-15 |
| A Drag Tensor Formulation for modelling Bottom Stress in wind-driven depth-averaged Flows<br><i>Harry L. Jenter and Ole Secher Madsen</i> . . . . .   | AOPE-15 |
| Generating Eigenray Tubes from two Solutions of the Wave Equation<br><i>James B. Bowlin</i> . . . . .   | AOPE-16 |
| A new Algorithm for Sound Speed in Water<br><i>John L. Spiesberger and Kurt Metzger</i> . . . . .   | AOPE-16 |
| Determination of the Sediment Shear Speed Profiles from SH Wave Phase and Group Velocity Dispersion Data<br><i>Subramaniam D. Rajan and Cinthia S. Howitt</i> . . . . .   | AOPE-16 |
| Effects of Stratification by suspended Sediments on Turbulent Shear Flows<br><i>Catherine Villaret and J. H. Trowbridge</i> . . . . .   | AOPE-16 |
| The Autonomous Benthic Explorer (ABE): A Deep Ocean AUV for Scientific Seafloor Survey<br><i>Dana R. Yoerger, Albert M. Bradley, and Barrie B. Walden</i> . . . . .   | AOPE-17 |
| Interpreting Shear and Strain Fine Structure from a neutrally Buoyant Float<br><i>Eric Kunze, Melbourne G. Briscoe, and A. J. Williams III</i> . . . . .  | AOPE-17 |
| Vertical Relationship of Acoustic Backscatter to Temperature Structure at the Western Edge of the Gulf Stream Using Optimal Least Squares Filtering<br><i>J. Michael Jech, C. S. Clay, J. J. Magnuson and T. K. Stanton</i> . . . . . | AOPE-18 |
| Precise Control of Underwater Robots: Why and How<br><i>Dana R. Yoerger</i> . . . . .   | AOPE-18 |
| Characterization of Deep Sea Storms<br><i>Thomas F. Gross and A. J. Williams III</i> . . . . .  | AOPE-18 |
| Design and Performance Evaluation of an actively compliant Underwater Manipulator for Full-Ocean Depth<br><i>Dana R. Yoerger, Hagen Schempf and David M. DiPietro</i> . . . . .   | AOPE-18 |



## DEPARTMENT OF BIOLOGY

|  |     |
|--|-----|
| Subnose-1: Electrochemical Tracking of Odor Plumes at 900 Meters Beneath the Ocean Surface<br><i>Jelle Atema, Paul A. Moore, Laurence P. Madin and Greg A. Gerhardt</i> . . . . .  | B-1 |
| <i>Archaeoglobus profundus</i> Sp. Nov., Represents a New Species Within the Sulfate-Reducing<br>Archaeobacteria<br><i>Siegfried Burggraf, Holger W. Jannasch, Barbara Nicolaus and Karl O. Stetter</i> . . . . .  | B-1 |
| Heterotrophic Flagellates Associated With Sedimenting Detritus<br><i>David A. Caron</i> . . . . .  | B-1 |
| Sensitivity Analysis of Periodic Matrix Models<br><i>Hal Caswell</i> . . . . .   | B-1 |
| The Time Required for Competitive Exclusion: Lotka-Volterra Systems<br><i>Hal Caswell</i> . . . . .  | B-2 |
| Disturbance, Interspecific Interaction, and Diversity in Metapopulations<br><i>Hal Caswell and Joel E. Cohen</i> . . . . .   | B-2 |
| From the Individual to the Population in Demographic Models<br><i>Hal Caswell and A. Meredith John</i> . . . . .   | B-2 |
| High Taurine Levels in the <i>Solemya velum</i> Symbiosis: Possible Sources and Functions<br><i>N. Conway and J. McDowell Capuzzo</i> . . . . .  | B-3 |
| Incorporation and Utilization of Bacterial Lipids by the <i>Solemya velum</i> Symbiosis<br><i>Noellette Conway and Judith McDowell Capuzzo</i> . . . . .   | B-3 |
| Vertical Distribution and Species Composition of Midwater Fishes in Warm-Core Gulf Stream<br>Meander/Ring 82-H<br><i>James E. Craddock, Richard H. Backus and Mary Ann Daher</i> . . . . .   | B-4 |
| Molecular Systematics, Microbial Ecology and Single Cell Analysis<br><i>E. F. DeLong</i> . . . . .   | B-4 |
| Fluorescent, Ribosomal RNA Probes for Identification of Single Cells: A Brief Review<br><i>Edward F. DeLong</i> . . . . .  | B-4 |
| Fluorescent, Ribosomal RNA Probes for Clinical Application<br><i>Edward F. DeLong and Jyotsna Shah</i> . . . . .   | B-5 |
| Phylogenetic Characterization and In Situ Localization of the Bacterial Symbiont of Shipworms<br>(Teredinidae: Bivalvia) using 16S rRNA Sequence Analysis and Oligonucleotide Probe Hybridization<br><i>D. L. Distel, E. F. DeLong and J. B. Waterbury</i> . . . . . | B-5 |
| The Role of Intercellular Chemical Communication in the <i>Vibrio fischeri</i> - Monocentrid Fish<br>Symbiosis<br><i>Paul V. Dunlap and E. P. Greenberg</i> . . . . .  | B-5 |
| Alongshore Transport of a Toxic Phytoplankton Bloom in a Buoyancy Current: <i>Alexandrium</i><br><i>tamarense</i> in the Gulf of Maine<br><i>Peter J. S. Franks and Donald M. Anderson</i> . . . . .   | B-6 |
| Toxic Phytoplankton Blooms in the Southwestern Gulf of Maine: Testing Hypotheses of Physical<br>Control Using Historical Data<br><i>Peter J. S. Franks and Donald M. Anderson</i> . . . . .  | B-6 |
| Regulation of Gutless Annelid Ecology by Endosymbiotic Bacteria<br><i>O. Giere, N. M. Conway, G. Gastrock and C. Schmidt</i> . . . . .   | B-7 |

|   |      |
|---|------|
| Sequential Utilization of Naturally Occurring Aromatic Hydrocarbons at the Guaymas Basin Hydrothermal Vent Site<br><i>Frederick E. Goetz and Holger W. Jannasch</i> . . . . .   | B-7  |
| Sex Differences in Hepatic Monooxygenases in Flounder and Scup and Regulation of P450 Forms by Estradiol<br><i>E. S. Gray, B. R. Woodin and J. J. Stegeman</i> . . . . .  | B-7  |
| Probing the Fine Structure of Ocean Sound-Scattering Layers Using ROVERSE Technology<br><i>Charles H. Greene, Peter H. Wiebe, Robert T. Miyamoto and Janusz Burczynski</i> . . . . .  | B-8  |
| Why Habitat Architecture and Color Are Important to Shrimp Living in Pelagic <i>Sargassum</i> : The Use of Camouflage and Plant-Part Mimicry<br><i>S. Hacker and L. P. Madin</i> . . . . .  | B-8  |
| The Role of Biotransformation in the Toxicity of Marine Pollutants<br><i>Mark E. Hahn and John J. Stegeman</i> . . . . .  | B-9  |
| Lake Zabuye and the Climatic History of the Tibetan Plateau<br><i>Heinrich D. Holland, George I. Smith, Holger W. Jannasch, Andrew G. Dickson, Zheng Miangping and Ding Tiping</i> . . . . .  | B-9  |
| Sulfur Cycling in a Permanently Ice-Covered Amictic Antarctic Lake, Lake Fryxell<br><i>Brian L. Howes and Richard L. Smith</i> . . . . .  | B-10 |
| Marine Microbiology: A Need for Deep-Sea Diving?<br><i>Holger W. Jannasch</i> . . . . .   | B-10 |
| Microbiological Processes in the Black Sea Water Column and Top Sediment: An Overview<br><i>Holger W. Jannasch</i> . . . . .  | B-10 |
| Thermophilic Bacterial Sulfate Reduction in Deep-Sea Sediments at the Guaymas Basin Hydrothermal Vent Site (Gulf of California)<br><i>Bo Barker Jørgensen, Leon X. Zawacki and Holger W. Jannasch</i> . . . . .                                     | B-10 |
| Microbial Oxidation of Sulfur in Dibenzothiophene<br><i>Judith P. Kitchell, Saraswathy V. Nochur, Judith K. Marquis, Dennis A. Bazylnski and Holger Jannasch</i> . . . . .  | B-11 |
| Cytochrome P-450E (P450IA1) Protein and Heme Turnover in <i>Fundulus heterochitus</i><br><i>Pamela J. Kloepper-Sams and John J. Stegeman</i> . . . . .  | B-11 |
| A Molecular Phylogeny of Dinoflagellate Protists (Pyrrhophyta) Inferred from the Sequence of 24S rRNA Divergent Domains D1 and D8<br><i>Guy Lenaers, Christopher Scholin, Yvonne Bhaud, Danielle Saint-Hilaire and Michel Herzog</i> . . . . .      | B-11 |
| A Comparison of Shipboard and <i>In Situ</i> Methods for Estimating Oceanic Primary Production<br><i>Steven E. Lohrenz, Denis A. Wiesenburg, Charles R. Rein, Robert A. Arnone, Craig D. Taylor, George A. Knauer and Anthony A. Knap</i> . . . . . | B-12 |
| Overview: Being There - The Role of In Situ Science in Oceanography<br><i>L. P. Madin</i> . . . . .   | B-12 |
| Cytochrome P450E (P450IA1) Induction and Inhibition in Winter Flounder by 3,3',4,4'-Tetrachlorobiphenyl: Comparison of Response in Fish from Georges Bank and Narragansett Bay<br><i>Emily Monosson and John J. Stegeman</i> . . . . .              | B-13 |
| Initial Contact, Exploration and Attachment of Barnacle Cyprids Settling in Flow<br><i>Lauren S. Mullineaux and Cheryl Ann Butman</i> . . . . .   | B-13 |

|   |      |
|---|------|
| Borrowed Proteins in Bacterial Bioluminescence<br><i>Dennis J. O'Kane, Bonnie Woodward, John Lee and Douglas C. Prasher</i>   | B-13 |
| Spatial and Temporal Distributions of Prochlorophyte Picoplankton in the North Atlantic Ocean<br><i>R. J. Olson, S. W. Chisholm, E. R. Zettler, M. A. Altabet and J. A. Dusenberry</i>  | B-14 |
| Pigments, Size and Distribution of <i>Synechococcus</i> in the North Atlantic and Pacific Oceans<br><i>R. J. Olson, S. W. Chisholm, E. R. Zettler and E. V. Armbrust</i>  | B-14 |
| Advances in Oceanography Using Flow Cytometry<br><i>Robert J. Olson, Erik R. Zettler and Sallie W. Chisholm</i>   | B-15 |
| The Dynamics of a Size-Classified Benthic Population with Reproductive Subsidy<br><i>Mercedes Pascual and Hal Caswell</i>   | B-15 |
| The Lumazine Protein Gene in <i>Photobacterium phosphoreum</i> is Linked to the <i>Lux</i> Operon<br><i>D. C. Prasher, D. O'Kane and B. Woodward</i>  | B-15 |
| Fixation and Drying of DNA Sequencing Gels on Glass Plates<br><i>Douglas Prasher and Bonnie Woodward</i>  | B-16 |
| Diel Patterns of Migration, Feeding, and Spawning by Salps in the Subarctic Pacific<br><i>Jennifer E. Purcell and Laurence P. Madin</i>   | B-16 |
| <i>Chaetoderma argenteum</i> , a Northeastern Pacific Aplacophoran Mollusk Redescribed<br>(Chaetodermomorpha, Chaetodermatidae)<br><i>A. H. Scheltema, J. Buckland-Nicks and F.-S. Chia</i>   | B-16 |
| Aplacophora<br><i>A. H. Scheltema, M. Tscherkassky and A. M. Kuzirian</i>   | B-16 |
| <i>Helicoradomenia juani</i> n.g. n.sp., a Pacific Hydrothermal Vent Aplacophora<br>(Mollusca, Neomeniomorpha)<br><i>Amelie H. Scheltema and Alan M. Kuzirian</i>   | B-17 |
| On the Children of Benthic Invertebrates: Their Ramblings and Migrations in Time and Space<br><i>R. S. Scheltema</i>  | B-17 |
| Prokaryotes and Their Habitats<br><i>Hans G. Schlegel and Holger W. Jannasch</i>  | B-17 |
| Fire, Fire Exclusion, and Seasonal Effects on the Growth and Survival of Two Savanna Grasses<br><i>Juan F. Silva, Jose Raventos and Hal Caswell</i>   | B-17 |
| Population Responses to Fire in a Tropical Savanna Grass: An Analysis Using Matrix Models<br><i>Juan F. Silva, Jose Raventos, Hal Caswell and Maria Cristina Trevisan</i>   | B-18 |
| Larval Development, Relationships, and Distribution of <i>Manducus maderensis</i> , with comments on the transformation of <i>M. greyae</i> (Pisces, Stomiiformes)<br><i>David G. Smith, Karsten E. Hartel and James E. Craddock</i>  | B-18 |
| Bacterial Biomass and Heterotrophic Activity in the Water Column of An Amictic Antarctic Lake<br><i>Richard L. Smith and Brian L. Howes</i>   | B-18 |
| Immunohistochemical Localization of Cytochrome P450IA1 Induced by 3,3',4,4'-Tetrachlorobiphenyl and by 2,3,7,8-Tetrachlorodibenzofuran in Liver and Extrahepatic Tissues of the Teleost ( <i>Stenotomus chrysops</i> Scup)<br><i>R. M. Smolowitz, M. E. Hahn and J. J. Stegeman</i> | B-19 |



|  |      |
|--|------|
| Structure and Morphology of Magnetite Anaerobically-Produced by a Marine Magnetotactic Bacterium and Dissimilatory Iron-Reducing Bacteria<br><i>N. H. C. Sparks, S. Mann, D. A. Bazylinski, D. R. Lovely, H. W. Jannasch and R. B. Frankel</i>   | B-19 |
| Predation on Protozoa: Its Importance to Zooplankton<br><i>Diane K. Stoecker and Judith McDowell Capuzzo</i>   | B-20 |
| Respiration, Photosynthesis and Carbon Cycling in Planktonic Ciliates<br><i>Diane K. Stoecker and Ann E. Michaels</i>  | B-20 |
| Photosynthesis in <i>Mesodinium rubrum</i> : Per Cell Measurements and Comparison to Community Rates<br><i>Diane K. Stoecker, Mary Putt, Linda H. Davis and Ann E. Michaels</i>  | B-20 |
| Patterns of Sarcodine Feeding in Epipelagic Oceanic Plankton<br><i>Neil R. Swanberg and David A. Caron</i>   | B-21 |
| A Datalogger to Identify Vocalizing Dolphins<br><i>Peter L. Tyack and Cheri A. Recchia</i>   | B-21 |
| Induced Cytochrome P-450 in Intestine and Liver of Spot ( <i>Leiostomus xanthurus</i> ) from a Polycyclic Aromatic Hydrocarbon-Contaminated Environment<br><i>Peter A. Van Veld, Donna J. Westbrook, Bruce R. Woodin, Robert C. Hale, Craig L. Smith, Robert J. Huggett and John J. Stegeman</i> | B-21 |
| The Application of a Pediveliger Oyster Larvae Bioassay for Determining the Toxicity of Contaminated Marine and Estuarine Sediments<br><i>K. A. Warner, J. McDowell Capuzzo, J. H. Gentile, H. L. Phelps and K. J. Scott</i>   | B-22 |
| Rates of Movement and Sedimentary Traces of Deep-Sea Foraminifera and Mollusca in the Laboratory<br><i>James R. Weinberg</i>   | B-22 |
| Sound Scattering by Live Zooplankton and Micronekton: Empirical Studies with a Dual-Beam Acoustical System<br><i>Peter H. Wiebe, Charles H. Greene, Timothy K. Stanton and Janusz Burczynski</i>   | B-22 |

## DEPARTMENT OF CHEMISTRY

### GEOCHEMISTRY

|   |     |
|---|-----|
| Aragonite and Magnesian Calcite Fluxes to the Deep Sargasso Sea<br><i>Victoria J. Fabry and Werner G. Deuser</i> . . . . .  | C-1 |
| Mahukona: The Missing Hawaiian Volcano<br><i>Michael O. Garcia, Mark D. Kurz, and David W. Muenow</i> . . . . .   | C-1 |
| Modeling Petroleum Generation in Sedimentary Basins<br><i>John M. Hunt and R. J.-C. Hennet</i> . . . . .  | C-1 |
| Modeling Oil Generation with Time-Temperature Index Graphs based on the Arrhenius Equation<br><i>John M. Hunt, M. D. Lewan, and R. J.-C. Hennet</i> . . . . .   | C-2 |
| Isotopic Evolution of Mauna Loa Volcano<br><i>Mark D. Kurz and David P. Kammer</i> . . . . .  | C-2 |
| The Organic Geochemistry of Peru Margin Surface Sediment: II. Paleoenvironmental Implications of Hydrocarbon and Alcohol Profiles<br><i>Mark A. McCaffrey, John W. Farrington, and Daniel J. Repeta</i> . . . . .   | C-3 |
| Measurements of Helium in Electrolyzed Palladium<br><i>John R. Morrey, Marc W. Caffee, Harry Farrar IV, Nathan J. Hoffman, G. Bryant Hudson, Russell H. Jones, Mark D. Kurz, John Lupton, Brian M. Oliver, Brian V. Ruiz, John F. Wacker, and A. van Veen</i> . . . . . | C-3 |
| Rare Earth Elements in Marine Sediments and Geochemical Standards<br><i>Edward R. Sholkovitz</i> . . . . .  | C-3 |
| Lipid Geochemistry of Remote Marine Aerosols in Southern Ocean Air<br><i>Marie-Alexandrine Sicre, Edward T. Peltzer, and Robert B. Gagosian</i> . . . . .   | C-4 |
| Photosynthesis, CaCO <sub>3</sub> Deposition and the Global Carbon Cycles<br><i>C. Steven Sikes and Victoria J. Fabry</i> . . . . .   | C-4 |
| Temperature Measurements during Initiation and Growth of a Black Smoker Chimney<br><i>M. K. Tivey, L. O. Olson, V. W. Miller, and R. D. Light</i> . . . . .   | C-4 |
| Diffusion of Cosmogenic <sup>3</sup> He in Olivine and Quartz: Implications for Surface Exposure Dating<br><i>T. W. Trull, M. D. Kurz and W. J. Jenkins</i> . . . . .   | C-5 |

### INSTRUMENTS

|  |     |
|--|-----|
| A Benthic Chamber with Electric Stirrer Mixing<br><i>Wayne Dickinson and F. L. Sayles</i> . . . . .  | C-5 |
| The ROLAI <sup>2</sup> D Lander: A Benthic Lander for the Study of Exchange across the Sediment-Water Interface<br><i>F. L. Sayles and W. H. Dickinson</i> . . . . . | C-5 |

### ORGANIC AND BIOLOGICAL CHEMISTRY

|  |     |
|--|-----|
| The Nature and Distribution of Fluorescent Dissolved Organic Matter in the Black Sea and the Cariaco Trench<br><i>Paula G. Coble and Robert B. Gagosian</i> . . . . .                      | C-6 |
| 3-D Fluorescence Characterization of Marine DOM from the Black Sea: Source Specificity at Last?<br><i>Paula G. Coble, Sarah A. Green, Neil V. Blough, and Robert B. Gagosian</i> . . . . . | C-6 |

|  |      |
|--|------|
| Identification of a Deep Marine Source of Particulate Organic Carbon using Bomb $^{14}\text{C}$<br><i>Ellen R. M. Druffel and Peter M. Williams</i> . . . . .  | C-6  |
| Pyrolytic Character of Organic Matter in Cenozoic Sediments on the Oman Shelf<br><i>Kay-Christian Emeis and Jean K. Whelan</i> . . . . .   | C-7  |
| Intramolecular Quenching of Excited Singlet States by Stable Nitroxyl Radicals<br><i>S. A. Green, D. J. Simpson, G. Zhou, P. S. Ho, and N. V. Blough</i> . . . . .   | C-7  |
| Generation of Gas and Oil from Coal and Terrestrial Kerogen<br><i>John M. Hunt</i> . . . . .   | C-8  |
| Generation and Migration of Petroleum from Abnormally Pressured Fluid Compartments: Reply<br><i>John M. Hunt</i> . . . . .   | C-8  |
| Determination of Carbon-Centered Radicals in Aqueous Solution by Liquid Chromatography with<br>Fluorescence Detection<br><i>David J. Kieber and Neil V. Blough</i> . . . . .   | C-8  |
| The Distribution and Recycling of Chlorophyll, Bacteriochlorophyll and Carotenoids in the Black Sea<br><i>Daniel J. Repeta and Daniel J. Simpson</i> . . . . .   | C-9  |
| RADIOCHEMISTRY   |      |
| Mixing between Oxidic and Anoxic Waters of the Black Sea as traced by Chernobyl Cesium Isotopes<br><i>Ken O. Buesseler, Hugh D. Livingston, and Susan A. Casso</i> . . . . .   | C-9  |
| Ruthenium-106 in the Black Sea<br><i>Ken O. Buesseler, Hugh D. Livingston, and Susan A. Casso</i> . . . . .  | C-9  |
| Growth Rate of a Deep-Sea Coral using $^{210}\text{Pb}$ and Other Isotopes<br><i>Ellen R. M. Druffel, Linda L. King, Rebecca A. Belostock, and Ken O. Buesseler</i> . . . . .  | C-10 |
| Thorium-230 Profiling in Deep-Sea Sediments: High-Resolution Records of Flux and Dissolution of<br>Carbonate in the Equatorial Atlantic during the Last 24,000 Years<br><i>Roger Francois, Michael P. Bacon, and Daniel O. Suman</i> . . . . . | C-10 |
| Variations in Terrigenous Input into the Deep Equatorial Atlantic during the Past 24,000 Years<br><i>Roger Francois and Michael P. Bacon</i> . . . . .   | C-11 |
| Determination of Isopycnal Diffusivity in the Sargasso Sea<br><i>W. J. Jenkins</i> . . . . .   | C-11 |
| The Photochemical Decomposition of Hydrogen Peroxide in Surface Waters of the Eastern Caribbean<br>and Orinoco River<br><i>James W. Moffett and Oliver C. Zafiriou</i> . . . . .   | C-11 |
| SEAWATER AND GEOCHEMISTRY  |      |
| A Chlorofluorocarbon Section in the Eastern North Atlantic<br><i>Scott C. Doney and John L. Bullister</i> . . . . .  | C-12 |
| Carbonate System in the Black Sea<br><i>Catherine Goyet, Alvin L. Bradshaw, and Peter G. Brewer</i> . . . . .  | C-12 |
| Seafloor Diagenetic Fluxes<br><i>W. R. Martin and F. L. Sayles</i> . . . . .   | C-12 |
| Carbon Cycling in Coastal Sediments: 2. An Investigation of the Sources of $\sum\text{CO}_2$ to Pore Water<br>using Carbon Isotopes<br><i>Ann P. McNichol, Ellen R. M. Druffel, and Cindy Lee</i> . . . . .                                    | C-13 |

|  |      |
|--|------|
| Cerium Redox Cycles and Rare Earth Elements in the Sargasso Sea<br><i>E. R. Sholkovitz and D. L. Schneider</i> . . . . .   | C-13 |
| Photochemical Free Radical Production Rates: Gulf of Maine and Woods Hole-Miami Transect<br><i>Oliver C. Zafriou and Brian Dister</i> . . . . .                      | C-14 |
| Molecular Probe Systems for Reactive Transients in Natural Waters<br><i>O. C. Zafriou, N. V. Blough, E. Micinski, B. Dister, D. Kieber, and J. Moffett</i> . . . . . | C-14 |
| Deep Nitrite Distributions in Oxidic Waters<br><i>O. C. Zafriou, L. A. Ball, and Q. Hanley</i> . . . . .   | C-15 |



## DEPARTMENT OF GEOLOGY AND GEOPHYSICS

### GEOCHEMISTRY

- Porewater Cadmium Geochemistry and the Pore Water Cadmium:  $\delta^{13}\text{C}$  Relationship  
*Daniel C. McCorkle and Gary P. Klinkhammer* . . . . . GG-1

- Carbon Cycling in Coastal Sediments: An Investigation of the Sources of  $\Sigma\text{CO}_2$  to Pore  $\text{H}_2\text{O}$  Using Carbon Isotopes  
*Ann P. McNichol, Ellen R. M. Druffel and Cindy Lee* . . . . . GG-1

### GEOLOGY

- Sequence Stratigraphy: Eustasy or Tectonic Imprint?  
*Marie-Pierre Aubry* . . . . . GG-1

- Deep Structure of the Earth: An Empirical Solution from its Gravity Field  
*Carl Bowin* . . . . . GG-2

- Microearthquake Characteristics of a Mid-Ocean Ridge Along-Axis High  
*Laura S. L. Kong, Sean C. Solomon and G. M. Purdy* . . . . . GG-2

- Late Weichselian glacier retreat in Kongsfjorden, West Spitsbergen, Svalbard  
*S. J. Lehman and Steven L. Forman* . . . . . GG-3

- Initiation of Fennoscandian Ice Sheet Retreat During the Last Deglaciation  
*S. J. Lehman, G. A. Jones, L. D. Keigwin, E. S. Andersen, G. Butenko and S-R Østmo* . . . . GG-3

- The Segmentation of the Mid-Atlantic Ridge Between  $24^\circ\text{N}$  and  $30^\circ 40'\text{N}$   
*Jean-Christophe Sempéré, G. M. Purdy and Hans Schouten* . . . . . GG-3

- Seafloor Topography: A Record of a Chaotic Dynamical System?  
*Deborah K. Smith and Peter R. Shaw* . . . . . GG-4

- The Three-Dimensional Seismic Velocity Structure of the East Pacific Rise Near Latitude  $9^\circ 30'\text{N}$   
*Douglas R. Toomey, G. M. Purdy, Sean C. Solomon and William S. D. Wilcock* . . . . . GG-4

- Evidence for Age and Evolution of Corner Seamounts and Great Meteor Seamount Chain from Multi-beam Bathymetry  
*Brian E. Tucholke and N. Christian Smoot* . . . . . GG-4

- Estimating Hypocentral Uncertainties for Marine Microearthquake surveys: A Comparison of Generalized Inverse and Grid Search Methods  
*William S. D. Wilcock and Douglas R. Toomey* . . . . . GG-5

### GEOPHYSICS

- Paleontological Evidence for Lateral Displacement of Deep Oceanic Crust Along the Vema Fracture Zone Southern Wall (Atlantic Ocean,  $10^\circ 45'\text{N}$ )  
*Marie-Pierre Aubry, William A. Berggren, André Schaaf, Jean-Marie Auzende, Yves Lagabirelle and Vassilios Mammaloukas-Frangoulis* . . . . . GG-5

- Predicting Relative and Absolute Variations of In-Situ Permeability From Full Waveform Acoustic Logs  
*Daniel R. Burns* . . . . . GG-5

- Sandstone Pore Aspect Ratio Spectra from Direct Observations and Velocity Inversion  
*Daniel R. Burns, C. H. Cheng and R. H. Wilkens* . . . . . GG-6

|   |       |
|---|-------|
| Lithologic Cycles and Paleo Fluid Flow Channels in Old Oceanic Crust From Geophysical Logs at ODP Site 418A<br><i>D. R. Burns, D. Thompson and C. H. Cheng</i> . . . . .          | GG-6  |
| The Spreading Rate Dependence of 3-D Mid-Ocean Ridge and Gravity Structure<br><i>J. Lin and J. Phipps Morgan</i> . . . . .  | GG-7  |
| The Sound Field Near Hydrothermal Vents on Axial Seamount, Juan de Fuca Ridge<br><i>Sarah A. Little, Keith D. Stolzenbach and G. Michael Purdy</i> . . . . .                      | GG-7  |
| Bathymetry of the Mid-Atlantic Ridge, 24°-31'N: A Map Series<br><i>G. M. Purdy, J.-C. Sempere, Hans Schouten, D. L. DuBois and R. Goldsmith</i> . . . . .                         | GG-7  |
| Imaging with Deep Water Multiples<br><i>Edmund C. Reiter, M. Nafi Toksöz, Timothy H. Keho and G. M. Purdy</i> . . . . .   | GG-8  |
| Robust Description of Statistically Heterogeneous Seafloor Topography through its Slope Distribution<br><i>Peter R. Shaw and Deborah K. Smith</i> . . . . .                       | GG-8  |
| Finite Difference Seismic Modeling of Axial Magma Chambers<br><i>Stephen A. Swift, Martin E. Dougherty and Ralph A. Stephen</i> . . . . .   | GG-8  |
| Thermal Modeling for Hole 735B<br><i>R. P. Von Herzen and J. H. Scott</i> . . . . .   | GG-9  |
| PALEOCEANOGRAPHY  |       |
| Reconstructing Past Particle Fluxes in the Tropical Atlantic Ocean<br><i>W. B. Curry and G. P. Lohmann</i> . . . . .  | GG-9  |
| Pangaeon Divergent Margins: Historical Perspective<br><i>Elazar Uchupi and K. O. Emery</i> . . . . .  | GG-10 |
| PALEONTOLOGY  |       |
| Neogene Planktonic Foraminifer Magnetobiostratigraphy of the Southern Kerguelen Plateau (Sites 747, 748 and 751)<br><i>W. A. Berggren</i> . . . . .                               | GG-10 |
| Paleogene Planktonic Foraminifer Magnetobiostratigraphy of the Southern Kerguelen Plateau (Sites 747-749)<br><i>W. A. Berggren</i> . . . . .                                      | GG-10 |
| Abyssal Agglutinates: Back to Basics<br><i>W. A. Berggren and M. A. Kaminski</i> . . . . .  | GG-11 |
| Calcareous Nannoplankton Changes Across the Cretaceous/Paleocene Boundary in the Southern Indian Ocean (Site 750)<br><i>Thomas Ehrendorfer and Marie-Pierre Aubry</i> . . . . .   | GG-11 |
| Cenozoic Biostratigraphy and Paleocanography in the North Sea and Labrador Shelf<br><i>F. M. Gradstein, M. A. Kaminski and W. A. Berggren</i> . . . . .                           | GG-12 |
| Paleogene Benthic Foraminifers from the Southern Indian Ocean (Kerguelen Plateau): Biostratigraphy and Paleoecology<br><i>Andreas Mackensen and William A. Berggren</i> . . . . . | GG-12 |
| Ontogeny and Habitat of Modern Menardiiform Planktonic Foraminifera<br><i>Peter N. Schweitzer and G. P. Lohmann</i> . . . . .   | GG-13 |

## PALEOCLIMATOLOGY

Holocene Paleoclimatic Evidence and Sedimentation Rates from a Core in southwestern Lake Michigan

*Steven M. Colman, Glenn A. Jones, Richard M. Forester and David S. Foster* . . . . . GG-13

## SEDIMENTOLOGY

An unusual organic chemical composition for interfacial sediment in the Black Sea

*J. A. Beier, Stuart G. Wakeham, C. H. Pilskaln and S. Honjo* . . . . . GG-14

Carbonate Accumulation in the Indian Ocean During the Pliocene: Evidence for a Change in Productivity and Preservation at about 2.4 Ma

*William B. Curry, James L. Cullen and Jan Backman* . . . . . GG-14

Intraspecific Differences in Temperature and Salinity Responses in the Coccolithophore *Emiliana huxleyi*

*Nicholas S. Fisher and Susumu Honjo* . . . . . GG-14

Sediment Deposition in the Late Holocene Abyssal Black Sea: Terrigenous and Biogenic Matter

*Bernward J. Hay, Michael A. Arthur, Walter E. Dean, Eric D. Neff and Susumu Honjo* . . . GG-15

Enhanced Particle Fluxes to the Deep Ocean Induced by Freshwater Input

*V. Ittekkot, R. R. Nair, V. Ramaswamy and S. Honjo* . . . . . GG-15

Fluxes of Reduced Sulfur, Iron and Organic Carbon in the Black Sea Using Time-Series Sediment Traps

*Jo Ann M. Nicholson, Susumu Honjo, Brian Fry, Bernward J. Hay, Robert W. Howarth and John L. Cisne* . . . . . GG-15

Lithogenic Fluxes to the Deep Arabian Sea Measured by Sediment Traps

*V. Ramaswamy, R. R. Nair, S. Manganini, B. Haake and V. Ittekkot* . . . . . GG-16





# DEPARTMENT OF PHYSICAL OCEANOGRAPHY

## OCEAN CIRCULATION & LOW FREQUENCY VARIABILITY

|   |      |
|---|------|
| Evidence for barotropic wave radiation from the Gulf Stream<br><i>Amy S. Bower and Nelson G. Hogg</i>   | PO-1 |
| Measurement of the flow through the Strait of Gibraltar<br><i>Harry L. Bryden and R. Dale Pillsbury</i>   | PO-1 |
| Ocean heat transport across 24°N in the Pacific<br><i>Harry L. Bryden, Dean H. Roemmich, and John A. Church</i>   | PO-1 |
| The Gibraltar Strait and its role in the dynamics of the Mediterranean Sea<br><i>Julio Candela</i>  | PO-2 |
| Evidence of Internal Swash Associated with Sulu Sea Solitary Waves?<br><i>David C. Chapman, Graham S. Giese, Margaret Goud Collins, Rolu Encarnacion, and Gil Jacinto</i>   | PO-2 |
| The Structure of the Kuroshio Southwest of Kyushu Part I: Comparison of winter and summer hydrographic observation in the Kuroshio and adjacent East China Sea during 1986<br><i>C. S. Chen, R. C. Beardsley, and R. Limeburner</i> | PO-2 |
| The Structure of the Kuroshio Southwest of Kyushu Velocity, Transport and Potential Vorticity Fields<br><i>C. S. Chen, R. C. Beardsley, and R. Limeburner</i>   | PO-3 |
| Water Discharged from the Gulf Stream North of Cape Hatteras<br><i>James C. Churchill and Peter C. Cornillon</i>  | PO-3 |
| Energetics of the Kuroshio Extension at 35°N, 152°E<br><i>Melinda M. Hall</i>   | PO-4 |
| Modeling the Geostrophic Adjustment and Spreading of Waters Formed by Deep Convection<br><i>A. J. Hermann and W B. Owens</i>  | PO-4 |
| Mooring Motion Corrections Revisited<br><i>Nelson G. Hogg</i>   | PO-4 |
| A simple one-layer model driven by combined wind and buoyancy flux<br><i>Rui Xin Huang</i>  | PO-5 |
| The three-dimensional structure of wind-driven gyres; ventilation and subduction<br><i>Rui Xin Huang</i>  | PO-5 |
| Convective flow patterns in an 8-box cube driven by combined wind-stress, thermal and saline forcing<br><i>Rui Xin Huang and Henry M. Stommel</i>   | PO-5 |
| Multiple Equilibrium States in Combined Thermal and Saline Circulation<br><i>Rui Xin Huang, James Luyten, and Henry M. Stommel</i>  | PO-5 |
| Flow of deep and bottom waters in the Pacific at 10°N<br><i>Gregory C. Johnson and John M. Toole</i>  | PO-6 |
| Flow of bottom water in the Somali Basin<br><i>Gregory C. Johnson, Bruce A. Warren, and Donald B. Olson</i>   | PO-6 |
| A deep boundary current in the Arabian Basin<br><i>Gregory C. Johnson, Bruce A. Warren, and Donald B. Olson</i>   | PO-6 |
| Review of U. S. Contributions to Warm-Core Rings<br><i>Terrence M. Joyce</i>  | PO-7 |

|  |       |
|--|-------|
| The Meandering Gulf Stream as Seen by the Geosat Altimeter: Surface Transport, Position and Velocity Variance from 73° to 46° W<br><i>Kathryn A. Kelly</i> . . . . .   | PO-7  |
| The Geoid and Mean Sea Surface Height Along the Geosat Subtrack from Bermuda to Cape Cod<br><i>Kathryn A. Kelly, Terrence M. Joyce, David M. Schubert, and Michael J. Caruso</i> . . . . .   | PO-7  |
| Can reflected extra-equatorial Rossby waves drive ENSO?<br><i>William S. Kessler</i> . . . . .   | PO-8  |
| Aspiration of Deep Waters through Straits<br><i>Thomas H. Kinder and Harry L. Bryden</i> . . . . .   | PO-8  |
| Recent Progress in Strait Dynamics<br><i>Thomas H. Kinder and Harry L. Bryden</i> . . . . .  | PO-8  |
| Observations of the Mindanao Current During the Western Equatorial Pacific Ocean Circulation Study (WEPOCS)<br><i>Roger Lukas, Eric Firing, Peter Hacker, Philip L. Richardson, Curtis A. Collins, Rana Fine, and Richard Gammon</i> . . . . . | PO-9  |
| A comparison of ship drift, drifting buoy and current meter mooring velocities in the Pacific South Equatorial Current<br><i>M. J. McPhaden, D. V. Hansen, and P. L. Richardson</i> . . . . .  | PO-9  |
| A Statistical Description of the Mean Circulation and Eddy Variability in the Northwestern Atlantic Using SOFAR Floats<br><i>W. Brechner Owens</i> . . . . .   | PO-9  |
| The Link Between Western Boundary Currents and the Equatorial Undercurrent<br><i>Joseph Pedlosky</i> . . . . .   | PO-10 |
| The Nonlinear Dynamics of Slightly Supercritical Baroclinic Jets<br><i>J. Pedlosky and P. Klein</i> . . . . .  | PO-10 |
| The Role of Finite Mixed-Layer Thickness in the Structure of the Ventilated Thermocline<br><i>Joseph Pedlosky and Paul Robbins</i> . . . . .   | PO-10 |
| Radiation-Induced Baroclinic Instability<br><i>J. Pedlosky and R. M. Samelson</i> . . . . .  | PO-11 |
| Space-Time Variability of the Deep Western Boundary Current Oxygen Core: Meandering and Variability<br><i>Robert S. Pickart</i> . . . . .  | PO-11 |
| Shallow and Deep Components of the North Atlantic Deep Western Boundary Current<br><i>Robert S. Pickart</i> . . . . .  | PO-11 |
| The Physical Oceanography of Sea Straits<br><i>L. J. Pratt</i> . . . . .   | PO-11 |
| Geostrophic vs. Critical Control in Straits<br><i>Lawrence J. Pratt</i> . . . . .  | PO-12 |
| A Search for Meddies in Historical Data<br><i>P. L. Richardson, M. S. McCartney, and C. Maillard</i> . . . . .   | PO-12 |
| Currents Forced by Stochastic Winds with Meridionally-Varying Amplitude<br><i>R. M. Samelson and B. Shroyer</i> . . . . .  | PO-12 |

|   |       |
|---|-------|
| Spectral Time Scales for Mid-Latitude Eddies<br><i>William J. Schmitz, Jr. and James R. Luyten</i>  | PO-13 |
| Diurnal Cycles of Current, Temperature, and Turbulent Dissipation in a Model of the Equatorial Upper Ocean<br><i>Rebecca R. Schudlich and James F. Price</i>  | PO-13 |
| Bottom water circulation in the western North Atlantic<br><i>Kevin G. Speer and Michael S. McCartney</i>  | PO-13 |
| Trans-Pacific sections at 47°N and 152°W: distribution of properties<br><i>Lynne D. Talley, Terrence M. Joyce, and Roland A. DeSzoeko</i>   | PO-14 |
| Deep Currents in the Arabian Sea in 1987<br><i>Bruce A. Warren and Gregory C. Johnson</i>   | PO-14 |
| Suppression of Deep Oxygen Concentrations by Drake Passage<br><i>Bruce A. Warren</i>  | PO-14 |
| FASINEX, A Study of Air-Sea Interaction in a Region of Strong Oceanic Gradients<br><i>Robert A. Weller</i>  | PO-15 |
| Riding the Crest: A Tale of Two Wave Experiments<br><i>R. A. Weller, M. A. Donelan, M. G. Briscoe and N. E. Huang</i>   | PO-15 |
| Forced Ocean Response during the Frontal Air-Sea Interaction Experiment (FASINEX)<br><i>R. A. Weller, D. L. Rudnick, C. C. Eriksen, K. L. Polzin, N. S. Oakey, J. W. Toole, R. W. Schmitt and R. T. Pollard</i> | PO-15 |
| On the Transport of Fresh Water by the Oceans<br><i>Susan Wijffels, Harry Bryden, Raymond Schmitt and Anders Stigebrandt</i>  | PO-16 |
| THEORETICAL AND LABORATORY MODELS   |       |
| Chaos in a Model of Forced Quasi-Geostrophic Flow Over Topography: An Application of Melnikov's Method<br><i>J. S. Allen, R. M. Samelson, and P. A. Newberger</i>   | PO-16 |
| The Interaction of an Eddy with an Unstable Jet<br><i>George I. Bell and Larry J. Pratt</i>   | PO-17 |
| A Review of Rotating Hydraulics<br><i>K. M. Borenäs and L. J. Pratt</i>   | PO-17 |
| Experiments on Baroclinic Vortex Shedding from Hydrothermal Plumes<br><i>Karl R. Helfrich and Thomas B. Battisti</i>  | PO-17 |
| Review of Dispersive and Resonant Effects in Internal Wave Propagation<br><i>K. R. Helfrich and W. K. Melville</i>  | PO-17 |
| Current Research Problems<br><i>Lawrence J. Pratt and Karl R. Helfrich</i>  | PO-18 |
| Hydraulics of Rotating Strait and Sill Flows<br><i>L. J. Pratt and P. A. Lundberg</i>   | PO-18 |
| Linear and Nonlinear Barotropic Instability of Geostrophic Shear Layers<br><i>L. J. Pratt and J. Pedlosky</i>   | PO-18 |
| Separation of a boundary jet in a rotating fluid<br><i>Melvin E. Stern and J. A. Whitehead</i>  | PO-18 |

|   |       |
|---|-------|
| Magma Waves and Diapiric Dynamics<br><i>J. A. Whitehead and Karl R. Helfrich</i> . . . . .  | PO-19 |
| Experimental Observations of Baroclinic Eddies on a Sloping Bottom<br><i>John A. Whitehead, Melvin E. Stern, Glenn R. Flierl, and Barry A. Klinger</i> . . . . .  | PO-19 |
| Instability of Flow with Temperature - Dependent Viscosity: A Model of Magma Dynamics<br><i>J. A. Whitehead and Karl R. Helfrich</i> . . . . .  | PO-20 |
| COASTAL CIRCULATION & DYNAMICS  |       |
| Coastal Ocean Processes (CoOP): Results of an Interdisciplinary Workshop<br><i>K. H. Brink, J. M. Bane, T. M. Church, C. W. Fairall, G. L. Geernaert, D. S. Gorsline,<br/>R. T. Guza, D. E. Hammond, G. A. Knauer, C. S. Martens, J. D. Milliman, C. A. Nittrouer,<br/>C. H. Peterson, D. P. Rogers, M. R. Roman, and J. A. Yoder</i> . . . . . | PO-20 |
| Formation and Maintenance of Shelfbreak Fronts in an Unstratified Flow<br><i>Glen Gawarkiewicz and David C. Chapman</i> . . . . .   | PO-21 |
| Evidence of a Critical Richardson Number in Moored Measurements During the Upwelling Season off<br>Northern California<br><i>Pijush K. Kundu and Robert C. Beardsley</i> . . . . .  | PO-21 |
| The Bottom Boundary Layer over the Northern California Shelf<br><i>Steve J. Lentz and John H. Trowbridge</i> . . . . .  | PO-21 |
| INSTRUMENTATION & EXPERIMENTAL METHODOLOGY  |       |
| Tests of Long-Range Ocean Data Telemetry using Frequency-Agile HF Packet-Switching Protocols<br><i>David A. Brooks and Melbourne G. Briscoe</i> . . . . .   | PO-22 |
| Ocean Frontal Variability in FASINEX<br><i>Charles C. Eriksen, Robert A. Weller, Daniel L. Rudnick, R. T. Pollard, and Lloyd A. Regier</i> . . . . .  | PO-22 |
| An Intelligent Chilled Mirror Humidity Instrument, D10IQ<br><i>David S. Hosom, James F. Price, Clifford Winget, Sumner Weisman, and Donald P. Doucet</i> . . . . .  | PO-22 |
| Error in Measurements of Incoming Shortwave Radiation made from Ships and Buoys<br><i>M. A. MacWhorter and R. A. Weller</i> . . . . .   | PO-23 |
| An Index of Refraction Algorithm For Seawater Over Temperature, Pressure, Salinity, Density, and<br>Wavelength<br><i>R. C. Millard and G. Seaver</i> . . . . .  | PO-23 |
| High-Speed, Real-Time Data Acquisition for Vector Measuring Current Meters<br><i>Melora M. Park, Robin C. Singer, Albert J. Plueddemann, and Robert A. Weller</i> . . . . .   | PO-24 |
| Biasing of the Covariance-Based Spectral Mean Estimator in the Presence of Band-Limited Noise<br><i>Albert J. Plueddemann and Robert Pinkel</i> . . . . .   | PO-24 |
| The Motion of a Solid Sphere in an Oscillating Flow: An Evaluation of Remotely-Sensed Doppler<br>Velocity Estimates in the Sea<br><i>David A. Siegel and Albert J. Plueddemann</i> . . . . .  | PO-24 |
| MISCELLANEOUS   |       |
| Geology of the Solitario, Trans-Pecos Texas<br><i>Charles E. Corry, Eugene Herrin, Fred W. McDowell, and Kenneth A. Phillips</i> . . . . .  | PO-25 |
| Andrew F. Bunker: Pioneering in Air-Sea Interaction Research 1946-79<br><i>Carl A. Friehe and Henry M. Stommel</i> . . . . .  | PO-26 |

## TECHNICAL REPORTS

- Altimeter Processing Tools for Analyzing Mesoscale Ocean Features  
*Michael J. Caruso, Ziv Sirkes, Pierre J. Flament, and M. K. Baker* . . . . . PO-26
- Hydrographic Observations from the US/PRC Cooperative Program in the Western Equatorial Pacific Ocean: Cruises 1-4  
*M. Cook, L. Mangum, R. Millard, G. LaMontagne, S. Pu, J. Toole, Z. Wang, K. Yang, and L. Zhao* . . . . . PO-26
- Improved Meteorological Measurements from Buoys and Ships (IMET): Preliminary comparison of Humidity Sensors  
*Gennaro H. Crescenti, Richard E. Payne, and Robert A. Weller* . . . . . PO-27
- The Seadata Program  
*Thomas W. Danforth* . . . . . PO-27
- Report on R.V. AKADEMIK VERNADSKY Cruise 39, Stage IV June 17 – July 19, 1989  
*Nick P. Fofonoff, Ellen Levy, A. James Kettle, and Richard C. Navitsky* . . . . . PO-27
- Automated Oxygen Titration and Salinity Determination  
*George P. Knapp, M. C. Stalcup, and R. J. Stanley* . . . . . PO-27
- Moored Current Meter, AVHRR, CTD, and Drifter Data From the Agulhas Current and Retroflexion Region (1985-1987) Volume XLII  
*J. Luyten, A. Spencer, S. Tarbell, K. Luetkemeyer, P. Flament, J. Toole, M. Francis, and S. Bennett* . . . . . PO-28
- US/PRC CTD Intercalibration Report 1986-1990  
*R. C. Millard, B. J. Lake, N. L. Brown, J. M. Toole, D. Schaaf, K. Yang, H. Yu, and L. Zhao* PO-28
- An Exploration of the North Atlantic Current and its Recirculation in the Newfoundland Basin using SOFAR Floats  
*W. Brechner Owens and Marguerite E. Zemanovic* . . . . . PO-28
- Surface Drifter Measurements in the Western Equatorial Pacific Ocean Circulation Study (WEPOCS III)  
*Christine M. Wooding, Philip L. Richardson, and Curtis A. Collins* . . . . . PO-28
- SOFAR Float Mediterranean Outflow Experiment Summary and Data from 1986 – 1988  
*Marguerite E. Zemanovic, Philip L. Richardson, and James F. Price* . . . . . PO-29



## MARINE POLICY CENTER

|   |       |
|---|-------|
| Multiple Use Planning for Coastal and Marine Protected Areas in the Caribbean<br><i>M. Tundi Agardy</i> . . . . .   | MPC-1 |
| Pacific Sea Turtles Under Threat<br><i>M. Tundi Agardy</i> . . . . .  | MPC-1 |
| Water Masses and Seabird Distributions in the Southern Chukchi Sea: The 1988 Joint<br>Soviet-American Expedition of the AKADEMIK KOROLEV<br><i>Jonathan M. Andrew and J. Christopher Haney</i> . . . . .                              | MPC-1 |
| The Soviet Maritime Arctic<br><i>Lawson W. Brigham</i> . . . . .  | MPC-1 |
| Nonfuel Minerals<br><i>James M. Broadus and Porter Hoagland III</i> . . . . .   | MPC-2 |
| Using Dynamic Optimization for Integrated Environmental Management: An Application to Solvent<br>Waste Disposal<br><i>Mark E. Eiswerth</i> . . . . .  | MPC-2 |
| Allocating Conservation Expenditures Across Habitats: Accounting for Inter-Species Genetic<br>Distinctiveness<br><i>Mark E. Eiswerth and J. Christopher Haney</i> . . . . .   | MPC-2 |
| Managing the Outer Continental Shelf Lands: Oceans of Controversy<br><i>R. Scott Farrow, James M. Broadus, Thomas A. Grigalunas, Porter Hoagland III,<br/>and James J. Opaluch</i> . . . . .  | MPC-3 |
| Developing a National Marine Electronics Agenda: Proceedings of the Marine Instrumentation Panel<br>Meeting, September 12-14, 1989<br><i>Arthur G. Gaines and Kristina L. C. Lindborg</i> . . . . .                                   | MPC-3 |
| Influence of Pycnocline Topography and Water Column Structure on Marine Distributions of Alcids<br>(Class Aves: Family Alcidae) in Anadyr Strait, Northern Bering Sea, Alaska<br><i>J. Christopher Haney</i> . . . . .                | MPC-3 |
| Variability in Distributions of Northern Fulmars ( <i>Fulmarus glacialis</i> ) and Short-Tailed Shearwaters<br>( <i>Puffinus tenuirostris</i> ) in the Southern Chukchi Sea<br><i>J. Christopher Haney and J. M. Andrew</i> . . . . . | MPC-4 |
| Analyzing Quantitative Relationships Between Seabirds and Marine Resource Patches<br><i>J. Christopher Haney and Andrew R. Solow</i> . . . . .  | MPC-4 |
| Some Initial Effects of Hurricane Hugo on Endangered and Endemic Species of West Indian Birds<br><i>J. Christopher Haney, Joseph M. Wunderle, Jr., Wayne J. Arendt</i> . . . . .  | MPC-4 |
| Coastal Zone Management in South Korea<br><i>Seoung-Yong Hong</i> . . . . .   | MPC-5 |
| Antarctic Treaty Diplomacy: Problems, Prospects and Policy Implications<br><i>Christopher C. Joyner</i> . . . . .   | MPC-5 |
| Antarctica and the Indian Ocean States: The Interplay of Law, Interests, and Geopolitics<br><i>Christopher C. Joyner</i> . . . . .  | MPC-5 |
| Geopolitics and Antarctica<br><i>Christopher C. Joyner</i> . . . . .  | MPC-6 |



|   |        |
|---|--------|
| CRAMRA: The Ugly Duckling of the Antarctic Treaty System?<br><i>Christopher C. Joyner</i> . . . . .   | MPC-6  |
| Maritime Zones in the Southern Ocean: Problems Concerning the Correspondence of Natural and<br>Legal Maritime Zones<br><i>Christopher C. Joyner</i> . . . . .                                   | MPC-6  |
| Plastic Pollution in the Marine Environment: Towards an International Solution<br><i>Christopher C. Joyner and Scot Frew</i> . . . . .  | MPC-7  |
| Key Problems in the Management of Sports Fisheries<br><i>Yoshiaki Kaoru</i> . . . . .   | MPC-7  |
| "Black Mayonnaise" and Marine Recreation: Methodological Issues in Valuing a Cleanup<br><i>Yoshiaki Kaoru and V. Kerry Smith</i> . . . . .  | MPC-7  |
| Gone Fishing, Be Back Later: Ending and Resuming Research Among Fishermen<br><i>Ilene M. Kaplan</i> . . . . .   | MPC-8  |
| Tourism in the Galápagos Islands: The Dilemma of Conservation<br><i>Richard A. Kenchington</i> . . . . .  | MPC-8  |
| Diablotin ( <i>Pterodroma hasitata</i> ): Biography of an Endangered Procellariiform<br><i>David S. Lee and J. Christopher Haney</i> . . . . .  | MPC-8  |
| Guiding the Ocean Search Process: Applying Public Land Experience to the Design of Leasing and<br>Permitting Systems for Ocean Mining and Ocean Shipwrecks<br><i>Robert H. Nelson</i> . . . . . | MPC-9  |
| The Detection of Greenhouse Warming<br><i>Andrew R. Solow</i> . . . . .   | MPC-9  |
| An Exploratory Analysis of the Occurrence of Explosive Volcanism in the Northern Hemisphere,<br>1851-1985<br><i>Andrew R. Solow</i> . . . . .   | MPC-9  |
| A Method of Approximate Multivariate Normal Orthant Probabilities<br><i>Andrew R. Solow</i> . . . . .   | MPC-10 |
| The Nonparametric Analysis of Point Process Data: The Freezing History of Lake Konstanz<br><i>Andrew R. Solow</i> . . . . .   | MPC-10 |
| A Note on the Statistical Properties of Animal Locations<br><i>Andrew R. Solow</i> . . . . .  | MPC-10 |
| A Randomization Test for Misclassification Probability in Discriminant Analysis<br><i>Andrew R. Solow</i> . . . . .   | MPC-10 |
| Testing for Density Dependence: A Cautionary Note<br><i>Andrew R. Solow</i> . . . . .   | MPC-10 |
| Decision-Making and the Value of Information Under Uncertainty<br><i>Andrew R. Solow and James M. Broadus</i> . . . . .   | MPC-11 |
| Global Warming: Quo Vadis?<br><i>Andrew R. Solow and James M. Broadus</i> . . . . .   | MPC-11 |
| Detecting Cluster in a Heterogeneous Community Sampled by Quadrats<br><i>Andrew R. Solow, Woolcott Smith and J. Frederick Grassle</i> . . . . .   | MPC-11 |

On Sample Size, Statistical Power, and the Detection of Density Dependence  
*Andrew R. Solow and John H. Steele* . . . . . MPC-11

Marine Instruments: User's Viewpoints  
*Glenn Woodsum and Hauke Kite-Powell* . . . . . MPC-11



## COASTAL RESEARCH CENTER

|   |       |
|---|-------|
| Tidal Velocity Asymmetries and Bedload Transport in Shallow Embayments<br><i>Virginia A. Fry and David G. Aubrey</i> . . . . .  | CRC-1 |
| Potential Impacts of Contemporary Changing Climate on South Asian Seas States<br><i>F. J. Gable and D. G. Aubrey</i> . . . . .  | CRC-1 |
| Potential Impacts of Contemporary Changing Climate on Caribbean Coastlines<br><i>Frank J. Gable and David G. Aubrey</i> . . . . .   | CRC-1 |
| Global Climatic Issues in the Coastal Wider Caribbean Region<br><i>Frank J. Gable, J. H. Gentile and D. G. Aubrey</i> . . . . .   | CRC-1 |
| Estimating the Value of Beach Recreation from Property Values: An Exploration with Comparisons to Nourishment Costs<br><i>Steven F. Edwards and Frank J. Gable</i> . . . . .  | CRC-2 |
| Global Environmental Change Issues in the Western Indian Ocean Region<br><i>Frank J. Gable, David G. Aubrey and John H. Gentile</i> . . . . .   | CRC-2 |
| Contemporary Climate Change and its Related Effects on Global Shorelines<br><i>Frank Gable</i> . . . . .  | CRC-2 |
| Potential Coastal Effects of Climate Change in the Caribbean<br><i>F. J. Gable and D. G. Aubrey</i> . . . . .   | CRC-2 |
| Changing Infrastructure of an Urban Waterfront: The South Boston Flats 1863-1920<br><i>Frank Gable</i> . . . . .  | CRC-3 |
| Caribbean Coastal and Marine Tourism - Coping with Climate Change and its Associated Effects<br><i>F. Gable</i> . . . . .   | CRC-3 |
| Recent Global Sea Levels and Land Levels<br><i>David G. Aubrey and K. O. Emery</i> . . . . .  | CRC-3 |
| <b>TECHNICAL REPORTS</b>  |       |
| Atlantic Shelf Sand Ridge Study: Physical Oceanography and Sediment Dynamics Data Report<br><i>Paul Dragos and David G. Aubrey</i> . . . . .  | CRC-4 |
| Sedimentation Study Environmental Monitoring and Operations Guidance System (EMOGS) Kings Bay, Georgia and Florida Phase III - FY 1989<br><i>David G. Aubrey, Thomas R. McSherry and Wayne D. Spencer</i> . . . . .   | CRC-4 |
| Geodetic Fixing of Tide Gauge Bench Marks<br><i>William E. Carter, David G. Aubrey, Trevor Baker, Claude Boucher, Christian LeProvost, David Pugh, W. R. Peltier, Mark Zumberge, Richard H. Rapp, Robert E. Schutz, K. O. Emery and David B. Endfield</i> . . . . . | CRC-5 |
| Development, Characteristics, and Effects of the New Chatham Harbor Inlet<br><i>Graham S. Giese, David G. Aubrey and James T. Liu</i> . . . . .   | CRC-5 |



## GRADUATE STUDENTS

|   |       |
|---|-------|
| Physiological Studies of Phototrophy and Heterotrophy in Two Algae with Contrasting Nutritional Characteristics, <i>Pyrenomonas salina</i> (Cryptophyceae) and <i>Poterioochromonas malhamensis</i> (Chrysophyceae)<br><i>Alan J. Lewitus</i> . . . . . | GS-1  |
| Analysis and Distribution of Integrins in Chicken Embryos<br><i>Lisa Andrea Urry</i> . . . . .  | GS-2  |
| Dinoflagellate Blooms and Physical Systems in the Gulf of Maine<br><i>Peter John Selwyn Franks</i> . . . . .  | GS-3  |
| Estimation and Correction of Geometric Distortions in Side-Scan Sonar Images<br><i>Daniel Tavora De Queiroz Cobra</i> . . . . .   | GS-3  |
| Stochastic Modeling of Seafloor Morphology<br><i>John Anson Goff</i> . . . . .  | GS-4  |
| Comparative Design, Modeling, and Control Analysis of Robotic Transmissions<br><i>Hagen Schempf</i> . . . . .   | GS-5  |
| Trace Element Geochemistry of Oceanic Peridotites and Silicate Melt Inclusions: Implications for Mantle and Ocean Ridge Magmagenesis<br><i>Kevin Todd Michael Johnson</i> . . . . .   | GS-6  |
| Detection and Characterization of Deep Water Wave Breaking using Moderate Incidence Angle Microwave Backscatter from the Sea Surface<br><i>Andrew Thomas Jessup</i> . . . . .   | GS-7  |
| Refinement and Application of a New Paleotemperature Estimation Technique<br><i>Elisabeth Lynn Sikes</i> . . . . .  | GS-8  |
| The Life Cycle of the Centric Diatom <i>Thalassiosira Weissflogii</i> : Control of Gametogenesis and Cell Size<br><i>Elizabeth Virginia Armbrust</i> . . . . .  | GS-8  |
| Evolution of Gaussian Vortices in Vertical Shear on the Beta Plane<br><i>James D. McLaren</i> . . . . .   | GS-9  |
| Variations in Structure and Tectonics Along the Mid-Atlantic Ridge, 23°N and 26°N<br><i>Laura Sau Lin Kong</i> . . . . .  | GS-9  |
| The Geochemistry of Beryllium Isotopes: Applications in Geochronometry<br><i>Erik Thorson Brown</i> . . . . .   | GS-11 |
| Inter-Annual Variability of Acoustic Ray Travel Times in the Northeast Pacific<br><i>John Alan Furgerson</i> . . . . .  | GS-12 |
| Observations of Ocean Fluctuations between 15 and 23 Hour Periods in the Pacific<br><i>Wayne Richard Blanding</i> . . . . .   | GS-12 |
| A Beam Pattern Design Procedure for Multidimensional Sonar Arrays Employing Minimum Variance Beamforming<br><i>Randall George Richards</i> . . . . .  | GS-13 |
| The Distribution of Wave Heights and Periods for Seas with Unimodal and Bimodal Power Density Spectra<br><i>Matthew Michael Sharpe</i> . . . . .  | GS-13 |

|  |       |
|--|-------|
| Basin-Scale Tidal Measurements using Acoustic Tomography<br><i>Robert Hugh Headrick</i> . . . . .  | GS-13 |
| Observation and Inversion of Seismo-Acoustic Waves in a Complex Arctic Ice Environment<br><i>Bruce Edward Miller</i> . . . . .                             | GS-14 |
| Relative Sea-Level Variations Revealed by Tide-Gauge Records of Long Duration<br><i>Anthony James Withnell</i> . . . . .                                   | GS-14 |
| Marine Bacteria as a Source of Dissolved Fluorescence in the Ocean<br><i>Paula G. Coble</i> . . . . .  | GS-15 |
| Foraminiferal and Coralline Barium as Paleooceanographic Tracers<br><i>David W. Lea</i> . . . . .  | GS-15 |
| Shipboard and Satellite Observations of Upper Ocean Velocity and Transport Variability in the Gulf Stream<br><i>David Michael Schubert, Jr.</i> . . . . .  | GS-16 |
| Sedimentary Lipids as Indicators of Depositional Conditions in the Coastal Peruvian Upwelling Regime<br><i>Mark A. McCaffrey</i> . . . . .                 | GS-17 |
| The Nutritional Role of Endosymbiotic Bacteria in Animal-Bacteria Symbioses: <i>Solemya Velum</i> , A Case Study<br><i>Noellette Mary Conway</i> . . . . . | GS-18 |

**DEPARTMENT OF APPLIED OCEAN PHYSICS & ENGINEERING**

**Albert J. Williams III, Chairman**





## **IMPROVED METEOROLOGICAL MEASUREMENTS FROM SHIPS AND BUOYS**

*Kenneth Prada, David Hosom and Alan Hinton*

The World Ocean Circulation Experiment (WOCE) is directed at understanding ocean circulation and its interrelation to climate. During WOCE, moored buoys and ships will be platforms for in-situ measurements of the basic observables: sea-surface temperature, air temperature, wind velocity, barometric pressure, solar and longwave radiation, humidity, and precipitation. Accurate estimates of the air-sea fluxes can be made from these measurements.

The IMET program (Improved Meteorological Measurements from Ships and Buoys) is responsible for the development of improved sensors and data logging systems for both ships and buoys. Objectives include increased resolution, accuracy and reliability; identical standards for sensors, data format and storage on both ships and buoys; and low cost production. The results are a series of discrete intelligent sensors that can be easily networked on both ships and buoys; shipboard and buoy data loggers with interactive or intelligent configuration capabilities and real-time color display of measurements; portable UHF-linked systems for volunteer and ship-of-opportunity applications; and improved calibration and documentation procedures.

Published in: *Proceedings of Marine Instrumentation* '90:178-182, 1990.

Supported by: NSF - Ocean Sciences Division Grant OCE-8709614.

WHOI Contribution No. 7282.

## **A MULTI-NODE THREE COMPONENT SEISMIC SYSTEM FOR DEEP SEA DRILLING PROJECT (DSDP) BOREHOLES**

*Donald E. Koelsch, Robert G. Goldsborough, Henri O. Berteaux and Ralph Stephen*

The Low Frequency Acoustic Seismic Experiment (LFASE) was conducted to measure low frequency seismic and acoustic ambient noise below the ocean floor. To perform this measurement sensors were clamped into a DSDP borehole.

For this experiment 4 three component geophone nodes were clamped in a bore hole at various depths below the ocean floor. The data were logged on special ruggedized high capacity write once read many (WORM) optical disk

recorders. There were two modes of operation. The first was to telemeter the data, via a conducting cable, to the attending ship where it was recorded by a PC/AT computer. The second was battery powered stand-alone mode which logged data at the ocean bottom on self contained optical disk recorders. The bottom package contained the equivalent of a PC/XT computer which controlled acquisition schedules and the data recording process.

This experiment marks the first time that ambient noise data from a multi-node, three component seismic array has been obtained from a DSDP borehole.

Published in: *Proceedings of Marine Instrumentation* '90:104-109, 1990.

Supported by: ONR Contract No. N00014-89-C-0018 and John Hopkins Applied Physics Labs Contract No. 602809-0.

WHOI Contribution No. 7283.

## **ROBUST 5000 BIT PER SECOND UNDERWATER COMMUNICATION SYSTEM FOR REMOTE APPLICATIONS**

*Lee E. Freitag and J. Stevens Merriam*

A compact, power efficient unit which operates as a two-way, single-duplex transmitter and receiver is being developed for operation as an underwater modem at speeds up to 5000 bits per second. The device is based on a fast digital signal processor that can run sophisticated communication algorithms in real-time. Reliable communication over fading, dispersive ocean channels is provided by incoherent MFSK signaling coupled with error correction coding and equalization. The unit is designed to operate as a transparent data link between user devices, but also allows control over communication system parameters. System hardware has been designed and built, and 300-1200 baud receiver software tested up to 2 km. Software allowing the unit to operate as a fast, fully operational, 5000 bit per second transceiver has been designed and is being implemented.

Published in: *Proceedings of Marine Instrumentation* '90:201-207, 1990.

Supported by: ONR Grant No. N00014-86-K-0751.

WHOI Contribution No. 7298.

## **DRAG FORCES AND FLOW-INDUCED VIBRATIONS OF LONG VERTICAL TOW CABLES PART I: STEADY STATE TOWING CONDITIONS**

*D. R. Yoerger, M. A. Grosenbaugh,  
M. S. Triantafyllou and J. J. Burgess*

The analysis of data of a unique experiment on the quasi-statics and vortex-induced dynamics of a long vertical tow cable is presented. The experiment consisted of measuring simultaneously the vortex-induced motions and the steady-state configuration of the tow cable. The measured steady-state configuration of the cable was used to calculate the cable's average drag coefficient which ranged from  $2.2 \pm 0.24$  to  $2.5 \pm 0.24$ . It was observed that the vortex-induced motion of the cable was modulated by a beat due to the presence of a shear current. This is confirmed here by spectral and time domain analysis of the acceleration records. The RMS motion of the cable varies with depth which indicates that the drag coefficient of the cable is spatially varying.

In Press: *ASME Transactions Journal of Offshore Mechanics and Arctic Engineering*.

Supported by: ONR Contract No. N00014-87-G-0111 and NSF Grant No. OCE-8511431.

WHOI Contribution No. 7306.

## **THE INFLUENCE OF THRUSTER DYNAMICS ON UNDERWATER VEHICLE BEHAVIOR AND THEIR INCORPORATION INTO CONTROL SYSTEM DESIGN**

*Dana R. Yoerger, John G. Cooke and  
Jean-Jacques E. Slotine*

The system dynamics of underwater vehicles can be greatly influenced by the dynamics of the vehicle thrusters. In this paper, a nonlinear parametric model of a torque-controlled thruster is developed and experimentally confirmed. The model shows that the thruster behaves like a sluggish nonlinear filter, where the speed of response depends on the commanded thrust level. A quasilinear analysis utilizing describing functions shows that the dynamics of the thruster produce a strong bandwidth constraint and a limit cycle, both of which are commonly seen in practice. Three forms of compensation were tested utilizing a hybrid simulation that combined an instrumented thruster with a real-time mathematical vehicle model. The first compensator, a linear lead network, was easy to implement and greatly improved performance over

the uncompensated system, but did not perform uniformly over the entire operating range. The second compensator, which attempts to cancel the nonlinear filtering effect of the thruster, was effective over the entire operating range but depends on an accurate thruster model. The final compensator, an adaptive sliding controller, was effective over the entire operating range and could compensate for uncertainties or degradation of the thruster.

Published in: *IEEE Journal of Ocean Engineering*, 15(3):167-178, 1990.

Supported by: ONR Contract No. N00014-86-C-0038, N00014-88-K-2022 and ONR Grant No. N00014-87-J-1111.

WHOI Contribution No. 7307.

## **A WAVETANK STUDY OF THE DEPENDENCE OF X-BAND CROSS SECTIONS ON WIND SPEED AND WATER TEMPERATURE**

*Mary Ruth Keller, William C. Keller and  
William J. Plant*

Measurements of normalized radar cross-sections of wind-generated waves were made at X-Band for both vertical and horizontal polarization for incidence angles of  $10^\circ$ ,  $28^\circ$ ,  $48^\circ$ , and  $68^\circ$ . The study, conducted in the NRL wind-wave facility, sought to measure effects on the backscatter of varying water temperature, wind speed, and wind stress. The measurements were averaged for 2.13 minutes simultaneously with wind speed and wind stress. Air and water temperature were measured periodically with mercury thermometers.

The results were compared with the empirical model functions developed for the SEASAT-A Satellite Scatterometer, SASS I, and SASS II, and with the physically-based models of Durden and Vesecky, Plant, and Donelan and Pierson. In these comparisons, differences between Ku and X-Bands were assumed to be small. When plotted versus 19.5 meter winds on a log-log scale, the cross sections do not fall on straight lines. Thus, a power law dependence of cross section on wind speed is not a good representation of that relationship. The data also exhibit large variations at low winds which are not related to system noise. This may indicate that the statistics of backscatter depend markedly on wind speed. Although the water temperature was varied from  $9^\circ\text{C}$  to  $36^\circ\text{C}$  when the measurements were made at a  $48^\circ$  incidence angle, no temperature dependence, as predicted by Donelan and Pierson, was detectable. The agreement between Plant's model and the data improved when the relationship between wind

speed, wind stress, and mean squared slope measured in the wavetank was used, instead of more general values. Nevertheless, neither this model nor any of the others was consistently accurate at all wind speeds, incidence angles, and polarizations.

The wavetank data compare well with 10 GHz, 3.0 cm (X-band) aircraft measurements, and with the 14.6 GHz, 2.1 cm (Ku-band) satellite data used in the SASS II model. Such agreement casts doubt on the hypothesis that cross section depends on antenna altitude.

Supported by: NRL Basic Research Funds  
83-1319-08 and NASA Grant NAGW-1675.

WHOI Contribution No. 7310.

### NEW CRITERIA FOR BLIND DECONVOLUTION OF NONMINIMUM PHASE SYSTEMS (CHANNELS)

*Ofir Shalvi and Ehud Weinstein*

We derive a necessary and sufficient condition for blind deconvolution (without observing the input) of nonminimum phase linear time-invariant systems (channels). Based on that, we propose several optimization criteria, and prove that their solution corresponds to the desired response. These criteria only involve the computation of second and fourth order moments, implying a simple tap up-date procedure. These criteria are universal in the sense that they do not impose any restrictions on the probability distribution of the (unobserved) input sequence. We also address the problem of additive noise in the system and show that in several important cases, e.g. when the additive noise is Gaussian, the proposed criteria are essentially unaffected.

Published in: *IEEE Transactions on Information Theory*, 36(2):312-321, 1990.

Supported by: ONR Contract No.  
N00014-85-K-0272.

WHOI Contribution No. 7334.

### A MODEL-BASED APPROACH TO 3-D IMAGING AND MAPPING UNDERWATER

*W. K. Stewart*

An approach to multidimensional representation of underwater environments is presented with results of applications in 3-D sonar mapping. A non-deterministic model incorporates information from multiple knowledge sources and creates a framework for real-time processing.

Probabilistic methods account for non-ideal sensors; spatial decomposition and numerical techniques treat amorphous underwater features and facilitate an incremental approach. An emphasis on representational and modeling issues is maintained with examples drawn from computer simulations and field data from profiling and imaging sonars.

Published in: *ASME Transactions Journal of Offshore Mechanics and Arctic Engineering*, 112:352-356, 1990.

Supported by: Sea Grant Program of the  
Massachusetts Institute of Technology, Monitor  
Marine Sanctuary Program of the National  
Oceanic and Atmospheric Administration and  
Deep Submergence Laboratory of W.H.O.I.

WHOI Contribution No. 7341.

### SOME OBSERVATIONAL EVIDENCE ON THE EFFECT OF ATMOSPHERIC FORCING ON TIDAL VARIABILITY IN THE UPPER DELAWARE BAY

*Kuo-Chuin Wong and John H. Trowbridge*

Until quite recently, most oceanographic research relating to the tidal variability in an estuary has ignored the effect of atmospherically forced motions on the tidal motions. Mechanisms exist, however, through which high frequency wind waves and low frequency subtidal variability can interact nonlinearly with the tide and modify the tidal response of an estuary significantly. A set of current and sea level observations in the upper Delaware Bay provides observational evidence which suggests that tidal variability in the interior of the bay was appreciably modified during two moderately strong atmospheric events.

Published in: *Journal of Geophysical Research*, 95(C9):16,229-16,240, 1990.

Supported by: NSF Grants OCE-8515735 and OCE  
87-10768.

WHOI Contribution No. 7347.

### WAVE INFLUENCES ON WIND PROFILES OVER WATER

*William J. Plant*

Wind profiles over water surfaces are shown to depend only on wind stress, wave state, and a constant roughness length which is on the order that for aerodynamically smooth flow. The model developed here is able to account for the observed wind speed dependence of the neutral drag coefficient over water surfaces. If an effective

roughness length is introduced to account for the influence of waves, as has been the common practice, then its wind speed dependence is also closely approximated by the present work. To a large extent, the ideas developed here explain the differences observed in the drag coefficient and effective roughness length when they are measured over bodies of water of different sizes. This work shows that these quantities are very sensitive to ambient wave conditions and could explain much of the variability observed in measurements of neutral drag coefficients. The model is developed assuming that the total wind stress as measured, for instance by a sonic anemometer, is the sum of a turbulent stress and a wave-induced stress and is constant in the surface layer. Turbulent stress is described by the usual Prandtl mixing-length hypothesis with a constant, small roughness length. A form for the wave-induced stress at the surface is derived directly from the Navier-Stokes equations subject to the assumption that gradients of wave-related fluctuations of stresses nearly cancel. This form depends on functions describing wave spectral densities, wave growth rates, wave phase speeds, and the surface drift current which are estimated from experimental data. The dependence of the normalized, wave-induced mean stress on height is shown to depend on wave-modulated viscous and Reynold's stresses in a complex manner. A simple form for this variation is chosen and shown to produce wind-profiles and effective roughness lengths in good agreement with experiment. These results indicate that for neutrally stratified conditions wind profiles are nearly logarithmic over water and vary in magnitude depending only on wind stress and wave state. The effective roughness length reaches a maximum for wave states corresponding to fetches on the order of a kilometer, in rough agreement with data. For short fetches, the influence of the surface wind drift reduces the effective roughness length while for long fetches, it is reduced due to the reduced wind input to the dominant waves. The form of the directional wave spectrum over a large range of wavenumbers is shown to be of primary importance in controlling the details of this behavior.

Supported by: ONR Grant N00014-89-J-1453 and  
NASA Grant NAGW-1675.

WHOI Contribution No. 7349.

### **SPECIFICATIONS & APPLICATIONS FOR AN ADVANCED ACOUSTIC TELEMETRY SYSTEM**

*Josko Catipovic, Daniel Frye and Dave Porta*

An acoustic telemetry system capable of reliable operation at data rates up to 5,000 bits

per second has been developed at the Woods Hole Oceanographic Institution and is being produced by Datasonics, Inc. of Cataumet, Massachusetts. This paper describes the telemetry system, summarizes results of recent at-sea tests, and discusses several upcoming operational applications of the equipment.

The telemetry technique makes use of MFSK acoustic data transmission where many tones are transmitted simultaneously and modulation and demodulation are done digitally with FFT's. Receiver software has been implemented on a digital signal processing chip, at AT&T DSP-32C.

Tests of prototype hardware have been performed in shallow water over path lengths of 800 to 2500 meters with baud rates up to 5000 bits per second. Vertical transmission tests in depths to 3000 meters have also been performed using low power transmitters operating at 600 to 1200 bits per second. Tests have been performed for both coded and uncoded data and acceptably low error rates have been achieved. Several upcoming deployments of the advanced acoustic telemetry system are described including a deep water moored array application, a bottom to surface link in shallow water, and a profiling application.

Supported by: ONR U.R.I.P. Contract No.  
N00014-86-K-0751.

WHOI Contribution No. 7352.

### **A COMPARISON OF BROADBAND AND NARROWBAND MODAL INVERSIONS FOR BOTTOM GEOACOUSTIC PROPERTIES AT A SITE NEAR CORPUS CHRISTI, TEXAS**

*James F. Lynch, Subramaniam D. Rajan and  
George V. Frisk*

In September, 1985, a series of narrowband shallow water acoustics experiments, collectively called project GEMINI, were performed in the Gulf of Mexico near Corpus Christi, Texas. The reasons for the experiments were threefold. The first was to obtain very accurate measurements of the pressure field versus range at a benign (i.e. range independent, geologically simple) site which had been well studied previously, and then determine how well one could predict the measured fields using state of the art propagation models with high quality geoacoustic information (both a priori and a posteriori) as input. The second reason was to utilize, extend, and benchmark the narrowband bottom measurement and inversion techniques previously developed by the authors [Rajan et. al., J. Acoust. Soc. Am., 82, 998-1017 (1987)]. The third reason was to compare bottom models generated by narrowband and broadband

techniques. Originally, this was to be restricted to the three-layer model inferred by L. Rubano in a previous study at the same site [L. Rubano, J. Acoust. Soc. Am., **67**, 1608-1613 (1980)]. However, by employing Rubano's original modal dispersion data with broadband perturbative inverse techniques also developed by the authors, we could make a more general comparison of narrowband and broadband inversions for the bottom properties. This paper is mainly devoted to answering the questions posed above. Detailed comparisons between narrowband and broadband techniques are presented with emphasis on: a) comparisons of the pressure field versus range predicted, b) comparisons of the bottom compressional wave speed model generated, c) the variance of the bottom model estimated, and d) the resolution of the bottom model generated. The range dependence of the bottom medium and the seasonal dependence of the near-surface sediment sound speed profile are observed and discussed (particularly the former effect – the latter is the subject of a separate paper). We have drawn the following conclusions from this study: (a) The geoacoustic models obtained using Narrowband perturbative inversion on the WHOI data (Model I), broadband perturbative inversion on Rubano's data (Model II), and J. Matthew's synthesis of archival data are generally consistent with one another for the top 90 m of sediment. Meaningful quantitative comparisons of Model I and II with Matthew's model are difficult because of the lack of error estimates for the archival data.

(b) The continuous compressional wave speed profile inferred using the narrowband perturbative inversion approach yields the best agreement between the theoretically computed and measured pressure fields. This result is partly due to the apparent inaccuracies of Matthews' model for the deeper sediment depths (> 90 m) the constraint of three homogeneous layers imposed by Rubano's original model, and some error in fitting the broadband dispersion curve and correcting for seasonal effects in the broadband perturbative inverse calculation based on Rubano's data.

(c) The differences between Model I and II fall within the error bounds predicted by linear inverse theory everywhere except the top 10 m of sediment. There the difference is attributed to the hypothesis that the compressional wave speed in the uppermost part of the sediment column is influenced by the water column temperature; the Rubano and WHOI experiments were conducted at different times of year with significantly different water temperatures, thereby yielding the differing sediment results.

In Press: *Journal of the Acoustical Society of America*.

Supported by: ONR Contract N00014-85-C-0379.

WHOI Contribution No. 7359.

## BASIN-SCALE TOMOGRAPHY: A NEW TOOL FOR STUDYING WEATHER AND CLIMATE

John L. Spiesberger and Kurt Metzger

We present the first experimental results demonstrating the use of acoustic tomography to observe the large-scale (>500 km) temperature fluctuations in ocean basins. Use of the tomographic technique, as presented here, will eventually lead to a better understanding of weather, climate, ocean circulation, and the distributions of marine organisms. From June to September 1987, tomographic signals were transmitted between four sources and nine receivers over a 3000 by 4000 km region (the basin-scale) in the northeast Pacific. This paper discusses five issues related to transmissions across one 3000 km section. First, basin-scale tomography is feasible because multipaths are stable in the presence of ocean fluctuations and the multipaths can be understood with ray theory (and its extensions). Second, the tomography problem can be initiated from climatological estimates. It is unnecessary to initiate with conventional measurements during the experiment (a prohibitively expensive proposition). Third, a description of the tomographic reconstruction procedure (Kalman filtering) is presented. The filter imposes temporal and spatial constraints on the solution for the thermal field. Fourth, the sensitivity of the estimated thermal field is examined with respect to variations of the constraints. Thermal maps are not very sensitive to variations of the constraints. Fifth, tomography is used to observe significant changes from month-to-month in the large-scale thermal field in the ocean, including the seasonal thermocline where week-to-week resolution can be obtained. In contrast, available point measurements appear to be insufficient for observing monthly changes in the large-scale thermal field in the ocean. These acoustic measures of weather and climate in the ocean cannot be verified with other data (e.g., satellites, point measurements) and thus provide an orthogonal perspective by which weather and climate may be observed and understood.

Published in: *Journal of the Acoustical Society of America*, 89(2):648-665, 1991.

Supported by: ONR Contract Nos.  
N00014-86-C-0358 and N00014-89-C-0179.

WHOI Contribution No. 7366.

## MEASURING WAVE DIRECTION USING UPWARD-LOOKING DOPPLER SONAR

*E. A. Terray, H. E. Krogstad, R. Cabrera,  
R. L. Gordon and A. Lohrmann*

There are a number of problems in coastal oceanography and engineering in which waves play a central role. These include sediment transport, the dispersal of contaminants air-sea interaction, wave agitation in harbors, and the hydrodynamic forces on offshore structures – both moored and fixed. As a result, there has been considerable recent interest in the use of acoustic Doppler techniques to measure wave direction. Several investigators have reported excellent results using sonars with horizontally-projected beams [1-3]. Such a configuration provides a dense set of spatial lags and permits measurement of the full frequency-wavenumber spectrum of the wave field.

Supported by: ONR Grant No. N00014-90-J-1464.

WHOI Contribution No. 7372.

## HIGH DATA RATE ACOUSTIC TELEMETRY FOR MOVING ROVS IN A FADING MULTIPATH SHALLOW WATER ENVIRONMENT

*Josko A. Catipovic and Lee E. Freitag*

A compact telemetry system for digital data telemetry at rates up to 10 kbits/sec over 1 to 10 km is presented. The system is designed for worst case ocean acoustic channel conditions, and operates in the presence of source/receiver motion, fading and multipath. In addition, the system incorporates spatial diversity by utilizing multiple hydrophones and data processing subsystems. This allows much more reliable operation under realistic circumstances where noise events and transducer masking are unavoidable. The result is a system specifically geared toward use at sea with a ROV. Preliminary dockside test results are presented to demonstrate the effectiveness of this multichannel system.

Published in: *Proceedings of the Symposium on Autonomous Underwater Vehicle Technology*, :296-303, 1990.

Supported by: ONR Contract No. N00014-86-K-0751.

WHOI Contribution No. 7386.

## NEW ESTIMATES OF SOUND-SPEED IN WATER

*John L. Spiesberger and Kurt Metzger*

Measured travel-times of acoustic pulses, propagated across a 3000 km section of the North Pacific, are inconsistent with travel-time predicted from the internationally accepted algorithm for the speed of sound. The sound-speed algorithm yields a speed which is too fast at oceanic pressures found below about 1 km depth. The speed of sound is of fundamental importance to acoustics and fluid dynamics.

In Press: *Journal of the Acoustical Society of America*.

Supported by: ONR Contract No. N00014-86-C-0358 and ONT Contract No. N00014-89-C-0179.

WHOI Contribution No. 7402.

## THE EFFECT OF SEASONAL TEMPERATURE FLUCTUATIONS IN THE WATER COLUMN ON SEDIMENT COMPRESSIONAL WAVE SPEED PROFILES IN SHALLOW WATER

*Subramaniam D. Rajan and George V. Frisk*

In shallow water areas, the temperature of the water column undergoes large fluctuations during the course of a year. In the Gulf of Mexico, for example, temperature fluctuations of as much as twelve degrees Centigrade have been observed. These seasonal variations in water column temperature affect the pore water temperature of the bottom sediments which, in turn, affects the compressional wave speed profile. Using Biot theory, it is shown that the sediment compressional wave speed varies approximately linearly with pore water temperature and this effect is, to first order, independent of the porosity and sediment type. It is also shown that the velocity ratio (ratio of sound speeds in water and the sediment at the sediment/water interface) is independent of the temperature but dependent on sediment type. These effects are demonstrated using two experimental measurements made at the same site in the Gulf of Mexico but during different seasons. In both cases, perturbative inversion techniques were used to infer the sound velocity profiles in the bottom. The differences between the two profiles fall within the error bounds predicted by linear inverse theory everywhere except the top 10 m of sediment, where the differences are attributed to the seasonal temperature fluctuation phenomenon. The experimental results suggest that the influence of the water column extends to greater depths than those predicted by theory.

Supported by: ONR Contract No.  
N00014-89-K-0055.

WHOI Contribution No. 7405.

## OPTICAL DISK RECORDERS IN ARCTIC INSTRUMENTATION

*Kenneth R. Peal and Kenneth E. Prada*

Arctic instrumentation designed for long-term emplacement presents a difficult challenge for traditional data recording methods. Optical disk recording offers permanent, high capacity storage with the promise of good performance at low temperatures. The results of the integration and testing of two optical disk recorders in an existing Arctic acquisition platform are reported. The platform can use either drive: one is a commercially available design, the other is a ruggedized unit. Problems discussed include temperature performance, power cycling, software operation in a PC environment, physical and electrical interfacing.

The results of freezer and cold chamber tests indicate that successful operation can be achieved in Arctic conditions.

Published in: *Oceans '90*, :550-555, 1990.

Supported by: ONR Contract No.  
N00014-86-C-0126.

WHOI Contribution No. 7411.

## TRANSIENT EDDY FORMATION AROUND HEADLANDS

*Richard P. Signell and W. Rockwell Geyer*

Eddies with length scales of 1-10 km are commonly observed in coastal waters and play an important role in the dispersion of water-borne materials. The generation and evolution of these eddies by oscillatory tidal flow around coastal headlands is investigated with analytical and numerical models. Using shallow water depth-averaged vorticity dynamics, eddies are shown to form when flow separation occurs near the tip of the headland, causing intense vorticity generated along the headland to be injected into the interior. An analytic boundary layer model demonstrates that flow separation occurs when the pressure gradient along the boundary switches from favoring (accelerating) to adverse (decelerating), and its occurrence depends principally on three parameters: the aspect ratio  $[b/a]$ , where  $b$  and  $a$  are characteristic width and length scales of the headland;  $[H/C_D a]$ , where  $H$  is the water depth,  $C_D$  is the depth-averaged drag coefficient; and  $[U_o/\sigma a]$ , where  $U_o$  and  $\sigma$  are the

magnitude and frequency of the far-field tidal flow. Simulations with a depth-averaged numerical model show a wide range of responses to changes in these parameters, including cases where no separation occurs, cases where only one eddy exists at a given time, and cases where bottom friction is weak enough that eddies produced during successive tidal cycles coexists, interacting strongly with each other. These simulations also demonstrate that in unsteady flow, a strong start-up vortex forms after the flow separates, leading to a much more intense patch of vorticity and stronger recirculation than found in steady flow.

In Press: *Journal of Geophysical Research*.

Supported by: NSF Grants OCE-87-11031 and  
OCE-89-17002.

WHOI Contribution No. 7412.

## FORTH INTERRUPT HANDLING

*Barrie B. Walden*

Microprocessor designers provide interrupt capabilities as a means for an external event to obtain the central processing unit's attention even while it is busy with another task. The power of this feature relies on a capable interrupt-handling routine. If multiple interrupt sources are available, the handler must be able to recognize and respond to each of them appropriately. This article provides a small set of Fourth words to simplify the use of interrupts and provides general insight into the process of working with interrupts. Code example for 6809 and 68CH11 microprocessors are provided.

In Press: *Forth Dimensions*.

Supported by: NSF grant OCE-86-16350.

WHOI Contribution No. 7428.

## DEVELOPMENT OF THE ARCTIC REMOTE AUTONOMOUS MEASUREMENT PLATFORM

*Kenneth R. Peal and Kenneth E. Prada*

Since the initial design of the Arctic Remote Autonomous Measurement Platform, several changes have been made to improve performance and reliability. The sea cable has been made more reliable and easier to deploy through the use of different connectors on the instruments and quick disconnect mechanical terminations. Several types of telemetry have been added.

Results of operational tests and field programs are reported using both helicopter and manual deployment methods.



Spectral and time series data from accelerometers and a hydrophone are recorded internally along with environmental sensor data. Selected data are available to the investigator in real time either via the ARGOS satellite system or high speed line-of-sight telemetry.

In situ recording capacity has been a major emphasis. Development of a reliable optical disk based system has involved laboratory and field testing to ensure satisfactory performance in Arctic field conditions.

Published in: *Oceans '90*, :556-561, 1990.

Supported by: ONR Contract No.  
N00014-86-C-0126.

WHOI Contribution No. 7429.

### **A STANDARDIZED ELECTRONIC PACKAGE FOR IMET SENSOR DEVELOPMENT**

*Geoff Allsup*

The World Ocean Circulation Experiment (WOCE) is directed at understanding the interrelationships of ocean circulation to climate. The IMET (Improved Meteorological Measurements from Ships and Buoys) program is charged with developing accurate and reliable methods of making meteorological measurements from ships and buoys. WOCE measurement requirements encompass the basic observables of air and sea surface temperature, wind velocity, barometric pressure, solar radiation, humidity, and precipitation. To integrate such a variety of new sensors easily and quickly, a standardized, core electronics module programmable in a common high level language is needed.

The IPACS standard electronics package (IMET Processor, A/D, Communications - Standard) is designed to meet these requirements. All IMET sensor development work is based on this 3 board core which integrates communications, A/D converter, 3 counter-timers, and parallel I/O. The Intel MCS-51 floating-point BASIC interpreter runs directly on the target IPACS hardware, allowing easy testing and debugging of sensor hardware and software by the individual designers. Standard IPACS support routines written in 'C' and assembler are easily added to the built-in BASIC interpreter, as are routines for specific sensor optimizations.

Published in: *Oceans '90*, :164-168, 1990.

Supported by: NSF grant OCE-8709614.

WHOI Contribution No. 7430.

### **MONITORING FISHBITE ACTIVITIES AND PROTECTING SYNTHETIC FIBER ROPES USED IN DEEP SEA MOORINGS**

*H. O. Berteaux, Bryce Prindle and  
Susan S. Putman*

Deep sea mooring lines are subjected to fishbite attacks which can and often do cause total failure of the mooring. The extent and the severity of this environmental problem has been recognized and means for reducing mooring degradation and material losses have been proposed (Berteaux and Prindle, 1987).

To better observe fishbite activities and determine the efficiency of protective jackets placed over wire and synthetic fiber ropes, a long term Experimental Surface Oceanographic Mooring (ESOM), supporting a number of rope specimens, was deployed offshore Bermuda in 1989 in 2900 meters of water depth. The mooring was recovered in March 1990. A careful inspection of the entire mooring revealed considerable fishbite occurrences, with exposed specimens showing a wide range of degradation. A description of the ESOM test platform and of the fishbite damages which occurred over the one year exposure *in situ* constitutes the first part of this paper.

As deep sea moorings proliferate, there is a need and a chance for the systematic acquisition of intelligent, authenticated and quantified fishbite information. Program managers and mooring designers could then use this valuable data base to assess the probability of fishbite attacks in a given geographical location and/or the efficiency of protective mooring materials. In the second part of the paper, the authors propose the creation of a Fishbite Research Group to pursue the systematic acquisition and the automated dissemination of worldwide fishbite information and the development of protective armors for mooring lines of smaller sizes.

Published in: *MTS '90*, 2:301-312, 1990.

Supported by: ONR Contract No. N00014-90-J-1719.

WHOI Contribution No. 7432.

### **AIR AND SEA TEMPERATURE MEASUREMENTS FOR IMET**

*Alan Hinton*

The World Ocean Circulation Experiment (WOCE) is directed at understanding ocean circulation and its interrelation to the climate. IMET (Improved Meteorological Measurements from Ships and Buoys) is a long lead time development effort to test and develop improved sensors for use in WOCE [1]. One of the objectives

of IMET is the development of an air and sea temperature sensor with high accuracy ( $\pm 0.005^\circ\text{C}$  accuracy,  $\pm 0.001^\circ\text{C}$  resolution) and long term stability (up to two year deployments) over the range of  $-40$  to  $+45^\circ\text{C}$ .

To meet this criteria a new programmable temperature sensor was developed that provides the high accuracy measurements and long term stability required for use in IMET. High accuracy is accomplished by making ratio-metric measurements of a PRT (Platinum Resistance Thermometer) with 18 bits of accuracy. The sensor makes use of the system calibration capability of a 20 bit ADC to adjust its output to compensate for system offsets. The temperature sensor uses an IPACS (IMET Processor, A/D, Communications Standard) system for its built in intelligence and I/O communications. IPACS is an electronics package developed at Woods Hole Oceanographic Institution for interfacing sensors to a standard electronics module.

Supported by: NSF grant OCE-8709614.

WHOI Contribution No. 7433.

### **ESTIMATES OF DIRECTIONAL SPECTRA FROM THE SURFACE ACOUSTIC SHEAR SENSOR (SASS)**

*Markku J. Santala and Albert J. Williams III*

The SASS (Surface Acoustic Shear Sensor) is a newly developed instrument platform designed to study upper ocean mixing processes. It consists of an array of six vector-measuring acoustic velocity sensors and a gyro stabilized motion sensing package mounted onto a moored surface-following float. Because SASS is instrumented with a motion sensing package, we are provided with an opportunity to discuss the effects of sensor motion on the estimation of directional wave spectra.

Published in: *Oceans '90*, 41-45, 1990.

Supported by: NSF grant OCE-87-16937.

WHOI Contribution No. 7434.

### **THE EFFECT OF UNSTEADY MOTION ON THE DRAG FORCES AND FLOW-INDUCED VIBRATIONS OF A LONG VERTICAL TOW CABLE**

*M. A. Grosenbaugh*

Drag coefficients and flow-induced vibrations of a long vertical tow cable are measured under steady and unsteady towing conditions. The steady-state drag coefficients range from 2.2 to 2.5. For unsteady towing conditions, the drag

coefficient was lower by as much as 40%, depending on the frequency content of the planar ship motion. For purely oscillatory motion, the drag coefficient decreased as the frequency of motion increased. The reduction in the drag coefficient may be related to the amplitude modulation of the flow-induced vibrations of the cable which are magnified during unsteady operations. When the surface ship changes speed, differences in the normal component of the velocity along the cable are present because of time delays in the response of the bottom of the cable to inputs at the top. The longer the cable, the greater are the delays. This creates large velocity gradients in the oncoming flow which are responsible for the intensification of the amplitude-modulation above the level that is observed during steady-state towing conditions. The overall effect of the amplitude modulation is a reduction in the hydrodynamic drag forces.

Supported by: ONR grant N00014-87-G-0111.

WHOI Contribution No. 7448.

### **MODELLING THE DYNAMICS OF A DEEPLY-TOWED UNDERWATER VEHICLE SYSTEM**

*Franz S. Hover, Michael S. Triantafyllou and Mark A. Grosenbaugh*

Towed underwater vehicle systems are influenced significantly by the presence of the cable, especially in deep water where cable drag and inertial effects are as important as, or even more important than, the drag and mass of the vehicle itself. This paper describes a numerical technique for simulating the dynamics of such a system, based on simplifications of the governing equations which retain the relevant motions and the accuracy of the solution. The ARGO/JASON system at the Woods Hole Oceanographic Institution is used as a case example; verification of some numerical predictions is shown, using full-scale sea data, and other illustrations are given.

Supported by: ONR Contract N00014-87-J-1111, NSF Contract OCE-8511431 and MIT Sea Grant Project Ru-21.

WHOI Contribution No. 7451.

### **BANDWIDTH-EFFICIENT TRELLIS-CODED MODULATION FOR PHASE RANDOM RAYLEIGH FADING CHANNELS**

*Josko A. Catipovic*

A bandwidth efficient modulation method for the incoherently demodulated Rayleigh fading

channel is analyzed and implementation results reported. The method is based on partitioning binary expurgated modulation (BEXPERM) codes into subsets with desirable minimum Hamming distance properties. The subsets are comparable to signal constellation subsets used for trellis coded modulation (TCM) over phase-coherent channels. A convolution code is used to generate a subset mapping rule; its free distance is chosen to match the Hamming distance distribution within a subset to produce an overall code with error correcting capabilities comparable to those of a single BEXPERM subset. The resulting modulation method is more bandwidth efficient than MFSK while exhibiting significant coding gain. BEXPERM allows 14 kbit/sec data rates over the 2 - 10 km shallow water fully saturated ocean acoustic channel. This data rate represents a 40% increase over that currently achievable for this type of conditions.

WHOI Contribution No. 7452.

# ALGORITHMS FOR JOINT CHANNEL ESTIMATION AND DATA RECOVERY - APPLICATION TO EQUALIZATION IN UNDERWATER COMMUNICATIONS

*Meir Feder and Josko A. Catipovic*

One of the main obstacles to reliable underwater acoustic communications is the relatively complex and unstable behavior of the ocean channel. Channel equalization method, that can estimate and track this complex and rapidly varying ocean response, may lead to reliable data communications at high rates that utilize fully the available bandwidth. Unfortunately, standard equalization techniques fail in this environment. In this paper we derive methods for joint ocean channel estimation and data recovery, using optimal, Maximum Likelihood (ML), estimation criterion. The resulting ML problems may be complex; thus, we will use iterative algorithms, e.g., the Expectation-Maximization (EM) algorithm. The different methods correspond to different assumptions about the ocean channel. The theoretical derivation of these methods, as well as preliminary results on a simulated ocean data experiments are presented.

WHOI Contribution No. 7453.

## THE NEED FOR GLOBAL OCEAN WAVE SPECTRAL INFORMATION

*Hans C. Graber, Vincent J. Cardone and Mark A. Donelan*

Within the last decade, scientists have come to view world climate variability as a response to the coupled atmosphere-ocean-cryosphere system. In such a system the air-sea interface is treated as a rough porous boundary and little recognition has been given to the ubiquitous ocean surface waves and the central role they play in many processes occurring at the air-water interface, in the deep ocean, over the continental shelves and in coastal waters. A good knowledge of the sea state is required to understand vertical mixing of mass, momentum and heat within the upper layers of the ocean, exchange and transfer processes between the atmosphere and ocean through the surface affecting winds stress, heat and mass transfer and ultimately climate response, the radar reflectivity to small-scale waves and the dynamics of coastal waters. Many studies of these processes have been carried out, though many of them suffer from an inadequate description of the wave field. Figure 1 illustrates the role of surface waves in atmospheric and oceanic processes and how satellite remote sensing could provide wave information on a global scale.

Following the innovative work of Pierson et al. (1966), several numerical models using the energy balance equation for the ocean wave spectrum, were developed to describe the evolution of the wave field under general meteorological conditions. When applied in the hindcast mode, each model performed well against observations. The generally poorer performance of wave models in the forecast mode was attributed by model proprietors to poor wind forecasts. However, any implication that wave modelling had approached something like a state of perfection was abruptly discredited by the results of the Sea Wave Modeling Project (SWAMP) intercomparison of wave models against simulated wind data. Almost an order of magnitude difference in the wave growth in even the simplest situations was noted. Such differences appeared to stem as much from a disagreement in deriving the correct growth rate from observations, as from deficiencies in knowledge of the underlying physics of wave growth and dissipation.

The wave modelling community continues to collaborate to a remarkable degree since SWAMP, and have collectively developed and tested an advanced third-generation wave model (3B-WAM, WAMDI-Group, 1989.) This model was developed not primarily to improve wave forecasting, but rather to serve as a critical part of an integrated system for the assimilation of in-situ and remotely

sensed wind and wave information, for the improvement of the initial state (especially surface wind fields) for numerical weather prediction (NWP) systems, and for accurate specification of surface stress and other air-sea fluxes for use in ocean models and coupled atmosphere-ocean climate models.

In this paper we will rationalize the increasingly recognized need to describe the global wave field routinely, give the general structure of the integrated NWP/wave model system which appears to be emerging, and indicate the new data and research which will be required. Much of this article is based on a status report by Graber et al. (1988); however, due to the quickly changing subject, some important new results have been included here. We begin with a brief review of the role of wave information in various processes.

Supported by: NASA Contract No. NAGW-1024.

WHOI Contribution No. 7454.

### **SEQUENTIAL ALGORITHMS FOR PARAMETER ESTIMATION BASED ON THE KULLBACK-LEIBLER INFORMATION MEASURE**

*Ehud Weinstein, Meir Feder and  
Alan V. Oppenheim*

Methods of stochastic approximation are used to convert iterative algorithms for maximizing the Kullback-Leibler information measure into sequential algorithms. Special attention is given to the case of incomplete data, and several algorithms are presented to deal with situations of this kind. The application of these algorithms to the identification of finite impulse response (FIR) systems is considered. Issues such as convergence properties of the proposed algorithms, choice of initial conditions, the limit distribution, and the associated regularity conditions are beyond the scope of this correspondence. However, the existing literature on stochastic approximation, together with the ideas presented in this paper should provide the starting point for such analyses.

Supported by: ONR Contract N00014-85-K-0272.

WHOI Contribution No. 7455.

### **ASYMMETRIC BEHAVIOR OF AN OCEANIC BOUNDARY LAYER ABOVE A SLOPING BOTTOM**

*J. H. Trowbridge and S. J. Lentz*

The effects of stratification, planetary rotation and sloping bottom combine to produce an

asymmetric response in which the characteristics of an oceanic bottom boundary layer depend on the direction, in addition to the magnitude, of the along-isobath velocity in the inviscid interior. The asymmetric response, which has been observed previously in oceanic measurements and numerical simulations, is examined through theoretical analysis of the low-frequency behavior of the boundary layer, under idealized conditions in which the motion begins from rest, the flow is uniform in the along-isobath and cross-isobath directions, and the water column is initially uniformly stratified. The first part of the analysis addresses the initial evolution of the boundary layer, and is based on an integrated model, in which the bottom stress is determined from a quadratic drag law and the height of the boundary layer is determined from a Pollard-Rhines-Thompson mixing criterion. The second part of the analysis addresses the behavior of the boundary layer at large times, focusing in particular on the case of down-slope Ekman transport, and is based on a model in which the cross-isobath momentum balance is inviscid, and a simple density structure is maintained by the combined effects of cross-isobath advection and vertical mixing. The models produce results in good agreement with previous numerical simulations. In addition, the models reproduce the asymmetric behavior apparent in observations, in which the boundary layer is thicker during flows favoring down-slope Ekman transport than it is during comparably strong flows favoring up-slope Ekman transport. The asymmetric behavior is caused primarily by cross-isobath Ekman transport of buoyancy, which increases or decreases the density in the boundary layer relative to the density in the interior, depending on the direction of the interior velocity.

In Press: *Journal of Physical Oceanography*.

Supported by: ONR grant N00014-89-J-1067 and grant N00014-89-J-1074.

WHOI Contribution No. 7456.

### **A REASSESSMENT OF THE ROLE OF TIDAL DISPERSION IN ESTUARIES AND BAYS**

*W. Rockwell Geyer and Richard P. Signell*

The role of tidal dispersion is reassessed, based on a consideration of the relevant physical mechanisms, particularly those elucidated by numerical simulations of tide-induced dispersion. It appears that the principal influence of tidal currents on dispersion occurs at length scales of the tidal excursion and smaller; thus the effectiveness of tidal dispersion depends on the relative scale of the tidal excursion to the size of the estuary or

bay. In many estuaries, where the tidal excursion length is small in comparison to the overall scale of the estuary, tidal processes alone cannot account for observed dispersion rates. Tidal dispersion is most pronounced in regions of abrupt topographic changes such as headlands and inlets, where flow separation occurs. The strong strain rate in the region of flow separation tends to stretch patches of fluid into long filaments, which are subsequently rolled up and distorted by the transient eddy field. The dispersion process accomplished by the tides varies strongly as a function of position and tidal phase and thus does not lend itself to parameterization by an eddy diffusion coefficient.

Supported by: NSF Grants OCE-87-11031 and OCE-89-17002.

WHOI Contribution No. 7457.

### SOUND SCATTERING BY DEFORMED WEDGES OF FINITE LENGTH

*Dezhang Chu and Timothy K. Stanton*

An approximate solution is derived describing the scattering of sound by wedges of finite length and deformed properties such as a curved apex and variable wedge angle. The analysis is based on the methods presented in an earlier article by Stanton [T.K. Stanton, J. Acoust. Soc. Am. 86, 691-705 (1989)] where the scattering of sound by deformed finite length cylinders was described. In an approach similar to that article, the solution to the deformed wedge is derived by first calculating the volume flow per unit length of the scattered field due to an infinitely long straight (undeformed) wedge and then integrating that solution over a finite distance while allowing the physical properties of the wedge to vary. As in the deformed cylinder formulation, the properties must vary slowly. Because the solution is based on the infinitely long wedge, the solution is restricted to angles of incidence and reception normal or near normal to the tangents of the apex (i.e. and effects are neglected). Explicit examples of the solution are given for the straight finite length wedge and uniformly bent finite wedge (using the geometric theory of diffraction (infinite wedge) formulation as a basis for calculating the volume flow per unit length). The scattered pressure is shown to spread spherically in these cases in contrast to the cylindrical spreading exhibited by wedges of infinite length. Dependence of the scattered field upon the length and orientation for the straight finite wedge and radius of curvature for the bent wedge are also demonstrated. The importance these results have in describing the scattering by naturally occurring rough surfaces that have deformed finite length features is discussed.

Supported by: WHOI Post Doctoral Fellowship.

WHOI Contribution No. 7459.

### THREE-DIMENSIONAL STOCHASTIC MODELING USING SONAR SENSING FOR UNDERSEA ROBOTICS

*W. Kenneth Stewart*

We describe an approach to the construction of three-dimensional stochastic models for intelligent systems exploring an underwater environment. The important characteristics shared by such applications are: real-time constraints; unstructured, three-dimensional terrain; high-bandwidth sensors providing redundant, overlapping coverage; lack of prior knowledge about the environment; and inherent inaccuracy or ambiguity in sensing and interpretation. The models are cast as three-dimensional spatial decompositions of stochastic feature vectors. Such models serve as intermediate descriptions that decouple low-level, high-bandwidth sensing from the higher-level, more asynchronous processes that extract information.

A numerical approach to incorporating new sensor information—*stochastic backprojection*—is derived from an incremental adaptation of the summation method for image reconstruction. Error and ambiguity are accounted for by blurring a spatial projection of remote-sensor data before combining them stochastically with the model. By exploiting the redundancy in high-bandwidth sensing, model certainty and resolution are enhanced as more data accumulate. In the case of a three-dimensional profiling sonar, the model converges to a “fuzzy” surface distribution from which a deterministic surface map is extracted. Computer simulations demonstrate the properties of stochastic backprojection and stochastic models.

Supported by: Sea Grant at MIT.

WHOI Contribution No. 7460.

### HYDRODYNAMIC FACILITATION OF GREGARIOUS SETTLEMENT OF A REEF-BUILDING TUBE WORM

*Joseph R. Pawlik, Cheryl Ann Butman, and Victoria R. Starczak*

Substrate-selection experiments testing the effects of both hydrodynamical processes and chemical cues were conducted with larvae of the reef-building polychaete *Phragmatopoma lapidosa californica* and larval mimics (plastic spheres). Previously still-water, single-substrate experiments demonstrated that larvae of this species settle

upon contact with specific free fatty acids (FFAs) isolated from the sand tubes of adult worms. In recirculating flume experiments, larvae were given a choice of five treatments, including two inductive substrates, arranged in a sediment array in a Latin-square design. Two flows were tested, with boundary shear velocities of 0.81 cm/s (fast) and 0.34 cm/s (slow), simulating typical tidal flows that are encountered by shallow, subtidal populations. The mimics fell to the bottom in both flow regimes but were transported as bedload only in fast flow. Larvae preferentially metamorphosed on tube sand or on sand treated with an isolated inductive compound (palmitoleic acid) in both fast and slow flow. Delivery to the array of both larvae and mimics was significantly higher in fast flow where larvae swam to the bottom and, like the mimics, tumbled as bedload. In slow flow, many larvae were observed to swim in the water column or near the surface. While physical processes are largely responsible for the delivery of larvae to potential habitats, larval behavior in response to flow conditions may facilitate substrate contact. The initiation of metamorphosis is ultimately a response to chemical cues.

Published in: *Science*, 251:421-424, 1991.

Supported by: NSF OCE88-12651, ONR N00014-89-J-1112, and Killam Memorial Postdoctoral Fellowship.

WHOI Contribution No. 7466.

### BASIN-SCALE ACOUSTIC TOMOGRAPHY: OBSERVATIONS OF BAROCLINIC TIDES GENERATED BY SEAMOUNTS

*Robert H. Headrick, John L. Spiesberger, and Paul J. Bushong*

Travel-times of acoustic signals were measured between a bottom-mounted source near Oahu and four bottom-mounted receivers located near Washington, Oregon, and California in 1988 and 1989. This paper discusses the observed tidal signals. At three out of four receivers, observed travel-times at  $M2$  and  $S2$  periods agree with predictions from a barotropic tide model to within  $\pm 30^\circ$  in phase and a factor of 1.6 in amplitude. The discrepancy at the fourth receiver can be removed by including the effects of phase-locked baroclinic tides generated by seamounts.

Our estimates of barotropic  $M2$  tidal dissipation by seamounts vary between  $2 \times 10^{16}$  and  $1 \times 10^{18}$  ergs $^{-1}$ . The variation by two orders of magnitude is due to uncertainties in the numbers and sizes of seamounts. The larger dissipation ( $1 \times 10^{18}$  ergs $^{-1}$ ) is the same order as previous estimates and amounts to 4 percent of the total dissipation at  $M2$ .

Supported by: ONR Contract N00014-86-C-0358 and ONT Contract N00014-89-C-0179.

WHOI Contribution No. 7473.

### A CHEBYCHEV TYPE INEQUALITY AND ITS APPLICATIONS

*Meir Feder*

Let  $X$  be a continuous/discrete random variable defined over the sample space,  $\Omega$ , and let  $p(x)$  be its probability density/mass function. Let  $q(x)$  be any other measurable integrable function defined over the sample space  $\Omega$ . Normalize  $q(x)$  so that  $\int_{\Omega} q(x)dx \leq 1$ , (e.g.  $q(x)$  can be an arbitrary probability density/mass function). Let  $\phi : (0, \infty) \rightarrow R^1$  be a measurable non-decreasing function. We prove that,

$$Pr \{ \phi(q(x)) \geq \phi(\alpha p(x)) \} \leq \frac{1}{\alpha}, \quad \alpha > 0$$

This inequality is found useful in analyzing the performance of data compression algorithms and sequential gambling schemes. The application of this inequality to hypothesis testing is briefly discussed.

WHOI Contribution No. 7483.

### DRAW FORCES AND FLOW-INDUCED VIBRATIONS OF A LONG VERTICAL TOW CABLE - PART II: UNSTEADY TOWING CONDITIONS

*M. A. Grosenbaugh, D. R. Yoerger, F. S. Hover, and M. S. Triantafyllou*

Full-scale experimental data on the dynamics and flow-induced vibrations of a long vertical tow cable are analyzed. The data were measured while the surface ship was going through a series of starting, stopping, and backing maneuvers. The results of the study show that the amplitude of the flow-induced vibrations of the cable is strongly modulated during maneuvering operations. Maneuvering creates situations where different sections of the cable are translating at different speeds. This causes an "artificial" shear current which at times is severe, depending on the difference in speed between the top and bottom of the cable. The artificial shear is responsible for the intensification of the amplitude-modulation above the level that is observed during steady-state towing conditions. The overall effect of the amplitude modulation is a reduction in the hydrodynamic drag forces. It is shown that the drag coefficient measured during maneuvering operations is lower than the steady-state value.

Supported by: NSF Grant OCE-8511431, ONR Grant N00014-87-G-0111, NSF Grant EID-8818653 and ONR Grant N00014-88-K-0765.

WHOI Contribution No. 7484.

## ROBUST CONTROL OF SURFACE-POSITIONED TETHERED UNDERWATER VEHICLE

*Michael S. Triantafyllou and Mark A. Grosenbaugh*

Tethered underwater vehicles that are positioned by controlling the motion of the surface-support ship are a reliable and economic means for continuous ocean exploration. However, the tether introduces long time delays (up to several minutes) which make control action difficult. Presented in this paper is a robust control scheme for controlling systems with time delays. The method is based on the Smith controller and the LQG/LTR methodology. An example, using full-scale data from the Woods Hole Oceanographic Institution's vehicle ARGO, demonstrates the developments. The methodology presented herein is applicable to other systems that exhibit time delays including autonomous vehicles that are controlled through an acoustic link.

In Press: *IEEE Journal of Ocean Engineering*.

Supported by: NSF Grant EID-8818653 and Dean at MIT support for class curriculum development.

WHOI Contribution No. 7485.

## SOUND SCATTERING BY RANDOMLY ROUGH ELONGATED OBJECTS. I. MEANS OF SCATTERED FIELD

*T. K. Stanton*

By use of the recently published deformed cylinder formulation [T.K. Stanton, J. Acoust. Soc. Am. 86, 691-705, (1989)], the scattered field due to randomly rough elongated dense elastic objects is derived. The radius of the deformed cylinder is allowed to vary with respect to position along the lengthwise axis resulting in a one-dimensional roughness. Explicit expressions are derived describing both the mean and mean square scattered field for the rough straight finite length cylinder (broadside incidence) for both  $ka \ll 1$  and  $ka \gg 1$  ( $k$  is the acoustic wavenumber and  $a$  is the radius) while only the mean is calculated for the prolate spheroid, uniformly bent finite cylinder, and infinitely long cylinder for  $ka \gg 1$  (again, all broadside incidence). Both types of means involve averages across an ensemble of statistically independent rough objects. The modal-series-based solution is used in the  $ka \ll 1$

case as the modal solution simplifies to the sum of two terms (monopole and dipole-like terms). For  $ka \gg 1$ , the modal solution does not converge very fast and a "ray" solution is therefore used in its place which involves a recently published form of the Sommerfeld Watson transformed solution where the coupling coefficients of the surface elastic wave components of the field are in simple approximate analytical form [P.L. Marston, J. Acoust. Soc. Am. 83, 25-37 (1988)]. All  $ka \gg 1$  results in this work demonstrate attenuation of the "specular" (echo from front face) and Rayleigh surface elastic wave components of the scattered field due to roughness. The attenuation of the mean specular component is  $\exp[-2k^2\sigma^2]$  (where  $\sigma$  is the rms roughness) which is also equal to the well known result describing attenuation of the specular wave from rough planar interfaces [C. Eckart, J. Acoust. Soc. Am. 25, 566-570 (1953)]. The attenuation of the Rayleigh wave is  $\exp\{-\frac{1}{2}k^2\sigma^2[(c/c_R)(2\pi - 2\theta_R) - 2\cos\theta_R + 2\pi mc/c_R]^2\}$  where  $c$  and  $c_R$  are the phase velocities of the surrounding medium and Rayleigh wave, respectively,  $\theta_R$  is the local "launching" angle of the Rayleigh wave, and  $m$  is related to the number of times the Rayleigh wave has circumnavigated the object ( $m=0$  is first echo,  $m=1$  is second, etc.). The attenuation of the Rayleigh wave is shown in the preceding equation to depend on the number of times it has circumnavigated the object resulting in a loss of the higher "m" terms in excess to that due to radiation damping alone. At high  $ka$ , it is shown that for rough tungsten carbide cylinders, the  $m=0$  Rayleigh wave dominates the scattering while the specular and  $m > 0$  waves are attenuated at greater rates. The analytical results are compared with 1) numerical simulations that cover all ranges of  $ka$  and 2) the scattering by rough planar interfaces with distinct differences arising because of effects specific to volumetric scattering.

Supported by: ONR Grant N00014-89-J-1729 and Grant N00014-90-J-1804.

WHOI Contribution No. 7496.

## ACOUSTIC ESTIMATES OF ANTARCTIC KRILL

*Charles H. Greene, Timothy K. Stanton,  
Peter H. Wiebe, and Sam McClatchie*

Everson *et al.*<sup>1</sup> discussed the implications of new measurements of target strength for estimating the abundance of krill in the Southern Ocean. Their conclusions were first, that previously used equations<sup>2</sup> relating target strength to physical size of these animals were greatly in error and, second, that the use of these equations

has resulted in gross underestimates of krill abundance in the Southern Ocean. As krill provides the basis of a large fishery and is the main component of the diet of many marine predators, accurate estimates are essential for management of this resource. We have collected data covering a broad size range of crustacean zooplankton and micronekton, and verify and elaborate the findings of Everson *et al.* We present new target-strength-by-size relationships over the full size range of krill at the acoustical frequencies commonly used in field studies<sup>3</sup>.

In Press: *Nature*.

Supported by: ONR Grant N00014-89-J-1729 and the American Antarctic Marine Living Resources Program.

WHOI Contribution No. 7497.

### FRESNEL ZONE EFFECTS IN THE SCATTERING OF SOUND BY INTERMEDIATE LENGTH CYLINDERS

*Daniel T. DiPerna and Timothy K. Stanton*

The backscattering behavior of straight cylinders is examined whose "intermediate" lengths are comparable to the diameter of the first Fresnel zone of the source/receiver pair. This "transitional region" is complex in nature as the cylinders occupy a finite number of Fresnel zones ( $\approx 1-5$ ) and, in general, can only be described numerically. The scattering is described by first adapting the deformed cylinder formulation [T.K. Stanton, J. Acoust. Soc. Am. 86, 691-705 (1989)] to the point-source/point-receiver combination. Numerically evaluating this expression showed the scattering characteristics to be dominated by Fresnel zone effects-oscillations in the backscatter versus length curve caused by constructive and destructive wave interferences due to phase shifts from contributions along the cylinder axis. An experiment was performed which involved measurement of backscatter versus cylinder length, and there is reasonable agreement between the results and the trend as predicted by the approximate theory.

In Press: *Journal of the Acoustical Society of America*.

Supported by: ONR Grant N00014-89-J-1729.  
WHOI Contribution No. 7498.

### IN SITU EVALUATION OF OCEAN PROFILING SENSORS

*Marinna A. Martini, James D. Irish,  
Albert M. Bradley, and Alan R. Duester*

The performance of ocean profilers operating

under real world conditions is difficult to evaluate. Profiles made simultaneously with two different instruments provide a unique opportunity to examine sensor performance under normal operating conditions. Comparisons are presented between data sets obtained with the following instruments: a UNH profiler, a Woods Hole Oceanographic Institution free falling hydrographic profiler, the Flying Fish, an EG&G Neil Brown Instrument Systems Mark III CTD and a Sea Bird Electronics SEACAT profiler. The comparisons raise issues of accuracy which must be addressed as efforts increase to combine hydrographic data sets from a variety sources to support research goals.

Published in: *MTS '90*, 338-343, 1990.

Supported by: NSF Grant OCE-8716018.

WHOI Contribution No. 7528.

### A DRAG TENSOR FORMULATION FOR MODELLING BOTTOM STRESS IN WIND-DRIVEN DEPTH-AVERAGED FLOWS

*Harry L. Jenter and Ole Secher Madsen*

The relationship between depth-averaged velocity and bottom stress for wind-driven flow in unstratified coastal waters is examined. Emphasis is placed on the adequacy of traditional linear and quadratic drag laws in comparison with a  $2\frac{1}{2}$ -D model. The  $2\frac{1}{2}$ -D model uses a simplified 1-D depth-resolving model (DRM) to provide a relationship between the depth-averaged velocity and bottom stress at each grid point of a depth-averaged model (DAM). Bottom stress information is passed from the DRM and DAM in the form of a drag tensor with two components: one which scales and one which rotates the velocity. This eliminates problems caused by traditional drag laws requiring the flow and bottom stress to be colinear. In addition, the drag tensor field is updated periodically so that the relationship between the velocity and bottom stress is time-dependent. Simplifications in the  $2\frac{1}{2}$ -D model restrict the time-scale of resolvable processes to be much longer than the vertical turbulent diffusion timescale.

The  $2\frac{1}{2}$ -D model is applied in four coastal scenarios: spin-up from rest of a flat shelf with a straight coastline subject to a constant wind stress, spin-up from rest of a linearly sloping shelf with a straight coastline subject to a constant wind stress, spin-up from rest of a linearly sloping shelf with a sinusoidal coastline subject to a constant wind stress, and the same geometry as the second scenario, but subject to a wind stress that is constant in space and rotating in time. The four scenarios reveal that choice of drag law affects



spin-up times and phase relationships significantly in typical coastal situations. In the scenarios examined, the  $2\frac{1}{2}$ -D model responds more quickly than traditional models. Likewise, steady-state responses are affected. The most important result is that failure to account for rotation in the drag law leads often to poor resolution of cross-shore bottom stress. Directly, this implies very poor prediction of such important processes as cross-shore sediment transport. Indirectly, the cross-shore momentum balance is altered causing the cross-shore pressure gradient to compensate, which, in turn, can cause significantly different predictions of coastal sea levels.

Supported by: ONR N00014-86-K-0061.

WHOI Contribution No. 7532.

### GENERATING EIGENRAY TUBES FROM TWO SOLUTIONS OF THE WAVE EQUATION

*James B. Bowlin*

A method is presented for calculating the paths taken by sound between a source and receiver. These paths, which we call eigenray tubes, are obtained from two solutions of the wave equation at finite frequency, one propagated from the source and the other propagated from the receiver. The results are not restricted to the high frequency limit as is the case with classical ray traces. This generalization of classical ray tracing could be an important new tool in acoustic tomography. A numerical example is included with plots of eleven eigenray tubes.

In Press: *The Journal of the Acoustical Society of America*.

Supported by: ONR Contract No.  
N00014-86-C-0358.

WHOI Contribution No. 7536.

### A NEW ALGORITHM FOR SOUND SPEED IN WATER

*John L. Spiesberger and Kurt Metzger*

Travel-times of acoustic pulses across a 3000 km section in the northeast Pacific are used to estimate an algorithm for the speed of sound in water. Our algorithm, derived from tomographic techniques, is inconsistent both with the international standard algorithm derived by Chen and Millero ["Speed of sound in seawater at high pressures", *J. Acoust. Soc. Am.* 62, 1129-1135 (1977)] and with the algorithm of Del Grosso ["New equation for the speed of sound in natural

waters (with comparisons to other equations)," *J. Acoust. Soc. Am.* 56, 1084-1091 (1974)]. Both previous algorithms were derived from laboratory experiments. The additive correction,  $\delta c$  ( $\text{m} \cdot \text{s}^{-1}$ ), to Del Grosso's sound speeds between 0 and 4 km depth is  $\delta c(p) = -0.1041898138 \times 10^{-2}p + 0.2101429060 \times 10^{-4}p^2 - 0.1414115788 \times 10^{-6}p^3 + 0.3178122360 \times 10^{-9}p^4 - 0.2178060243 \times 10^{-12}p^5$  with  $p$  being pressure-gauge units in  $\text{kg} \cdot \text{cm}^{-2}$ . The rms error of  $\delta c$  is about  $0.05 \text{ m} \cdot \text{s}^{-1}$  and  $0.1 \text{ m} \cdot \text{s}^{-1}$  between the intervals of 0 to 2 km and 2 to 4 km respectively. At about 3 km depth, sound speeds predicted by Chen and Millero and Del Grosso are about  $0.7 \text{ m} \cdot \text{s}^{-1}$  and  $0.2 \text{ m} \cdot \text{s}^{-1}$  too fast respectively. An accurate algorithm for sound-speed is of fundamental importance in acoustics and in tomographic measures of ocean temperature.

In Press: *Journal of the Acoustical Society of America*.

Supported by: ONR Contract No. N00014-86-C-0358  
and ONR Contract No. N00014-90-C-0098.

WHOI Contribution No. 7537.

### DETERMINATION OF THE SEDIMENT SHEAR SPEED PROFILES FROM SH WAVE PHASE AND GROUP VELOCITY DISPERSION DATA

*Subramaniam D. Rajan and Cinthia S. Howitt*

In modeling ocean sediments it is common to assume that the medium is a fluid. This implies that the shear properties of the sediment material can be neglected. While this approximation is valid at higher frequencies, at lower frequencies (below say 50 Hz) shear properties of the sediment become important. It is therefore necessary to be able to determine the shear characteristics of the sediments. We present methods for extracting the density and shear speed profiles in the sediment material from the phase velocity and group velocity dispersion relationships of SH waves. The performance of this approach is studied using noise free and noisy synthetic data. The method is then applied to group velocity dispersion relationship obtained from field data.

Supported by: ONR N00014-89-K-0055.

WHOI Contribution No. 7542.

### EFFECTS OF STRATIFICATION BY SUSPENDED SEDIMENTS ON TURBULENT SHEAR FLOWS

*Catherine Villaret and J. H. Trowbridge*

Sediments suspended in turbulent flows of water over plane beds are known to influence the

structure of the flows by which they are carried. Past attempts to model this effect have been based almost exclusively on a theoretical framework in which the dense solid particles stratify the flow and have an influence analogous to that of a downward heat flux in the stably stratified atmospheric surface layer. We compare results from a model based on this theoretical framework with laboratory measurements of ensemble-averaged velocity and ensemble-averaged particle concentration obtained by previous investigators, in order to test the applicability of the theoretical approach to dilute suspensions of sand in turbulent flows of water. We find that the stratification effect can be observed qualitatively in measured velocity profiles, except in one series of experiments in which systematic measurement errors may have obscured the effect. Estimates of model constants based on measured velocity profiles are, overall, roughly consistent with expectations based on measurements in thermally stratified flows, although there is substantial variability in individual profiles. Some of this variability is explainable as a consequence of existence of a parameter range in which stratification effects are too weak to be detected accurately, other variability is explainable as a consequence of approximations in the model, and still other variability is possibly a consequence of weak dependence of model constants on sediment grain size, which was not expected based on the theoretical development. The stratification effect is not observed in individual particle concentration profiles, but must instead be observed in experiments in which the flow conditions and particle properties are held fixed while the particle load is increased.

Supported by: Sea Grant R/0-5 and ONR Grant No. N00014-89-J-1067.

WHOI Contribution No. 7544.

### THE AUTONOMOUS BENTHIC EXPLORER (ABE): A DEEP OCEAN AUV FOR SCIENTIFIC SEAFLOOR SURVEY

*Dana R. Yoerger, Albert M. Bradley, and  
Barrie B. Walden*

The Autonomous Benthic Explorer (ABE) is a vehicle that will perform scientific survey of the seafloor over an extended period of time without a support vessel. The vehicle has been designed to complement the existing manned submersible and remotely operated vehicle systems available to the scientific community. A primary application of ABE will be repeated surveys of hydrothermal vent areas at depths of 4000 meters. Specifically, ABE will be able to provide data concerning the

long term variability of hydrothermal vents, a task that existing assets cannot accomplish. This paper discusses the motivation for ABE, outlines the specifications and basic design approach, and describes critical technical problems. Initial and future ABE mission scenarios are also discussed.

Supported by: NSF Grant OCE 8820227.

WHOI Contribution No. 7569.

### INTERPRETING SHEAR AND STRAIN FINE STRUCTURE FROM A NEUTRALLY BUOYANT FLOAT

*Eric Kunze, Melbourne G. Briscoe, and  
A. J. Williams III*

The 1-5 m shear and strain spectra from a neutrally buoyant float reveal more strain in the near-inertial band ( $f < \omega < 2f \sim M_2$ ) and more shear in the continuum internal wave band ( $2f < \omega < N$ ) than can be accounted for by linear internal gravity waves. The shape of the 1-m shear spectrum can be reproduced by vertically advecting low-frequency  $\sim 2$ -m wavelength fine structure past the float sensors with the observed displacement time series. Advection smears the encounter frequency across the internal wave band, aliasing and Doppler shifting some low intrinsic frequency variance into the continuum band and some high intrinsic frequency wave variance into the near-inertial band. Past observations of the excess shear variance at high frequencies led to speculation that it may be stratified two-dimensional turbulence having the same spatial scales as internal waves but carrying fine-scale potential vorticity anomalies (Holloway, 1983). The high shear relative to strain ( $V_z/(\bar{N}\zeta_z) = 2.2$ ) and high Froude number ( $V_z/\bar{N} = 1.23$ ) would restrict stratified two-dimensional turbulence to having average relative vorticity more negative than  $-f$ . This limitation makes a stratified turbulence explanation for the fine structure impossible. On the other hand, the shear and strain characteristics are consistent with the Garrett and Munk (1979) internal wave model and could easily be explained by near-inertial internal waves. There may be no efficient means of generating potential vorticity anomalies away from boundaries.

Published in: *Journal of Geophysical Research*, 95(C10):18,111-18,125, 1990.

Supported by: ONR Project N00014-85-C-0001, OCE 86-20101 and "Mesoscale-to-Mixing" University Research Initiative.

WHOI Contribution No. 7579.

**VERTICAL RELATIONSHIP OF  
ACOUSTIC BACKSCATTER TO  
TEMPERATURE STRUCTURE AT THE  
WESTERN EDGE OF THE GULF  
STREAM USING OPTIMAL LEAST  
SQUARES FILTERING**

*J. Michael Jech, C. S. Clay, J. J. Magnuson and  
T. K. Stanton*

A quantitative approach, optimal least squares filtering, was used to determine the linear correlation between the physical and biological structure at the western edge of the Gulf Stream. Coordinated temperature and acoustic backscatter data (70 and 120 kHz) were obtained 105 km northeast of Cape Hatteras along a transect perpendicular to the Gulf Stream front. We determined temperature, vertical temperature gradient and diurnal effects on the vertical distribution of biological sound scatterers in the top 200 m of a Gulf Stream frontal region. Our data show that temperature is a better predictor of acoustic scattering than is temperature gradient at the meso to finescale. Diurnal differences in the predictability of scattering suggest other abiotic and biotic factors influence nekton and zooplankton distribution. This technique is new in its application to marine ecology and we feel that optimal filtering may be a powerful tool in applying sonar to aquatic ecology.

In Press: *Journal of Geophysical Research*.

Supported by: ONR Grant N00014-89-J-1729.

WHOI Contribution No. 7580.

**PRECISE CONTROL OF UNDERWATER  
ROBOTS: WHY AND HOW**

*Dana R. Yoerger*

This paper addresses two issues that are fundamental to the evolution of today's Remotely Operated Vehicles (ROV's) into teleoperated or autonomous robots. First, the paper addresses how precise control makes an underwater vehicle more effective as a sensing or work platform. These points are illustrated with results from sonar and optical surveys of two ships from the War of 1812, the HAMILTON and the SCOURGE. Second, the paper presents key technical issues that make underwater vehicles difficult to control and illustrates solutions based on recent tests with an experimental underwater vehicle.

Supported by: ONR Contract N00014-86-C-0038,  
N00014-88-K-2022 and ONR Grant  
N00014-87-J-1111.

WHOI Contribution No. 7581.

**CHARACTERIZATION OF DEEP SEA  
STORMS**

*Thomas F. Gross and A. J. Williams III*

To describe and quantify the physical forcing of sediment transport events at the HEBBLE site, velocity, stress and sediment concentration data were obtained during a year long deployment. Through the year a variety of intense sediment transporting "events" were recorded. Careful analysis of these "events" reveals that only small proportion of the peaks in suspended sediment concentration correspond to "local" erosion. Most sediment "events" were clouds of fine suspended material advected into the region. Analysis of progressive vector diagrams reveal that these advected clouds were bounded by regions with concentration gradients as high as  $200\mu\text{g}/\text{l}/\text{km}$ . The high gradients suggest streams of sediment-bearing water, with sharp fronts of sediment concentration along their sidewalls, were veering across the region. The largest concentrations of suspended sediment were observed during local suspension events. The growth and decay of the sediment clouds during the "local" events did not exactly track the boundary shear stress. Rapid erosion occurred as the stress exceeded a critical shear stress. Maximum suspended concentrations occurred shortly after erosion began, indicating a source limited erosion process. The depositional period lasted for several weeks, whereas the erosion occurred in only a few days. Photographs of the bottom reveal depositional features (crag and tail dunes) which are aligned with the post storm flow, not the erosional flow direction.

Supported by: ONR Contract N00014-85-C-0001 and  
NR 083-004.

WHOI Contribution No. 7582.

**DESIGN AND PERFORMANCE  
EVALUATION OF AN ACTIVELY  
COMPLIANT UNDERWATER  
MANIPULATOR FOR FULL-OCEAN  
DEPTH**

*Dana R. Yoerger, Hagen Schempf and  
David M. DiPietro*

An underwater manipulator is described that can exhibit a wide range of compliance through a combination of mechanical design and software control and its performance characterized. The manipulator has been used in conjunction with the JASON Remotely Operated Vehicle at full-ocean depth. The major goal of the design was to produce a manipulator that can actively control

the interaction forces with the work task in the hostile deep-ocean environment. The manipulator's performance has been characterized in the lab and its overall operational utility has been confirmed during tests to depths of approximately 4000 meters, including an archaeological excavation at 700 meters depth in the Mediterranean.

The manipulator uses high performance brushless DC servomotors driving the joints through low-friction, zero-backlash reductions of moderate ratio consisting of cables and pulleys. Each joint is highly backdriveable and has a large range of rotation. This approach permits a variety of force control schemes such as impedance control to be implemented with no sensors other than the displacement sensors integrated with the brushless motor. It also permits high-quality torque servomechanisms to be directly implemented.

This paper outlines the design and illustrates the performance of a single joint in terms of friction, stiffness, and in implementing variable compliance and as a closed-loop torque servo.

In Press: *Journal of Robotic Systems Special Issue on Underwater Robotics.*

Supported by: ONR contract N00014-86-C-0038,  
N00014-88-K-2022 and ONR grant  
N00014-87-J-1111.

WHOI Contribution No. 7594.



**DEPARTMENT OF BIOLOGY**

**Peter H. Wiebe, Chairman**

**BIOLOGY**



**SUBNOSE-1: ELECTROCHEMICAL  
TRACKING OF ODOR PLUMES AT 900  
METERS BENEATH THE OCEAN  
SURFACE**

*Jelle Atema, Paul A. Moore, Laurence P. Madin  
and Greg A. Gerhardt*

High-resolution (18.75 Hz) microscale (3; 200 micron average diameter sensors) measurements of the turbulent distribution of chemicals from an odor source initiated from a platform at 900 meters beneath the ocean surface were studied from a deep diving submersible, the Johnson Sea-Link. The recording sensors were attached to a movable mechanical arm on the submersible and signals from the chemical sensor were recorded using a specially designed battery-powered microcomputer-controlled instrument. The recordings showed that both rapid and slow time course chemical signals existed in the odor plume at distances of even 50 meters from the chemical source. In addition, these studies suggest that this new technology can be successfully employed to study the dynamics of odor dispersal and/or nutrient chemical dynamics in a remote marine environment.

Supported by: NOAA/NURP Grant  
NA88AA-H-UR020, Subcontract No. 88-9; and  
NSF Grant BNS88-12952.

WHOI Contribution No. 7598.

**ARCHAEOGLOBUS PROFUNDUS SP. NOV.,  
REPRESENTS A NEW SPECIES  
WITHIN THE SULFATE-REDUCING  
ARCHAEBACTERIA**

*Siegfried Burggraf, Holger W. Jannasch,  
Barbara Nicolaus and Karl O. Stetter*

Eleven isolates of immotile coccoid hyperthermophilic archaeobacteria growing at temperatures up to 90°C were obtained from the walls of active smokers and from sediments from a deep-sea hydrothermal system at Guaymas, Mexico. Similar to *Archaeoglobus fulgidus*, they were sulfidogens showing a blue-green fluorescence at 420 nm. Sulfate, thiosulfate and sulfite served as electron acceptors. Elemental sulfur inhibited growth. In contrast to *A. fulgidus*, the new isolates were obligate mixotrophs strictly requiring H<sub>2</sub> and an organic carbon source (e.g., acetate). One of the new isolates was studied in more detail. It could be further distinguished from *A. fulgidus* by a 5 mol% lower GC-content of its DNA (41 mol%), a different pattern of complex lipids, and by insignificant DNA homology. On the basis of these distinguishing features, a new species,

*Archaeoglobus profundus* is described in this paper. Type strain is *A. profundus* AV 18 (DSM 5631).

Published in: *Systematic and Applied Microbiology*,  
13:24-28, 1990.

Supported by: NSF Grant OCE87-00581; and ONR  
Contract N00014-88-K-0386.

WHOI Contribution No. 7281.

**HETEROTROPHIC FLAGELLATES  
ASSOCIATED WITH SEDIMENTING  
DETRITUS**

*David A. Caron*

Suspended detrital aggregates in aquatic environments are specialized microenvironments for the existence of heterotrophic protists in planktonic ecosystems. Ranging in size from a few micrometers to several centimeters, many of these aggregates harbour rich communities of bacteria, cyanobacteria and photosynthetic eukaryotes, thereby constituting patches of highly elevated abundances of prey for many species of protozoa. Because these particles often contain abundances of protozoan prey many times greater than in the surrounding seawater, suspended particles often are sites for the aggregation and growth of phagotrophic flagellates and other protozoa in pelagic ecosystems. Abundances of flagellated protozoa on particles in the plankton can be more than two orders of magnitude greater than abundances in an equivalent volume of water in the same environment but without visible particles. Many of these species are "particle-associated" forms and similar to benthic species, poorly adapted to planktonic existence but capable of capturing and utilizing microorganisms loosely associated with, or attached to, the particle surfaces. Protozoa on suspended detrital aggregates play a significant role in the remineralization of organic carbon and nutrients contained in suspended particulate material, and undoubtedly contribute to the flux of these elements in aquatic ecosystems.

In Press: *The Biology of Free-Living Heterotrophic Flagellates*, D. J. Patterson and J. Larsen, eds., Oxford University Press.

Supported by: ONR Grant N00014-89-J-1075; and  
NSF Grants OCE88-18503 and OCE89-01005.

WHOI Contribution No. 7558.

**SENSITIVITY ANALYSIS OF PERIODIC  
MATRIX MODELS**

*Hal Caswell*

Population growth in periodic environments can be modelled by periodic matrix products. The



sensitivity analysis of population growth rate in such models is complicated because (1) entries in the periodic product matrix do not correspond to easily interpreted life history parameters, whereas (2) the entries in each individual matrix do not relate directly to the eigenvalues of the product matrix. In this paper I derive a simple expression for the sensitivity of population growth rate to changes in the entries in the individual matrices of a periodic matrix product. The formula is particularly useful for annual species living in seasonal environments.

Supported by: NSF Grants OCE89-00231, BSR87-04936; and DOE Grant DE-FG02-89ER60882.

WHOI Contribution No. 7500.

### THE TIME REQUIRED FOR COMPETITIVE EXCLUSION: LOTKA-VOLTERRA SYSTEMS

*Hal Caswell*

The time required for local competitive exclusion plays an important role in theories of non-equilibrium coexistence. It has been hypothesized that environmental fluctuations on the same scale as this exclusion time may lead to long-term non-equilibrium coexistence. This paper examines the factors determining exclusion time in a two-species system described by the Lotka-Volterra competition equations. The most important parameters are the intrinsic rate of increase of the losing competitor and the competition coefficient giving the effect of the winning competitor on the loser. Interactions involving exploitation competition between very similar, large long-lived species lead to very long exclusion times. In general, exclusion is expected to require tens of generations, unless intense interference competition is involved. This agrees with the results of laboratory experiments. These results are applied to the highly diverse communities in tropical rain forests and in the deep sea.

Supported by: NSF Grants OCE85-16177, OCE89-00231 and BSR87-04936; and DOE Grant DE-FG02-89ER60882.

WHOI Contribution No. 7449.

### DISTURBANCE, INTERSPECIFIC INTERACTION, AND DIVERSITY IN METAPOPULATIONS

*Hal Caswell and Joel E. Cohen*

In this paper, we explore some relationships between disturbance (biotic and abiotic) and

diversity (both species diversity and spatial heterogeneity) in a family of simple metapopulation models. These models describe, in schematic form, alternative mechanisms of succession, transitive and intransitive competitive relations in communities, and predator-mediated coexistence. Theories of ecological diversity have traditionally been based on results about species coexistence. A major implication of metapopulations is that coexistence may result from mechanisms which do not apply to single, undivided populations. In particular, in metapopulations the interaction of competition and disturbance can maintain *fugitive* or *nonequilibrium* species (Hutchinson 1951, 1952) which persist regionally even though they are excluded locally whenever they come into contact with superior competitors.

These theories suggest that coexistence and diversity in metapopulations are determined by the interaction of rates operating on several scales – competition (and other interspecific interactions) within patches, dispersal among patches, and disturbance operating across a landscape of patches. To explore these relations, we examine a family of simple models in which these rates appear explicitly.

Published in: *Biological Journal of the Linnaean Society*, 42:193-218, 1991.

Supported by: NSF Grants OCE85-16177, BSR87-04936 and BSR87-05047.

WHOI Contribution No. 7325.

### FROM THE INDIVIDUAL TO THE POPULATION IN DEMOGRAPHIC MODELS

*Hal Caswell and A. Meredith John*

All demographic models of populations are, in a sense, individual-based. Individuals are described in terms of their states (*i*-states, *sensu* Metz and Diekmann). The state of the population (*p*-states, *sensu* Metz and Diekmann) is then derived from the states of the individuals. Much demographic theory is based on a mixing assumption which guarantees that the distribution of individuals among *i*-state classes is a satisfactory *p*-state. When the mixing assumption fails, for example due to interactions among individuals, it is necessary to record the entire *i*-state configuration, keeping track of each individual in the population. This leads to individual-based models *sensu* Huston et al. We discuss several examples from demography of the relation between the individual and the population: multi-type branching processes as the *i*-state model underlying stable population theory, micro-simulations of

reproduction and family structure, age-classified epidemic models, and hazard analysis.

Supported by: NSF Grants OCE89-00231 and BSR87-04936; and DOE Grant DE-FG02-89ER60882.

WHOI Contribution No. 7415.

## HIGH TAURINE LEVELS IN THE *SOLEMYA VELUM* SYMBIOSIS: POSSIBLE SOURCES AND FUNCTIONS

N. Conway and J. McDowell Capuzzo

In order to determine comparative biochemical differences between bivalves with and without endosymbiotic chemoautotrophic bacteria, specimens of *Solemya velum*, a bivalve species known to contain bacterial endosymbionts, and the symbiont-free soft-shelled clam *Mya arenaria*, were collected from the same subtidal reducing sediments during October and November 1988. Total and free amino acid compositions were determined for both species. Protein-bound amino acids were calculated as the difference between total and free amino acids. In addition, stable isotope ratios of the total and free amino acids of each species were measured in order to determine potential sources for these molecules. Both species had similar total hydrolyzable- and protein-bound amino acid compositions; approximately 50% of the protein-bound amino acids were essential amino acids. In *S. velum*, the large reduction of the digestive system suggests these amino acids are probably synthesized by the endosymbiotic bacteria and translocated to the animal tissue. These results are supported by the  $\delta^{13}\text{C}$  and  $\delta^{15}\text{N}$  ratios of the amino acids of *S. velum* which were very similar to the isotope ratios previously found in both the endosymbionts and whole tissues of *S. velum*. Both the relative and absolute amounts of free amino acids differed significantly between the two species. In *S. velum*, the absolute concentrations of taurine, a sulfur-containing amino acid, were greater than the total free amino acid concentrations typically found in bivalves. The  $\delta^{34}\text{S}$  ratios of the free amino acids of *S. velum* were extremely negative ( $-17.2\text{‰}$ ) suggesting that taurine is synthesized using sulfur originally derived from external reduced sulfur sources, such as pore water sulfides. The possible roles for taurine in this animal-bacteria symbiosis are discussed.

Supported by: Ocean Ventures Fund; NOAA, Office of Sea Grant Award NA86-AA-D-S6090, RP/22 and RP/17.

WHOI Contribution No. 7575.

## INCORPORATION AND UTILIZATION OF BACTERIAL LIPIDS BY THE *SOLEMYA VELUM* SYMBIOSIS

Noellette Conway and Judith McDowell Capuzzo

We undertook a detailed analysis of the lipid composition of *Solemya velum*, a bivalve containing endosymbiotic chemoautotrophic bacteria, in order to determine the presence of lipid biomarkers of endosymbiont activity. The symbiont-free clam *Mya arenaria* and the sulfur-oxidizing bacterium, *Thiomicrospira crunogena* were analyzed for comparative purposes. The  $\delta^{13}\text{C}$  ratios of the fatty acids and sterols were also measured to elucidate potential carbon sources for the lipids of each bivalve species. Both fatty acid and sterol composition differed markedly between the two bivalves. The lipids of *Solemya* were characterized by large amounts of 18:1 $\omega$ 7 (*cis*-vaccenic acid), 16:0 and 16:1 $\omega$ 7 fatty acids and low concentrations of the highly unsaturated fatty acids characteristic of most marine bivalves. Cholesta-5-en-3- $\beta$ -ol (cholesterol) accounted for greater than 95% of the sterols in *S. velum*; small amounts of 24-ethycholesta-5-en-3- $\beta$ -ol were found in some specimens. In contrast, *Mya arenaria* had fatty acid and sterol compositions similar to typical marine bivalves characterized by large amounts of the highly unsaturated fatty acids 20:5 $\omega$ 3 and 22:6 $\omega$ 3 and a variety of plant-derived sterols. The fatty acids of *T. crunogena* were similar to those of *Solemya velum* and were dominated by 18:1 $\omega$ 7, 16:0 and 16:1 $\omega$ 7 fatty acids. None of the organisms studied contained hydrocarbons or hopanoids exceeding amounts found in analytical blanks.

The *cis*-vaccenic acid found in *S. velum* is almost certainly symbiont-derived and serves as a potential biomarker for symbiont-lipid incorporation by the animal host. The high concentrations of *cis*-vaccenic acid (up to 35% of the total fatty acid content) in both symbiont-containing and symbiont-free tissues of *S. velum* demonstrate the importance of the endosymbionts in the lipid metabolism of this bivalve. Furthermore, the presence of *cis*-vaccenic acid in all the major lipid classes of *S. velum* demonstrates both incorporation and utilization of this compound. The small amounts of polyunsaturated fatty acids found in *S. velum* and the absence of sterols of plant origin further suggests that this symbiosis relies on endosymbiont chemoautotrophy for the majority of its nutritional requirements.

The  $\delta^{13}\text{C}$  ratios of the fatty acids and sterols of *S. velum* were significantly lighter ( $-38.4\text{‰}$  to  $-45.3\text{‰}$ ) than those of *M. arenaria* ( $-23.8\text{‰}$  to  $-24.2\text{‰}$ ) and were similar to the values found for the fatty acids of *T. crunogena* ( $-45\text{‰}$ ); this

suggests that the lipids of *S. velum* are either derived directly from the endosymbionts or are synthesized using endosymbiont-derived carbon.

In Press: *Marine Biology*.

Supported by: NOAA Grant NA87AA-0-0M093; Ocean Ventures Fund; and WHOI Education Program.

WHOI Contribution No. 7356.

## **VERTICAL DISTRIBUTION AND SPECIES COMPOSITION OF MIDWATER FISHES IN WARM-CORE GULF STREAM MEANDER/RING 82-H**

*James E. Craddock, Richard H. Backus and Mary Ann Daher*

The integrated abundance and vertical distribution of midwater fishes in the upper 1000 m of warm-core Gulf Stream ring 82-H show that the fauna of the ring was very similar to that of the northern Sargasso Sea. The data indicate that warm-core rings have a large impact on the fauna of the Slope Water even though only a small fraction of the volume of rings is mixed into the Slope Water and that the fishes (mostly non-migratory) are located in the 'unreactive' parts of the ring.

Supported by: NSF Grants OCE81-17270 and OCE87-20402.

WHOI Contribution No. 7339.

## **MOLECULAR SYSTEMATICS, MICROBIAL ECOLOGY AND SINGLE CELL ANALYSIS**

*E. F. DeLong*

Molecular approaches in taxonomy and systematics are providing a unifying framework for understanding the phylogenetic relationships of diverse biological species. The methods rely on comparison of nucleic acid or amino acid sequences, which can serve as "yardsticks" for measuring evolutionary divergence. Direct sequence analysis can largely circumvent problems inherent in phenotypic comparisons of widely divergent taxa. Macromolecular sequence data bases are valuable resources for determining the phylogenetic affiliations of previously unstudied or uncharacterized organisms. In particular, current understanding of the evolutionary relationships of microbial species has been greatly advanced through molecular phylogenetic comparisons of small subunit ribosomal RNA (rRNA) sequences.

The molecular data employed in systematic and evolutionary studies are also proving useful for ecological studies. By directly retrieving phylogenetically informative gene sequences from mixed microbial populations, it is possible to infer phylogenetic affiliations of individual population constituents. This allows identification of community members without requiring their cultivation, and so avoids some selective biases associated with pure culture methods. In addition, short segments of sequence, such as those found in small subunit rRNA, can be taxa-specific. These sequences may therefore serve as diagnostic markers for particular groups. In conjunction with epifluorescence microscopy, fluor-labeled, rRNA-targeted probes that bind to these diagnostic sequences may be used to determine the phylogenetic identity of individual cells. Thus, macromolecular sequence information can be employed to detect the presence of particular species, and to study their spatial and temporal variability. Recent applications, including molecular phylogenetic analyses of mixed bacterioplankton populations, demonstrate the utility of this approach.

Supported by: ONR Grant N00014-90-J-1917.

WHOI Contribution No. 7564.

## **FLUORESCENT, RIBOSOMAL RNA PROBES FOR IDENTIFICATION OF SINGLE CELLS: A BRIEF REVIEW**

*Edward F. DeLong*

A method for fluorescence detection and phylogenetic identification of single microbial cells is described. The procedure uses fluorescently labeled oligonucleotide probes, complementary to ribosomal RNA (rRNA) sequences. In their entirety, small subunit rRNA sequences contain highly, moderately and modestly conserved nucleotide positions. This allows the design of rRNA-targeted probes diagnostic for both broad phylogenetic groups (kingdoms), and closely related species. Ribosomal RNA-specific hybridization probes are quite sensitive, due to the cellular abundance of ribosomes. In conjunction with epifluorescence microscopy, fluorescently labeled, rRNA-targeted oligonucleotide probes can be used to detect and identify individual cells.

Supported by: WHOI.

WHOI Contribution No. 7416.

## FLUORESCENT, RIBOSOMAL RNA PROBES FOR CLINICAL APPLICATION

Edward F. DeLong and Jyotsna Shah

A method for detecting and phylogenetically identifying single microbial cells is described. The procedure uses fluorescently labeled nucleic acid probes, complementary to diagnostic ribosomal RNA (rRNA) sequences. As a group, rRNA sequences contain highly, moderately and modestly conserved nucleotide positions, so probes diagnostic for both broad phylogenetic groups (kingdoms) and narrow ones (species) can be designed. In situ, rRNA-specific hybridization probes are quite sensitive, because most cells contain large numbers of ribosomes. The simplicity, rapidity and sensitivity of the technique render it useful for a variety of clinical and research applications.

Published in: *Diagnostics and Clinical Testing*,  
28:41-44, 1990.

Supported by: ONR Contract N14-87-K-081; WHOI;  
and Gene Trak Systems.

WHOI Contribution No. 7364.

## PHYLOGENETIC CHARACTERIZATION AND IN SITU LOCALIZATION OF THE BACTERIAL SYMBIONT OF SHIPWORMS (TEREDINIDAE: BIVALVIA) USING 16S rRNA SEQUENCE ANALYSIS AND OLIGONUCLEOTIDE PROBE HYBRIDIZATION

D. L. Distel, E. F. DeLong and J. B. Waterbury

It has been proposed that a bacterium isolated from the gills of shipworms (teredinid mollusks) is, by virtue of its ability to both degrade cellulose and fix dinitrogen, the symbiont that enables these mollusks to utilize wood as their principal food source. The phylogenetic affiliation of four of these bacteria isolated from wood-boring bivalve mollusks was determined by 16S rRNA sequence analysis using the reverse transcriptase method with six oligonucleotide primers. The four bacterial strains tested had indistinguishable 16S rRNA sequences supporting the previous conclusion, based on phenotypic characterization, that these isolates represent a single species. Evolutionary distance matrix analysis of the RNA sequence indicated that the bacterial symbiont falls within the gamma-3 subdivision of the Proteobacteria and is unique from other known bacterial genera. In situ localization of the bacterial symbiont in tissue sections of the shipworm *Lyrodus pedicellatus* was

determined using a 16S rRNA directed oligodeoxynucleotide hybridization probe specific for the bacterium isolated from shipworm gill tissue. Fluorescence microscopy showed that the specific probe bound to *L. pedicellatus* tissue at sites coincident with the location of symbiont cells and that it did not bind to other host tissues. This technique provided direct visual evidence that the cellulolytic, nitrogen-fixing bacterial isolates were the gill symbionts observed within *L. pedicellatus*.

Supported by: WHOI Postdoctoral Fellowship.

WHOI Contribution No. 7602.

## THE ROLE OF INTERCELLULAR CHEMICAL COMMUNICATION IN THE *VIBRIO FISCHERI* - MONOCENTRID FISH SYMBIOSIS

Paul V. Dunlap and E. P. Greenberg

Three species of luminous bacteria (*Vibrio fischeri*, *Photobacterium leiognathi*, and *Photobacterium phosphoreum*) presently are known to enter into light-organ symbiosis with marine fishes and squid. These associations are recognized as having the potential to provide insight into cellular and sub-cellular interactions between the animal host and its bacterial symbiont. Of these three species, *V. fischeri* is the most thoroughly understood with regard to its luminescence system. This chapter addresses current and past work on cellular interactions between *V. fischeri* and its fish host, fishes of the family Monocentridae (pinecone fish), and presents an analysis of current molecular genetic studies of the cell density-dependent autoinduction of luminescence in *V. fischeri*, a cardinal feature of the bioluminescent symbiosis. Specific topics include: the systematics and distribution of monocentrid fishes, developmental biology of the symbiotic association, function of the symbiosis for host and symbiont, morphology and ultrastructure of the fish light organ, symbiotic state of *V. fischeri* in the fish light organ, organization of the *V. fischeri* luminescence genes, molecular mechanisms of the cell density-dependent autoinduction of luminescence in *V. fischeri*, control of autoinduction by cyclic AMP, and control of luminescence by other genetic and environmental factors potentially involved in the symbiosis.

Supported by: New York State Sea Grant.

WHOI Contribution No. 7524.

**ALONGSHORE TRANSPORT OF A  
TOXIC PHYTOPLANKTON BLOOM IN  
A BUOYANCY CURRENT:  
*ALEXANDRIUM TAMARENSE* IN THE  
GULF OF MAINE**

*Peter J. S. Franks and Donald M. Anderson*

The present study examines the mechanisms controlling blooms of the toxic dinoflagellate *Alexandrium tamarense* and the concomitant patterns of shellfish toxicity in the southwestern Gulf of Maine. During a series of cruises over three years, various hydrographic parameters were measured to elucidate the physical factors affecting the distribution and abundance of dinoflagellates along this coast. In two years when toxicity was detected in the southern part of this region, *A. tamarense* cells were apparently transported into the study area between Portsmouth and Cape Ann, Massachusetts, in a coastally trapped buoyant plume. This plume appears to have been formed off Maine by the outflow from the Androscoggin and Kennebec Rivers. Flow rates of these rivers, hydrographic sections, and satellite images suggest that the plume had a duration of about a month, and extended alongshore for several hundred kilometers. The distribution of cells followed the position of the plume as it was influenced by wind and topography. Thus when winds were downwelling-favorable, cells were moved alongshore to the south, and were held to the coast; when winds were upwelling-favorable, the plume sometimes separated from the coast, advecting the cells offshore.

The alongshore advection of toxic cells within a coastally trapped buoyant plume can explain the details of the temporal and spatial patterns of shellfish toxicity along the coast. The general observation of a north-to-south temporal trend of toxicity is consistent with the southward advection of the plume. In 1987 when no plume was present, *Alexandrium tamarense* cells were scarce, and no toxicity was recorded at the southern stations. A testable hypothesis was formulated explaining the development and spread of toxic dinoflagellate blooms in this region. The hypothesis included: source of *A. tamarense* populations in the north, possibly associated with the Androscoggin and Kennebec estuaries; a relationship between toxicity patterns and river flow volume and timing of flow peaks; and a relationship between wind stresses and the distribution of low salinity water and cells. Local, in situ growth of dinoflagellates can be an important factor initiating toxic dinoflagellate blooms. However, these data demonstrate the significant role of alongshore transport of established populations of *Alexandrium tamarense* in controlling the location and timing of paralytic

shellfish poisoning (PSP) outbreaks in May and June along the southwestern coast of the Gulf of Maine.

Supported by: ONR Contract N00014-87-K-0007; ONR Grant N00014-89-J-1111; NOAA, Office of Sea Grant Awards NA86-AA-D-SG090, R/B-92 and NA90-AA-D-SG480, R/B-100; and NSF Grant OCE89-11226.

WHOI Contribution No. 7522.

**TOXIC PHYTOPLANKTON BLOOMS IN  
THE SOUTHWESTERN GULF OF  
MAINE: TESTING HYPOTHESES OF  
PHYSICAL CONTROL USING  
HISTORICAL DATA**

*Peter J. S. Franks and Donald M. Anderson*

Blooms of the toxic dinoflagellate, *Alexandrium tamarense* have been nearly annual features along the coasts of southern Maine, New Hampshire and Massachusetts since 1972. Two hypotheses which have been used to explain the initiation of these blooms were tested using historical records of shellfish toxicity, wind, and river flow. The first hypothesis states that the blooms were initiated or advected to shore by wind-driven coastal upwelling. The second states that established blooms were advected from north to south alongshore in a coastally trapped buoyant plume of water. Of the eleven years examined, we found seven cases inconsistent with the wind-driven upwelling hypothesis, and only one case (1985) which contradicts the plume-advection hypothesis. Nineteen hundred and eighty-five was an unusual year in many respects, and we suggest that some other mechanism was responsible for the toxic outbreaks. In addition, the wind-driven upwelling hypothesis could not explain the observed north-to-south temporal progression of toxicity each year. The plume advection hypothesis was found to best explain the details of the timing and spread of shellfish toxicity. These include the variable north-to-south progression with time, the presence of a toxin-free zone south of Cape Ann, MA, the sporadic nature of toxic outbreaks south of Massachusetts Bay, and the apparently rare occurrence of toxicity well offshore on Nantucket Shoals and Georges Bank.

Supported by: ONR Contract N00014-87-K-0007; ONR Grant N00014-89-J-1111; NOAA, Office of Sea Grant Awards NA86-AA-D-SG090, R/B-92 and NA90-AA-D-SG480, R/B-100; and the Florence and John Schumann Foundation.

WHOI Contribution No. 7523.

## REGULATION OF GUTLESS ANNELID ECOLOGY BY ENDOSYMBIOTIC BACTERIA

*O. Giere, N. M. Conway, G. Gastrock and  
C. Schmidt*

In studies on invertebrates from sulphidic environments (thiobios) exploiting reduced substances through symbiosis with bacteria, ecological results are underrepresented and experimental work is generally lacking. The gutless oligochaete *Inanidrilus leukodermatus* contains endosymbiotic sulphur-oxidizing bacteria and inhabits the sediment layers around the redox potential discontinuity (RPD) where there is access to both microoxic and sulphidic conditions. This annelid species is highly suitable for ecological studies, notably on the distributional effects of symbiotic associations with sulphur bacteria as it is very mobile and locally abundant.

By experimental manipulation of physico-chemical gradients, we have shown for the first time that the distribution pattern of these worms directly results from active migrations towards the variable position of the RPD, demonstrating the ecological relevance of the concomitant chemical conditions for these worms. Their distributional behaviour probably helps to optimize the metabolic conditions for the endosymbiotic bacteria coupling the needs of symbiont physiology with host behaviour and ecology. The prevailing bacterial role in the ecophysiology of the symbiosis was confirmed by biochemical analyses (stable isotope ratios for C and N; assays of lipid and amino acid composition) which showed that a dominating portion of the biochemical fluxes in the symbiosis is bacteria-based.

It appears that the distributional and nutritional ecology of the gutless annelids is regulated by their symbiosis with sulphur bacteria. These ecological and biochemical data supplement and confirm our earlier structural, microbiological and physiological results underlining the importance of the prokaryotes in this highly evolved and much integrated mutualistic bacteria-animal association.

In Press: *Marine Ecology Progress Series*.

Supported by: Ocean Ventures Fund.

WHOI Contribution No. 7392.

## SEQUENTIAL UTILIZATION OF NATURALLY OCCURRING AROMATIC HYDROCARBONS AT THE GUAYMAS BASIN HYDROTHERMAL VENT SITE

*Frederick E. Goetz and Holger W. Jannasch*

Petroleum rich surface sediments and the overlying water at the Guaymas Basin hydrothermal vent site yielded 151 strains of aerobic, mesophilic, marine bacteria that grew on aromatic compounds as sole sources of carbon. The isolates fall into two physiological groups: (1) capable of metabolizing toluene, naphthalene, biphenyl, dibenzofuran, or phenanthrene and (2) unable to grow on toluene or the polycyclic compounds tested but able to metabolize one or more of the following: p-hydroxybenzoate, phenylacetate, salicylate, m-hydroxybenzoate, benzoate, hydrocinnamate, D/L-mandelate, cinnamate, phthalate. These latter compounds are of biological (secondary) origin and represent metabolites derived from the polycyclic and other naturally occurring aromatic compounds. A similarity analysis of 135 of the isolates on the basis of substrate use, sodium chloride requirement, and growth in complex marine media identified 90 metabolically distinct bacterial strains. The results suggest that the petroleum rich hydrothermal sediments of the Guaymas Basin vent site support a heterogeneous microbial population that is engaged in the stepwise breakdown of aromatic hydrocarbons.

Supported by: NSF Grant OCE89-22854; and ONR Contract N00014-86-K-0386.

WHOI Contribution No. 7526.

## SEX DIFFERENCES IN HEPATIC MONOOXYGENASES IN FLOUNDER AND SCUP AND REGULATION OF P450 FORMS BY ESTRADIOL

*E. S. Gray, B. R. Woodin and J. J. Stegeman*

Details concerning the endogenous regulation of hepatic cytochrome P450 monooxygenase in teleosts, and the features of this regulation common among fish species, are poorly known. Gonadally mature female winter flounder (*Pseudopleuronectes americanus*) have been reported to have several-fold lower levels of microsomal cytochromes P450 and b<sub>5</sub> and NADPH-cytochrome c reductase than do males (Mar. Environ. Res., 1984, 14:422-435). These strong sex differences prompted more detailed study of P450 regulation in winter flounder liver, and a comparison with sex differences in another marine teleost scup (*Stenotomus chrysops*).

Ethoxyresorufin O-deethylase (EROD) activity/nmol P450 was less in gonadally mature females than in males of both species. Immunoblot analysis with MAb 1-12-3 to P450E (the EROD catalyst) showed that the content of P450E counterpart was also much less in females of both species. Aminopyrine N-demethylase (APND) and testosterone 6 $\beta$ -hydroxylase (6 $\beta$ -OHase) activities per nmol P450 were higher in gonadally mature female than in mature male flounder, differences not seen in scup. Polyclonal antibodies to scup P450A were shown to detect proteins in a number of teleosts. The levels of anti-P450A cross-reacting protein were greater in mature female than in male flounder, but as with 6 $\beta$ -OHase activity, the content of this protein was not sexually differentiated in scup. Estradiol treatment of winter flounder depressed rates of EROD, APND, 6 $\beta$ -OHase and estradiol 2-OHase activities per mg protein, but APND and 6 $\beta$ -OHase activities per nmol P450 were unchanged. Thus, E<sub>2</sub> promotes general decreases in some hepatic P450-catalyzed activities, but in achieving sex differences there is also specific regulation of the P450E counterpart, and possibly of the 6 $\beta$ -OHase (P450A?). Other factors, temporal or hormonal, can modify the effect of E<sub>2</sub> treatment, and may contribute to the specific regulation of P450 forms in naturally-maturing fish, and to species differences in this regulation.

Supported by: EPA Cooperative Agreement CR-813155; and PHS Grants ES-04220 and CA-44306.

WHOI Contribution No. 7423.

### PROBING THE FINE STRUCTURE OF OCEAN SOUND-SCATTERING LAYERS USING ROVERSE TECHNOLOGY

Charles H. Greene, Peter H. Wiebe,  
Robert T. Miyamoto and Janusz Burczynski

A 420-kHz, dual-beam SONAR system, deployed on a remotely operated vehicle (ROV), was used to examine the fine structure of sound-scattering layers (SSL's) in Puget Sound and the Arctic Ocean. The Puget Sound SSL, initially detected with a shipboard, 200-kHz, single-beam SONAR system, was correlated with a high biomass of sound scatterers in the size range of macrozooplankton and micronekton. Its vertical position appeared unrelated to profiles of temperature, salinity, or chlorophyll fluorescence. The Arctic SSL was composed of similar sized sound scatterers, although its volume backscattering intensity was 10 to 100 times lower than that observed for the Puget Sound SSL. The vertical position of the Arctic SSL was closely

associated with the thermocline separating Arctic Water from North Atlantic Water.

The fine-scale, horizontal variability of water-column volume backscattering was examined at both study sites. The highest variability observed was associated with the Puget Sound SSL where the mean intensity of volume backscattering was also the highest. These findings are consistent with the common observation that, whatever methods are used to measure zooplankton and micronekton abundance, sampling variance nearly always increases with the mean.

In Press: *Limnology and Oceanography*.

Supported by: ONR Contract N00014-88-K-0116.

WHOI Contribution No. 7508.

### WHY HABITAT ARCHITECTURE AND COLOR ARE IMPORTANT TO SHRIMP LIVING IN PELAGIC SARGASSUM: THE USE OF CAMOUFLAGE AND PLANT-PART MIMICRY

S. Hacker and L. P. Madin

Camouflage and plant-part mimicry, two forms of resemblance of animals to their habitat, were investigated for two species of shrimp living in pelagic *Sargassum natans* (Linnaeus) Gaillon in the Sargasso Sea. We used field collections and laboratory experiments to correlate the size, shape, color, and behavior of *Latreutes fucorum* (Fabricius) and *Hippolyte coerulescens* (Fabricius) with the architecture and color of the *Sargassum* habitat. Habitat architecture (sensu Hacker and Steneck) is a measure of the number, size, shape and arrangement of structural and spatial components of the habitat. Components of the structural architecture of *Sargassum* and plastic plants were measured and related to shrimp number, body size and shape. *Latreutes* most resembled *Sargassum* fronds, while *Hippolyte* resembled the gas-filled bladders (vesicles). Behavioral observations showed that *Latreutes* characteristically clings to the fronds and *Hippolyte* to the main stalk and vesicles of *Sargassum* plants.

In habitat selection experiments, the shrimp were offered *Sargassum* and artificial algae with different architectures and colors. Both species were found in equal densities on *Sargassum* and artificial algae suggesting that food value was unimportant relative to habitat architecture. When offered a modified habitat architecture of *Sargassum*, *Latreutes* preferred a "fronds only" to a "vesicles only" plant while the reverse was true for *Hippolyte*. When plastic plants with small and large fronds were offered, small *Latreutes* showed a significant preference for small-frond plants, while large shrimp showed no preference. *Latreutes* was

found in yellow plants significantly more than in brown plants but *Hippolyte* was found in equal densities on both plants. In general, small shrimp tend to be solid-colored or transparent, while large shrimp have disruptive color patterns corresponding to their habitat. It may be that there is an ontogenetic shift from use of plant-part mimicry to camouflage. As shrimp outgrow the specific plant parts they mimic, they use color patterns to camouflage themselves and generally resemble the *Sargassum* habitat matrix. In this system, camouflage and plant-part may depend, in large part, on the size, shape and color of the shrimp relative to elements of the *Sargassum* habitat, and change in importance of fish predation is discussed in relation to the shrimp and fish found in *Sargassum* collections from this study.

Supported by: NSF Grant OCE88-18503.

WHOI Contribution No. 7530.

## THE ROLE OF BIOTRANSFORMATION IN THE TOXICITY OF MARINE POLLUTANTS

Mark E. Hahn and John J. Stegeman

Marine organisms are exposed to a variety of environmental contaminants via food, water, and sediments. Some of these chemicals are toxic at the levels encountered in the environment. They produce toxicity by interacting with essential cellular macromolecules - including proteins, lipids, and nucleic acids (DNA, RNA) - and disrupting their normal functions. Many chemicals can produce such toxicity only after they are enzymatically transformed to toxic derivatives. The major enzyme system involved in this biotransformation is cytochrome P-450 (P-450), a group of related proteins that are also involved in the synthesis and degradation of endogenous compounds such as steroid hormones. The content of some cytochrome P-450 enzymes increases in response to certain chemicals, a phenomenon known as induction. We have studied the cytochrome P-450 system in several species of marine fish and have recently begun to investigate this system in whales. In particular, we have characterized several types of cytochrome P-450 from the marine fish scup (*Stenotomus chrysops*). One form, cytochrome P-450E, is similar to a form of P-450 that is found in terrestrial mammals (rats, mice, humans) and is involved in the transformation of certain pollutants to toxic and carcinogenic derivatives. Scup P-450E is induced (increased) following exposure to polycyclic aromatic hydrocarbons (PAH), polychlorinated biphenyls (PCB), and polychlorinated dibenzofurans (PCDF). In addition, elevated levels

of cytochrome P-450E are found in fish from polluted areas of the ocean as compared to fish from less-polluted sites. Using antibody probes and measurements of enzymatic activity, we have detected a related cytochrome P-450 in minke whales (*Balaenoptera acutorostrata*) from the North Atlantic. Clearly, whales possess a form or forms of cytochrome P-450 that are similar to those found in other vertebrate animals, including terrestrial mammals and marine fish. However, further investigations will be needed to determine the role of these enzymes in the toxicity of environmental contaminants found in whales.

Published in: *Pour L'Avenir du Béluga (For the Future of the Beluga)* Proceedings of the International Forum for the Future of the Beluga, J. Prescott and M. Gauguelin, eds., Presses de l'Université du Québec, pp. 185-198, 1990.

Supported by: Surdna Foundation; and PHS Grant ES-04220.

WHOI Contribution No. 7552.

## LAKE ZABUYE AND THE CLIMATIC HISTORY OF THE TIBETAN PLATEAU

Heinrich D. Holland, George I. Smith,  
Holger W. Jannasch, Andrew G. Dickson,  
Zheng Miangping and Ding Tiping

Lake Zabuye is one of many highly saline lakes on the Qinghai-Xizang (Tibetan) Plateau. Well developed lake terraces indicate that lake level was at one time 180 m higher than at present. Preliminary observations suggest that there have been at least two high stands of the lake, one *ca.*  $10^5$  years B.P., the other *ca.*  $10^4$  years B.P. The present, highly concentrated alkaline chloride-sulfate brines of Lake Zabuye evolved by the evaporation of spring waters and surface runoff, probably during the last several thousand years. The brines are abnormally rich in several trace elements and could become a source of lithium for the Peoples' Republic of China. The distribution of microorganisms in Lake Zabuye during the summer of 1988 reflected the abnormal aridity of the several previous years. Nevertheless, halobacteria and photosynthetic sulfur bacteria were successfully isolated; their presence indicates that their distribution is worldwide.

Supported by: U.S. National Academy of Sciences.

WHOI Contribution No. 7543.



**SULFUR CYCLING IN A  
PERMANENTLY ICE-COVERED  
AMICTIC ANTARCTIC LAKE, LAKE  
FRYXELL**

*Brian L. Howes and Richard L. Smith*

The ice free valleys of southern Victoria Land contain a variety of perennially ice-covered closed-basin lakes. The lack of wind driven mixing and the saline bottom waters has resulted in an amictic redox stratified water column with oxygen concentrations in excess of air equilibration in the euphotic zone and anoxic conditions with concentrations of  $\text{H}_2\text{S}$  approaching 1.25 mM in the hypolimnion. We are constructing a sulfur balance for the lake to determine: 1) the long-term fate of S entering the lake; 2) the importance of organic matter remineralization by microbial  $\text{SO}_4^{2-}$  reduction to the C and N cycles; 3) the rate of internal recycling of S; and 4) the long-term redox stability of Lake Fryxell.

Measurements of  $[\text{Cl}^-]$  in the water column supported the concept of amixis and diffusion dominated transport. Estimates of water column sulfate and sulfide diffusion and measured rates of sediment  $\text{SO}_4^{2-}$  reduction indicate a system in relative balance and a turnover of the water column  $\text{SO}_4^{2-}$  pool of approximately 1,750 yrs, emphasizing the long-time scales upon which the biogeochemical cycling within Lake Fryxell must be gauged. Inorganic reduced sulfur pools are significantly higher than found in freshwater sediments and are similar to marine sediments consistent with the saline nature of the lake waters. Sediment carbon/sulfur ratios suggest that anoxic bottom waters have persisted over the past 10,000 years. The present S balance of the anoxic basin of Lake Fryxell suggests a sediment sink for  $\text{SO}_4^{2-}$  input from glacial streams after microbial transformation to inorganic reduced forms, and a system in near equilibrium with  $\text{SO}_4^{2-}$  inputs.

Supported by: NSF Grants DPP89-18782 and BSR87-17701.

WHOI Contribution No. 7442.

**MARINE MICROBIOLOGY: A NEED  
FOR DEEP-SEA DIVING?**

*Holger W. Jannasch*

Studies in deep-sea microbiology are an essential part of global biogeochemistry and of biological oceanography in particular. Discovering the heterogeneity of microbial populations and their activities on the deep-sea floor had not been possible without the capability of visual surveying and sample collecting during manned diving

operations. This lack of uniformity does not only refer to hydrothermal vents and cold seeps but also to the discontinuous accumulations of organic deposits in sea floor depressions at a large range of scales and the resulting formation of nutrient enriched anoxic pockets. Aiding in this work has been the use of free vehicles. More recently the rapid developments of ROV capabilities promise wide geographical spread of microbial deep-sea studies. In planning to extend our diving operations to the oceans' maximum depths, the simultaneous development and use of all of these approaches will be essential, and it is greatly hoped that economic consideration will not force us into making premature choices. From our experiences in diving-related research over the last two decades, it appears evident that manned and unmanned operations complement each other for the various, often unexpected tasks in deep-sea studies.

Published in: *Marine Technology Society Journal*, 24(2):28-31, 1990.

Supported by: NSF Grant OCE87-00581; and ONR Contract N00014-88-K-0386.

WHOI Contribution No. 7384.

**MICROBIOLOGICAL PROCESSES IN  
THE BLACK SEA WATER COLUMN  
AND TOP SEDIMENT: AN OVERVIEW**

*Holger W. Jannasch*

Biochemical transformations catalyzed enzymatically by various metabolic types of microorganisms are discussed in connection with the specific projects to be studied during Leg 2 of the R/V KNORR Black Sea Cruise No. 134-9, May 1988.

Supported by: NSF Grant OCE86-08124.

WHOI Contribution No. 7514.

**THERMOPHILIC BACTERIAL SULFATE  
REDUCTION IN DEEP-SEA SEDIMENTS  
AT THE GUAYMAS BASIN  
HYDROTHERMAL VENT SITE (GULF  
OF CALIFORNIA)**

*Bo Barker Jørgensen, Leon X. Zawacki and  
Holger W. Jannasch*

Sulfate reduction was studied by radiotracer methods in geothermally heated mud near black smokers in the southern trough of the Guaymas Basin at 2000 m water depth. Sediment cores were retrieved by the submersible ALVIN from three closely spaced sites. Steep hydrothermal gradients

from 2.7°C at the surface up to 126°C at 75 cm depth were measured in the sediments. Extensive conversion of sulfate to H<sub>2</sub>S, with 4 mM SO<sub>4</sub><sup>2-</sup> and 15 mM H<sub>2</sub>S at 5 cm depth, indicated thermogenic reduction at depth in the upwards percolating hot pore fluid. Pyrite concentrations were high, 200 μmol S cm<sup>-3</sup>, while FeS was low near detection limit. Bacterial sulfate reduction showed maximum rates of 30-140 nmol SO<sub>4</sub><sup>2-</sup> cm<sup>-3</sup> d<sup>-1</sup>. While mesophilic sulfate reduction occurred near the cold (2-3°C) sediment surface, extremely thermophilic activity was observed in deeper, hot layers, the actual depth dependent on the temperature profile of the particular core. In the subsurface sediment at 10 to 45 cm depth, optimum temperatures for sulfate reduction increased from 63°C to 83°C with corresponding maximum temperatures of 66°C to 90°C.

Published in: *Deep-Sea Research*, 37(4):695-710, 1990.

Supported by: NSF Grant OCE87-00581; and ONR Contract N00014-88-K-0386.

WHOI Contribution No. 7160.

## MICROBIAL OXIDATION OF SULFUR IN DIBENZOTHIOPHENE

Judith P. Kitchell, Saraswathy V. Nochur,  
Judith K. Marquis, Dennis A. Bazylinski and  
Holger Jannasch

An aerobic microorganism isolated from deep-sea thermal vents in the Gulf of California and grown with the model coal compound dibenzothiophene (DBT) was found to produce DBT oxidation products, including DBT-sulfoxide and DBT-sulfone. The organism can utilize DBT as sole carbon and sulfur source, but grows better when the medium is supplemented with yeast extract. After five to seven days of incubation with DBT, some DBT-sulfoxide and, to a lesser extent, DBT-sulfone, intermediates in the desulfurization of DBT, were detected. When the culture was grown in medium with DBT-sulfoxide as substrate, little oxidation occurred, but when DBT-sulfone was used as substrate, it was rapidly degraded. The extracellular extract is also active against DBT, producing sulfur oxidation products.

Published in: *Resources, Conservation and Recycling*, 5:1-9, 1991.

Supported by: DOE Grant DE-AC22-88PC-88855.

WHOI Contribution No. 7513.

## CYTOCHROME P-450E (P450IA1) PROTEIN AND HEME TURNOVER IN *FUNDULUS HETEROCLITUS*

Pamela J. Kloepper-Sams and John J. Stegeman

The in vivo turnover rates of P450IA1 (P-450E) apoprotein and heme moieties were examined in an estuarine fish. The decay in radiolabel was followed by 192 h after injection of [<sup>3</sup>H]leucine and [<sup>14</sup>C]delta aminolevulinic acid (ALA) into β-naphthoflavone pretreated *Fundulus heteroclitus*. All microsomal [<sup>3</sup>H] was incorporated into the trichloroacetic acid-precipitable fraction (protein), whereas about 55% of the microsomal [<sup>14</sup>C] was found in this fraction. Peak incorporation of [<sup>3</sup>H]leucine into total microsomal protein and into P-450E apoprotein preceded peak incorporation of [<sup>14</sup>C]ALA into the heme prosthetic group of either. Total ("average") hepatic microsomal protein had an apparent biphasic turnover, with half-lives of 8 and 138 h, while total microsomal heme prosthetic groups in protein had apparent half-lives of 66 and 141 h. P-450E, at induced steady state levels, was isolated by immunoprecipitation with anti-scup P-450E antibodies. The apoprotein had a half-life of 39 h by the isotopic decay method, comparable to a half-life of 43 h when incorporating the kinetics of enzyme induction into the calculation. The P-450E heme moiety had a half-life of 93 h. Thus, teleost P450IA1 apoprotein has a shorter apparent half-life than does the heme moiety, in contrast to the half-lives of mammalian P-450. Studies on the turnover of fish P-450 may provide new insights into heme/protein interactions potentially involved in the regulation of P450IA1 expression.

Supported by: PHS Grants CA-44306 and ES-04220.

WHOI Contribution No. 7333.

## A MOLECULAR PHYLOGENY OF DINOFLAGELLATE PROTISTS (PYRRHOPHYTA) INFERRED FROM THE SEQUENCE OF 24S rRNA DIVERGENT DOMAINS D1 AND D8

Guy Lenaers, Christopher Scholin, Yvonne Bhaud,  
Danielle Saint-Hilaire and Michel Herzog

The sequence of two divergent domains (D1 and D8) from dinoflagellate 24S large subunit rRNA was determined by primer extension using total RNA as template. Nucleotide sequence alignments over 401 bases have been analyzed in order to investigate phylogenetic relationships within this highly divergent and taxonomically controversial group of protists of the division Pyrrhophyta. Data are provided confirming that

dinoflagellates represent a monophyletic group. For 11 out of the 13 investigated laboratory grown species, an additional domain (D2) could not be completely sequenced by reverse transcription because of a hidden break located near its 3'-terminus. Two sets of sequence alignments were used to infer dinoflagellate phylogeny. The first (199 nt) included conservative sequences flanking the D1 and D8 divergent domains. It was used to reconstruct a broad evolutionary tree for the dinoflagellates, which was rooted using *Tetrahymena thermophila* as the outgroup. To confirm the tree topology, and mainly the branchings leading to closely related species, a second alignment (401 nt) was considered, which included the D1 and D8 variable sequences in addition to the more conserved flanking regions. Species which showed sequence similarities with other species lower than 60% on average (Knuc values higher than 0.550), were removed from this analysis. A coherent and convincing evolutionary pattern was obtained for the dinoflagellates, also confirmed by the position of the hidden break within the D2 domain which appears to be group specific. The reconstructed phylogeny indicates that the early emergence of *Oxyrrhis marina* preceded that of most Peridiniales, a large order of thecate species, whereas the unarmored Gymnodiniales appeared more recently, along with members of the Prorocentrales characterized by two thecal plates. In addition, the emergence of heterotrophic species preceded that of photosynthetic species. These results provide new perspectives on proposed evolutionary trees for the dinoflagellates based on morphology, biology and fossil records.

In Press: *Journal of Molecular Evolution*, 1990.

Supported by: French Centre National de la Recherche Scientifique; and NSF Grant OCE89-11226.

WHOI Contribution No. 7520.

#### A COMPARISON OF SHIPBOARD AND *IN SITU* METHODS FOR ESTIMATING OCEANIC PRIMARY PRODUCTION

Steven E. Lohrenz, Denis A. Wiesenburg,  
Charles R. Rein, Robert A. Arnone,  
Craig D. Taylor, George A. Knauer and  
Anthony A. Knap

Primary production data measured by *in situ* (IS) and "simulated" *in situ* (SIS) incubations were compared. To minimize differences between the two types of incubations, SIS experiments were conducted in temperature-controlled incubators in which the spectral distribution and quantity of irradiance was adjusted to approximate IS

conditions. IS irradiance was estimated using a spectral irradiance model, validated by profiles of the vertical attenuation coefficient. IS incubations were done using two methods. The first involved deployment of bottles on a drifting array for whole day (dawn to dusk) incubations. The second method employed an autonomous submersible incubation device that performed short term (< 1 h) incubations at multiple depths. Differences between whole day IS and SIS incubation estimates were attributed mainly to differences between IS and SIS available irradiance. This view was supported by the observation that  $\ln(\text{photosynthesis})$  versus  $\ln(\text{available irradiance})$  regressions derived from IS and SIS measurements were not significantly different. Differences in available irradiance also apparently contributed to differences between short term IS and SIS treatments, although near surface differences may have been caused by differential ultraviolet suppression of photosynthesis. Water column composite photosynthesis-irradiance models derived from whole day SIS data were used to predict water column-integrated production at IS irradiance levels. These estimates of water column-integrated primary production were within 15% of those determined by conventional IS methods. The results provide justification for use of SIS incubation techniques to estimate primary production when IS measurements are not feasible.

Supported by: NSF Grants OCE88-01089 and OCE87-08958; and ONR Contracts N00014-88-K-0155 and N00014-85-K-0155.

WHOI Contribution No. 7320.

#### OVERVIEW: BEING THERE - THE ROLE OF *IN SITU* SCIENCE IN OCEANOGRAPHY

L. P. Madin

*In situ* approaches to biological, chemical and geological oceanography allow scientists to work directly in the ocean using diving, manned submersibles or robotic devices. An important characteristic of this *in situ* research is the immediacy of direct visual contact for observation, pattern recognition and control of manipulations. Many oceanographic questions must be investigated on more than one scale of time and space. *In situ* work is well suited to small scales, and permits access to environments that cannot be sampled or inspected remotely. Most importantly, these methods reveal aspects of biology, geology and chemistry which exist only *in situ*, and cannot be adequately reconstructed or understood without being seen as, and where, they are. With the continued development of robotic technology, the quality of "being there" should eventually become

an integral part of most oceanographic investigations.

Published in: *Marine Technology Society Journal*, 24(2):19-21, 1990.

Supported by: NSF Grant OCE88-18503.

WHOI Contribution No. 7387.

**CYTOCHROME P450E (P450IA1)  
INDUCTION AND INHIBITION IN  
WINTER FLOUNDER BY  
3,3',4,4'-TETRACHLOROBIPHENYL:  
COMPARISON OF RESPONSE IN FISH  
FROM GEORGES BANK AND  
NARRAGANSETT BAY**

*Emily Monosson and John J. Stegeman*

Induction of liver microsomal cytochrome P450 by 3,3',4,4'-tetrachlorobiphenyl (TCB) was evaluated in winter flounder from two different sites; one offshore (Georges Bank), and one coastal (Narrow River, Narragansett, Rhode Island). Immunoblot analysis of liver microsomes with monoclonal antibody 1-12-3 to scup P450E (P450IA1) revealed P450IA protein content of 0.01 nmol/mg in Georges Bank fish that were not treated with TCB. By comparison, untreated Narrow River fish had an 80-fold greater content of immunodetected P450IA protein, indicating a strong environmental induction in these fish. In Georges Bank fish the total (spectrophotometrically measured) microsomal P450 content and the content of P450IA protein were induced progressively by intraperitoneal doses of TCB ranging from 0.1-10.0 mg/kg. Ethoxyresorufin-O-deethylase specific activity (activity per mg protein) was also progressively induced, but the catalytic efficiency or turnover number, (i.e., activity/nmol P450IA) was less in fish given the greater doses of TCB. In Narrow River fish TCB-treatment resulted in no significant change (at  $P \leq 0.05$ ) in total microsomal P450 content or in P450IA protein content, although these tended to be less (total P450) or greater (P450IA) in fish given the greater doses. EROD activity per mg protein was less in Narrow River fish given greater TCB doses than in control fish. EROD activities per nmol of P450IA protein in control Narrow River fish were less than those in any treatment group of Georges Bank fish, and tended to diminish even further with TCB treatment. The results show that 3,3',4,4'-TCB induces P450IA in winter flounder, and that TCB acts in vivo to inhibit the activity of P450IA enzyme, by mechanisms not yet known. The lower catalytic efficiency of P450IA enzyme in Narrow River fish than in Georges Bank fish indicates that P450IA inhibition, whether caused by TCB or

some other agent, does occur in the environment. The data also indicate that prior condition, including existing environmental induction, can strongly influence the responses of P450IA protein to additional chlorobiphenyl exposure.

Supported by: EPA Cooperative Agreement CR-131155; and PHS Grants CA-44306 and ES-04220.

WHOI Contribution No. 7357.

**INITIAL CONTACT, EXPLORATION  
AND ATTACHMENT OF BARNACLE  
CYPRIDS SETTLING IN FLOW**

*Lauren S. Mullineaux and Cheryl Ann Butman*

Settlement responses of barnacle (*Balanus amphitrite*) cyprids to boundary-layer flows were examined in laboratory flume experiments. The leading-edge configuration of flat plates were altered in order to manipulate flows without changing surface topography or free-stream velocity. Settlement along the plates correlated strongly with downstream gradients in shear stress. Analyses of video images taken during the experiments indicate that cyprids first contact plates in regions where plate-ward advection is high, and subsequent exploratory movement along the plate is oriented with flow direction at the plate surface. After exploration, cyprids reject a surface more frequently in a fast ( $10 \text{ cm s}^{-1}$ ) mean-stream velocity than in a slow ( $5 \text{ cm s}^{-1}$ ) flow, but rejection occurs in shear stresses well below the threshold that would prevent attachment and exploration. A higher rejection rate does not result in lower settlement however, since contact rate is higher in fast than slow flows. The response of cyprids to flow thus appears to be a passive transport process during the initial contact stage of settlement, but an active behavioral response to flow direction and shear stress during later stages of exploration and attachment.

In Press: *Marine Biology*.

Supported by: ONR Grant N00014-89-J-1112; and Coastal Research Center.

WHOI Contribution No. 7419.

**BORROWED PROTEINS IN BACTERIAL  
BIOLUMINESCENCE**

*Dennis J. O'Kane, Bonnie Woodward, John Lee  
and Douglas C. Prasher*

A partial amino acid sequence of lumazine protein from *Photobacterium phosphoreum* was determined by gas-phase sequencing. Two

degenerate 17-mer oligonucleotide probes, deduced from the N-terminal sequence and from an internal amino acid sequence respectively, were used to screen a library of *P. phosphoreum* DNA inserted in  $\lambda 2001$ . Three  $\lambda$  clones that hybridized with both oligonucleotide probes were purified. The lumazine protein gene was localized to a 3.4 kb *Bam*HI/*Eco*RI fragment in the clone  $\lambda 75B$ . Nucleotide sequences for both strands of this fragment were determined by the dideoxy-chain termination method. The fragment contained an open reading frame, encoding a 189 residue protein, which had a predicted amino acid sequence that concurred with the partial sequence determined for lumazine protein. Considerable sequence similarity was detected between lumazine protein, the yellow fluorescence protein from *Vibrio fischeri*, and the  $\alpha$ -subunit of riboflavin synthetase (E. C. 2.5.1.9). A highly conserved sequence in lumazine protein corresponds to the proposed lumazine binding sites in the  $\alpha$ -subunit of riboflavin synthetase. Several secondary structure programs predict the conformation of this site in lumazine protein to be a  $\beta$ -sheet. This constraint permitted modeling of the potential interactions between the lumazine ligand and the apoprotein. A minimal model with three interactions between the ligand and the  $\beta$ -sheet structure is proposed which is consistent with the results of NMR and ligand binding studies.

In Press: *Proceedings of the National Academy of Sciences, USA*.

Supported by: American Cancer Society Grant NP-640.

WHOI Contribution No. 7540.

## SPATIAL AND TEMPORAL DISTRIBUTIONS OF PROCHLOROPHYTE PICOPLANKTON IN THE NORTH ATLANTIC OCEAN

R. J. Olson, S. W. Chisholm, E. R. Zettler,  
M. A. Altabet and J. A. Dusenberry

Extremely abundant red-fluorescing picoplankton cells, believed to be prochlorophytes, were recently revealed by seagoing flow cytometry, but the dim fluorescence of these tiny cells initially limited studies to the relatively highly pigmented cells near the bottom of the euphotic zone. Improvements in sensitivity of the flow cytometer now enable us to detect the prochlorophytes in surface waters as well. In the Sargasso Sea in May 1988 and May 1989, prochlorophytes were present throughout the upper water column and in fact we observed the highest concentrations in surface waters within the Gulf Stream. Further south, the prochlorophytes formed subsurface maxima; the

median depth of prochlorophyte (but not *Synechococcus*) populations followed the deepening of the nitracline. Prochlorophytes were not present in waters north of the Gulf Stream in May, although we had observed them there on a previous September cruise. Prochlorophytes were present year-round near Bermuda, with lowest concentrations in the winter, when *Synechococcus* was most numerous; the prochlorophytes appear to "bloom" later than the cyanobacterial picoplankton, after the onset of seasonal stratification. The latitudinal variations in prochlorophyte and *Synechococcus* distributions during spring resembled the seasonal pattern near Bermuda.

Published in: *Deep-Sea Research*, 37(6):1033-1051, 1990.

Supported by: NSF Grants OCE83-16616, OCE84-21041, OCE84-16964, OCE85-08032, OCE86-14332, OCE86-14488 and OCE87-17508; and ONR Contracts N00014-83-K-0661, N00014-84-C-0278 and N00014-87-K-0007.

WHOI Contribution No. 7330.

## PIGMENTS, SIZE AND DISTRIBUTION OF SYNECHOCOCCUS IN THE NORTH ATLANTIC AND PACIFIC OCEANS

R. J. Olson, S. W. Chisholm, E. R. Zettler and  
E. V. Armbrust

Dual-beam flow cytometry was used to analyze the distribution and optical characteristics of *Synechococcus* in the N. Atlantic and Pacific Oceans. The depth range over which *Synechococcus* cells were abundant was related to the depth of the nitrite maximum and the chlorophyll maximum, but was not significantly correlated with the depth of the surface isothermal layer. Dual-beam analysis of chromophore pigment types revealed that the majority of the populations were of the high-urobilin type; low-urobilin types, similar to the isolate WH7803, were found only in coastal waters where they almost always co-occurred with high-urobilin strains.

Phycoerythrin fluorescence intensity per cell increased dramatically with depth in the lower euphotic zone at all stations; at some open-ocean stations, very deep cells were as much as 100 times brighter than those at the surface. The maximal fluorescence intensity per cell was about the same at the coastal and oceanic stations, and the depth of maximal fluorescence was closely related to the depth of the nitrite maximum. At most stations, fluorescence per cell was constant throughout the mixed layer, but at some open-ocean stations it decreased continuously to the surface. The latter pattern suggests that mixing rates in these areas

are slow relative to the abilities of the cells to photoacclimate. A distinct diel pattern in forward-angle light scatter was observed in cells in the mixed layer over vast regions, which we hypothesize to be coupled to growth of the cells during daylight hours.

Published in: *Limnology and Oceanography*,  
35(1):45-58, 1990.

Supported by: NSF Grants OCE82-11525,  
OCE83-16616, OCE84-21041, OCE84-16964,  
OCE85-08032, OCE86-14332 and OCE86-14488;  
and ONR Contracts N00014-83-K-0661,  
N00014-84-C-0278 and N00014-87-K-0007.

WHOI Contribution No. 7331.

## ADVANCES IN OCEANOGRAPHY USING FLOW CYTOMETRY

*Robert J. Olson, Erik R. Zettler and  
Sallie W. Chisholm*

The development of flow cytometry as an oceanographic tool over the past decade has yielded a new perspective on plankton community structure. We are less tempted to regard all cells as identical, or inclined to model communities as black boxes, because of the application of flow cytometry to plankton ecology. It serves as a model example of technology-driven research, and illustrates the power of cross-disciplinary applications of existing technology. Biological oceanographers, who were previously limited to either bulk measurements of average community properties or to tedious and slow microscopic analyses, were presented with an exciting new tool with which they could obtain near-real-time, objective measurements of plankton communities on an individual cell basis. The ways in which this technology has been employed, and the ways in which it has shaped some of the research directions in our field, form the subject of this paper. We will review applications of this technology to oceanographic questions, and point out some directions in which the technology will need to develop further in order to fulfill its potential.

Supported by: NSF Grants OCE88-14332,  
OCE83-16616, OCE84-21041, OCE85-08032,  
OCE86-14488; and ONR Contracts  
N00014-83-K-0661, N00014-84-C-0278 and  
N00014-K-0007.

WHOI Contribution No. 7588.

## THE DYNAMICS OF A SIZE-CLASSIFIED BENTHIC POPULATION WITH REPRODUCTIVE SUBSIDY

*Mercedes Pascual and Hal Caswell*

This work presents a discrete time model for the dynamics of a size-classified benthic population with planktonic larvae. Recruitment, decoupled from local reproduction by larval dispersal, is represented in the model as an external subsidy to the local population. Analysis of the model reveals the importance of recruitment and growth plasticity in determining the stability of an equilibrium which always exists. Growth plasticity promotes stability while recruitment plays the opposite role. The stability results provide a scale to which observed levels of recruitment, mortality and growth can be compared, in terms of their effects on population dynamics.

In Press: *Theoretical Population Biology*, 39, 1991.

Supported by: NSF Grants BSR87-04936 and  
OCE89-00231; and DOE Grant  
DE-FG02-89ER60882.

WHOI Contribution No. 7300.

## THE LUMAZINE PROTEIN GENE IN *PHOTOBACTERIUM PHOSPHOREUM* IS LINKED TO THE *LUX* OPERON

*D. C. Prasher, D. O'Kane and B. Woodward*

The bioluminescent bacteria emit light in a broad spectral distribution with a spectral maximum in the range 472-505 nm. The emission maxima ( $\lambda_{max} = 475-486$  nm) from some strains of *Photobacterium phosphoreum* and *P. leiognathi* are blue-shifted with respect to the emission spectra ( $\lambda_{max} = \approx 495$  nm) from the in vitro reaction of their luciferases with FMNH<sub>2</sub>, aldehyde and oxygen alone. The lumazine protein (LumP) has been determined to be the emitter in these strains. The gene encoding lumazine protein from *P. phosphoreum* strain A13 has recently been cloned and sequenced. The gene was localized to a 3.4 kb *Bam*HI/*Eco*RI DNA fragment. After sequencing the entire fragment, a large open reading frame was discovered to run in the opposite direction from the LumP gene. The translation product of the open reading frame is shown here to have homology to the *luxC* gene of *Vibrio harveyi*. Of the 361 residues aligned, 204 are identical for 56.5% identity. *LuxC* of *P. phosphoreum*, *V. harveyi*, and *V. fischeri* is part of the *lux* operon. DNA sequence analysis of *luxC* and the upstream region has been reported from only the *Vibrio* species. In the region upstream to

*luxC*, *V. fischeri* contains the regulatory gene *luxI* while *Vibrio harveyi* contains an open reading frame encoding a protein of unknown function and no similarity to LumP.

Published in: *Nucleic Acids Research*, 18:6450, 1990.

Supported by: American Cancer Society Grant NP-640.

WHOI Contribution No. 7538.

## FIXATION AND DRYING OF DNA SEQUENCING GELS ON GLASS PLATES

Douglas Prasher and Bonnie Woodward

The enzymatic method of using Klenow or modified T7 polymerase to generate DNA sequence has traditionally utilized a <sup>32</sup>P or <sup>35</sup>S-labelled nucleotide. The molecules synthesized in vitro are separated via polyacrylamide gel electrophoresis. The positions of the DNA fragments are localized in the gel by placing X-ray film next to the gel.

The DNA sequence is determined directly from the band pattern produced on the film. The resolution of the band pattern can be improved if the gel is dried before exposing the X-ray film to it. A commonly used method of drying the gel involves transferring it to filter paper and then drying it on a vacuum gel dryer. Alternatively, the gel can be dried directly on one of the glass plates used to prepare and pour the gel. We describe a modification of the method described by Garoff and Ansorge (*Anal. Biochem.* 115:450, 1981) such that the process of drying sequencing gels on a glass plate is 100% effective, even for a novice.

Published in: *Biotechniques*, 8(4):391-393, 1990.

Supported by: WHOI Independent Study Award; American Cancer Society Grant NP-640.

WHOI Contribution No. 7539.

## DIEL PATTERNS OF MIGRATION, FEEDING, AND SPAWNING BY SALPS IN THE SUBARCTIC PACIFIC

Jennifer E. Purcell and Laurence P. Madin

The common pattern of diel vertical migration by zooplankton alternates diurnal quiescence at depth with nocturnal feeding near the surface. In contrast to this pattern, the pelagic tunicate *Cyclosalpa bakeri* feeds actively during the day at depths of 30 to 60 m, but ceases to feed after nighttime migration into the surface layer (< 30 m). This behavior cannot be explained satisfactorily by current hypotheses that vertical migration serves to reduce visual predation,

minimize photodamage, promote dispersion, reduce metabolic costs, or increase fecundity. We offer evidence that vertical migration of *C. bakeri* is part of their reproductive behavior. The nighttime ascent acts to concentrate the salps near the surface where spawning occurs, and filter-feeding ceases so that the swimming sperm are not trapped and ingested before they can enter the oviduct.

Supported by: NSF Grant OCE87-00776.

WHOI Contribution No. 7351.

## CHAETODERMA ARGENTEUM, A NORTHEASTERN PACIFIC APLACOPHORAN MOLLUSK REDESCRIBED (CHAETODERMOMORPHA, CHAETODERMATIDAE)

A. H. Scheltema, J. Buckland-Nicks and F.-S. Chia

*Chaetoderma argenteum* Heath 1911 has been collected in the northeast Pacific from Point Conception, California, to southeast Alaska between 70 and 600 m. Synonyms are *C. attenuata* Heath 1911 and *C. montereyensis* Heath 1911. Since 1960, several surveys have taken *C. argenteum* from the Santa Maria Basin, from off the Oregon coast, and from both offshore and inshore waters of southwest British Columbia in numbers large enough to provide material for experimental research.

*Chaetoderma argenteum* is redescribed and illustrated. It is distinguished from other *Chaetoderma* species of the east Pacific by the anterior trunk spicules, which are bent and thickened on each side of an abfrontal groove, and by the large radula cone, which is curved in lateral view.

In Press: *Veliger*.

Supported by: Partial Support, NSERC of Canada; and MMS Contract No. 14-35-0001-30484.

WHOI Contribution No. 7512.

## APLACOPHORA

A. H. Scheltema, M. Tscherkassky and A. M. Kuzirian

The anatomy of eighteen species of Aplacophora, many of them new, is described and illustrated by drawings, light microscopy, scanning electron microscopy (SEM), and transmission electron microscopy (TEM).

In Press: *Microscopic Anatomy of Invertebrates*, F. W. Harrison, ed., Wiley-Liss, New York.

Supported by: Partial Support, Conchologists of America, Inc.

WHOI Contribution No. 7401.

**HELICORADOMENIA JUANI N.G. N.SP., A  
PACIFIC HYDROTHERMAL VENT  
APLACOPHORA  
(MOLLUSCA, NEOMENIOMORPHA)**

*Amelie H. Scheltema and Alan M. Kuzirian*

*Helicoradomenia juani* n.g. n.sp. is found in large numbers at the northeast Pacific vent sites of Juan de Fuca Ridge, Explorer Ridge and Gorda Ridge. It is placed in the family Simrothiellidae based on radula morphology (distichous bars with paired ventral pockets) and separated from other genera in the family by the presence of solid epidermal spicules.

In Press: *Veliger*.

Supported by: Partial Support, Conchologists of America, Inc.

WHOI Contribution No. 7465.

**ON THE CHILDREN OF BENTHIC  
INVERTEBRATES: THEIR RAMBLINGS  
AND MIGRATIONS IN TIME AND  
SPACE**

*R. S. Scheltema*

The contemporary spatial distribution of benthic invertebrate species may be enlarged by the capacity to disperse while conversely limited by ecological constraints, i.e., by the physical and biologic factors that control survival and reproduction. Past historic events or "accidents" at various time scales also have contributed to the present geographic distribution of species or sometimes whole faunas, e.g., short-term physical catastrophes such as storms over hours or days, climatic and sea level changes over periods of thousands of years, the opening or closing of seaways and the drift of continents over geologic epochs. One principal means of dispersal among benthic temperate and tropical invertebrates is the transport of their planktonic larvae; rafting, adult migration and human intervention provide alternative or sometimes additional means. The scale at which human intervention is now possible can result in profound changes to benthic populations over very short time intervals, indeed such alterations may be equivalent to natural processes that have required thousands to millions of years.

Published in: *Environmental Quality and Ecosystem Stability, Environmental Quality, Israel Society for Ecology and Environmental Quality Science Publication*, E. Spanier, Y. Steinberger and M. Luria, eds., Jerusalem, Israel, Vol. IV-B:93-107, 1989.

Supported by: NSF Grant OCE86-14579.

WHOI Contribution No. 7301.

**PROKARYOTES AND THEIR HABITATS**

*Hans G. Schlegel and Holger W. Jannasch*

Updated and greatly extended chapter in this Handbook discussing recent research from about 600 references.

Supported by: NSF Grant OCE89-22854.

WHOI Contribution No. 7378.

**FIRE, FIRE EXCLUSION, AND  
SEASONAL EFFECTS ON THE  
GROWTH AND SURVIVAL OF TWO  
SAVANNA GRASSES**

*Juan F. Silva, Jose Raventos and Hal Caswell*

We followed the fate of seedlings and adult plants of two grass species: *Andropogon semiberbis* and *Sporobolus cubensis* in two plots, in a savanna community in western Venezuela. One plot was burnt at the end of the first dry season whereas the other was excluded of fire. The results expressed as probabilities of survival in the case of seedlings and as transition probabilities to different size classes and probabilities of death for adults, were subjected to log linear analysis. We considered the effects on seedling's fate of the following variables: treatment (burnt or excluded), season (dry or wet), and species. In the case of adults, the analysis included the effects of treatment and season, condition to the initial stage, for each species separately.

Seedlings of *S. cubensis* were more susceptible to fire and drought whereas *A. semiberbis* seedlings and adults were more susceptible for fire exclusion, and this treatment a higher cause of mortality than fire itself. Both species seem to depend on the occurrence of periodic fires for vigorous vegetative growth and seed production, but the negative responses of *A. semiberbis* to fire exclusion were faster. Differences between the two species suggest that *A. semiberbis* is a better colonizer under burnt savanna conditions, but that once established, *S. cubensis* resistance to unfavorable changes is higher.

In Press: *Acta Oecologica*.



Supported by: NSF Grant BSR87-04936; and EPA Grant CR-814895-01-1.

WHOI Contribution No. 7383.

## POPULATION RESPONSES TO FIRE IN A TROPICAL SAVANNA GRASS: AN ANALYSIS USING MATRIX MODELS

Juan F. Silva, Jose Raventos, Hal Caswell and Maria Cristina Trevisan

We used field data from our previous research on populations of *Andropogon semiberbis* to construct size-classified matrix population models for an annually burnt population and for a population protected from fire. We used these models to examine the effects of fire on population growth rate, stable size distributions, and reproductive value, and to simulate different fire regimes. The burnt population increases rapidly ( $\lambda = 1.2524$ ,  $r = 0.2251$ ), whereas the unburnt population declines to extinction ( $\lambda = 0.2762$ ,  $r = -1.2886$ ). Most of this difference is due to effects on the growth, survival, and reproduction of the smallest two size classes, which are shown by elasticity analysis to be the most important to population growth in both populations. The stable size and reproductive value distributions are similar in both models. Both deterministic and stochastic analyses reveal a critical frequency of fire (approximately 0.85) below which this species is unable to maintain itself. This apparent reliance on fire frequency suggests that the spread and evolution of this species has been closely related to human occupation of neotropical savannas.

In Press: *Journal of Ecology*.

Supported by: NSF Grant BSR87-04936; and EPA Grant CR-814895-01-1.

WHOI Contribution No. 7326.

## LARVAL DEVELOPMENT, RELATIONSHIPS, AND DISTRIBUTION OF *MANDUCUS MADERENSIS*, WITH COMMENTS ON THE TRANSFORMATION OF *M. GREYAE* (PISCES, STOMIIFORMES)

David G. Smith, Karsten E. Hartel and James E. Craddock

Larval development of *Manducus maderensis* is described for the first time and additional information is presented on the development of *M. greyae*. Relationships of *Manducus* and its close relative, *Diplophos*, are discussed based on larval pigmentation, transformation size, and the degree of development of annular mucosal intestinal folds. Distribution of *M. maderensis* is updated with extensive new material.

WHOI Contribution No. 7404.

## BACTERIAL BIOMASS AND HETEROTROPHIC ACTIVITY IN THE WATER COLUMN OF AN AMICTIC ANTARCTIC LAKE

Richard L. Smith and Brian L. Howes

Antarctic Dry Valley lake systems have several unique physical characteristics that make them unusual environments for aquatic microorganisms. The thick, permanent ice cover maintains a constant temperature within each lake which insulates the water column, reduces light penetration, prevents exchange of gases and nutrients between the water column and the atmosphere, and maintains a geochemically stratified water column in which solute movement is predominantly a diffusion-controlled process. Little is known about microorganisms in such systems, especially the planktonic bacteria. Our work has focused on enumerating and characterizing the total microbial populations within one of these lakes, Lake Fryxell.

The water column of this lake is composed of an upper aerobic zone with oxygen concentrations in excess of air equilibration and an anoxic zone that contains reduced compounds such as ammonium, hydrogen sulfide and methane. The oxycline has a very steep oxygen gradient; immediately beneath the oxic-anoxic interface there is a turbidity maximum partially due to high populations of large bacteria as compared to other portions of the water column. Adenylate energy charge values indicate extremely stressed conditions for these organisms; some EC values were characteristic of actively growing populations of microorganisms. Bacterial abundance was 2-3 times higher in the deeper, anoxic zones than in the aerobic zone which may be the result of grazing by protozoan populations in the aerobic zone. Heterotrophic activity was very low below 12 m and above 8 m (constituting 75% of the water column), however, no significant increases in heterotrophy were found in the depth intervals where photosynthesis was actively occurring.

Supported by: NSF Grant DPP89-18782.

WHOI Contribution No. 7441.

**IMMUNOHISTOCHEMICAL  
LOCALIZATION OF CYTOCHROME  
P450IA1 INDUCED BY**

**3,3',4,4'-TETRACHLOROBIPHENYL  
AND BY**

**2,3,7,8-TETRACHLORODIBENZOFURAN  
IN LIVER AND EXTRAHEPATIC  
TISSUES OF THE TELEOST  
(*STENOTOMUS CHRYSOPS* SCUP)**

*R. M. Smolowitz, M. E. Hahn and J. J. Stegeman*

The regulation of different cytochrome P450 forms and their functions in different organs and cell types could determine the susceptibility of those cells and organs to toxic effects of xenobiotics, including chemical carcinogenesis. Here we describe the cellular localization of cytochrome (P450E) P450IA1 induced in 10 major organs or organ systems of a marine vertebrate species, the fish, *Stenotomus chrysops* (scup). Scup were injected intraperitoneally with 3,3',4,4'-tetrachlorobiphenyl (TCB) at 1 mg/kg, or with 2,3,7,8-tetrachlorodibenzofuran (TCDF) at 3 µg/kg. Induction was verified by Western blot analysis of microsomes from selected organs (liver, kidney, and gill) using monoclonal antibody (MAb) 1-12-3 to scup P450IA1. The localization of P450E was subsequently determined in sections prepared by standard histological methods (10% buffered formalin fixation, paraffin embedding), and stained with MAb 1-12-3 and peroxidase-labelled second antibody. P450IA1 was induced in epithelial and endothelial cells in liver (including pancreatic tissue), kidney, gill, gut, spleen, testis, and ovary. Induction was also detected in endothelial cells but not other cell types in brain, spleen and heart. In heart, the staining was present in the endocardium as well as in endothelium of the coronary vasculature and great vessels. Although TCDF and TCB both induced P450E in various cells of all organs examined, the effect of TCB was in most cases greater than that of TCDF. This may be due to a relatively higher TCB dosage. A wider staining distribution was seen in gut, gill, kidney and gonad of TCB-treated fish, which might be explained by a greater penetration, or by excretion of parent TCB, as opposed to TCDF. In any case, the results show that these important environmental agents induce P450IA1 in generally similar patterns in all organs examined. The common finding of a strong induction of P450IA1 in endothelial cells in all organs supports the suggestion that endothelium may be a primary site of P450IA induction.

Published in: *Drug Metabolism and Disposition*,  
19(1):113-123, 1991.

Supported by: PHS Grants ES-04220 and CA-44306;  
Donaldson Charitable Trust; and Surdna  
Foundation.

WHOI Contribution No. 7390.

**STRUCTURE AND MORPHOLOGY OF  
MAGNETITE  
ANAEROBICALLY-PRODUCED BY A  
MARINE MAGNETOTACTIC  
BACTERIUM AND DISSIMILATORY  
IRON-REDUCING BACTERIA**

*N. H. C. Sparks, S. Mann, D. A. Bazylinski,  
D. R. Lovely, H. W. Jannasch and R. B. Frankel*

Intracellular crystals of magnetite synthesized by the magnetotactic vibroid organism, MV-1, and extracellular crystals of magnetite produced by the non-magnetotactic dissimilatory iron-reducing bacteria, designated GS-15, were examined using high resolution transmission electron microscopy, electron diffraction and <sup>57</sup>Fe Mössbauer spectroscopy. The magnetotactic bacterium contained a single chain of approximately 10 crystals aligned along the long axis of the cell. The crystals were essentially pure stoichiometric magnetite. When viewed along the crystal long axis the particles had a hexagonal cross-section whereas side-on they appeared as rectangles or truncated rectangles of average dimension, 53 x 35 nm. These findings are explained in terms of a three-dimensional morphology comprising a hexagonal prism of {110} faces which are capped and truncated by {111} end faces. Electron diffraction and lattice imaging studies indicated that the particles were structurally well-defined single crystals. In contrast, magnetite produced by the organism, GS-15, was irregular in shape and had smaller mean dimensions (14 nm). Single crystals were imaged but these were not of high structural perfection. These results highlight the influence of intracellular control on the crystallochemical specificity of bacterial magnetites. The characterization of these crystals is important in aiding the identification of biogenic magnetic materials in paleomagnetism and in studies of sediment magnetization.

Published in: *Earth and Planetary Science Letters*,  
98:14-22, 1990.

Supported by: NSF Grant OCE89-22854.

WHOI Contribution No. 6956.

## PREDATION ON PROTOZOA: ITS IMPORTANCE TO ZOOPLANKTON

Diane K. Stoecker and Judith McDowell Capuzzo

Protozoa are an important component of both the nano- and microplankton in marine and freshwater environments and are preyed upon by zooplankton, including suspension-feeding copepods, some gelatinous zooplankters and some first-feeding fish larvae. The clearance rates of suspension-feeding zooplankton for ciliates, in particular, are higher than for most phytoplankton. For at least some suspension-feeding zooplankton, protozoans are calculated to be quantitatively an important component of the diet during certain seasons. In laboratory studies, protozoan components in the diet appear to enhance growth and survival of certain life history stages or enhance fecundity. These data suggest that protozoans are qualitatively as well as quantitatively important in the diets of marine zooplankton.

Most studies of predation on Protozoa have focused on the euphotic zone in nearshore waters. Predation on Protozoa however, is expected to be particularly important both quantitatively and qualitatively in marine environments and seasons in which primary production is dominated by cells  $< 5 \mu\text{m}$  in size, such as nearshore environments after the spring phytoplankton bloom, in oligotrophic waters, and in environments dominated by detritus-dominated food webs, such as the deep sea. In detritus-dominated food webs, Protozoa may be a source of essential nutrients and may thus facilitate utilization of bacterial and detrital carbon by metazoan plankton.

Published in: *Journal of Plankton Research*,  
12(5):891-908, 1990.

Supported by: NSF Grant OCE86-00684.

WHOI Contribution No. 7385.

## RESPIRATION, PHOTOSYNTHESIS AND CARBON CYCLING IN PLANKTONIC CILIATES

Diane K. Stoecker and Ann E. Michaels

Release of  $^{14}\text{C}$  labelled carbon dioxide from uniformly-labelled cells was used to measure respiration by individual ciliates in 2h incubations. In a strictly heterotrophic ciliate, *Strombidium spiralis* (Leegaard, 1915), release of labelled carbon dioxide was equivalent to  $\sim 2.8\%$  of cell  $\text{C h}^{-1}$  at  $20^\circ\text{C}$ , and there was no difference between rates in the dark and light. In the chloroplast-retaining ciliates, *Laboea strobila* Lohmann, 1908, *Strombidium conicum* (Lohmann, 1908) Wulff,

1919 and *Strombidium capitatum* (Leegaard, 1915) Kahl, 1932, release of labelled carbon dioxide was less in the light than in the dark in experiments done at  $15^\circ\text{C}$ . In *L. strobila* release of radiolabel as carbon dioxide was equivalent to  $\sim 2.4\%$  of cell  $\text{C h}^{-1}$  in the dark but  $\sim 1\%$  at  $50 \mu\text{E m}^{-2} \text{s}^{-1}$ , an irradiance limiting to photosynthesis. In *S. conicum* release of radiolabel as carbon dioxide was equivalent to  $\sim 4.4\%$  of cell  $\text{C h}^{-1}$  in the dark but at an irradiance saturating to photosynthesis ( $250\text{--}300 \mu\text{E m}^{-2} \text{s}^{-1}$ ) there was no detectable release of labelled carbon dioxide. In *S. capitatum* release of radiolabel as carbon dioxide was equivalent to  $\sim 4.3\%$  of cell  $\text{C h}^{-1}$  in the dark but at an irradiance saturating to photosynthesis was  $\sim 2.4\%$  of cell  $\text{C h}^{-1}$ . These data, combined with data from photosynthetic uptake experiments, indicate that  $^{14}\text{C}$  uptake underestimates the total benefit of photosynthesis by 50% or more in chloroplast-retaining ciliates.

Supported by: NSF Grant OCE88-00684.

WHOI Contribution No. 7510.

## PHOTOSYNTHESIS IN MESODINIUM RUBRUM: PER CELL MEASUREMENTS AND COMPARISON TO COMMUNITY RATES

Diane K. Stoecker, Mary Putt, Linda H. Davis and  
Ann E. Michaels

The photosynthetic ciliate, *Mesodinium rubrum*, is a common component of the plankton in estuarine, coastal and offshore areas. Unusually high photosynthetic rates have been measured during visible blooms (red-waters) of this species, but little data were available on photosynthesis by *Mesodinium* during more routine conditions. We used single cell techniques to measure chlorophyll content and rates of photosynthesis in *Mesodinium* ( $16\text{--}18 \times 21\text{--}22 \mu\text{m}$  in size) that were part of mixed-species phytoplankton assemblages in small estuaries and salt ponds. The C: chl. *a* ratio for *Mesodinium* ranged from 47 to 78. Rates of photosynthesis ranged from 13 to  $88 \text{ pg C cell}^{-1} \text{ h}^{-1}$  [ $1.8$  to  $8.6 \text{ pg C (pg chl. } a)^{-1} \text{ h}^{-1}$ ] at saturating irradiance. The assimilation ratios (chlorophyll specific rate at saturating irradiance) were within the mid-range reported for bulk measurements made during *Mesodinium* red-waters and within the range reported for phytoplankton.  $I_k$  values for *Mesodinium* were  $\geq 275 \mu\text{E m}^{-2} \text{s}^{-1}$  in all experiments. At saturating irradiance, carbon fixation ranged up to a ca. 14% of body  $\text{C h}^{-1}$ . In our incubations, *Mesodinium* accounted for from  $< 1\%$  to  $\geq 70\%$  of the community primary production in surface water samples although at no time during our studies did it cause red-waters.

In Press: *Marine Ecology Progress Series*.

Supported by: NSF Grant OCE87-09961.

WHOI Contribution No. 7570.

## **PATTERNS OF SARCODINE FEEDING IN EPIPELAGIC OCEANIC PLANKTON**

*Neil R. Swanberg and David A. Caron*

The range of in situ prey composition was determined in marine planktonic acantharia, foraminifera, and radiolaria collected by divers, and quantitatively compared to the prey available, as determined by surface plankton hauls on cruises in the Florida Current, Gulf Stream and Sargasso Sea. A relatively large percentage of the sarcodines (60% of acantharia, 48% of foraminifera and 46% of radiolaria) had no detectable prey. Of those which had fed on identifiable prey, there was considerable overlap between sarcodine species in the types of prey captured. Nevertheless, some partitioning of food resources was evident. Foraminifera consumed greater numbers of diatoms and copepods than other prey types, radiolaria consumed more tintinnids and mollusc larvae, and acantharia consumed mostly tintinnids. Copepods and their nauplii dominated the biomass consumed for all three groups, though mollusc larvae were significant for both acantharia and radiolaria. The results of parametric univariate statistical analyses done on each major predator group and multivariate analysis on a species-by-species basis confirmed that there was evidence for some partitioning of prey resources among the major sarcodine predators. The partitioning appeared to follow primarily morphological rather than taxonomic criteria, however, and may have been at least partially a mechanical effect.

In Press: *Journal of Plankton Research*.

Supported by: NSF Grant OCE81-17715.

WHOI Contribution No. 7589.

## **A DATALOGGER TO IDENTIFY VOCALIZING DOLPHINS**

*Peter L. Tyack and Cheri A. Recchia*

A datalogger was developed to identify dolphins within socially interacting groups. Every 50 msec the logger stores data on the level and frequency of detected sound. Dataloggers are temporarily attached to dolphins by suction cups for data collection sessions lasting up to 45 minutes. Later computer analysis of data from the dataloggers reveals which dolphin produced each vocalization recorded during the session. Results from use of dataloggers with two captive bottlenose

dolphins (*Tursiops truncatus*) at the New England Aquarium in Boston are presented. The possible use of dataloggers with wild dolphins is discussed.

Supported by: ONR Contract N00014-87-K-0236.

WHOI Contribution No. 7586.

## **INDUCED CYTOCHROME P-450 IN INTESTINE AND LIVER OF SPOT (*LEIOSTOMUS XANTHURUS*) FROM A POLYCYCLIC AROMATIC HYDROCARBON-CONTAMINATED ENVIRONMENT**

*Peter A. Van Veld, Donna J. Westbrook,  
Bruce R. Woodin, Robert C. Hale, Craig L. Smith,  
Robert J. Huggett and John J. Stegeman*

Levels of total cytochrome P-450, of specific P-450 (determined immunologically with MAb 1-12-3 and referred to as P-450E) and ethoxyresorufin O-deethylase (EROD) were elevated in intestine and liver microsomes of spot (*Leiostomus xanthurus*) collected from the Elizabeth River, a polycyclic aromatic hydrocarbon (PAH) contaminated tributary of Chesapeake Bay. Fish were collected over a sediment PAH concentration gradient that ranged from 9 to 96,000 µg PAH/kg dry sediment. Intestinal P-450E was near the lower limits of detection in fish collected at the relatively clean sites but was elevated 80- to 100-fold in fish collected from contaminated sites. Intestinal EROD activity exhibited a similar trend. Liver P-450E and associated EROD activity was detectable in all samples and was induced approximately eight-fold at the most heavily contaminated site. Despite the sensitivity of the intestine to PAH inducing agents, intestinal P-450E levels did not correlate well with sediment PAH whereas liver P-450E did. Instead, the intestinal enzyme was induced to similar and high levels at all contaminated sites. The results suggest that the intestine plays an important role in the absorption and metabolism of dietary PAH and/or PAH type inducing agents and that intestinal P-450E may be a useful indicator of exposure to these compounds via the diet.

Published in: *Aquatic Toxicology*, 17:119-132, 1990.

Supported by: PHS Grants CA-44306 and ES-04220; and EPA Grant CR-813155.

WHOI Contribution No. 7332.

# THE APPLICATION OF A PEDIVELIGER OYSTER LARVAE BIOASSAY FOR DETERMINING THE TOXICITY OF CONTAMINATED MARINE AND ESTUARINE SEDIMENTS

K. A. Warner, J. McDowell Capuzzo,  
J. H. Gentile, H. L. Phelps and K. J. Scott

A sediment bioassay, that measures acute mortality and failure of metamorphosis in pediveliger larvae of the oysters *Crassostrea gigas* and *Crassostrea virginica*, was used to determine the toxicity of sediment-associated contaminants from the marine superfund site in New Bedford Harbor, MA. Pediveliger larval mortalities at stations NBH-7 and -8 were significantly different from each other, from station NBH-5 and the reference stations. There was excellent correspondence among station dependent patterns of acute mortality for the pediveliger larval bioassays and the amphipod, *Ampelisca abdita*. *C. gigas* metamorphosis which was 86% in reference sediment and 78% in seawater controls, decreased to 12% or less at NBH-stations. Metamorphosis of *C. virginica* pediveliger larvae in reference sediments was only 10-23% which precluded statistical comparison to NBH-sediments. The results from these studies suggest that the acute mortality response of the oyster pediveliger is of comparable sensitivity to the amphipod, and that pediveliger larval metamorphosis is a more sensitive response than acute mortality. Linear regressions of sediment PCB, copper, and chromium concentrations and acute mortality were significant for all three bioassay species. One cannot determine from these analyses, however, which contaminant or combination of contaminants was responsible for the observed toxicity.

Supported by: WHOI Summer Fellowship Program;  
and EPA Grant CR-814895-01.

WHOI Contribution No. 7576.

## RATES OF MOVEMENT AND SEDIMENTARY TRACES OF DEEP-SEA FORAMINIFERA AND MOLLUSCA IN THE LABORATORY

James R. Weinberg

Living calcareous foraminifera (*Laticarinina pauperata*), bivalves (*Nucula* sp., *Thyasira* sp.) and gastropods (*Frigidoalvania brychia*), from 775 m depth in the northwest Atlantic, were collected and maintained in the laboratory at 1 atm for up to 772 days in cups containing sediment and sea water at 5°C. Crawling rates, and sizes of burrows and traces in sediments were measured. Taxonomic groups differed in degree of movement

and in sizes and kinds of biogenic structures produced in sediments. Rates of movement at the substrate surface by *L. pauperata* and *F. brychia* were 12-16 and 150 mm individual<sup>-1</sup> day<sup>-1</sup>, respectively. These individuals were less than 4 mm in size. *L. pauperata* moved in and out of sediments, suggesting that in nature it may occupy a range of depths within the sediment. This study shows that it is feasible to measure movements of individual organisms from the continental slope in the laboratory without using chambers that replicate *in situ* pressure. Data from such laboratory studies could complement field studies.

Supported by: WHOI; and NOAA's National Undersea Research Center.

WHOI Contribution No. 7400.

## SOUND SCATTERING BY LIVE ZOOPLANKTON AND MICRONEKTON: EMPIRICAL STUDIES WITH A DUAL-BEAM ACOUSTICAL SYSTEM

Peter H. Wiebe, Charles H. Greene,  
Timothy K. Stanton and Janusz Burczynski

Measurements and analysis are presented of the backscattering of 420 kHz sound by 43 individual animals of representative zooplanktonic and micronektonic taxa. Direct measurements of an individual's target strength were made with a commercial dual-beam sonar system in an enclosure filled with seawater deployed off a dock at Friday Harbor, Washington. The dependence of target strengths upon individual length, wet weight, and dry weight was investigated. In addition, the target strength and statistical variations of echo amplitude due to variations in shape and orientation of the organism were compared with acoustic scattering models involving different shapes (the general shapes of the sphere, and straight and uniformly bent finite cylinders were used along with attempts to take into account roughness). We found that: 1) backscattering cross sections are proportional to volume of the organisms rather than area as would be predicted by a sphere scattering model, 2) mean target strength based on average backscattering cross section is best described by the bent cylinder model whose model series solution is truncated, and 3) the fluctuations of the echo amplitudes are well described by the Rice probability density function whose shape parameter is related to the randomly rough straight cylinder model. These extensive studies showed conclusively that the elongated animals scattered sound more like elongated targets than spherical ones, thus demonstrating the need for models more sophisticated than the spherical ones routinely used to date. The data and model analyses provide

a basis for devising future acoustical data acquisition and processing techniques for bioacoustical field studies.

Published in: *Journal of the Acoustical Society of America*, 88(5):2346-2360, 1990.

Supported by: ONR Contracts N00014-87-K-007 and N00014-89-J-1729; and NSF Grant OCE87-09962.

WHOI Contribution No. 7427.

**SUBJECT HEADING INDEX**  
**Department of Biology**  
**1990**

---

**ANIMAL BEHAVIOR**

|  |      |
|--|------|
| <i>Jelle Atema, Paul A. Moore, Laurence P. Madin, and Greg A. Gerhardt</i> ..... | B-1  |
| <i>S. Hacker and L. P. Madin</i> .....   | B-8  |
| <i>Jennifer E. Purcell and Laurence P. Madin</i> .....                           | B-16 |
| <i>Peter L. Tyack and Cheri A. Recchia</i> .....                                 | B-21 |

**BENTHIC ECOLOGY**

|  |      |
|--|------|
| <i>O. Giere, N. M. Conway, G. Gastrock, and C. Schmidt</i> ..... | B-7  |
| <i>Lauren S. Mullineaux and Cheryl Ann Butman</i> .....          | B-13 |
| <i>Mercedes Pascual and Hal Caswell</i> .....                    | B-15 |
| <i>R. S. Scheltema</i> .....                                     | B-17 |

**BENTHOS**

|   |      |
|---|------|
| <i>Hal Caswell</i> .....                              | B-2  |
| <i>Amelie H. Scheltema and Alan M. Kuzirian</i> ..... | B-17 |
| <i>R. S. Scheltema</i> .....                          | B-17 |
| <i>James R. Weinberg</i> .....                        | B-22 |

**BIOACOUSTICS**

|   |      |
|---|------|
| <i>Charles H. Greene, Peter H. Wiebe, Robert T. Miyamoto, and Janusz Burczynski</i> ..... | B-8  |
| <i>Peter L. Tyack and Cheri A. Recchia</i> .....  | B-21 |
| <i>Peter H. Wiebe, Charles H. Greene, Timothy K. Stanton, and Janusz Burczynski</i> ..... | B-22 |

**BIOCHEMISTRY**

|  |      |
|--|------|
| <i>Noellette Conway and Judith McDowell Capuzzo</i> .....                        | B-3  |
| <i>E. S. Gray, B. R. Woodin and J. J. Stegeman</i> .....                         | B-7  |
| <i>Mark E. Hahn and John J. Stegeman</i> .....                                   | B-9  |
| <i>Pamela J. Kloepper-Sams and John J. Stegeman</i> .....                        | B-11 |
| <i>Emily Monosson and John J. Stegeman</i> .....                                 | B-13 |
| <i>Dennis J. O'Kane, Bonnie Woodward, John Lee, and Douglas C. Prasher</i> ..... | B-13 |
| <i>R. M. Smolowitz, M. E. Hahn, and J. J. Stegeman</i> .....                     | B-19 |

**BIOGEOCHEMISTRY**

|  |      |
|--|------|
| <i>Heinrich D. Holland, George I. Smith, Holger W. Jannasch, Andrew G. Dickson,<br/>Zheng Miangping, and Ding Tiping</i> .....                   | B-9  |
| <i>Brian L. Howes and Richard L. Smith</i> .....   | B-10 |
| <i>Richard L. Smith and Brian L. Howes</i> .....   | B-18 |
| <i>Peter A. Van Veld, Donna J. Westbrook, Bruce R. Woodin, Robert C. Hale, Craig L. Smith,<br/>Robert J. Huggett, and John J. Stegeman</i> ..... | B-21 |

## **BIOGEOGRAPHY**

|  |      |
|--|------|
| <i>E. F. DeLong</i> .....  | B-4  |
| <i>Heinrich D. Holland, George I. Smith, Holger W. Jannasch, Andrew G. Dickson, Zheng Miangping, and Ding Tiping</i> ..... | B-9  |
| <i>R. J. Olson, S. W. Chisholm, E. R. Zettler, M. A. Altabet, and J. A. Dusenberry</i> .....                               | B-14 |
| <i>R. J. Olson, S. W. Chisholm, E. R. Zettler, and E. V. Armbrust</i> .....  | B-14 |
| <i>Robert J. Olson, Erik R. Zettler, and Sallie W. Chisholm</i> .....  | B-15 |
| <i>A. H. Scheltema, J. Buckland-Nicks, and F.-S. Chia</i> .....  | B-16 |
| <i>R. S. Scheltema</i> .....   | B-17 |

## **BIOLOGICAL/CHEMICAL/PHYSICAL INTERACTIONS**

|  |      |
|--|------|
| <i>Jelle Atema, Paul A. Moore, Laurence P. Madin, and Greg A. Gerhardt</i> ..... | B-1  |
| <i>Peter J. S. Franks and Donald M. Anderson</i> .....                           | B-6  |
| <i>Brian L. Howes and Richard L. Smith</i> .....                                 | B-10 |
| <i>Pamela J. Kloepper-Sams and John J. Stegeman</i> .....                        | B-11 |
| <i>Lauren S. Mullineaux and Cheryl Ann Butman</i> .....                          | B-13 |
| <i>Robert J. Olson, Erik R. Zettler, and Sallie W. Chisholm</i> .....            | B-15 |
| <i>Richard L. Smith and Brian L. Howes</i> .....                                 | B-18 |
| <i>R. M. Smolowitz, M. E. Hahn, and J. J. Stegeman</i> .....                     | B-19 |
| <i>Neil R. Swanberg and David A. Caron</i> .....                                 | B-21 |

## **BIOTECHNOLOGY**

|  |      |
|--|------|
| <i>Edward F. DeLong</i> .....  | B-4  |
| <i>Edward F. DeLong and Jyotsna Shah</i> .....   | B-5  |
| <i>Judith P. Kitchell, Saraswathy V. Nochur, Judith K. Marquis, Dennis A. Bazylnski, and Holger Jannasch</i> ..... | B-11 |

## **COMMUNITY ECOLOGY**

|  |      |
|--|------|
| <i>Hal Caswell</i> .....   | B-2  |
| <i>Hal Caswell and Joel E. Cohen</i> .....   | B-2  |
| <i>O. Giere, N. M. Conway, G. Gastrock, and C. Schmidt</i> .....                             | B-7  |
| <i>R. J. Olson, S. W. Chisholm, E. R. Zettler, M. A. Altabet, and J. A. Dusenberry</i> ..... | B-14 |
| <i>R. J. Olson, S. W. Chisholm, E. R. Zettler, and E. V. Armbrust</i> .....                  | B-14 |
| <i>Neil R. Swanberg and David A. Caron</i> .....   | B-21 |

## **DESCRIPTIVE/FUNCTIONAL MORPHOLOGY**

|   |      |
|---|------|
| <i>D. L. Distel, E. F. DeLong, and J. B. Waterbury</i> .....      | B-5  |
| <i>S. Hacker and L. P. Madin</i> .....                            | B-8  |
| <i>A. H. Scheltema, J. Buckland-Nicks, and F.-S. Chia</i> .....   | B-16 |
| <i>A. H. Scheltema, M. Tscherkassky, and A. M. Kuzirian</i> ..... | B-16 |
| <i>Amelie H. Scheltema and Alan M. Kuzirian</i> .....             | B-17 |

## **ECOSYSTEM STUDIES**

|  |      |
|--|------|
| <i>Peter J. S. Franks and Donald M. Anderson</i> .....                                       | B-6  |
| <i>Brian L. Howes and Richard L. Smith</i> .....   | B-10 |
| <i>R. J. Olson, S. W. Chisholm, E. R. Zettler, M. A. Altabet, and J. A. Dusenberry</i> ..... | B-14 |
| <i>R. J. Olson, S. W. Chisholm, E. R. Zettler, and E. V. Armbrust</i> .....                  | B-14 |
| <i>Richard L. Smith and Brian L. Howes</i> .....   | B-18 |



## **EVOLUTION**

|  |      |
|--|------|
| <i>E. F. DeLong</i> .....  | B-4  |
| <i>D. L. Distel, E. F. DeLong, and J. B. Waterbury</i> .....   | B-5  |
| <i>Guy Lenaers, Christopher Scholin, Yvonne Bhaud, Danielle Saint-Hilaire, and Michel Herzog</i> ..... | B-11 |
| <i>Dennis J. O'Kane, Bonnie Woodward, John Lee, and Douglas C. Prasher</i> .....                       | B-13 |
| <i>R. S. Scheltema</i> .....   | B-17 |

## **FISHERIES**

|  |      |
|--|------|
| <i>Diane K. Stoecker and Judith McDowell Capuzzo</i> ..... | B-20 |
|--|------|

## **FISHES**

|  |      |
|--|------|
| <i>James E. Craddock, Richard H. Backus, and Mary Ann Daher</i> .....  | B-4  |
| <i>Paul V. Dunlap and E. P. Greenberg</i> .....  | B-5  |
| <i>E. S. Gray, B. R. Woodin, and J. J. Stegeman</i> .....  | B-7  |
| <i>Mark E. Hahn and John J. Stegeman</i> .....   | B-9  |
| <i>Pamela J. Kloepper-Sams and John J. Stegeman</i> .....  | B-11 |
| <i>Emily Monosson and John J. Stegeman</i> .....   | B-13 |
| <i>David G. Smith, Karsten E. Hartel, and James E. Craddock</i> .....  | B-18 |
| <i>R. M. Smolowitz, M. E. Hahn, and J. J. Stegeman</i> .....   | B-19 |
| <i>Peter A. Van Veld, Donna J. Westbrook, Bruce R. Woodin, Robert C. Hale, Craig L. Smith, Robert J. Huggett, and John J. Stegeman</i> ..... | B-21 |

## **GENETICS**

|  |      |
|--|------|
| <i>Paul V. Dunlap and E. P. Greenberg</i> .....  | B-5  |
| <i>Guy Lenaers, Christopher Scholin, Yvonne Bhaud, Danielle Saint-Hilaire, and Michel Herzog</i> ..... | B-11 |

## **INSTRUMENTATION**

|  |      |
|--|------|
| <i>Jelle Atema, Paul A. Moore, Laurence P. Madin, and Greg A. Gerhardt</i> .....   | B-1  |
| <i>Charles H. Greene, Peter H. Wiebe, Robert T. Miyamoto, and Janusz Burczynski</i> .....  | B-8  |
| <i>Steven E. Lohrenz, Denis A. Wiesenburg, Charles R. Rein, Robert A. Arnone, Craig D. Taylor, George A. Knauer, and Anthony A. Knap</i> ..... | B-12 |
| <i>L. P. Madin</i> .....   | B-12 |
| <i>R. J. Olson, S. W. Chisholm, E. R. Zettler, M. A. Altabet, and J. A. Dusenberry</i> .....   | B-14 |
| <i>R. J. Olson, S. W. Chisholm, E. R. Zettler, and E. V. Armbrust</i> .....  | B-14 |
| <i>Robert J. Olson, Erik R. Zettler, and Sallie W. Chisholm</i> .....  | B-15 |
| <i>Peter L. Tyack and Cheri A. Recchia</i> .....   | B-21 |

## **LARVAL ECOLOGY**

|   |      |
|---|------|
| <i>Lauren S. Mullineaux and Cheryl Ann Butman</i> ..... | B-13 |
| <i>Mercedes Pascual and Hal Caswell</i> .....           | B-15 |
| <i>R. S. Scheltema</i> .....                            | B-17 |

## **LIFE HISTORY**

|                              |      |
|------------------------------|------|
| <i>Hal Caswell</i> .....     | B-1  |
| <i>R. S. Scheltema</i> ..... | B-17 |

## **MARINE MAMMALS**

|  |      |
|--|------|
| <i>Mark E. Hahn and John J. Stegeman</i> .....   | B-9  |
| <i>Peter L. Tyack and Cheri A. Recchia</i> ..... | B-21 |

## **MARINE POLLUTION**

|  |      |
|--|------|
| <i>Peter J. S. Franks and Donald M. Anderson</i> .....   | B-6  |
| <i>Mark E. Hahn and John J. Stegeman</i> .....   | B-9  |
| <i>Pamela J. Kloepper-Sams and John J. Stegeman</i> .....  | B-11 |
| <i>Emily Monosson and John J. Stegeman</i> .....   | B-13 |
| <i>R. M. Smolowitz, M. E. Hahn, and J. J. Stegeman</i> .....   | B-19 |
| <i>Peter A. Van Veld, Donna J. Westbrook, Bruce R. Woodin, Robert C. Hale, Craig L. Smith, Robert J. Huggett, and John J. Stegeman</i> ..... | B-21 |
| <i>K. A. Warner, J. McDowell Capuzzo, J. H. Gentile, H. L. Phelps and K. J. Scott</i> .....  | B-22 |

## **MATHEMATICAL ECOLOGY**

|   |        |
|---|--------|
| <i>Hal Caswell</i> .....  | B-1, 2 |
| <i>Hal Caswell and Joel E. Cohen</i> .....  | B-2    |
| <i>Hal Caswell and A. Meredith John</i> .....                                       | B-2    |
| <i>Mercedes Pascual and Hal Caswell</i> .....                                       | B-15   |
| <i>Juan F. Silva, Jose Raventos, and Hal Caswell</i> .....                          | B-17   |
| <i>Juan F. Silva, Jose Raventos, Hal Caswell, and Maria Cristina Trevisan</i> ..... | B-18   |

## **MICROBIAL ECOLOGY**

|  |      |
|--|------|
| <i>Siegfried Burggraf, Holger W. Jannasch, Barbara Nicolaus, and Karl O. Stetter</i> .....   | B-1  |
| <i>David A. Caron</i> .....  | B-1  |
| <i>N. Conway and J. McDowell Capuzzo</i> .....   | B-3  |
| <i>Noellette Conway and Judith McDowell Capuzzo</i> .....                                    | B-3  |
| <i>E. F. DeLong</i> .....  | B-4  |
| <i>Edward F. DeLong</i> .....  | B-4  |
| <i>D. L. Distel, E. F. DeLong, and J. B. Waterbury</i> .....                                 | B-5  |
| <i>O. Giere, N. M. Conway, G. Gastrock, and C. Schmidt</i> .....                             | B-7  |
| <i>Frederick E. Goetz and Holger W. Jannasch</i> .....                                       | B-7  |
| <i>Brian L. Howes and Richard L. Smith</i> .....   | B-10 |
| <i>Holger W. Jannasch</i> .....  | B-10 |
| <i>Bo Barker Jørgensen, Leon X. Zawacki, and Holger W. Jannasch</i> .....                    | B-10 |
| <i>R. J. Olson, S. W. Chisholm, E. R. Zettler, M. A. Altabet, and J. A. Dusenberry</i> ..... | B-14 |
| <i>R. J. Olson, S. W. Chisholm, E. R. Zettler, and E. V. Armbrust</i> .....                  | B-14 |
| <i>Robert J. Olson, Erik R. Zettler, and Sallie W. Chisholm</i> .....                        | B-15 |
| <i>Hans G. Schlegel and Holger W. Jannasch</i> .....   | B-17 |
| <i>Richard L. Smith and Brian L. Howes</i> .....   | B-18 |
| <i>Diane K. Stoecker and Judith McDowell Capuzzo</i> .....                                   | B-20 |
| <i>Diane K. Stoecker, Mary Putt, Linda H. Davis, and Ann E. Michaels</i> .....               | B-20 |
| <i>Neil R. Swanberg and David A. Caron</i> .....   | B-21 |

## **MICROBIAL GENETICS**

|   |     |
|---|-----|
| <i>Paul V. Dunlap and E. P. Greenberg</i> ..... | B-5 |
|---|-----|

## **MICROBIOLOGY**

|  |      |
|--|------|
| <i>Siegfried Burggraf, Holger W. Jannasch, Barbara Nicolaus, and Karl O. Stetter</i> .....                                     | B-1  |
| <i>E. F. DeLong</i> .....  | B-4  |
| <i>Edward F. DeLong</i> .....  | B-4  |
| <i>Edward F. DeLong and Jyotsna Shah</i> .....   | B-5  |
| <i>Paul V. Dunlap and E. P. Greenberg</i> .....  | B-5  |
| <i>Frederick E. Goetz and Holger W. Jannasch</i> .....   | B-7  |
| <i>Heinrich D. Holland, George I. Smith, Holger W. Jannasch, Andrew G. Dickson,<br/>Zheng Miangping, and Ding Tiping</i> ..... | B-9  |
| <i>Holger W. Jannasch</i> .....  | B-10 |
| <i>Bo Barker Jørgensen, Leon X. Zawacki, and Holger W. Jannasch</i> .....  | B-10 |
| <i>Judith P. Kitchell, Saraswathy V. Nochur, Judith K. Marquis, Dennis A. Bazylnski,<br/>and Holger Jannasch</i> .....         | B-11 |
| <i>Dennis J. O'Kane, Bonnie Woodward, John Lee, and Douglas C. Prasher</i> .....   | B-13 |
| <i>R. J. Olson, S. W. Chisholm, E. R. Zettler, M. A. Altabet, and J. A. Dusenberry</i> .....                                   | B-14 |
| <i>R. J. Olson, S. W. Chisholm, E. R. Zettler, and E. V. Armbrust</i> .....  | B-14 |
| <i>D. C. Prasher, D. O'Kane, and B. Woodward</i> .....   | B-15 |
| <i>N. H. C. Sparks, S. Mann, D. A. Bazylnski, D. R. Lovely, H. W. Jannasch, and R. B. Frankel</i> .....                        | B-19 |
| <i>Diane K. Stoecker and Ann E. Michaels</i> .....   | B-20 |

## **MODELLING**

|  |      |
|--|------|
| <i>Hal Caswell and A. Meredith John</i> .....              | B-2  |
| <i>Peter J. S. Franks and Donald M. Anderson</i> .....     | B-6  |
| <i>Juan F. Silva, Jose Raventos, and Hal Caswell</i> ..... | B-17 |

## **MOLECULAR BIOLOGY**

|  |      |
|--|------|
| <i>E. F. DeLong</i> .....  | B-4  |
| <i>Edward F. DeLong</i> .....  | B-4  |
| <i>Edward F. DeLong and Jyotsna Shah</i> .....                                   | B-5  |
| <i>D. L. Distel, E. F. DeLong, and J. B. Waterbury</i> .....                     | B-5  |
| <i>Paul V. Dunlap and E. P. Greenberg</i> .....                                  | B-5  |
| <i>Dennis J. O'Kane, Bonnie Woodward, John Lee, and Douglas C. Prasher</i> ..... | B-13 |
| <i>D. C. Prasher, D. O'Kane, and B. Woodward</i> .....                           | B-15 |
| <i>Douglas Prasher and Bonnie Woodward</i> .....                                 | B-16 |

## **PATHOLOGY**

|  |     |
|--|-----|
| <i>Edward F. DeLong and Jyotsna Shah</i> ..... | B-5 |
|--|-----|

## **PHYSIOLOGY**

|  |      |
|--|------|
| <i>N. Conway and J. McDowell Capuzzo</i> .....   | B-3  |
| <i>Noellette Conway and Judith McDowell Capuzzo</i> .....                                    | B-3  |
| <i>Paul V. Dunlap and E. P. Greenberg</i> .....  | B-5  |
| <i>O. Giere, N. M. Conway, G. Gastrock, and C. Schmidt</i> .....                             | B-7  |
| <i>E. S. Gray, B. R. Woodin, and J. J. Stegeman</i> .....                                    | B-7  |
| <i>R. J. Olson, S. W. Chisholm, E. R. Zettler, M. A. Altabet, and J. A. Dusenberry</i> ..... | B-14 |
| <i>R. J. Olson, S. W. Chisholm, E. R. Zettler, and E. V. Armbrust</i> .....                  | B-14 |
| <i>Diane K. Stoecker and Ann E. Michaels</i> .....   | B-20 |
| <i>Diane K. Stoecker, Mary Putt, Linda H. Davis, and Ann E. Michaels</i> .....               | B-20 |

## **PHYTOPLANKTON**

|  |      |
|--|------|
| <i>Peter J. S. Franks and Donald M. Anderson</i> .....   | B-6  |
| <i>Guy Lenaers, Christopher Scholin, Yvonne Bhaud, Danielle Saint-Hilaire, and Michel Herzog</i> .....   | B-11 |
| <i>Steven E. Lohrenz, Denis A. Wiesenburg, Charles R. Rein, Robert A. Arnone, Craig D. Taylor, George A. Knauer, and Anthony A. Knap</i> ..... | B-12 |
| <i>R. J. Olson, S. W. Chisholm, E. R. Zettler, M. A. Altabet, and J. A. Dusenberry</i> .....   | B-14 |
| <i>R. J. Olson, S. W. Chisholm, E. R. Zettler, and E. V. Armbrust</i> .....  | B-14 |
| <i>Robert J. Olson, Erik R. Zettler, and Sallie W. Chisholm</i> .....  | B-15 |
| <i>Diane K. Stoecker, Mary Putt, Linda H. Davis, and Ann E. Michaels</i> .....   | B-20 |

## **PHYTOPLANKTON ECOLOGY**

|  |      |
|--|------|
| <i>Peter J. S. Franks and Donald M. Anderson</i> .....   | B-6  |
| <i>Steven E. Lohrenz, Denis A. Wiesenburg, Charles R. Rein, Robert A. Arnone, Craig D. Taylor, George A. Knauer, and Anthony A. Knap</i> ..... | B-12 |
| <i>R. J. Olson, S. W. Chisholm, E. R. Zettler, M. A. Altabet, and J. A. Dusenberry</i> .....   | B-14 |
| <i>R. J. Olson, S. W. Chisholm, E. R. Zettler, and E. V. Armbrust</i> .....  | B-14 |
| <i>Robert J. Olson, Erik R. Zettler, and Sallie W. Chisholm</i> .....  | B-15 |
| <i>Diane K. Stoecker and Ann E. Michaels</i> .....   | B-20 |
| <i>Diane K. Stoecker, Mary Putt, Linda H. Davis, and Ann E. Michaels</i> .....   | B-20 |

## **POPULATION ECOLOGY**

|   |        |
|---|--------|
| <i>David A. Caron</i> .....   | B-1    |
| <i>Hal Caswell</i> .....  | B-1, 2 |
| <i>Hal Caswell and A. Meredith John</i> .....                                       | B-2    |
| <i>E. F. DeLong</i> .....   | B-4    |
| <i>Mercedes Pascual and Hal Caswell</i> .....                                       | B-15   |
| <i>Juan F. Silva, Jose Raventos, and Hal Caswell</i> .....                          | B-17   |
| <i>Juan F. Silva, Jose Raventos, Hal Caswell, and Maria Cristina Trevisan</i> ..... | B-18   |

## **RECRUITMENT**

|   |      |
|---|------|
| <i>Lauren S. Mullineaux and Cheryl Ann Butman</i> ..... | B-13 |
| <i>Mercedes Pascual and Hal Caswell</i> .....           | B-15 |
| <i>R. S. Scheltema</i> .....                            | B-17 |

## **REMOTE SENSING**

|   |      |
|---|------|
| <i>Charles H. Greene, Peter H. Wiebe, Robert T. Miyamoto, and Janusz Burczynski</i> ..... | B-8  |
| <i>Robert J. Olson, Erik R. Zettler, and Sallie W. Chisholm</i> .....                     | B-15 |

## **SYSTEMATICS**

|  |      |
|--|------|
| <i>Guy Lenaers, Christopher Scholin, Yvonne Bhaud, Danielle Saint-Hilaire, and Michel Herzog</i> ..... | B-11 |
| <i>A. H. Scheltema, J. Buckland-Nicks, and F.-S. Chia</i> .....  | B-16 |
| <i>A. H. Scheltema, M. Tscherkassky, and A. M. Kuzirian</i> .....                                      | B-16 |
| <i>Amelie H. Scheltema and Alan M. Kuzirian</i> .....  | B-17 |

## **TAXONOMY**

|   |      |
|---|------|
| <i>E. F. DeLong</i> .....   | B-4  |
| <i>A. H. Scheltema, J. Buckland-Nicks, and F.-S. Chia</i> .....   | B-16 |
| <i>A. H. Scheltema, M. Tscherkassky, and A. M. Kuzirian</i> ..... | B-16 |
| <i>Amelie H. Scheltema and Alan M. Kuzirian</i> .....             | B-17 |

## **TOXICOLOGY**

|  |      |
|--|------|
| <i>Mark E. Hahn and John J. Stegeman</i> .....   | B-9  |
| <i>Pamela J. Kloepper-Sams and John J. Stegeman</i> .....  | B-11 |
| <i>Emily Monosson and John J. Stegeman</i> .....   | B-13 |
| <i>R. M. Smolowitz, M. E. Hahn, and J. J. Stegeman</i> .....   | B-19 |
| <i>Peter A. Van Veld, Donna J. Westbrook, Bruce R. Woodin, Robert C. Hale, Craig L. Smith,<br/>Robert J. Huggett, and John J. Stegeman</i> ..... | B-21 |
| <i>K. A. Warner, J. McDowell Capuzzo, J. H. Gentile, H. L. Phelps and K. J. Scott</i> .....  | B-22 |

## **ZOOPLANKTON**

|   |      |
|---|------|
| <i>R. S. Scheltema</i> .....  | B-17 |
| <i>Neil R. Swanberg and David A. Caron</i> .....  | B-21 |
| <i>Peter H. Wiebe, Charles H. Greene, Timothy K. Stanton, and Janusz Burczynski</i> ..... | B-22 |

## **ZOOPLANKTON ECOLOGY**

|   |      |
|---|------|
| <i>David A. Caron</i> .....   | B-1  |
| <i>Charles H. Greene, Peter H. Wiebe, Robert T. Miyamoto, and Janusz Burczynski</i> ..... | B-8  |
| <i>Jennifer E. Purcell and Laurence P. Madin</i> .....                                    | B-16 |
| <i>Diane K. Stoecker and Judith McDowell Capuzzo</i> .....                                | B-20 |
| <i>Diane K. Stoecker and Ann E. Michaels</i> .....  | B-20 |
| <i>Neil R. Swanberg and David A. Caron</i> .....  | B-21 |

**DEPARTMENT OF CHEMISTRY**

**Frederick L. Sayles, Chairman**

**CHEMISTRY**



## GEOCHEMISTRY

### ARAGONITE AND MAGNESIAN CALCITE FLUXES TO THE DEEP SARGASSO SEA

Victoria J. Fabry and Werner G. Deuser

Aragonite and magnesian calcite fluxes were estimated from a 14-month series of sediment trap samples from depths of 500, 1500, and 3200 m in the Sargasso Sea. No significant difference with depth was observed in fluxes of either carbonate phase. At 3200 m the mean aragonite flux was  $2.8 \text{ mg m}^{-2}\text{d}^{-1}$ , or 13% of the total  $\text{CaCO}_3$  flux. At all depths pteropods were the major source of aragonite, contributing more carbonate than heteropods by a factor of 3–24. Most of the pteropod aragonite occurred in the size fraction  $>0.5 \text{ mm}$ . At 3200 m more than half of the pteropod mass flux in the size fraction  $>0.5 \text{ mm}$  was comprised of four species: *Styliola subula*, *Clio pyramidata*, *Limacina inflata*, and *Cuvierina columnella*. The mean magnesian calcite flux at 3200 m was  $1.7 \text{ mg m}^{-2}\text{d}^{-1}$  or 8% of the total  $\text{CaCO}_3$  flux. The majority of the magnesian calcite (9–12 mole %  $\text{MgCO}_3$ ) occurred in the finest size fraction,  $<37 \mu\text{m}$ . Evidence suggests that bryozoans attached to floating *Sargassum* are the source of this magnesian calcite. The combined fluxes of aragonite and magnesian calcite accounted for 21–25% of the mean annual  $\text{CaCO}_3$  flux to 1500 and 3200 m.

In Press: *Deep-Sea Research*.

Supported by: NSF Grants OCE84-17909 and OCE87-16589.

WHOI Contribution No. 7493.

### MAHUKONA: THE MISSING HAWAIIAN VOLCANO

Michael O. Garcia, Mark D. Kurz, and  
David W. Muenow

New bathymetric and geochemical data indicate that a seamount west of the island of Hawaii, Mahukona, is a Hawaiian shield volcano. Mahukona has weakly alkalic lavas that are geochemically distinct. They have high  $^3\text{He}/^4\text{He}$  ratios (12–21 times atmosphere), and high  $\text{H}_2\text{O}$  and Cl contents, which are indicative of the early stage of development of Hawaiian volcanoes. The He and Sr isotopic values for Mahukona lavas are intermediate between those for lavas from Loihi and Mauna Loa volcanoes and may be indicative of a temporal evolution of Hawaiian magmas. Mahukona volcano became extinct at about 500

ka, perhaps before reaching sea level. It fills the previously assumed gap in the parallel chains of volcanoes forming the southern segment of the Hawaiian hotspot chain. The paired sequence of volcanoes was probably caused by the bifurcation of the Hawaiian mantle plume during its ascent, creating two primary areas of melting 30 to 40 km apart that have persisted for at least the past 4 m.y.

Published in: *Geology*, 18:1111-1114, 1990.

Supported by: NSF Grant OCE87-16970.

### MODELING PETROLEUM GENERATION IN SEDIMENTARY BASINS

John M. Hunt and R. J.-C. Hennet

This paper presents a graphical method for defining the oil and gas windows in sedimentary basins based on the Arrhenius equation. Time-temperature index (TTI) graphs for kerogen Types I, II, and III, plus a graph for the conversion of oil to gas, were constructed and tested in various basin configurations. Application of these graphs showed them to match the oil window indicated by other maturation parameters more closely than the Lopatin method with fast reacting kerogens. However, both methods defined approximately the same oil window in the examples tested for medium and slow reacting Type II kerogens and for a medium reacting Type I and Type III kerogen at moderate heating rates.

A large spread was found between the kinetic parameters of different Type I and Type II kerogens so it is not valid to use a fixed set of kinetic parameters within each of these groups. Type II kerogens ranged in activation energies (E) from 144 kJ/mol to 218 kJ/mol. The kerogens with the highest sulfur contents had the lowest E values and were the fastest in generating oil, while the kerogens with the lowest sulfur contents had the highest E values and were the slowest in generating oil. Type I kerogens ranged from 194 to 269 kJ/mol due to other compositional differences.

A comparison of oil windows in a cratonic basin showed that the slowest reacting Type II kerogen required 2,800 m more of burial to generate oil compared to the fastest reacting Type II kerogen. The slowest Type I required 2,000 m more of burial compared to the fastest Type I to generate oil.

These graphs are simple and accurate enough to have wide application in making preliminary evaluations of the depth of the oil and gas windows in exploration areas.

In Press: *Productivity, Accumulation and Preservation of Organic Matter: Recent and*



*Ancient Sediments*, Jean K. Whelan and John W. Farrington, eds., Columbia University Press.

Supported by: DoE Grant DE-FG02-86ER13466.

WHOI Contribution No. 7346.

## MODELING OIL GENERATION WITH TIME-TEMPERATURE INDEX GRAPHS BASED ON THE ARRHENIUS EQUATION

*John M. Hunt, M. D. Lewan, and R. J.-C. Henket*

The time and depth of oil generation from petroleum source rocks containing Type II kerogens can be determined using time-temperature index (TTI) graphs based on the Arrhenius equation. Activation energies (E) and the frequency factors (A) used in the Arrhenius equation were obtained from hydrous pyrolysis experiments on rock samples in which the kerogens represent the range of Type II kerogen compositions encountered in most petroleum basins. The E and A values obtained were used to construct graphs which can define the beginning and end of oil generation for most Type II kerogens having chemical compositions in the range of these standards. Activation energies of these standard kerogens vary inversely with their sulfur content. The kerogen with the highest sulfur content had the lowest E value and was the fastest in generating oil while the kerogen with the lowest sulfur content had the highest E value and was the slowest to generate oil. These standard kerogens were designated as Types IIA, B, C and D based on decreasing sulfur content and corresponding increasing time-temperature requirements for generating oil.

The  $\sum TTI_{ARR}$  values determined graphically with these Type II kerogen standards in two basin models were compared with a computer calculation using 2,000 increments. The graphical method came within  $\pm 3\%$  of the computer calculation.

As Type II kerogens are the major oil generators in the world, these graphs should have wide application in making preliminary evaluations of the depth of the oil window in exploration areas.

In Press: *Bulletin of the American Association of Petroleum Geologists*.

Supported by: DoE Grant DE-FG02-86ER13466.

WHOI Contribution No. 7318.

## ISOTOPIC EVOLUTION OF MAUNA LOA VOLCANO

*Mark D. Kurz and David P. Kammer*

In an effort to understand the temporal helium isotopic variations in Mauna Loa volcano, we have

measured helium, strontium and lead isotopes in a suite of Mauna Loa lavas that span most of the subaerial eruptive history of the volcano. These data are important because Mauna Loa is the largest volcano on the planet and the exposed basalts provide ideal samples of the shield building tholeiitic stages of Hawaiian volcanism. The lavas range in age from historical flows to the Ninole basalts which are thought to be several hundred thousand years of age. Most of the samples younger than 30,000 years in age (Kau Basalts) are radiocarbon dated flows, while the samples older than 30,000 years are stratigraphically controlled (Kahuku and Ninole Basalts). The data reveal a striking change in the geochemistry of the lavas approximately 10,000 years before present. The lavas older than 10,000 years are characterized by high  $^3\text{He}/^4\text{He}$  ( $\sim 16$ – $20$  times atmospheric), higher  $^{206}\text{Pb}/^{204}\text{Pb}$  ( $\sim 18.2$ ), and lower  $^{87}\text{Sr}/^{86}\text{Sr}$  ( $\sim 0.70365$ ) ratios than the younger samples (having He, Pb and Sr ratios of approximately 8.5 x atmospheric, 18.1, and 0.70390, respectively). There are also smaller but significant isotopic variations between historical lava flows. The isotopic variations are on shorter time scale (100 to 10,000 years) than has previously been observed for Hawaiian volcanoes, and demonstrate the importance of geochronology and stratigraphy to geochemical studies. The data show consistency between all three isotope systems, which suggests that helium is correlated with the other isotopes, that the variations are not related to magma chamber degassing processes, and that helium is not decoupled from the other isotopes. The Mauna Loa isotopic variations could be explained by mixing between a plume type source, similar to Loihi, and an asthenospheric source with helium isotopic composition close to MORB and elevated Sr isotopic values. An asthenospheric source, or variation within the plume source, is considered more likely than lithospheric sources due to the elevated  $^{87}\text{Sr}/^{86}\text{Sr}$  ratios in the recent Kau Basalts. Consideration of the Mauna Loa data in conjunction with results from other Hawaiian volcanoes suggests that more than three different mantle sources are required to explain the isotopic characteristics of Hawaiian volcanism.

In Press: *Earth and Planetary Science Letters*.

Supported by: NSF Grant OCE87-16970.

WHOI Contribution No. 7399.

# THE ORGANIC GEOCHEMISTRY OF PERU MARGIN SURFACE SEDIMENT: II. PALEOENVIRONMENTAL IMPLICATIONS OF HYDROCARBON AND ALCOHOL PROFILES

Mark A. McCaffrey, John W. Farrington, and  
Daniel J. Repeta

We assess the utility of sedimentary hydrocarbons and alcohols as indicators of short-term changes in depositional conditions in the coastal Peruvian upwelling regime at 15°S. The distribution of 35 lipids (*n*-alkanes, *n*-alkanols, hopanols, keto-ols, lycopane, phytol, stenols, stanols, sterenes, and tetrahymanol) in a 1 m dated core from 253 m water depth are interpreted by: (1) a principal components analysis, and (2) a consideration of individual source-specific biomarkers. Profiles of odd-carbon-number *n*-alkanes (C<sub>25</sub>–C<sub>33</sub>) and even-carbon-number *n*-alkanols (C<sub>24</sub>–C<sub>28</sub>) reflect changes in the input of terrigenous sediment relative to marine sediment during deposition, as indicated by the correlations between these lipids and inorganic indicators of terrigenous clastic debris. The *n*-alkane carbon preference index (CPI) provides a less-sensitive record of fluctuations in the terrestrial input than the concentration profiles of the individual *n*-alkanes and *n*-alkanols, and these lipids are *not* well-correlated with the historical El Niño record. The similarity of all the stenol profiles measured and the lack of concordance between these profiles and inorganic indicators of terrigenous input suggest that any fluctuations in the abundance of higher-plant stenols are obscured by the larger marine contribution of these compounds. Similarities between the profiles of total organic carbon (TOC) and cholesterol/cholesterol are consistent with stenol hydrogenation being influenced by the sediment redox conditions.

In Press: *Geochimica et Cosmochimica Acta*, 55, 1991.

Supported by: NSF Grant OCE88-11409.

WHOI Contribution No. 7374.

## MEASUREMENTS OF HELIUM IN ELECTROLYZED PALLADIUM

John R. Morrey, Marc W. Caffee,  
Harry Farrar IV, Nathan J. Hoffman,  
G. Bryant Hudson, Russell H. Jones,  
Mark D. Kurz, John Lupton, Brian M. Oliver,  
Brian V. Ruiz, John F. Wacker, and A. van Veen

The results of a double-blind, cold fusion experiment are reported, in which six laboratories

measured the helium content of five identically shaped 2-mm-diam × 10-cm-long palladium rods supplied by Fleischmann and Pons. Three rods were initially implanted with <sup>4</sup>He. Before analysis, three of the rods had served as cathodes during electrolysis in cold fusion experiments: two in 0.1 M LiOD, and one in 0.1 M LiOH. The other two, one implanted and one not, served as references. The major observations are as follows:

1. All the materials, including the as-received palladium stock, contained easily measured quantities of <sup>4</sup>He—well above amounts normally found in high-purity palladium.
2. The <sup>4</sup>He could be totally removed from at least two of the materials, including the as-received palladium stock, by surface etching the samples to a depth of ~25 μm.
3. Helium implanted by alpha-particle bombardment remained in the electrodes throughout the electrolysis.
4. No <sup>3</sup>He was measured above detection limits in any of the materials by any of the six laboratories.

It cannot be proven that the minimal excess heating in one of the rods reported by Fleischmann and Pons can be attributed to the formation of <sup>4</sup>He, although the possibility that some <sup>4</sup>He could have formed during electrolysis cannot be ruled out. If <sup>4</sup>He were generated, the mechanism must be surface related, not bulk related. No attempt was made to measure any helium or tritium that might have left the cathode surface as gas during electrolysis. The results presented cannot, unfortunately, confirm the existence or nonexistence of cold fusion via helium production. However, they provide a basis for follow-on experiments that should lead to a final conclusion.

Published in: *Fusion Technology*, 18(4):659–668, 1990.

## RARE EARTH ELEMENTS IN MARINE SEDIMENTS AND GEOCHEMICAL STANDARDS

Edward R. Sholkovitz

A comparison was made of sediment dissolution methods used for analysis of rare earth elements (REE) and major elements (Fe, Al, Ti, Zr, P). Dissolution by HF and lithium metaborate fusion were compared in seven Geochemical Standards and twenty marine sediments.

Using HF dissolution of shelf and slope sediments, this author previously observed that these marine sediments were significantly depleted in heavy REE (HREE) relative to the crustal abundance (*i.e.*, shale). This observation, plus published REE compositions of river particles lead to the conclusion that the riverine input of

particles to the oceans cannot be assumed to have the crustal abundance for REE.

Comparisons of fusion (total) to HF dissolutions for marine sediments show that the latter method misses between 20% and 100% of the HREE (i.e., Dy, Er, Yb, Lu) and large percentages of Zr. In contrast, fusion and HF dissolutions yield similar concentrations for the light (La, Ce, Nd) and middle (Eu, Gd) REE and other major elements. The fusion data show that the marine sediments are more similar in REE composition to shales than previously reported by this author who underestimated the contribution of HF-insoluble residues to the concentration of HREE. The heavy mineral zircon is the most likely cause of this observation. Zircons, known to be enriched in HREE were identified by X-ray diffraction as a major component of the HF-insoluble residues. Geochemical standards also have a significant, but usually smaller fraction of their HREE associated with HF-insoluble phases. These compositional differences have significance with respect to interpreting river inputs, oceanic abundances and diagenesis of REE.

Published in: *Chemical Geology*, 88:333-347, 1990.

Supported by: NSF Grant OCE85-15695.

WHOI Contribution No. 7379.

## LIPID GEOCHEMISTRY OF REMOTE MARINE AEROSOLS IN SOUTHERN OCEAN AIR

*Marie-Alexandrine Sicre, Edward T. Peltzer, and Robert B. Gagosian*

Aerosol samples collected on Ninety Mile Beach on the west coast of the North Island of New Zealand were analyzed for three classes of naturally occurring organic compounds. These compounds are major components of the epicuticular waxes of terrestrial plants. The hydrocarbon and fatty alcohol compound classes have provided important biomarker information in previous studies. In this study, we have added the long-chain n-aldehydes. The source marker information contained in these three compound classes provides a clear signal of the terrestrial source of the aerosols. In the eight samples analyzed, we have identified three distinct regional source signatures for these aerosols depending upon their origin: Southern Ocean air, New Zealand or Australia. These source identifications were entirely consistent with isentropic air mass trajectories. Impactor studies provided additional information as to the source of the aerosols and the mode of introduction of the material into the atmosphere. This approach clearly identified marine hydrocarbons and fatty

alcohols in the aerosol which were obscured by the strong terrestrial signature in bulk aerosol samples.

Supported by: NSF Grants OCE87-16954 and OCE84-06666.

WHOI Contribution No. 7317.

## PHOTOSYNTHESIS, $\text{CaCO}_3$ DEPOSITION AND THE GLOBAL CARBON CYCLES

*C. Steven Sikes and Victoria J. Fabry*

The principal groups of photosynthetic, calcifying organisms in the oceans are: (1) reef-building corals that are replete with symbiotic algae; (2) calcareous algae often associated with reef communities; (3) planktonic foraminifera that have symbiotic algae; and (4) coccolithophorids, the group that may produce the greatest amount of  $\text{CaCO}_3$  on a global basis. Among the coccolithophorids, *Emiliana huxleyi* is the most abundant and widely distributed. The purpose of this paper is to review the general aspects of the relationship between photosynthesis and calcification, using *E. huxleyi* as a model system. The possibilities for interactions between photosynthetically-linked calcification and atmospheric  $\text{CO}_2$  are discussed. Available evidence suggests that photosynthetically-enhanced coccolith formation is a sink for oceanic dissolved inorganic carbon (DIC) that may act as a demand on atmospheric  $\text{CO}_2$  as well, due to the way that cells utilize DIC and its fate after fixation. The size of this sink is unknown, however.

In Press: *Photosynthetic Carbon Metabolism and Regulation of Atmospheric  $\text{CO}_2$  and  $\text{O}_2$* .

Supported by: NSF Grant OCE87-16589.

WHOI Contribution No. 7488.

## TEMPERATURE MEASUREMENTS DURING INITIATION AND GROWTH OF A BLACK SMOKER CHIMNEY

*M. K. Tivey, L. O. Olson, V. W. Miller, and R. D. Light*

Black smoker chimneys are hollow spires formed by mineral deposition at sea-floor hydrothermal vent sites. They grow in two stages: formation of a sulphate-dominated wall (stage I), followed by precipitation of sulphide minerals on the inner side, and in pore spaces, of the wall (stage II). Here we present the results of an *in-situ* 46-day experiment which allows direct observation of stage I growth processes by monitoring wall and fluid temperatures. The position and thickness of

stage I chimney walls can change on short timescales, and are controlled by the dynamics of fluid flow both during and after initial wall emplacement. The temperature in the main flow remained stable at  $353 \pm 2^\circ\text{C}$  throughout the experiment, including the period during which the chimney wall was constructed. Six thermocouples, however, recorded maximum temperatures between  $365$  and  $405^\circ\text{C}$ , which are significantly higher than most exit temperatures documented previously. These latter observations bear on the question of the maximum temperatures attainable in sea-floor hydrothermal systems.

Published in: *Nature*, 346(6279):51-54, 1990.

Supported by: Woods Hole Oceanographic Institution and NSF Grant OCE89-16643.

WHOI Contribution No. 7422.

### DIFFUSION OF COSMOGENIC $^3\text{He}$ IN OLIVINE AND QUARTZ: IMPLICATIONS FOR SURFACE EXPOSURE DATING

*T. W. Trull, M. D. Kurz and W. J. Jenkins*

The *in situ* production of  $^3\text{He}$  in surface rocks by cosmic ray induced nuclear reactions offers an important geochronological tool. To evaluate helium loss problems in this technique, cosmogenic  $^3\text{He}$  diffusivities were measured in quartz and olivine by incremental heating at  $150$ – $600^\circ\text{C}$ . Arrhenius temperature dependences were observed in both minerals with similar activation energies ( $E_a = 25 \pm 4$  Kcal/mole,  $\log D^\circ = -3.7 \pm 0.9$  in olivine and  $E_a = 25.2 \pm 0.9$ ,  $\log D^\circ = +0.2 \pm 0.4$  in quartz) and imply very low diffusivities when extrapolated to environmental temperatures (less than  $10^{-18}$   $\text{cm}^2/\text{s}$  in quartz and  $10^{-22}$   $\text{cm}^2/\text{s}$  in olivine at  $20^\circ\text{C}$ ). These low diffusivities suggest helium loss will not significantly affect cosmogenic helium exposure dating for timescales on the order of  $10^6$  years in quartz and  $10^9$  years in olivine, provided large (2 mm) sample grains are used. Exposure ages obtained with smaller grains need to be corrected for diffusive helium loss and equations are provided for this purpose.

Cosmogenic  $^3\text{He}$  diffuses more than 100 times faster than trapped magmatic  $^3\text{He}$  in olivine or radiogenic  $^4\text{He}$  in quartz. The mechanisms responsible for these differences have yet to be determined, but may involve both trapping processes at mineral defects and enhanced mobility associated with spallation produced crystal damage. Therefore, it is possible that helium diffusivities may depend on a sample's cosmic ray exposure or radiogenic production history. Whatever the precise mechanism, the higher mobility of  $^3\text{He}$  suggests that incremental heating

will be useful in separating cosmogenic helium from inherited or radiogenic helium in future studies.

Comparison of the diffusivity results with total cosmogenic  $^3\text{He}$  contents of different quartz size fractions for an Antarctic quartzite suggests that He loss may have occurred more rapidly than predicted by the laboratory measurements. Nonetheless, retention of cosmogenic  $^3\text{He}$  in the sample is quite high (equivalent to more than a million years of exposure) and cosmogenic  $^3\text{He}$  geochronology is feasible in this and other quartz containing rocks.

In Press: *Earth and Planetary Science Letters*.

Supported by: NSF Grants EAR88-3783 and DPP88-17406.

WHOI Contribution No. 7489.

## INSTRUMENTS

### A BENTHIC CHAMBER WITH ELECTRIC STIRRER MIXING

*Wayne Dickinson and F. L. Sayles*

Benthic chambers incorporating electric stirrer mixing have been designed and tested and have proven reliable during seven 18–31 day, 4300 m ocean deployments. The chambers are 21 cm diameter by 31 cm long acrylic tubes sealed with pvc lids. A stepper motor and pressure tolerant electronics contained within the lids are magnetically coupled to stirring paddles to provide mixing within the chambers. The stirrers exhibit stable mixing rates and uniform speeds between chambers, require less than  $1/3$  watt of power, and are maintenance free. Laboratory calibration of stirring and mixing characteristics demonstrate the areal averaged equivalent seawater-sediment boundary layer thickness can be set to agree with *in situ* measured values.

Supported by: NSF Grant OCE87-11962.

WHOI Contribution No. 7462.

### THE ROLAI<sup>2</sup>D LANDER: A BENTHIC LANDER FOR THE STUDY OF EXCHANGE ACROSS THE SEDIMENT-WATER INTERFACE

*F. L. Sayles and W. H. Dickinson*

A free vehicle benthic lander designed to characterize reaction at and transport across the sediment-water interface has been built, tested, and is being utilized in deep sea experiments. The lander has been designed for long duration

deployments (>30 days) in order to measure the small fluxes and low reaction rates typical of most of the deep ocean. To characterize fluxes and determine the nature and sites of reactions producing them, the lander autonomously collects sediment and pore water samples as well as samples from benthic chambers. Tracers can be released into the chambers to define such processes as non-diffusive exchange across the interface. Pore water samples are collected with millimeter scale resolution in the uppermost sediments to determine diffusive fluxes across the interface. O<sub>2</sub> concentration in the chambers is measured *in-situ* and standardized relative to bottom water at preset times throughout a deployment. To avoid disturbance of material at and on the interface during landing, the lander buoyancy becomes positive ~10 m above the bottom and the instrument is winched onto the sea floor at a fixed rate of 3 m/min.

The lander has been deployed a number of times in deep water (4400 m) off Bermuda. The results obtained verify the operation of the various systems and confirm the need for long deployments in the acquisition of accurate flux data in mid-ocean environments.

In Press: *Deep-Sea Research*.

Supported by: NSF Grant OCE87-11962.

WHOI Contribution No. 7409.

## ORGANIC AND BIOLOGICAL CHEMISTRY

### THE NATURE AND DISTRIBUTION OF FLUORESCENT DISSOLVED ORGANIC MATTER IN THE BLACK SEA AND THE CARIACO TRENCH

*Paula G. Coble and Robert B. Gagosian*

Depth profiles of some of the chemical components of dissolved fluorescence in the Black Sea and the Cariaco Trench were measured using ion-pairing high performance liquid chromatography. Both individual compounds and unresolvable complex material were observed in the fraction retained by C18-bonded silica adsorbent. Identifiable individual compounds included riboflavin, lumiflavin, lumichrome, FAD, and FMN. Maxima in riboflavin concentrations occurred in association with maxima in chl *a*, bchl *e*, ETS, and bacterial cell numbers. The concentration of the complex material increased with depth, corresponding to an increase in the total dissolved fluorescence. The relative contribution of individual fluorescent compounds to total extractable fluorescence decreased from 13% at the surface to 2% at 270 m.

In Press: *Black Sea Oceanography*, E. Izdar and J. M. Murray, eds. NATO ARW Cesme, Turkey, 1989.

Supported by: NSF Grant OCE87-001368.

WHOI Contribution No. 7340.

### 3-D FLUORESCENCE CHARACTERIZATION OF MARINE DOM FROM THE BLACK SEA: SOURCE SPECIFICITY AT LAST?

*Paula G. Coble, Sarah A. Green, Neil V. Blough,  
and Robert B. Gagosian*

The natural fluorescence properties of seawater provide a means of elucidating the complex chemical composition and diverse sources of dissolved organic matter (DOM) in sea water. The positions of excitation and emission maxima for a wide range of natural water samples show remarkable similarity. High-sensitivity fluorescence spectroscopic studies have shown recently that emission maxima for marine and coastal waters differ by 20 nm when the excitation wavelength is 313 nm. Here we present evidence from three-dimensional excitation emission matrix (EEM) spectroscopy that at least three fluorophores are present in waters of the Black Sea. Distinct changes in the relative abundance of these fluorophores are observed as a function of depth. We suggest that three-dimensional fluorescence spectroscopy can be used to distinguish between different types and sources of DOM in natural waters. These findings may have important applications in the field of remote sensing of phytoplankton pigments. For example, a better understanding of the sources of DOM components will help in correcting remotely sensed data for the presence of gelbstoff (yellow-coloured DOM, which plays an important part in radiation absorption by surface waters).

Published in: *Nature*, 348:432-435, 1990.

Supported by: NSF Grant OCE87-01386.

WHOI Contribution No. 7444.

### IDENTIFICATION OF A DEEP MARINE SOURCE OF PARTICULATE ORGANIC CARBON USING BOMB <sup>14</sup>C

*Ellen R. M. Druffel and Peter M. Williams*

The influx of bomb radiocarbon (<sup>14</sup>C) into the oceanic food chain has been evaluated by radiocarbon dating of pelagic organisms in the North Pacific. These studies found a significant gradient with depth of Δ<sup>14</sup>C (per mil deviation from the 'standard' activity of nineteenth century

wood). Such a gradient is not expected according to long-standing assumptions about carbon cycling in the water column; instead, one could expect the  $\Delta^{14}\text{C}$  of organisms throughout the water column to have become equal to that in surface-water dissolved inorganic carbon (DIC) by about 1970 (10–20 years after the production of bomb radiocarbon). Here we present  $\Delta^{14}\text{C}$  values measured in the profiles of suspended and sinking particulate organic carbon (POC) from an open-ocean site and a coastal basin. The  $^{14}\text{C}$  activity of suspended POC decreases significantly with depth, as is observed in organisms, whereas that of sinking POC is only slightly lower than that in surface DIC and surface suspended POC. All POC  $\Delta^{14}\text{C}$  results, however, are greater than the corresponding pre-bomb, surface-derived DIC values, and therefore contain bomb  $^{14}\text{C}$ . This decrease in  $^{14}\text{C}$  activity requires a deep source (or sources) of carbon to sub-surface POC pools. Adsorptive processes involving low- $^{14}\text{C}$ -activity dissolved organic carbon (DOC) may provide a mechanism for lowering  $\Delta^{14}\text{C}$  values in suspended and (to a lesser extent) sinking POC.

Published in: *Nature*, 347(6289):172–174, 1990.

Supported by: NSF Grant OCE87-16590.

WHOI Contribution No. 7345.

#### PYROLYTIC CHARACTER OF ORGANIC MATTER IN CENOZOIC SEDIMENTS ON THE OMAN SHELF

*Kay-Christian Emeis and Jean K. Whelan*

Analysis of the molecular composition and quantity of pyrolytic hydrocarbons in 4 $\ell$  samples from Owen Ridge and the Oman margin enabled us to identify chemical differences in the organic matter from Owen Ridge and the Oman margin. The differences may be attributed to regional variability in organic matter composition between margin and ridge, effects of kerogen formation and condensation with age, and effects of changes in the depositional environment on the Oman margin. Pyrolytic hydrocarbons from ridge sediments are relatively more enriched in heterocompounds, aromatic molecules, and *n*-alkanes, and *n*-monoalkenes in the range *n*-C<sub>9</sub> to *n*-C<sub>14</sub> when compared to margin sediments. This may be indicative of input of degraded organic material on Owen Ridge and less degraded material on the Oman margin. Increases of long-chain *n*-alkanes and *n*-monoalkenes with depth in sediments from the Oman margin are a result of the concentration of precursor moieties in the kerogen during low-temperature diagenesis. Differences in the depositional environment during deposition of sediments on the Oman margin (changes in the oxygen content of bottom waters and changing

benthic activity in a variable oxygen minimum zone) appear to be mirrored in the distribution of monounsaturated isoprenoid hydrocarbons prist-1-end and prist-2-end and alkylbenzene.

In Press: Prell, W. L., Niitsuma, N., *et al.*  
*Proceedings of Ocean Drilling Program, Scientific Results*, 117, 1991.

Supported by: NSF Grant OCE85-09859.

WHOI Contribution No. 7527.

#### INTRAMOLECULAR QUENCHING OF EXCITED SINGLET STATES BY STABLE NITROXYL RADICALS

*S. A. Green, D. J. Simpson, G. Zhou, P. S. Ho, and N. V. Blough*

Absorbance and steady-state and time-resolved fluorescence measurements were employed to examine the mechanism(s) of excited singlet state quenching by nitroxides in a series of nitroxide-fluorophore adducts. This work establishes the following: 1) the absorption and emission energies of the fluorophores are unaffected by the presence of the nitroxide substituent(s), and the residual emission that is observed from the adducts arises from the locally excited singlet of the fluorophore, not from charge recombination; 2) rate constants for intramolecular quenching by the nitroxides ( $k_q$ ) are high ( $10^8$ – $10^{10}$  s<sup>-1</sup>) and decrease significantly with increasing nitroxide to fluorophore distance—however, relatively high rates of quenching ( $>10^8$  s<sup>-1</sup>) are observed over distances as great as 12 Å; 3) Förster energy transfer does not contribute significantly to the quenching due to the low values for the spectral overlap integrals; 4) the  $k_q$ 's do not increase proportionally to the solvent-dependent increases in the Dexter overlap integral, indicating that energy transfer by the Dexter mechanism is not responsible for the quenching; 5) the values of  $k_q$  show no obvious correlation with the calculated free energies for photo-induced electron transfer, suggesting that this quenching pathway is also unimportant; 6) for hematoporphyrin-nitroxide adducts, which contain a fluorophore whose singlet energy is below that of the first excited state energy of the nitroxide (thus precluding energy transfer), significant rates of quenching are still observed. These results suggest that the quenching arises through electron exchange which causes relaxation of the (local) singlet state to the triplet and/or ground state of the fluorophore.

Published in: *Journal of American Chemical Society*, 112(20):7337–7346, 1990.

Supported by: ONR Grants N00014-87-K-007 and N00014-89-J-1260.

WHOI Contribution No. 7348.

## GENERATION OF GAS AND OIL FROM COAL AND TERRESTRIAL KEROGEN

*John M. Hunt*

Late Carboniferous-Permian sedimentary rocks contain the world's largest coal reserves which have generated and released gas but very little oil.

Terrestrial kerogen, in comparison, has sourced large quantities of waxy oils in countries such as China, Australia, the U.S.A., Argentina, Venezuela, and Indonesia, plus gas and condensate in deltas worldwide. Why is more oil coming from terrestrial kerogen than from coal?

The answer appears to be in the hydrogen content and the ease of migration. When terrestrial kerogens and coals have high hydrogen contents relative to carbon they can form oil. When the hydrogen is low, mainly gas is formed. Most of the world's coal is low in hydrogen whereas terrestrial (lacustrine) kerogen tends to be high in hydrogen so it forms more oil. Also, oil is adsorbed on coal more strongly than on the disseminated kerogen of sedimentary rocks, and the micropores of bedded coals may trap liquid hydrocarbons until the pores are fractured. This makes migration out of the coal more difficult compared to conventional source rocks.

Supported by: DoE Grant DE-FGO2-86ER13466.

WHOI Contribution No. 7478.

## GENERATION AND MIGRATION OF PETROLEUM FROM ABNORMALLY PRESSURED FLUID COMPARTMENTS: REPLY

*John M. Hunt*

Reply to Discussion of Douglas W. Waples (1990).

Waples comments on the cause of overpressures are important. The existence of overpressured fluid compartments can be identified with RFT and DST pressure measurements. Also, we can prove that oil has moved vertically out of the overpressured compartments into the overlying normally pressured rocks with biomarkers. But we cannot establish the dominant cause of overpressures except in a few cases. My paper briefly mentions compaction, the thermal expansion of pore fluids and hydrocarbon generation from kerogen as possible causes. These and other causes of overpressures have been discussed in some detail in several publications (Bradley, 1975; Fertl, 1976; Hunt, 1979, p. 237-241; Gretener, 1981; Spencer, 1987). But high overpressures cannot exist without a hydraulic seal so the cause of overpressures is really related to the

cause and timing of seal formation. When we more fully understand why, when, and where these seals form, we will be in a better position to evaluate the various causes of overpressures in each basin.

In Press: *AAPG Bulletin*.

Supported by: Gas Research Institute Contract No. 5088-260-1746.

WHOI Contribution No. 7480.

## DETERMINATION OF CARBON-CENTERED RADICALS IN AQUEOUS SOLUTION BY LIQUID CHROMATOGRAPHY WITH FLUORESCENCE DETECTION

*David J. Kieber and Neil V. Blough*

A simple method to detect subnanomolar to micromolar levels of photochemically generated carbon-centered radicals in aqueous solutions has been developed and optimized. This method is based on the efficient trapping of radicals by a water-soluble amino nitroxide, followed by derivatization of the trapped products with fluorescamine to produce highly fluorescent adducts. These adducts can be separated by reversed-phase high-performance liquid chromatography and detected fluorometrically. The fluorescent derivatives are stable over a period of days. The detection limit, primarily determined by reagent interferences, ranged from 0.3 to 1 nM per analyte for a 500  $\mu$ L injection at a signal-to-noise ratio of two. The precision of the method for the determination of adduct concentrations in the 1-10 nM range varied from 2.4 to 8.4% relative standard deviation ( $n = 6$ ). A direct comparison with electron paramagnetic resonance spectroscopy/spin trapping illustrates the advantages of our technique. One important feature of the method is that it permits the simultaneous detection of an array of radicals, as demonstrated through the study of the photochemical production of radicals in a variety of natural water samples and in Suwannee River fulvic acid.

Published in: *Analytical Chemistry*, 62(21):2275-2283, 1990.

Supported by: ONR Grant Nos. N00014-87-K-007 and N00014-89-J-1260.

WHOI Contribution No. 7410.

# THE DISTRIBUTION AND RECYCLING OF CHLOROPHYLL, BACTERIOCHLOROPHYLL AND CAROTENOIDS IN THE BLACK SEA

Daniel J. Repeta and Daniel J. Simpson

Chlorophyll, bacteriochlorophyll-*e*, carotenoids, and particulate organic carbon were measured in a suite of suspended particulate matter and sediment trap samples collected from three stations in the Black Sea. Vertical profiles of particulate Chlorophyll-*a* display well developed subsurface maxima with concentrations of up to 465 ng/ℓ between 30–40 m. Associated with these maxima are the carotenoids 19'-hexanoyloxyfucoxanthin from prymnesiophytes and fucoxanthin from diatoms. Subsurface maxima in bacteriochlorophyll-*e*, characteristic of the obligate photoautotroph *Clorobium phaeobacterioides* and *C. phaeovibrioides*, were also observed between 80–100 m in all samples. Vertical profiles of bacteriochlorophyll-*e* display maxima at the H<sub>2</sub>S interface (chemocline) and provide the first evidence for anoxygenic photosynthesis in the Black Sea. Bacteriochlorophyll-*e* was present at stations separated by 450 Km, implying a large areal extent to the bacterial plate. The Black Sea therefore supports the largest and deepest contemporary anoxygenic photosynthetic system in the world, and may provide a suitable model for carbon cycling in anoxic seas of Cambrian and Precambrian times.

Pigments are rapidly recycled with high efficiency in the euphotic zone. The distribution of pigments in our sediment trap samples is considerably different from reported distributions of pigments in sediment trap samples collected from oxic open ocean systems. High concentrations of unaltered algal pigments, originating at the base of the euphotic zone, were measured in sediment trap samples collected in and immediately below the chemocline. The carotenoid 19'-hexanoyloxyfucoxanthin, abundant in samples collected from depths <35 m, was not detected in any of our trap samples.

In Press: *Deep-Sea Research*.

Supported by: NSF Grant OCE88-14398.

WHOI Contribution No. 7501.

# RADIOCHEMISTRY

## MIXING BETWEEN OXIC AND ANOXIC WATERS OF THE BLACK SEA AS TRACED BY CHERNOBYL CESIUM ISOTOPES

Ken O. Buesseler, Hugh D. Livingston, and  
Susan A. Casso

The Chernobyl nuclear power station accident in 1986 released readily measurable quantities of fallout <sup>134</sup>Cs and <sup>137</sup>Cs to Black Sea surface waters. This pulse-like input of tracers can be used to follow the physical mixing of the surface oxic waters, now labeled with the Chernobyl tracers, and the deeper anoxic waters, which are initially Chernobyl free. By 1988, there is clear evidence of Chernobyl Cs penetration below the oxic/anoxic interface at deep water stations in the western and eastern basins of the Black Sea. This rapid penetration of surface waters across the pycnocline cannot be explained by vertical mixing processes alone. Data from profiles at the mouth of the Bosphorus suggest significant ventilation of intermediate depths can occur as the outflowing Black Sea waters are entrained with the inflowing Mediterranean waters, forming a sub-surface water mass which is recognized by its surface water characteristics, *i.e.*, initially a relatively high oxygen content and Chernobyl Cs signal. The lateral propagation of this signal along isopycnals into the basin interior would provide a quite rapid and effective mechanism for ventilating intermediate depths of the Black Sea. This process could also account for the lateral injection of resuspended margin sediments into the basin interior. The temperature and salinity data suggest that the entrainment process occurs at depths of 50–80 m, mixing waters from the Cold Intermediate Layer with the incoming, denser Mediterranean waters.

In Press: *Deep-Sea Research*.

Supported by: NSF Grant OCE87-00715, ONR Grant N00014-85-C-007, and Coastal Research Center.

WHOI Contribution No. 7376.

## RUTHENIUM-106 IN THE BLACK SEA

Ken O. Buesseler, Hugh D. Livingston, and  
Susan A. Casso

Profiles of Chernobyl <sup>106</sup>Ru and <sup>137</sup>Cs were obtained at margin and interior sites in the Black Sea between 1986 and 1988. The data show a vertical separation in the activity distributions of these two tracers. Ruthenium-106 is found at



depths below the Chernobyl  $^{137}\text{Cs}$ , indicating that  $^{106}\text{Ru}$  is removed via particle scavenging processes, unlike the Cs isotopes which serve primarily as tracers of physical mixing. In 1988, more detailed measurements at depths near the oxic/anoxic interface suggest that a subsurface maximum in  $^{106}\text{Ru}$  occurs at the same depth as the particulate Mn maximum above oxygen zero, with perhaps a secondary peak below. Inventory calculations indicate that while  $^{106}\text{Ru}$  has been significantly scavenged from the upper 50 m, the net loss of  $^{106}\text{Ru}$  from the upper 200 m has been relatively small since its input in 1986. This implies that substantial  $^{106}\text{Ru}$  is remineralized from sinking particles, and returns to the dissolved pool, thus limiting net export and increasing the apparent residence time of Ru. Relatively high deep water  $^{106}\text{Ru}$  inventories (50% of total) suggest that a substantial fraction of the  $^{106}\text{Ru}$  transient tracer reaches the deep waters as a pulse shortly after delivery. This is analogous to what has been seen for the weapons testing fallout radionuclide,  $^{239,240}\text{Pu}$ .

In Press: NATO Advanced Workshop, *Black Sea Oceanography*.

Supported by: NSF Grants OCE87-00715 and OCE89-17465, ONR Contract No. N00014-85-C-007, Coastal Research Center, Turkish Research Council, and German Federal Ministry for Research and Technology Grant No. MFU005438.

WHOI Contribution No. 7509.

### GROWTH RATE OF A DEEP-SEA CORAL USING $^{210}\text{Pb}$ AND OTHER ISOTOPES

*Ellen R. M. Druffel, Linda L. King, Rebecca A. Belostock, and Ken O. Buesseler*

A deep-sea coral was studied to determine its growth rate and to reconstruct time histories of isotope distributions in the deep ocean. The specimen was collected at a depth of 600 m off Little Bahama Banks using the Deep Submergence Vehicle (DSV) *Alvin*. The growth rate of the calcitic coral trunk was determined using excess  $^{210}\text{Pb}$  measured in concentric bands. Excess  $^{210}\text{Pb}$  was found in the outer half of the coral's radius, and a growth rate of  $0.11 \pm 0.02$  mm/yr is calculated. Assuming a constant growth rate during formation of the entire trunk, an age of  $180 \pm 40$  years is estimated for the coral. The decrease observed in radiocarbon activities measured on the same bands (Griffin and Druffel, 1989) concurred with the growth rate estimated from excess  $^{210}\text{Pb}$  activity.  $^{239,240}\text{Pu}$  activities measured by mass spectrometry were also detected in the outer two

bands of the coral, as expected from the  $^{210}\text{Pb}$  chronology. Stable oxygen and carbon isotopes measured in samples collected by a variety of techniques are positively correlated. This is evidence of a variable kinetic isotope effect most likely caused by variations in the skeletal growth rate. Long-lived corals such as this specimen have the potential for serving as integrators of seawater chemistry in the deep-sea over several century timescales.

Published in: *Geochimica et Cosmochimica Acta*, 54:1493-1500, 1990.

Supported by: NSF Grant OCE86-8263, DoE Contract DE-FGO2-85ER60358, and Arthur Vining Davis Foundation.

WHOI Contribution No. 7311.

### THORIUM-230 PROFILING IN DEEP-SEA SEDIMENTS: HIGH-RESOLUTION RECORDS OF FLUX AND DISSOLUTION OF CARBONATE IN THE EQUATORIAL ATLANTIC DURING THE LAST 24,000 YEARS

*Roger Francois, Michael P. Bacon, and Daniel O. Suman*

Variations in carbonate flux and dissolution, which occurred in the equatorial Atlantic during the last 24,000 years, have been estimated by a new approach that allows the point-by-point determination of paleofluxes to the seafloor. An unprecedented time resolution can thus be obtained which allows sequencing of the relatively rapid events occurring during deglaciation. The method is based on observations that the flux of unsupported  $^{230}\text{Th}$  into deep-sea sediments is nearly independent of the total mass flux and is close to the production rate. Thus excess  $^{230}\text{Th}$  activity in sediments can be used as a reference against which fluxes of other sedimentary components can be estimated. The study was conducted at two sites (Ceará Rise; western equatorial Atlantic, and Sierra Leone Rise; eastern equatorial Atlantic) in cores raised from three different depths at each site. From measurements of  $^{230}\text{Th}$  and  $\text{CaCO}_3$ , changes in carbonate flux with time and depth were obtained. A rapid increase in carbonate production, starting at the onset of deglaciation, was found in both areas. This event may have important implications for the postglacial increase in atmospheric  $\text{CO}_2$  by increasing the global carbonate carbon to organic carbon rain ratio and decreasing the alkalinity of surface waters (and possibly the North Atlantic Deep Water). Increased carbonate dissolution occurred in the two regions during deglaciation,

followed by a minimum during mid-Holocene and renewed intensification of dissolution in late Holocene. During the last 16,000 years, carbonate dissolution was consistently more pronounced in the western than in the eastern basin, reflecting the influence of Antarctic Bottom Water in the west. This trend was reversed during stage 2, possibly due to the accumulation of metabolic CO<sub>2</sub> below the level of the Romanche Fracture Zone in the eastern basin.

Published in: *Paleoceanography*, 5(5):761-787, 1990.

Supported by: NSF Grant OCE86-620.

WHOI Contribution No. 7474.

### VARIATIONS IN TERRIGENOUS INPUT INTO THE DEEP EQUATORIAL ATLANTIC DURING THE PAST 24,000 YEARS

*Roger Francois and Michael P. Bacon*

Estimates of terrigenous fluxes at three different water depths at two sites in the equatorial Atlantic by normalization against excess <sup>230</sup>Th flux indicate that the flux of terrigenous material to the seafloor was significantly higher during the last glacial period. Fluxes started to decrease during deglaciation and reached minimal values in the middle of the Holocene. From 15 to 5 thousand years ago, there was a substantial increase in flux with increasing water depth below 2800 m; this increase may reflect resuspension and lateral transport of slope and rise sediment, possibly because of intensification of deep water circulation during that period.

In Press: *Science*.

Supported by: NSF Grants OCE86-620 and OCE89-22707.

WHOI Contribution No. 7486.

### DETERMINATION OF ISOPYCNAL DIFFUSIVITY IN THE SARGASSO SEA

*W. J. Jenkins*

Using observed space and time derivatives of the distributions of <sup>3</sup>He, tritium and tritium-helium age in the Sargasso Sea, and the tritium-helium age equation, I estimate the isopycnal eddy diffusivity to be 1840 ± 440 m<sup>2</sup> s<sup>-1</sup> within the main thermocline.

In Press: *Journal of Physical Oceanography*.

Supported by: NSF Grant OCE89-11697 and ONR Contract No. N00014-89-J-1312.

WHOI Contribution No. 7515.

### THE PHOTOCHEMICAL DECOMPOSITION OF HYDROGEN PEROXIDE IN SURFACE WATERS OF THE EASTERN CARIBBEAN AND ORINOCO RIVER

*James W. Moffett and Oliver C. Zafriou*

The photochemical decomposition of hydrogen peroxide has been studied in surface waters collected on a transect from the Atlantic Ocean north of Puerto Rico through the eastern Caribbean Sea to the mouth of the Orinoco River. Absolute rates of photochemical decomposition were measured by adding <sup>18</sup>O labelled H<sub>2</sub>O<sub>2</sub> to the water samples and irradiating with a shipboard solar simulator. Photochemical decomposition was measurable at all station locations. Decomposition rates increased along the transect towards the Orinoco and were directly proportional to photochemical production rates, which also increased. Photodecomposition rates were also linearly related to the intensity of absorption of samples at 300 nm. Decomposition rates were generally ~5% of formation rates, indicating that photochemical decomposition is probably a minor sink for H<sub>2</sub>O<sub>2</sub> in the mixed layer compared to biological decomposition.

In all seawater samples photodecomposition led exclusively to <sup>18</sup>O<sub>2</sub>, indicating that reaction with photochemically produced oxidants was the dominant reaction mechanism. The oxidizing species are not the best known photooxidants in seawater, singlet oxygen and OH and O<sub>2</sub> radicals. Unidentified oxidants with formation rates ~5% of the H<sub>2</sub>O<sub>2</sub> formation flux are required.

In contrast, H<sub>2</sub><sup>18</sup>O<sub>2</sub> decomposition in unfiltered samples or Orinoco River water led solely to H<sub>2</sub>O<sup>18</sup>, indicating reaction with a photochemically produced reductant was the dominant mechanism. Further experiments indicated that the reductant was probably Fe(II) produced by photoreduction of particulate Fe(III), a known process. This pathway would produce an equivalent flux of OH radical: Fe(II) + HOOH → Fe(III) + OH + OH<sup>-</sup>.

Supported by: NSF Grants OCE84-17770 and OCE87-00576, and ONR Grants N00014-85-C-001, N00014-87-K-0007, N00014-89-J-1258 and N00014-89-J-1260.

WHOI Contribution No. 7471.

## SEAWATER AND GEOCHEMISTRY

### A CHLOROFLUOROCARBON SECTION IN THE EASTERN NORTH ATLANTIC

Scott C. Doney and John L. Bullister

We present the distributions of two chlorofluorocarbons, CFC-11 and CFC-12, measured as part of a hydrographic section between Iceland and the equator during July and August of 1988. CFC tagged water has filled the entire subpolar water column and subtropical thermocline in the eastern North Atlantic. Measurable CFC concentrations are observed at the ocean bottom as far south as 35°N, and the CFC penetration depth shoals to ~750 meters in the tropics. Specific features in the CFC distributions include a clear signal of Labrador Sea mid-depth ventilation, a CFC-enriched overflow water boundary current along the Iceland slope, and a mid-depth, equatorial plume of upper North Atlantic Deep Water. The CFC data are used, in conjunction with the hydrographic data from the cruise, to illustrate the ventilation time scales and pathways for the water masses in the eastern basin and to estimate oxygen utilization rates in the subtropical thermocline. We show that the CFC distribution along the 20°W section is generally consistent with the available data for the other transient tracers in the eastern basin and with what is known about the formation mechanisms and circulation patterns for the different water masses in the eastern basin. The evolution of the tropical and subtropical CFC distributions over the five-year period between the TTO/TAS survey and our cruise is also examined.

Supported by: NSF Grants OCE88-00957 and OCE86-15289.

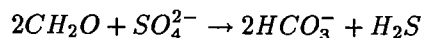
WHOI Contribution No. 7600.

### CARBONATE SYSTEM IN THE BLACK SEA

Catherine Goyet, Alvin L. Bradshaw, and  
Peter G. Brewer

We have measured both alkalinity and total carbon dioxide on a selected set of Black Sea samples from cruise 134 of *R/V Knorr*, using gas extraction/coulometry techniques, and improved titration procedures, that permit more accurate data than that obtained in earlier expeditions. Earlier results had shown an apparent excess in alkalinity, by a factor of 1.6, from the stoichiometric ratio predicted from the sequential oxidation of Redfield ratio organic matter by the

species  $O_2$ ,  $NO_3^-$ , and  $SO_4^{2-}$ . Thus both the nature of the organic substrate, and our fundamental knowledge of reaction stoichiometry in anoxic systems, were called into question. We show that the total  $CO_2$  balance is consistent with oxidation of organic matter by sulfate:



and consistent with work on sediment interstitial waters in anoxic conditions (Berner *et al.*, 1970; Ben Yaakov, 1973). The total  $CO_2$  results are lower by 300  $\mu\text{m/kg}$  in surface waters, and 50  $\mu\text{m/kg}$  in deep waters, than data reported from the 1969 *Atlantis II* expedition. While changes in Black Sea hydrography have taken place and been documented (Murray *et al.*, 1989), the  $CO_2$  system changes are far too large to be accounted for by these processes, and are more likely the result of improved technique, rather than geochemical evolution.

In Press: *Deep-Sea Research*.

Supported by: NSF Grants OCE88-14393 and OCE87-1461.

WHOI Contribution No. 7475.

### SEAFLOOR DIAGENETIC FLUXES

W. R. Martin and F. L. Sayles

Early diagenesis is an important contributor to the oceanic cycles of many components of seawater. In many cases, the flux across the sediment-water interface resulting from early diagenesis is comparable to input rates to the ocean from other sources. In the cases of many bioactive elements, the early diagenetic flux is considerably larger than, for instance, the riverine input to the ocean, as early diagenesis is intimately involved in the rapid cycling of these elements within the ocean. However, a general characteristic of early diagenetic fluxes, both for bioactive components of seawater and for the major seawater ions, is that they affect oceanic concentrations on long time-scales, ranging from  $10^4$  to  $10^7$  years.

The study of early diagenesis is important to the study of ocean history as early diagenetic reactions play an important role in fixing sediment composition. Diagenetic fluxes exceed burial rates for the major bioactive elements: about 90% of the organic carbon rain to the seafloor degrades during early diagenesis; over 60% of the biogenic silica, and about 80% of the  $CaCO_3$  reaching the seafloor dissolve. Thus, variations in diagenetic reaction rates can have disproportionately large effects on sedimentary concentrations and accumulation rates of these components.

It is important to recognize that, at the present time, any analysis of the role of early diagenesis in oceanic processes is data-limited. The spatial coverage of measurements is limited; more importantly, the interpretation of results often depends on the measurement technique used. For this reason, we begin our evaluation of early diagenetic fluxes with a review of measurement techniques and uncertainties. Then, we examine the ways in which early diagenesis affects the modern oceanic cycles of the major seawater ions, carbon, and silicon; and we examine its effects on the sedimentary record of ocean history as it is interpreted using organic carbon,  $\text{CaCO}_3$ , and opal data.

In Press: *National Academy of Sciences/National Resource Council Panel on Global Surficial Geofluxes: Glacial to Modern.*

Supported by: NSF Grant OCE87-11962.

WHOI Contribution No. 7297.

## CARBON CYCLING IN COASTAL SEDIMENTS: 2. AN INVESTIGATION OF THE SOURCES OF $\sum \text{CO}_2$ TO PORE WATER USING CARBON ISOTOPES

*Ann P. McNichol, Ellen R. M. Druffel, and Cindy Lee*

A study of seasonal variations in the  $\delta^{13}\text{C}$  of  $\sum \text{CO}_2$  was conducted at a site in Buzzards Bay, MA. The depth profiles of  $\delta^{13}\text{C}$ - $\sum \text{CO}_2$ ,  $\sum \text{CO}_2$  and Ca were measured in five cores collected over an 18-month period. Gradients of up to  $1.3^\circ/\infty/\text{cm}$  in  $\delta^{13}\text{C}$ - $\sum \text{CO}_2$  were observed with the largest gradients present in the summer months. Maxima and minima were observed in the isotopic profile due to the activity of burrowing organisms. A model used to describe the isotopic profiles indicated that the  $\delta^{13}\text{C}$  of  $\sum \text{CO}_2$  added to pore water during early diagenesis ( $-6.3$  to  $-14.6^\circ/\infty$ ) was enriched in  $^{13}\text{C}$  with respect to the organic matter in the sediments ( $-20.6^\circ/\infty$ ). The difference could not be explained by the dissolution of  $\text{CaCO}_3$ . The results of a laboratory study of the oxidation of organic carbon in sediments indicate that the  $\delta^{13}\text{C}$  of  $\sum \text{CO}_2$  added from the oxidation of organic carbon is  $-18.5 \pm 1.5^\circ/\infty$ . These results indicate that some of the enrichment of  $^{13}\text{C}$  in pore water  $\sum \text{CO}_2$  is due to fractionation during oxidation. The rest of the enrichment may be due to isotopic exchange with bottom water or the production of  $^{13}\text{C}$ -depleted dissolved organic carbon.

In Press: *ACS Symposium Volume*, Division of Environmental Chemistry, American Chemical Society, Boston, MA, April 1990.

Supported by: NSF Grants OCE83-15412 and OCE84-16632.

WHOI Contribution No. 7413.

## CERIUM REDOX CYCLES AND RARE EARTH ELEMENTS IN THE SARGASSO SEA

*E. R. Sholkovitz and D. L. Schneider*

Two profiles of the rare earth elements are reported for the upper water column of the Sargasso Sea. The trivalent-only REE have remarkably constant concentrations in the upper 500 m of April 1989 and 200 m of the May 1989 profiles. In contrast, Ce concentrations decrease smoothly with increasing depth. In April 1989 Ce decreases from  $15.7 \text{ pmol/kg}$  at 20 m to  $5.1 \text{ pmol/kg}$  at 750 m. Ce behaves anomalously with respect to its REE neighbors. While both dissolved Ce and Mn have elevated concentrations in the upper 200 m, their vertical gradients are distinctly different. In contrast to Mn, which reaches a minimum dissolved concentration near the zone (150–250 m) of a particulate Mn maximum, Ce is being removed both near this zone and to depths of at least 750 m.

These new profiles indicate that Ce is involved in an upper ocean redox cycle. This interpretation is consistent with Moffett's (1990) incubation tracer experiments on the same May 1989 seawater. He showed that Ce(III) oxidation is biologically mediated, probably light inhibited, increases with depth and is 3–4 times slower than Mn(II) oxidation in the 100–200 m zone. "CERoclines" provide new information into the fine scale zonation of redox processes operating in the upper columns of oligotrophic oceans.

While the trivalent-only REE have similar concentrations, striking differences exist between our Ce profiles and Ce-anomalies and those of de Baar *et al.* (1983) from an August 1980 profile. The increase in their Ce concentration in the upper 150 m is ten times greater than ours. This leads to large positive Ce-anomalies while our samples show well-developed negative anomalies. Causes for the Ce-anomalies in the Sargasso Sea are discussed in light of new data reported in this paper and in the literature.

Supported by: NSF Grant OCE87-11032.

WHOI Contribution No. 7571.

## PHOTOCHEMICAL FREE RADICAL PRODUCTION RATES: GULF OF MAINE AND WOODS HOLE-MIAMI TRANSECT

*Oliver C. Zafriou and Brian Dister*

The total free-radical fluxes generated by illumination of surface water samples with a solar simulator were measured in a variety of coastal surface waters along the east coast of the United States in summer, 1987.

Photochemically-generated free radicals were scavenged with a known excess of added nitric oxide and the nitric oxide losses were measured by difference using a semi-automated, computer-controlled system coupled to the ship's clean surface water intake system.

This first large free-radical flux data set shows that radical production occurs at significant rates that are relatively uniform over large regions. However, at the time of this cruise, a strong photo-reactivity front divided coastal waters north of Cape Cod ( $3.85 \pm 0.82$  nmoles liter<sup>-1</sup> min<sup>-1</sup> sun<sup>-1</sup>, n=8 sites) from coastal waters south to northern Florida ( $1.67 \pm 0.32$  nmoles liter<sup>-1</sup> min<sup>-1</sup> sun<sup>-1</sup>, n=20).

The mean flux on an areal basis is estimated to be  $\sim 0.7$  mM m<sup>-2</sup>d<sup>-1</sup>, or about 20 mM m<sup>-2</sup> for the summer season.

These values are sufficiently large to produce interesting but unknown geochemical consequences. The regional uniformity and wavelength dependence of the rates are consistent with the concept that the principal mechanism of radical production is photolysis of long-lived humic-like dissolved chromophores of unknown structure. A vertical profile shows strong near-surface depletion of reactive materials under calm conditions.

The dependence of total radical production rates on irradiation time, light intensity, concentration of added NO, and wavelength range of polychromatic radiation are also reported. The results support the conclusion that the method produces an operationally consistent, well-behaved estimate of photochemical free-radical production potential that is not strongly affected by biological processes.

In Press: *Journal of Geophysical Research*.

Supported by: NSF Grants OCE84-17770 and OCE87-00576.

WHOI Contribution No. 7421.

## MOLECULAR PROBE SYSTEMS FOR REACTIVE TRANSIENTS IN NATURAL WATERS

*O. C. Zafriou, N. V. Blough, E. Micinski, B. Dister, D. Kieber, and J. Moffett*

Many natural water transformations are mediated by reactive transients (RT's) too fleeting to measure directly. The concepts of molecular probe methods that can uniquely characterize these otherwise inaccessible species are critically reviewed in the context of environmental studies.

Photochemically produced free radicals exemplify important RT's. A photooxidation scheme characterizing the radical chemistry of seawater and emphasizing the reactions of oxygen species is presented. All the hypothesized radicals are measurable only as reactive transients with lifetimes <10 s; many undergo critical reactions on the 1  $\mu$ s timescale.

New probe systems have been designed for use at sea and to explore and test the photooxidation hypothesis. These stable free radical probes exhibit kinetic and thermodynamic advantages compared to conventional even-electron probes as a result of elementary chemical considerations. Their selectivity profiles match well the properties of the primary and secondary radical groups postulated by the hypothesis, and initial data demonstrates that these systems are sensitive, give oceanographically consistent results, and tentatively confirm or constrain the scheme.

Organic nitroxide probes confirm the postulated fast radical + O<sub>2</sub> reactions, and can be used to separate and identify trace organic radicals in model systems and natural waters. The inorganic probe nitric oxide has been used extensively to measure total radical fluxes of  $\sim 0.1$ -1 nM/kg/min of noon surface insolation in "blue" waters ( $\sim 10$ -100  $\mu$ M per calendar year), confirming geochemically significant flux magnitudes. The fluxes of the superoxide ion-radical have been measured at sea using related 15-N labelled NO probes. Values approximately one-third of the total flux at the same sites confirm that this previously postulated species is a major component of the photochemical radical array, qualitatively strengthening the hypothesis that they are the source of photochemically produced HOOH.

Testing the robustness of results from probe studies of the photooxidation hypothesis requires intercalibration methods and probe-independent validation experiments. Prospects for realizing these constraints are surveyed.

Published in: *Marine Chemistry*, 30:45-71, 1990.

Supported by: NSF Grants OCE84-17770 and  
OCE87-00576, and ONR Contracts  
N00014-85-C-0001, N000-14-87-K-0007;  
N00014-89-J-1258, and N00014-89-J-1260.

WHOI Contribution No. 7308.

## DEEP NITRITE DISTRIBUTIONS IN OXIC WATERS

*O. C. Zafiriou, L. A. Ball, and Q. Hanley*

We describe a modification of the Garside (1982) method for trace nitrite analysis that is able to measure subnanomolar concentrations of this important intermediate in the nitrogen cycle, and present the first Atlantic and Caribbean deepwater profiles. Nitrite was detected in all samples. Concentrations were consistently lowest (0.1-0.4 nM) in oligotrophic surface waters. Profiles in the upper kilometer beneath the classical primary nitrite maximum (PNM) were qualitatively similar, exhibiting a smooth supra-exponential drop with depth to values of  $\sim 1$  nM at 1 km. Below 1 km nitrite concentrations were 0.4-1 nM, continuing to decrease with increasing depth.

The nitrite inventory in this "tail" of the PNM with  $1 \text{ nM} \leq [\text{NO}_2^-] \leq 50 \text{ nM}$  roughly equals that in the classical PNM. Significant quantitative differences among profiles were observed, consistent with estimated rapid nitrite pool turnover times, 3-7 days in the 0.1-1 km region. Thus we suggest that seasonally and/or regionally variable factors altering the nitrite production — consumption balance, rather than transport processes — are mainly responsible for profile variability. Larger differences between these profiles and a deep Pacific nitrite section may reflect additional large influences of denitrification on  $[\text{NO}_2^-]$  in the strong Pacific oxygen minimum.

Nitrite profiles with anomalous midwater or deep fine structure, including multi-point maxima and minima, were also measured at three sites along the Venezuelan continental margin and at  $\sim 13^\circ\text{N}$ . These features are tentatively attributed to boundary effects, as hydrographic or circumstantial evidence suggests that the anomalous waters have recently interacted with the bottom.

Supported by: NSF Grants OCE86-1618 and  
OCE87-00576.

WHOI Contribution No. 7481.



**DEPARTMENT OF GEOLOGY AND GEOPHYSICS**

**David A. Ross, Chairman**

**GEOLOGY and GEOPHYSICS**





## GEOCHEMISTRY

### POREWATER CADMIUM GEOCHEMISTRY AND THE PORE WATER CADMIUM: $\delta^{13}\text{C}$ RELATIONSHIP

*Daniel C. McCorkle and Gary P. Klinkhammer*

Results from two continental margin cores collected off Pt. Sur, California make possible a direct determination of the relationship between dissolved cadmium and the carbon isotopic composition of dissolved inorganic carbon in the interstitial water of suboxic marine sediments. The  $\delta^{13}\text{C}$  values of dissolved inorganic carbon decrease nearly 1‰ in the top 0.5 cm of the sediments, and display a more gradual decrease through the top 20 cm of the sediments. Dissolved cadmium concentrations increase by 0.6 to 1.5 nmol/kg in the top 0.5 cm of the sediments, and then rapidly decrease to values of approximately 0.12 nmol/kg between 5 and 10 cm into the sediments, apparently as a result of scavenging onto iron oxide surfaces. This pattern contrasts with pore water cadmium profiles previously reported for pelagic sediments, which show no evidence of cadmium scavenging by the sediments. However, pore water cadmium concentrations are poorly correlated with pore water  $\delta^{13}\text{C}$  values in both oxic and suboxic sediments. These results suggest that the cadmium/calcium ratios and  $\delta^{13}\text{C}$  values of infaunal benthic foraminifera need not be tightly linked, and that the relationship between these two aspects of foraminiferal shell chemistry may vary in response to changes in sediment geochemistry.

Published in: *Geochimica et Cosmochimica Acta*,  
55:161-168, 1991.

Supported by: NSF Grant OCE88-12901.

WHOI Contribution No. 7388.

### CARBON CYCLING IN COASTAL SEDIMENTS: AN INVESTIGATION OF THE SOURCES OF $\Sigma\text{CO}_2$ TO PORE $\text{H}_2\text{O}$ USING CARBON ISOTOPES

*Ann P. McNichol, Ellen R. M. Druffel and  
Cindy Lee*

A study of seasonal variations in the  $\delta^{13}\text{C}$  of  $\Sigma\text{CO}_2$  was conducted at a site in Buzzards Bay, MA. The depth profiles of  $\delta^{13}\text{C}$ - $\Sigma\text{CO}_2$  and Ca were measured in five cores collected over an 18-month period. Gradients of up to 1.3 ‰/cm in  $\delta^{13}\text{C}$ - $\Sigma\text{CO}_2$  were observed with the largest gradients present in the summer months. Maxima and minima were observed in the isotopic profile

due to the activity of burrowing organisms. A model used to describe the isotopic profiles indicated that the  $\delta^{13}\text{C}$  of  $\Sigma\text{CO}_2$  added to pore water during early diagenesis (-6.3 to 14.6 ‰) was enriched in  $^{13}\text{C}$  with respect to the organic matter in the sediments (-2.0.6 ‰). The difference could not be explained by the dissolution of  $\text{CaCO}_3$ . The results of a laboratory study of the oxidation of organic carbon in sediments indicate that the  $\delta^{13}\text{C}$  of  $\Sigma\text{CO}_2$  added from the oxidation of organic carbon is  $-18.5 \pm 1.5$  ‰. These results indicate that some of the enrichment of  $^{13}\text{C}$  in pore water  $\Sigma\text{CO}_2$  is due to fractionation during oxidation. The rest of the enrichment may be due to isotopic exchange with bottom water or the production of  $^{13}\text{C}$ -depleted dissolved organic carbon.

In Press: *Organic Substances and Sediments in  
Water: Volume II. Processes and Analytical*. R.  
A. Baker, ed. Lewis Publishers, Inc. Chelsea,  
Michigan.

Supported by: NSF Grants OCE83-15412,  
OCE84-2179, OCE84-16632, Education  
WHOI/MIT and Coastal Research Center,  
WHOI.

WHOI Contribution No. 7413.

## GEOLOGY

### SEQUENCE STRATIGRAPHY: EUSTASY OR TECTONIC IMPRINT?

*Marie-Pierre Aubry*

Sequence stratigraphy is viewed by many geologists as the expression in the stratigraphic record of the history of sea level changes. Sequence boundaries are its most distinctive elements and are used for global correlations. Until now, correlations between unconformities and postulated lowerings of sea level have been primarily seen in terms of cause and effect relationships, the postulated fall providing an explanation for the presence of an unconformity. They have not been truly perceived in terms of stratigraphic correlations which would imply the establishment of synchrony between the cause and the effect. To decipher the presence of a global sea level signal in the stratigraphic record, the synchrony of sea level related unconformities in widely separated basins must be established, which can be achieved by comparing the degree of overlap between hiatuses in different stratigraphic sections.

Outcrop sections, wells and the deep sea record reveal an apparently worldwide unconformity(ies) across the lower/middle Eocene boundary, characterized by intensive reworking, and/or relatively rapid shallowing in some areas

(e.g., Cyrenaica, NE Libya; California; Egypt). The lower to middle Eocene intervals in sections on the North Atlantic margins have been correlated through magnetobiostratigraphy and the durations of the hiatuses have been precisely determined. This record is compared with that in sections in other basins where shallowing and intensive reworking occur.

This study shows that there are two groups of unconformities and associated hiatuses around the lower/middle Eocene boundary. The older hiatuses, in the latest early middle Eocene, are generally short, even on the shelf (~1m.y.); the younger hiatuses, in the early Eocene are somewhat longer (>2 m.y.). The stratigraphic record around the lower/middle Eocene boundary suggests that there may be two mechanisms acting simultaneously to produce unconformities. Unconformities of a given age on the shelf may result from a global fall in sea level while their stratigraphically correlative unconformities on the slope and rise may result from tectonic instability. Unconformities related to the third order cycles in sea level changes in Vail's model primarily may reflect tectono-eustasy.

In Press: *Journal of Geophysical Research*.

Supported by: A Consortium of Oil Companies.

WHOI Contribution No. 7375.

## DEEP STRUCTURE OF THE EARTH: AN EMPIRICAL SOLUTION FROM ITS GRAVITY FIELD

*Carl Bowin*

It is a common consensus that the ambiguity of gravity anomalies in distinguishing deep compact, from shallow broad, or intermediate, mass distributions makes impossible the task indicated in the title. The truism of the above consensus has been assumed so implicitly, that its limits in real situations were never before tested. The methodology of Cumulative Contribution Curves (CCC methodology) of Bowin (1983, 1985, 1986) is further developed and demonstrates that the earth is not big enough, or the core/mantle boundary (CMB) not shallow enough, for a thin tapered surface mass distribution to match the characteristics of a compact mass anomaly at the CMB. A substantial (thick) non-tapered mass anomaly would be required of a surface mass anomaly distribution to match the New Guinea high 2-3 harmonic degree geoid pattern in order to make the strong geoid horizontal gradient observed. Such a surficial mass anomaly (equal to the earth's greatest mass anomaly), if it existed at the earth's surface, would certainly be in evidence geologically. Thus, this paper demonstrates that

the large geoid anomalies of the earth's spherical harmonic degree 2-3 field arises from topography at the CMB, and that this topography is produced by convective motions within the core (not the mantle) that produce the earth's magnetic field. Evidence is also presented that the 4-10 geoid anomaly field indicates that subducted slabs extend into the lower mantle and hence that whole mantle convection contributes to plate tectonics.

Supported by: A Consortium of Oil Companies.

WHOI Contribution No. 7503.

## MICROEARTHQUAKE CHARACTERISTICS OF A MID-OCEAN RIDGE ALONG-AXIS HIGH

*Laura S. L. Kong, Sean C. Solomon and  
G. M. Purdy*

We report results from a three-week microearthquake survey of the segment of the Mid-Atlantic Ridge centered near 26°N, in the area of the TAG hydrothermal field. The seismic network, consisting of seven ocean bottom hydrophones and two ocean bottom seismometers, spanned the median valley inner floor and eastern valley wall. Hypocenters were determined for 189 earthquakes, with good resolution of focal depth obtained for 105 events. Almost all events occurred at depths between 3 and 7 km beneath the seafloor, with earthquakes occurring at shallower depths (less than 4 km) beneath the along-axis high. No events were detected in the immediate vicinity of the hydrothermal field. The along-axis high is the site of a mid-crustal low velocity zone, significant attenuation of P wave energy, and high b-values; the low-velocity volume extends about 10 km south of the high to the vicinity of a volcano within the axial neovolcanic zone. Fault plane solutions indicate high-angle (or very low angle) normal faulting beneath the along-axis high and the base of the adjacent western wall, reverse faulting beneath the axial volcano, and a more conventional normal faulting geometry for earthquakes beneath the eastern wall. The distribution of seismicity and the diversity of faulting styles suggests a spatially variable tectonic state for the ridge segment at 26°N. These variations are likely a signature of along-axis differences in thermal structure and state of stress. We suggest that the low-velocity volume beneath the along-axis high is the site of a relatively recent crustal injection of magma that migrated southward by at least 10 km. Continued cooling of the now largely solid, but still hot intrusion, and associated thermal stress and fracturing in the immediately surrounding crust, can account generally for the distribution of areas of most

intense earthquake activity, the diversity of observed faulting mechanisms, and the presence of the high-temperature vent field. These results are supportive of the spreading cell model for segmentation of magmatism and thermal structure along a slowly spreading ridge.

Supported by: NSF Grants EAR84-07798, EAR84-07754 and EAR88-17173, and the WHOI/MIT Joint Program in Oceanography.

WHOI Contribution No. 7494.

### **LATE WEICHSELIAN GLACIER RETREAT IN KONGSFJORDEN, WEST SPITSBERGEN, SVALBARD**

*S. J. Lehman and Steven L. Forman*

The chronology of late Weichselian to Holocene deglaciation of Kongsfjorden, West Spitsbergen has been reconstructed based on the geomorphic and stratigraphic record of ice retreat, relative sea level relationships, and  $^{14}\text{C}$  dating of associated marine organic materials. The seaward extent of glacial drift and fjord bathymetry constrain a secure reconstruction for the ice sheet near the mouth of the fjord at ca. 13,000 yrs B.P., but do not rule out the possibility that more extensive glaciation was achieved earlier during the Late Weichselian. Regional shoreline relations indicate that deglaciation occurred in two steps, one beginning during or just prior to the Late Weichselian Marine Limit phase at 13,000 - 12,000 yr B.P. and another beginning at 10,000 - 9,500 yr B.P. The fjord was completely deglaciated by  $9,440 \pm 130$  yr B.P. A period of stable relative sea level began 10,700 yr B.P. and ended between 10,000 and 9500 yr B.P., which we take to indicate renewed glacial loading during the Younger Dryas. Glacier re-advance within Kongsfjorden at this time was diminutive, suggesting that most of the Younger Dryas ice sheet growth was confined to the eastern part of the archipelago and/or to the Barents Shelf.

The two-step deglaciation of Kongsfjorden occurred during intervals of accelerated global ice sheet melting and rapid oceanic and atmospheric warming in temperate latitudes of the circum-Atlantic region. This coincidence most likely resulted from contemporaneous increases in the poleward transport of oceanic heat.

In Press: *Quaternary Research Research*.

Supported by: NSF Grants DPP88-13875 and DPP90-01468.

WHOI Contribution No. 7601.

### **INITIATION OF FENNOSCANDIAN ICE SHEET RETREAT DURING THE LAST DEGLACIATION**

*S. J. Lehman, G. A. Jones, L. D. Keigwin,  
E. S. Andersen, G. Butenko and S-R Østmo*

Although the retreat history of the southern margin of the Laurentide ice sheet during the last deglaciation has been well known for several decades (1-3) and recently supported by evidence from accelerator mass spectrometer (AMS) radiocarbon dating of meltwater in the Gulf of Mexico and the North Atlantic subtropical gyre, the retreat history of the Fennoscandian ice sheet before 13 kyr ago is still poorly documented. From AMS  $^{14}\text{C}$  dating and isotopic analysis of a rapidly deposited series of supra-till sediments in the Norwegian Channel (North Sea), we find that the southern margin of the Fennoscandian ice sheet was in retreat by 15 kyr BP (before present), approximately 2,000 yr earlier than previously supposed. Oxygen isotope analyses in the channel sediments confirm earlier evidence from deep Norwegian Sea sediment cores for low salinity due to ice sheet discharge beginning ~15-14.5 kyr BP (ref. 6). Recent recalibration of the  $^{14}\text{C}$  timescale indicates that the onset of deglaciation within the Norwegian Sea occurred during an interval of rapidly increasing summer insolation beginning ~18,000 calendar yr BP (ref. 7), suggesting that ice-sheet retreat may have been caused by increasing insolation acting on a particularly climate-sensitive ice-sheet configuration. Freshwater and icebergs discharged into the Norwegian Sea at this time reached the North Atlantic and may have contributed to a brief interval of extreme oceanic cooling and reduced production of North Atlantic Deep Water. These factors may also have helped to briefly reverse the deglaciation trend (Erie Interstade) already underway in North America.

Published in: *Nature*, 349:513-516, 1990.

Supported by: NSF Grants DPP88-13875 and DPP87-22235.

WHOI Contribution No. 7491.

### **THE SEGMENTATION OF THE MID-ATLANTIC RIDGE BETWEEN 24°N AND 30°40'N**

*Jean-Christophe Sempéré, G. M. Purdy and  
Hans Schouten*

The Mid-Atlantic Ridge (MAR) extends for over 12,000 km from Iceland to the Bouvet Triple Junction. Most of our knowledge of the geology of this slow-spreading centre comes either from

widely-spaced, low-resolution, echo-sounding lines or from detailed studies of small areas using deep-towed instruments or submarines. The high-resolution multibeam bathymetry coverage available up to now has been insufficient to define the variability of accretionary processes along this plate boundary. In this paper, we present the results of a recent investigation of an  $\approx 800$  km-long section of the MAR carried out using the multibeam echo-sounder Sea Beam. Analysis of these data reveals the scale and nature of the segmentation of the MAR between the Kane Fracture Zone ( $24^{\circ}\text{N}$ ) and latitude  $30^{\circ}40'\text{N}$ .

Published in: *Nature*, 344(6265):427-431, 1990.

Supported by: NSF Grant OCE87-09615.

WHOI Contribution No. 7303.

### SEAFLOOR TOPOGRAPHY: A RECORD OF A CHAOTIC DYNAMICAL SYSTEM?

*Deborah K. Smith and Peter R. Shaw*

We suggest that limits on the number of independent variables that play a role in controlling the shape of the seafloor can be obtained directly from bathymetry data. To obtain this information, seafloor topography is considered as a product of a larger system that produces the oceanic lithosphere. We hypothesize that this dynamical system is chaotic, and use bathymetric depth values to search for evidence of a strange attractor, the dimension of which estimates the number of degrees of freedom in the system. An analysis of Sea Beam multibeam data collected along a flow line of seafloor spreading in the Northeast Pacific Ocean indicates that the dynamical system that forms the topography (on the length scale of 100's of meters) has an underlying structure that is contained in the bathymetry, but this structure cannot be completely specified by a low order attractor.

Published in: *Geophysical Research Letters*, 17(10):1541-1544, 1990.

Supported by: ONR Contracts N00014-87-K-0508 and N00014-89-J-1021.

WHOI Contribution No. 7440.

### THE THREE-DIMENSIONAL SEISMIC VELOCITY STRUCTURE OF THE EAST PACIFIC RISE NEAR LATITUDE $9^{\circ}30'\text{N}$

*Douglas R. Toomey, G. M. Purdy,  
Sean C. Solomon and William S. D. Wilcock*

Three-dimensional images of crustal seismic structure beneath the East Pacific Rise show

pronounced axial heterogeneity over distances of a few kilometers. A linear high-velocity anomaly, approximately 1-2 km in width and restricted to the uppermost 1 km of the crust, is centered over the rise axis. The magnitude of an axial low-velocity anomaly varies along-axis in a pattern consistent with higher crustal temperatures at depths of 1-3 km midway between two axial morphologic discontinuities. This apparent thermal segmentation along axis is consistent with injection of mantle-derived melt midway along a locally linear, 12-km-long segment of the rise.

Published in: *Nature*, 347(6294):639-645, 1990.

Supported by: NSF Grant OCE90-00458.

WHOI Contribution No. 7463.

### EVIDENCE FOR AGE AND EVOLUTION OF CORNER SEAMOUNTS AND GREAT METEOR SEAMOUNT CHAIN FROM MULTIBEAM BATHYMETRY

*Brian E. Tucholke and N. Christian Smoot*

The Corner seamounts in the western North Atlantic and Great Meteor seamount "chain" in the eastern North Atlantic are thought to progress in age from Late Cretaceous through late Cenozoic. They were both presumably formed by volcanism above the New England hotspot when first the North American plate, and then the Mid-Atlantic Ridge axis and African plate, moved over the hotspot. High-resolution, multibeam bathymetry of the seamounts shows geomorphic features such as guyots, terraces, and a base-level plateau (Cruiser plateau) that we interpret to have formed at sea level. We have backtracked these features to sea level along the North Atlantic crustal age-depth curve in order to estimate their age. The derived age-pattern of volcanism indicates formation of the Corner seamounts at ca. 80 Ma to 76 Ma, with migration of the Mid-Atlantic Ridge plate boundary over the hotspot and formation of the Cruiser plateau about 76 Ma. Seamount ages suggest that subsequent volcanism on the African plate moved first *northward*, in the Lake Cretaceous to early Cenozoic (Plato, Tyro, and Atlantis seamount groups), then southward to Great Meteor Seamount in the late Cenozoic. Recurrent volcanism appears to have occurred at some seamounts up to 20-30 m.y. after their initial passage over the hotspot. It would thus appear that intralithospheric conduits can link the hotspot to old seamounts several hundred kilometers away.

Published in: *Journal of Geophysical Research*, 95(B11):17,555-17,569, 1990.

Supported by: ONR Contract N00014-82-C-0019.

WHOI Contribution No. 7377.

# **ESTIMATING HYPOCENTRAL UNCERTAINTIES FOR MARINE MICROEARTHQUAKE SURVEYS: A COMPARISON OF GENERALIZED INVERSE AND GRID SEARCH METHODS**

*William S. D. Wilcock and Douglas R. Toomey*

For microearthquake surveys conducted with small networks in regions where the local velocity structure has large vertical gradients, the formal errors accompanying hypocentral solutions obtained by a generalized inverse method may be misleading since they do not incorporate the effects of nonlinearity in travel times. An alternative method for estimating uncertainties involves calculating travel time residuals over a regular grid and using F statistics to contour confidence volumes. We present a statistical expression for the latter confidence limits that is applicable when an independent estimate of arrival time errors is available from observations accumulated for a number of earthquakes. Synthetic experiments comparing the results of the grid search and generalized inverse methods show that in cases where solutions are obtained either without S wave information or for epicenters which lie well outside the network the effects of nonlinearity on the shape of the confidence regions may be significant. However, for the well-located events both methods yield very similar confidence volumes which predict well the distribution of hypocenters obtained from repeated locations incorporating random errors. The generalized inverse method has the advantage that it can be more easily applied to the examination of systematic errors in hypocentral parameters produced by uncertainties in the velocity structure, since the effects of laterally varying velocity models can be studied in a computationally efficient manner. Except in the cases of very poorly resolved earthquakes, the effects of nonlinearity on uncertainties in hypocentral parameters can be observed by the application of F statistics to the variation of generalized inverse travel time residuals with focal depth.

Supported by: NSF Grants EAR88-17173 and  
EAR85-17137.

WHOI Contribution No. 7511.

# *GEOPHYSICS*

## **PALEONTOLOGICAL EVIDENCE FOR LATERAL DISPLACEMENT OF DEEP OCEANIC CRUST ALONG THE VEMA FRACTURE ZONE SOUTHERN WALL (ATLANTIC OCEAN, 10°45'N)**

*Marie-Pierre Aubry, William A. Berggren,  
Andr  Schaaf, Jean-Marie Auzende,  
Yves Lagabir lle and  
Vassilios Mammaloukas-Frangoulis*

Lateral displacement of oceanic lithosphere along transform faults has first been suggested by geophysical methods, especially by analysis of magnetic anomalies. Theoretical ages have been confirmed by paleontological studies of sediments recovered from non-transform areas, but until no direct geological evidence from fracture zones such as increasing age of sediments along transform fault walls have been reported. In this paper we present the results of a paleontological study of samples collected during the VEMANAUTE cruise on the Vema Fracture Zone southern wall where an almost complete section of oceanic crust is exposed. Our results are compared to theoretical ages proposed earlier for the crust in the surveyed area. The timing and location of mechanisms responsible for the exposure of the observed section suggest that early morphologies and structures may be preserved during the transform wall's displacement.

Supported by: A Consortium of Oil Companies.

WHOI Contribution No. 7561.

## **PREDICTING RELATIVE AND ABSOLUTE VARIATIONS OF IN-SITU PERMEABILITY FROM FULL WAVEFORM ACOUSTIC LOGS**

*Daniel R. Burns*

This paper provides a review of the application of full waveform acoustic logs to in-situ permeability estimation. The slowness and attenuation of the tube wave arrival in full waveform acoustic logs has been observed to be sensitive to variations in the in-situ permeability. The tube wave slowness can provide a measure of permeability variations if corrections are made for formation and borehole variations unrelated to permeability. The Biot model can be used to estimate absolute permeability values from tube wave attenuation measurements if all model parameters are known. However, the effect of mudcake on the tube wave properties must be

explicitly addressed before absolute estimates can be made with confidence. Shear wave acoustic logs, used in conjunction with the tube wave data, provide additional constraints on the permeability estimation problem.

In Press: *The Log Analyst* - Special issue on Acoustic Logging.

Supported by: NSF Grant OCE89-00316.

WHOI Contribution No. 7565.

### **SANDSTONE PORE ASPECT RATIO SPECTRA FROM DIRECT OBSERVATIONS AND VELOCITY INVERSION**

*Daniel R. Burns, C. H. Cheng and R. H. Wilkens*

Measurements of pore shapes from Scanning Electron Microscope (SEM) images for three sandstone samples (the Navajo Sandstone, the Weber Sandstone, and the Kayenta Sandstone) are compared with the aspect ratio spectra obtained from inverting laboratory velocity versus pressure data using the method of Cheng and Toksoz [1]. The two spectra can only be compared over a narrow range of aspect ratios due to the poor resolution of the inversion method at high aspect ratios and the SEM method at low aspect ratios. Over the narrow aspect ratio range of 0.001 to 0.01 the two spectra are in good agreement for the Navajo Sandstone which contains no clay. The agreement is poor for the Weber and Kayenta Sandstone samples both of which contain clay. The Navajo sample is composed primarily of quartz with pressure dissolution apparent along most grain contacts. The result is smooth, flat cracks along grain boundaries. The Navajo sample, then, is closest to the ideal "two-phase" material modelled by the inversion technique. Because of the presence of clay, the Kayenta and Weber samples are not accurately modelled by this technique, resulting in poor agreement between the inversion and SEM observations. The SEM derived aspect ratio spectra for the three samples are very similar. The spectral peak for all three samples corresponds to an aspect ratio of between 0.2 and 0.4 which is in agreement with other results in the literature [2,3].

Published in: *International Journal of Rock Mechanics and Mining Sciences & Geomechanics Abstracts*, 27(4):315-323, 1990.

Supported by: NSF Grant OCE89-00316.

WHOI Contribution No. 7350.

### **LITHOLOGIC CYCLES AND PALEO FLUID FLOW CHANNELS IN OLD OCEANIC CRUST FROM GEOPHYSICAL LOGS AT ODP SITE 418A**

*D. R. Burns, D. Thompson and C. H. Cheng*

Using some new processing of the multichannel sonic (MCS) log data from Site 418A, the resulting P, S, and Stoneley wave velocity estimates and apparent attenuation were integrated with the natural gamma, spectral gamma, resistivity, neutron, density, and caliper logs and core lithology information for interpretation of lithologic cycles and possible paleo fluid flow. These data indicate the presence of multiple breccia or rubble zones in the lower portions of the borehole. These zones are interpreted as the last stages of eruptive cycles as described by Hyndman and Salisbury (1984). The results of permeability (packer) tests and temperature gradient measurements at Sites 395A and 504B indicate that fluid flow in the crust at those sites is localized to brecciated zones which are capped by massive flow basalts. By analogy, the breccia zones interpreted at Site 418A may have acted as fluid flow channels at an earlier time. Six major paleo fluid flow zones are interpreted at Site 418A. These breccia zones have low velocities (P, S, and Stoneley), increased apparent attenuation, and an increase in gamma activity. These intervals are interpreted as permeable pathways which may have been altered by the second stage of oxidizing alteration as described by Holmes (1988). Each breccia unit is capped by a massive basalt flow unit which marks the start of the next eruptive cycle. The massive basalt flow units are identified in the MCS data by high velocities and low attenuation. The resistivity log data suggest that each major eruptive cycle trend is made up of several smaller sub-cycles. The MCS data can provide great insight into the variations in lithology in ODP boreholes if both the velocity and amplitude information is fully utilized. The inverse of the trace energy is a stable measure of apparent attenuation which may be related to alteration, fracturing, or permeability (if there are open fractures). Velocity estimates for P, S, and Stoneley waves provide useful information about lithologic variability if interpreted in detail.

Supported by: NSF Grant OCE89-00316.

WHOI Contribution No. 7406.

## THE SPREADING RATE DEPENDENCE OF 3-D MID-OCEAN RIDGE AND GRAVITY STRUCTURE

*J. Lin and J. Phipps Morgan*

Analyses of newly collected three-dimensional gravity data at mid-ocean ridges spreading at half-rates from 1.5 cm/yr to 5.5 cm/yr reveal that variations in along-axis seafloor depth and sub-seafloor density increase dramatically with decreasing spreading rate. These observations suggest that mantle flow has a three-dimensional 'string of plumes'-like structure beneath slow-spreading ridges and has a more sheet-like upwelling structure beneath fast-spreading ridges. We speculate that this may reflect a dominant compositionally driven mantle flow component beneath slow-spreading ridges and a dominant plate-separation induced mantle flow component beneath fast-spreading ridges.

In Press: *Geophysical Research Letters*.

Supported by: WHOI Culpeper Young Scientist Award and NSF Grant OCE90-20408.

WHOI Contribution No. 7319.

## THE SOUND FIELD NEAR HYDROTHERMAL VENTS ON AXIAL SEAMOUNT, JUAN DE FUCA RIDGE

*Sarah A. Little, Keith D. Stolzenbach and  
G. Michael Purdy*

High-quality acoustic noise measurements were obtained by two hydrophones located 3 m and 40 m from an active hydrothermal vent on Axial Seamount, Juan de Fuca Ridge, in an effort to determine the feasibility of monitoring hydrothermal vent activity through flow noise generation. Most of the measured noise field could be attributed to ambient ocean noise source of microseisms, distant shipping, and weather, punctuated by local ships and biological sources. Long-period, low-velocity, water/rock interface waves were detected with high amplitudes which rapidly decayed with distance from the seafloor. Detection of vent signals was hampered by unexpected spatial non-stationarity due to the shadowing effects of the caldera wall. No continuous vent signals were deemed significant based on a criterion of 90% probability of detection and 5% probability of false alarm. However, a small signal near 40 Hz, with a power level of  $10^{-4} \text{Pa}^2/\text{Hz}$  was noticed on two records taken within 3 m of the Inferno black smoker. The frequency of this signal is consistent with predictions, and the power level suggests the

occurrence of jet noise amplification due to convected density inhomogeneities.

Published in: *Journal of Geophysical Research*, 95(B8):12,927-12,945, 1990.

Supported by: NOAA Sea Grant  
NA86-AA-D-SG090, ONR Contract  
N00014-87-K-0007, and NOAA Vents Program.

WHOI Contribution No. 7122.

## BATHYMETRY OF THE MID-ATLANTIC RIDGE, 24°-31'N: A MAP SERIES

*G. M. Purdy, J.-C. Sempere, Hans Schouten,  
D. L. DuBois and R. Goldsmith*

This paper accompanies a series of twelve color maps that present the seafloor morphology of a 900 km-long section of the crestal region of the Mid-Atlantic Ridge (MAR) in a degree of detail never before published. The area covered by these maps, in the regional context of the Central Atlantic Ocean, is shown in Fig. 1. Interpretations of these data in terms of mid-ocean ridge processes are presented elsewhere (Sempere et al., 1990; Lin et al., 1990). The function of this article is simply to present the data, and to do so in a format that is of immediate utility to students of the Mid-Atlantic Ridge. The richness of these data and their potential for tackling a wide range of problems in mid-ocean ridge research is compelling motivation for their release in a timely manner. They are deserving of study by those with a broader range of expertise than exists within the small group of investigators involved in their collection. It is hoped that these results will serve as a stimulus for further geological and geophysical studies in this region by providing a high quality base map, a clear view of the regional setting of at least fifteen individual spreading center segments and, for the first time, an insight into the variability in morphological character of these segments and the discontinuities by which they are separated (Sempere et al., 1990).

Although these data are available in digital form, so that investigators could generate displays specifically to their individual requirements, we decided that in this case it was useful to produce and publish a hard copy map series at a scale that would permit them to be directly useful for investigations of mid-ocean ridges. Only a small portion of the community has been exposed to the incredible detail that modern multibeam bathymetry systems provide and to the unique view of the ocean floor they reveal when used to produce near 'full-coverage' maps of the type presented. Publication of these data in this form is something of an experiment that is practical only because of new facilities for computer generation of



large format displays and for low-cost color reproduction. If successful, we hope this will stimulate other investigators to publish their multibeam bathymetry data in a similar form thus making available this exciting new resource to the broader community.

Published in: *Marine Geophysical Researches*,  
12:247-252, 1990.

Supported by: NSF Grant OCE87-09615.

WHOI Contribution No. 7420.

## IMAGING WITH DEEP WATER MULTIPLES

*Edmund C. Reiter, M. Nafi Toksöz,  
Timothy H. Keho and G. M. Purdy*

Traditional methods of seismic processing treat energy which does not correspond to primary reflection paths as noise. In deep water seismic data, water column multiples are often coherent and separate enough from the primary reflections to be helpful in improving subsurface imaging. In this paper we demonstrate the utility of water column multiples using a field data set from a digitally recording stationary Ocean Bottom Hydrophone (OBH) (Koelsch et al. 1982) in 2300 m of water recording a 10,800 cubic inch airgun array (Figure 1a). We use a ray based Kirchhoff two dimensional (2-D) pre-stack depth migration to extrapolate and image the data along raypaths corresponding to the first order water column multiples in addition to the traditional primary reflection paths. This allows the primary reflections and the first order water column multiple to be processed separately and combined after polarity correction. The final composite image differs from the primary reflection image in two main aspects. First, the signal to noise ratio is improved in regions of the x - z plane insonified by both the primary and multiple reflections. Second, the lateral coverage of the image is extended as a result of including the water column multiple. Two dimensional synthetic data are used to examine the difficulties in identifying the true travel path of the multiple reflected energy. One possible path involves a reflection from the seafloor beneath the source, hereafter called the "source multiple" (Figure 1b) and the other a reflection from the free surface above the receiver called the "receiver multiple" (Figure 1c). We show that a reliable 2-D image may be extracted from the larger amplitude receiver multiple while the smaller amplitude source multiple provides a poor image.

In Press: *Geophysics*.

Supported by: NSF Grant EAR84-18120.

WHOI Contribution No. 7314.

## ROBUST DESCRIPTION OF STATISTICALLY HETEROGENEOUS SEAFLOOR TOPOGRAPHY THROUGH ITS SLOPE DISTRIBUTION

*Peter R. Shaw and Deborah K. Smith*

Statistical heterogeneity of abyssal hill properties is often evident in seafloor topography, even under periods of relatively constant spreading direction and rate. In this paper we relate the statistics of topographic slopes computed on finite spatial scales to the autocovariance function, and investigate the practicality of using these functions in describing such heterogeneous abyssal hill terrains. For a two-dimensional homogeneous surface, a direct relation exists between the sample autocovariance and the slope distribution at different spatial scales. However, for a heterogeneous field characterized by large transient signals, the computed autocovariance estimate no longer has a clear statistical interpretation, and becomes dominated by the transients. In contrast, the family of slope distributions can still be used to derive stable descriptors of the field. Slope statistics are thus useful in deriving a more robust estimate of the autocovariance than the usual sample autocovariance. Moreover, slope statistics may also be used to derive stable estimates of quantities not measurable with the autocovariance function or power spectra, such as the statistical asymmetry of features. Examples of the use of slope statistics and a comparison with autocovariance methods are presented. We document and quantify evidence of statistical asymmetry in a region of abyssal hills in the Northeast Pacific, and in a second example, the presence of multiple lineations in a region where a fracture zone cuts through abyssal hill terrain.

Published in: *Journal of Geophysical Research*,  
95(B6):8705-8722, 1990.

Supported by: ONR Contracts N00014-87-K-0087,  
N00014-87-K-0508 and N00014-89-J-1021.

WHOI Contribution No. 7335.

## FINITE DIFFERENCE SEISMIC MODELING OF AXIAL MAGMA CHAMBERS

*Stephen A. Swift, Martin E. Dougherty and  
Ralph A. Stephen*

We tested the feasibility of using finite difference methods to model seismic propagation at ~10Hz through a two-dimensional representation of an axial magma chamber with a thin, liquid lid. Our technique produces time series of displacement or pressure at seafloor receivers to mimic a seismic

reflection experiment and snapshots of P and S energy propagation. The results indicate that our implementation is stable for models with sharp velocity contrasts and complex geometries. We observe a high-energy, downward-traveling shear phase, observable only with borehole receivers, that would be useful in studying the nature and shape of magma chambers. The ability of finite difference methods to model high-order wave phenomena makes this method ideal for testing velocity models of spreading axes and for planning near-axis drilling of the East Pacific Rise in order to optimize the benefits from shear wave imaging of sub-axis structure.

Published in: *Geophysical Research Letters*,  
17(12):2105-2108, 1990.

Supported by: NSF Grant OCE87-01132.

WHOI Contribution No. 7299.

## THERMAL MODELING FOR HOLE 735B

*R. P. Von Herzen and J. H. Scott*

Two temperature logs subsequent to the drilling of the 500-m deep hole 735B on the flank of the Atlantis-II fracture zone in the SW Indian Ocean are used to determine the equilibrium temperature profile beneath the sea floor. The overall equilibrium temperature gradient with depth is negative at the surface, changing to a positive gradient at about 300 m which gradually increases to the bottom of the hole. Positive excursions of the temperature profile are centered at depths of about 30, 190, and 260 m below the sea floor. The data are interpreted with two different models: 1) Advection of sea water into permeable zones in the upper 400 m beneath the seafloor, and 2) warming by conduction from the surface since the last glacial maximum. The heat flow implied by the temperature profile in the deepest part of the hole is quite low,  $<30 \text{ mW m}^{-2}$ , but even at this depth the temperature gradient may not be representative of the heat flux from below.

Published in: *Proceedings of the Ocean Drilling Program, Scientific Results*, Leg 118.

Supported by: USSAC, Joint Oceanographic Institutions, Inc. JPO 799.

WHOI Contribution No. 7338.

## PALEOCEANOGRAPHY

### RECONSTRUCTING PAST PARTICLE FLUXES IN THE TROPICAL ATLANTIC OCEAN

*W. B. Curry and G. P. Lohmann*

Using a research strategy analogous to modern sediment trap studies, sediment accumulation patterns on submarine rises can be interpreted in terms of past ocean chemistry and circulation. We have followed this research strategy to reconstruct the history of surface water productivity and deep-water chemistry and circulation in the eastern equatorial Atlantic (Sierra Leone Rise) and western equatorial Atlantic (Ceara Rise) during the last glacial maximum ( $\sim 18,000 \text{ B.P.}$ ). On shallow sections of these rises, at depths with little carbonate particle degradation, we assume that the accumulation of skeletal carbonate approximates the carbonate production rate in surface water. During the last glacial maximum, the rate of carbonate productivity was lower in the eastern Atlantic than it is today, while the western Atlantic exhibited no glacial-interglacial difference in carbonate productivity. Based on the difference in carbonate accumulation rates between shallow and deep cores on the rises, we observed greater dissolution in both basins during the last glaciation. The eastern Atlantic always had a lower rate of dissolution than the western Atlantic, despite having deep water with a lower  $\delta^{13}\text{C}$  during the last glacial maximum. Organic carbon accumulation in the eastern Atlantic increased with depth in the water column during the last glaciation, suggesting that there was a bathymetric decrease in dissolved oxygen concentration at that time. These observations are consistent with a glacial decrease in the production rate of northern source deep water during the last glaciation. At that time, the mixing zone between northern source and southern source deep water migrated to the north in the Atlantic, resulting in a greater proportion of corrosive, southern source deep water in the western Atlantic, and entering the eastern Atlantic through low-latitude fracture zones. Today the ratio of northern and southern components entering the eastern Atlantic is about 4:1. Based on  $\delta^{13}\text{C}$  and carbonate accumulation, our best estimate of this ratio during the last glaciation is 1:1.

Published in: *Paleoceanography*, 5(4):487-505, 1990.

Supported by: NSF Grants OCE80-10935,  
OCE82-151, OCE84-10203 and OCE85- 11014.

WHOI Contribution No. 7398.

## PANGAEAN DIVERGENT MARGINS: HISTORICAL PERSPECTIVE

*Elazar Uchupi and K. O. Emery*

Pangaeon divergent margins caused by the breakup by rifting of that mega-continent display three distinct evolutionary stages. In their youth or rift stage divergent margins display a syn-sediment style fault that has considerable tectonic instability. During the mature or drift stage (sea-floor spreading) the continental margins are relatively stable and are dominated by thermal subsidence. These two stages (rifting and drifting) are separated in many areas by an unconformity coeval with the oldest oceanic crust—the break-up unconformity; in some areas the onset of seafloor spreading is marked by intense magmatic activity. Sediment facies during the rifting stage range from continental clastics landward of the continental basement hinge and along the flanks of the basin to saline deposits and more open water carbonates in the axial zone of the rift. Lithologies emplaced during the drift or mature stage of margin development range from shallow clastics/carbonates to deep-water carbonate/siliceous oozes, turbidites and contourites some of which were deposited in an anoxic environment. Deposition then is controlled by changes in the configuration of the basins, changes in sea level, and plate migration through several climatic belts. During the final or old-age stage of margin development divergence gives way to convergence. This stage, which generally terminates with continental collision, is characterized by tectonism, magmatic activity, and crustal shortening. Mesozoic divergent margins along the east-west trending Tethys Ocean have reached this stage in their evolution.

In Press: *Marine Geology*.

WHOI Contribution No. 7414.

## PALEONTOLOGY

### NEOGENE PLANKTONIC FORAMINIFER MAGNETOBIOSTRATIGRAPHY OF THE SOUTHERN KERGUELEN PLATEAU (SITES 747, 748 AND 751)

*W. A. Berggren*

With the exception of a brief (2 m.y.) late Miocene-early Pliocene hiatus, an essentially complete Neogene record was recovered on the Kerguelen Plateau in a calcareous biofacies. The

stratigraphic distribution of about 30 taxa of Neogene planktonic foraminifers recovered at Sites 747, 748, and 751 (Central and Southern Kerguelen Plateau; approximately 54°–58°S) is recorded. Faunas are characterized by low diversity and high dominance and exhibit a gradual decline in species numbers (reflecting a concomitant increase in biosiliceous forms, particularly diatoms) from about 10 in the early Miocene to 5 to 8 in the middle Miocene, 3–4 in the late Miocene to essentially a long (*Neogloboquadrina pachyderma*) form in the Pliocene-Pleistocene. A provisional seven-fold biostratigraphic zonation has been formulated which, together with the recovery of a representative Neogene magnetostratigraphic record, may ultimately lead to a correlation with low latitude magnetobiostratigraphies. The initial appearance of *Neogloboquadrina pachyderma* is associated with Magnetic Polarity Chron (MPC) 4 (~7 Ma) and MPC 4A (>8 Ma) at sites 747 and 751, respectively.

In Press: *Proceedings of the Ocean Drilling Program*.

Supported by: JOI-USSAC PO20228.

WHOI Contribution No. 7566.

### PALEOGENE PLANKTONIC FORAMINIFER MAGNETOBIOSTRATIGRAPHY OF THE SOUTHERN KERGUELEN PLATEAU (SITES 747-749)

*W. A. Berggren*

An essentially complete Paleogene record was recovered on the Central and Southern Kerguelen Plateau (~55°–59°S) in a calcareous biofacies. Recovery deteriorates within the middle Eocene and down to the upper Paleocene owing to the presence of interbedded cherts and chalks. The stratigraphic distribution of about 70 taxa of planktonic foraminifers recovered at Sites 747-749 is reported. Faunas exhibited relatively high diversity (approximately 20-25 species) in the early Eocene followed by a gradual reduction in diversity in the middle Eocene. A brief incursion of tropical keeled morozovellids occurs near the Paleocene/Eocene boundary similar to that recorded on the Maud Rise (ODP Sites 689 and 690).

The high latitude Paleogene zonal scheme developed by ODP Leg 113 has been adopted (with minor modifications) for the lower Eocene-Oligocene part of the Kerguelen Plateau record. A representative Oligocene (polarity chronozones 7-13) and late Eocene-late middle Eocene (questionably polarity chronozones 16-18) magnetostratigraphic record has allowed the calibration of several biostratigraphic datum levels

to the standard Global Polarity Time Scale (GPTS) and has established their essential synchrony between low and high latitudes.

In Press: *Proceedings of the Ocean Drilling Program*.

Supported by: JOI-USSAC PO20228.

WHOI Contribution No. 7567.

## ABYSSAL AGGLUTINATES: BACK TO BASICS

W. A. Berggren and M. A. Kaminski

We live in a world of ever increasing complexity. In the 25 years since the publication of the Treatise volumes by Loeblich and Tappan (1964), the number of validly described foraminiferal genera have more than doubled from 1192 in 1964 to at least 2455 in 1988. Agglutinated foraminifera (including the proteinaceous allogromiids) occupy about 180 pages of the recently revised version (Loeblich and Tappan, 1988). From the astrorhizids to the chrysalidinids, there are now at least 624 valid agglutinated genera, nearly as many genera as in the hyaline calcareous benthic suborder Rotaliina.

Taxonomy is a science which is intimately, if not wholly, devoted to the organization of observational data. It occupies a central role in the hierarchy of scientific activities, for without it any attempts at understanding or delineating relationships in the natural world are doomed to flounder on the scrapheap of chaos and obscurity.

Despite being one of the oldest of scientific endeavours, taxonomy does not yet benefit from widely observed principles and procedures. In practice, taxonomy can be regarded as a chaotic system (in the scientific sense of the word). It often seems that any initial uncertainties or minor oversights when a taxon is first described can lead to compounded errors at a later date. As in any chaotic system, the concept of a given taxon is generally constrained at some higher-order taxonomic level, such as at the genus or family level. But within these loose constraints, it is sometimes difficult to predict the course a given taxon definition will take when it is used by subsequent authors. Once a taxon becomes established in the literature, the history of taxonomic concepts surrounding a given species name often turns out to be an exercise in uncertainty, and one cannot escape the analogy with that of well-aged mystery novel.

The source of this chaos, ultimately, is the general practice of using only modern references when studying the history of a particular species concept. Often, modern taxonomists fail to refer to original material when using established, or so-called "well-known" names. In this essay, we

would like to point out some examples of chaos in the taxonomy of agglutinated foraminifera and identify some of the pitfalls which are likely to be encountered in the taxonomic history of any fossil group. The light-hearted approach we have taken here is not to be misconstrued as disrespect for our subject, but rather as an indication of the "human aspect" of research of this type as well as the fact that humour resides in the simplest as well as the most abstruse of all human endeavors. The theme of our discussion is that in the continuing effort to achieve a more realistic and "natural" classification of this "complex" group of organisms, we can achieve these objectives only by adopting a "Back to Basics" approach wherein we (re)examine original material, original sources and see for the first time the object of our scrutiny.

Published in: *Paleoecology, Biostratigraphy, Paleooceanography and Taxonomy of Agglutinated Foraminifera*, Hemleben, C. et al., eds. Kluwer Academic Publishers, Dordrecht, NATO ASI Series; Series C: Mathematical and Physical Sciences, Vol. 327:53-75, 1990.

Supported by: A Consortium of Oil Companies.

WHOI Contribution No. 7296.

## CALCAREOUS NANNOPLANKTON CHANGES ACROSS THE CRETACEOUS/PALEOCENE BOUNDARY IN THE SOUTHERN INDIAN OCEAN (SITE 750)

Thomas Ehrendorfer and Marie-Pierre Aubry

The changes in composition that the calcareous nannoplankton underwent across the Cretaceous/Paleocene boundary at southern high-latitude Ocean Drilling Program Hole 750A are documented through a semi-quantitative study. These changes are compared with changes described from other localities at high- and low-latitudes. This study provides additional data toward a detailed documentation of the paleontologic changes that occurred in the late Maestrichtian and the early Paleocene, despite limitations to the interpretation caused by coring gaps, drilling disturbance, and the presence of an unconformity at the boundary in this site.

In Press: *Proceedings of the Ocean Drilling Program, Scientific Results*, Vol. 120B.

Supported by: A Consortium of Oil Companies and the WHOI/MIT Joint Program in Oceanography.

WHOI Contribution No. 7519.

# CENOZOIC BIOSTRATIGRAPHY AND PALEOCEANOGRAPHY IN THE NORTH SEA AND LABRADOR SHELF

F. M. Gradstein, M. A. Kaminski and  
W. A. Berggren

We use Ranking and Scaling (RASC), a new method of "Graphic Correlation" (STRATCOR), and conventional comparison of foraminifer and dinoflagellate events in over 60 wells, to arrive at a new and detailed Cenozoic biostratigraphy for Paleogene bathyal and Neogene neritic strata in the North Sea-Haltenbanken and Labrador Shelf-Grand Banks. We emphasize ease of zonal recognition and reliability in correlation rather than maximum stratigraphic resolution. All zones are calibrated to standard planktonic foraminiferal and nannofossil zonations, and we present an interregional range chart for 43 agglutinated benthic foraminiferal taxa.

A fourteen fold (RASC) interval zonation of benthic and some planktonic foraminifera involves the average last occurrence of 64 taxa present in a minimum of 7 of 33 North Sea wells studied. In addition, eighteen rare, but stratigraphically important shelly microfossils and dinoflagellates were inserted as "unique events". A composite standard sequence (using STRATCOR) of 60 foraminiferal and 39 dinocyst events in 3 of the same North Sea wells improves chronostratigraphic resolution over previously published zonations. The interval zones are (from oldest to youngest): NSR1 - *Subbotina pseudobulloides* Zone, Danian; NSR2a,b - *Trochammina ruthven murrayi* - *Reticulophragmium paupera* Zone, late Lutetian to Bartonian; NSR7a,b - *Globigerina* ex gr. *officinalis* Zone, Chattian; NSR9 - *Globorotalia* ex tr. *praescitula* Zone, early-middle Miocene; NSR10 - *Bolboforma metzmacheri* Zone, late Miocene; NSR11 - *Neoglobobulimina atlantica* Zone, early Pliocene; NSR12 - *Cassidulina teretis* Zone, late Pliocene.

The quantitative biozonation for the Labrador Shelf and Grand Banks is calculated from the last occurrences distribution of 186 foraminifera and a few miscellaneous events in 27 wells. The 12 fold (RASC) zonation is quantitatively integrated with palynomorph events in 16 of the same wells, and the final zonation retains 85 of the 437 microfossil taxa, present in 7 or more wells. The interval zones are: LGR1 - *Gavelinella beccariiiformis* Zone, Danian to Selandian; LGR2 - *Subbotina patagonica* Zone, Ypresian; LGR3 - *Acarinina densa* Zone, early Lutetian; LGR4 - *Plectofrondicularia* aff *paucicostata* Zone, middle Lutetian; LGR5 - *Reticulophragmium amplexans* Zone, late Lutetian to Bartonian; LGR6 - *Turborotalia pomeroli* Zone, Priabonian; LGR7 - *Turritina alsatica* Zone,

Rupelian; LGR8 *Uvigerina* ex gr. *miozea nuttali* Zone, middle Miocene; LGR10 - *Ceratobulimina contraria* Zone, late middle Miocene; LGR11 - *Cassidulina teretis* Zone, Pliocene. Several zones may be split in subzones for more detailed subsurface correlations.

Paleoecological analysis reveals 5 microfossil assemblages, which characterize inner shelf through middle slope (bathyal) depth regimes. The Late Paleocene-Eocene middle slope assemblage lived at 750-1000 m water depth. The diversity and specimen abundance of agglutinated benthic foraminifera along two basinward seismic transects in the North Sea and Grand Banks, increases basinward. The genera *Rhabdammina*, *Kalamopsis*, *Karrierella*, *Hormosina*, *Ammosphaeroidina*, *Cystammina*, *Recurvoides*, *Rzehakina*, *Cyclammina* and *Pseudobulimina* are more typical for the deeper part of the basins. The observed paleoecological trends are of importance in the evaluation of subsidence and burial history trends, using the program BURSUB.

The tectonic and burial history of the Central North Sea basin is characterized by phases of rapid subsidence and sedimentation in the middle Paleocene and Pliocene, and little or no subsidence and widespread non-deposition or erosion in the Late Eocene, Early Miocene and Late Miocene. Relative geographic isolation of the North Sea in latest Paleocene through earliest Eocene time created a deep basin with lower salinity surface water.

In Press: Kluwer Academic and K.N.G.N.G. Book Series.

Supported by: A Consortium of Oil Companies.

WHOI Contribution No. 7529.

## PALEOGENE BENTHIC FORAMINIFERS FROM THE SOUTHERN INDIAN OCEAN (KERGUELEN PLATEAU): BIOSTRATIGRAPHY AND PALEOECOLOGY

Andreas Mackensen and William A. Berggren

Benthic foraminifera have been studied from lower Paleocene through upper Oligocene sections from Sites 747 and 748. The composition of the benthic foraminifer special suggests middle to lower bathyal (600-2000 m) paleodepth during the Neogene and probably upper abyssal (2000-3000 m) paleodepth during the Paleocene at Site 747. Site 748 is thought to have remained at middle to lower bathyal paleodepth throughout the Cenozoic. Principal component analysis distinguished four major benthic foraminifer assemblages: (1) a Paleocene *Stensioina beccariiiformis* assemblage at

Sites 747 and 748, (2) an early Eocene *Nuttallides truempyi* assemblage at a lower bathyal paleodepth at Site 747, (3) an early through middle Eocene *Stilostomella-Lenticulina* assemblage at middle bathyal Site 748, and (4) a latest Eocene through Oligocene *Cibicidoides-Astrononion pusillum* assemblage at both sites. Major benthic foraminifer changes, as indicated by the principal components and first and last appearances, occurred at or close to the Paleocene/Eocene boundary and in the late Eocene close to the middle/late Eocene boundary.

In Press: *Proceedings of the Ocean Drilling Program*, Vol. 120.

Supported by: JOI/USSAC PO20228.

WHOI Contribution No. 7467.

### ONTOGENY AND HABITAT OF MODERN MENARDIIFORM PLANKTONIC FORAMINIFERA

*Peter N. Schweitzer and G. P. Lohmann*

Ontogeny is an important source of variability in morphology and stable-isotopic composition in planktonic foraminifera. Through careful morphological analysis the populations of *Globorotalia menardii* and *G. tumida* were studied in detail at a single locality, the Ceara Rise. The foraminiferal test is dominated by two processes of growth, the accretion of chambers and the formation of an enveloping calcite crust. These are recognized through measurements of shell size, shape, and density. The populations are divided into groups according to their stage of chamber and crust development.

For both *Globorotalia menardii* and *G. tumida* the measured isotopic composition of whole specimens indicates that the organisms grow in the upper 50m of the water. The crust is emplaced at depths of between 50m and 100m, assuming that the shell is precipitated in isotopic equilibrium with seawater  $\delta^{18}\text{O}$ .

Assuming the smaller specimens lacking the crust represent the early stages of larger crusted specimens, one can calculate the oxygen- and carbon-isotopic compositions of the calcite added by the two processes. Crust composition in *Globorotalia tumida* appears to be in equilibrium with seawater  $\delta^{18}\text{O}$ , while in *G. menardii* the crust is lighter in  $\delta^{13}\text{C}$  than the equilibrium values.

Similar measures of isotopic composition from the Sierra Leone Rise and the Bermuda Rise support these findings. At the Bermuda Rise, the isotopic data suggests growth in shallow water during the summer months, when a seasonal thermocline is well developed.

In Press: *Journal of Foraminiferal Research*.

Supported by: OCE Grants 84-17040 and OCE89-12280.

WHOI Contribution No. 7557.

## PALEOCLIMATOLOGY

### HOLOCENE PALEOCLIMATIC EVIDENCE AND SEDIMENTATION RATES FROM A CORE IN SOUTHWESTERN LAKE MICHIGAN

*Steven M. Colman, Glenn A. Jones,  
Richard M. Forester and David S. Foster*

Preliminary results of a multidisciplinary study of cores in southwestern Lake Michigan suggest that the materials in these cores can be interpreted in terms of both isostatically and climatically induced changes in lake level. Ostracodes and mollusks are well preserved in the Holocene sediments, and they provide paleolimnologic and paleoclimatic data, as well as biogenic carbonate for stable-isotope studies and radiocarbon dating. Pollen and diatom preservation in the cores is poor, which prevents comparison with regional vegetation records. New accelerator-mass spectrometer  $^{14}\text{C}$  ages, from both carbon and carbonate fractions, provide basin-wide correlations and appear to resolve the longstanding problem of anomalously old ages that result from detrital organic matter in Great Lakes sediments.

Several cores contain a distinct unconformity associated with the abrupt fall in lake level that occurred about 10.3 ka when the isostatically depressed North Bay outlet was uncovered by the retreating Laurentide ice sheet. Below the unconformity, ostracode assemblages imply cold water with very low total dissolved solids (TDS), and bivalves have  $\delta^{18}\text{O}$  (PDB) values as light as -10. Samples from just above the unconformity contain littoral to sublittoral ostracode species that imply warmer, higher-TDS (though still dilute) water than that inferred below the unconformity. Above this zone, another interval with  $\delta^{18}\text{O}$  values less than -10 occurs. The isotopic data suggest that two influxes of cold, isotopically light meltwater from Laurentide ice entered the lake near the Holocene- Pleistocene boundary. These influxes, which occurred shortly before 10.3 ka and between 9 and 9.5 ka, were separated by a period during which the lake was warmer, shallower, but still very low in dissolved solids. One or both of the meltwater influxes may be related to discharge from Lake Agassiz into the Great Lakes.

Sedimentation rates appear to have been constant from about 10 ka to 5 ka. Bivalve shells deposited between about 8 and 5 ka have  $\delta^{18}\text{O}$  values that range from -2.3 to -3.3 and appear to

decrease toward the end of the interval. The ostracode assemblages and the stable isotopes suggest changes that are climatically controlled, including fluctuating water levels and increasing dissolved solids, though the water remained relatively dilute (TDS < 300 mg/l).

A dramatic decrease in sedimentation rates occurred at about 5 ka, possibly associated with the peak of the Nipissing high lake stage. A dramatic reduction in ostracode and mollusk abundances during the late Holocene is probably due to this decrease in sedimentation rates, which would result in increased carbonate dissolution. Ostracode productivity may also have declined due to a reduction in bottom-water oxygen caused by increased epilimnion algal productivity.

Published in: *Journal of Paleolimnology*, 4:269-284, 1990.

Supported by: USGS/WHOI Cooperative Agreement.

WHOI Contribution No. 7492.

## SEDIMENTOLOGY

### AN UNUSUAL ORGANIC CHEMICAL COMPOSITION FOR INTERFACIAL SEDIMENT IN THE BLACK SEA

*J. A. Beier, Stuart G. Wakeham, C. H. Pilskaln and S. Honjo*

Particulate material deposited at the sediment-water interface of the ocean represents the transition between material raining down to the sediment from overlying waters and material eventually buried. The organic chemical composition of this interfacial sediment tends to be a mix of compounds derived from sources in the water column and compounds produced during early stages of diagenesis. We report here that the uppermost 1 mm of sediment, or flocculant material ("floc"), in the Black Sea is unusually enriched in saturated organic compounds, in contrast to both water column particles and the underlying sediment in which unsaturated compounds are dominant. The floc may contain a rich microbial community capable of efficiently altering unsaturated organic compounds delivered to the sediment/water interface, leaving behind a compound distribution high in saturated components. In addition, the floc may be enriched in fine, low density material in which this microbial reduction has been shown to occur in the water column.

Supported by: NSF Grant OCE88-14228.

WHOI Contribution No. 7572.

### CARBONATE ACCUMULATION IN THE INDIAN OCEAN DURING THE PLIOCENE: EVIDENCE FOR A CHANGE IN PRODUCTIVITY AND PRESERVATION AT ABOUT 2.4 MA

*William B. Curry, James L. Cullen and Jan Backman*

We measured carbonate concentrations in Pleistocene and Pliocene sediments deposited at Sites 709, 710, and 711. Carbonate concentrations exhibit low-amplitude, long-wave length (300-400 k.y. period) variations at the shallowest sites (709 and 710). Before 2.47 Ma, all three sites exhibit higher frequency (100-k.y. period) variations. The deepest site (711) exhibited low-amplitude variations and very low concentrations up to the Gauss/Matuyama magnetic reversal (2.47 Ma), then concentrations abruptly increased. After 2.47 Ma, carbonate concentrations at Site 711 exhibited the same periodic changes as at Site 709. Although a long wave-length periodicity (260-280 k.y.) occurs at these sites after 2.47 Ma, the 100-k.y. period is absent. The dominant periods observed in these data are those found in the eccentricity component of the earth's orbital geometry.

Estimates of carbonate accumulation at Sites 709 and 710 document that surface-water productivity decreased near the Gauss/Matuyama magnetic reversal whereas accumulation at Site 711 increased. These results indicate that the rate of carbonate preservation in the deep Indian Ocean increased at that time. This increase in preservation may have resulted from a decrease in the production rate of carbonate in tropical oceans of the world. Carbonate accumulation estimated from sediments in shallow locations (~3000-3800 m) of the Atlantic and Pacific oceans also indicates that carbonate production decreased at this time. A consequence of lowered surface-water productivity is increased carbonate ion concentration of the deep ocean and better preservation of carbonate on the seafloor.

Published in: *Proceedings of the Ocean Drilling Program, Scientific Results*, Vol. 115, 1990.

Supported by: Various NSF Grants.

WHOI Contribution No. 7397.

### INTRASPECIFIC DIFFERENCES IN TEMPERATURE AND SALINITY RESPONSES IN THE COCCOLITHOPHORE *EMILIANA HUXLEYI*

*Nicholas S. Fisher and Susumu Honjo*

The growth of two clones of the oceanic

coccolithophore, *Emiliania huxleyi*, isolated from the Sargasso Sea and the Hudson Canyon, under 25 different salinity-temperature regimes was contrasted. The temperature range studied was from 8 to 27 °C; the salinity range was from 20 ‰ to 45 ‰. The isolate from the Sargasso Sea grew better at higher salinities than did the Hudson Canyon isolate, although not as well at the highest temperature. Generally, the Sargasso Sea clone had a narrower optimal temperature range (18 - 23 °C) and wider salinity range than did the Hudson Canyon clone. The results suggest that, as with diatoms, physiologically distinct races exist in coccolithophores, as indicated by the intraspecific differences in growth response to temperature and salinity in *E. huxleyi*. Further, these different growth responses of the two clones are consistent with the prevailing environmental conditions in their sites of isolation.

In Press: *Biological Oceanography*.

Supported by: NSF Grant OCE88-10657.

WHOI Contribution No. 7499.

#### SEDIMENT DEPOSITION IN THE LATE HOLOCENE ABYSSAL BLACK SEA: TERRIGENOUS AND BIOGENIC MATTER

Bernward J. Hay, Michael A. Arthur,  
Walter E. Dean, Eric D. Neff and Susumu Honjo

The temporal sedimentary patterns in the Late Holocene central eastern and western Black Sea are very similar. The sedimentary history was most visibly affected by the coccolithophorid species *Emiliania huxleyi* which briefly invaded the Black Sea for the first time ('First Invasion Period'), nearly disappeared again shortly afterwards ('Transition Sapropel'), but returned permanently several centuries later ('Final Invasion Period'). The temporary near-disappearance of *E. huxleyi* was probably caused by a temporary drop in salinity. Accumulation of *E. huxleyi* was on average about 40% higher in the western than in the eastern Black Sea. Highest coccolithophorid production occurred basin-wide during part of the Little Ice Age. The accumulation of terrigenous matter was generally higher in the eastern than in the western Black Sea by about 20%.

In Press: *Deep-Sea Research*.

Supported by: NSF Grants OCE86-114363 and OCE87-11741.

WHOI Contribution No. 7599.

#### ENHANCED PARTICLE FLUXES TO THE DEEP OCEAN INDUCED BY FRESHWATER INPUT

V. Ittekkot, R. R. Nair, V. Ramaswamy and  
S. Honjo

The Bay of Bengal is a gigantic catch basin for freshwater and sediment inputs from some of the world's largest rivers and as such exhibits drastic seasonal changes in its surface salinity. In order to study the dynamics of particle flux to the deep ocean in response to large scale freshwater inputs, we deployed three sediment trap moorings (two traps each) in the northern, central and southern Bay of Bengal, respectively (Fig. 1). Seasonally, the maximum river discharge during the SW monsoon coincides with maximum particle flux in the water column at all stations. Geographically, the fluxes of carbonate increase whereas those of total particles, opal, lithogenics and organic carbon decrease from north to south. The overall flux pattern appears to be controlled by seasonally varying inputs from land and accompanying shifts in marine biogenic production. World-wide freshwater pulses during deglaciation may have involved similar shifts in marine biogenic production, with concurrent changes in oceanic carbon removal processes.

Supported by: NSF Grant OCE88-14228.

WHOI Contribution No. 7573.

#### FLUXES OF REDUCED SULFUR, IRON AND ORGANIC CARBON IN THE BLACK SEA USING TIME-SERIES SEDIMENT TRAPS

Jo Ann M. Nicholson, Susumu Honjo, Brian Fry,  
Bernward J. Hay, Robert W. Howarth and  
John L. Cisne

In the southern and central Black Sea basin, reduced sulfur comprises nearly 1% of the total particulate flux, as measured by time-series sediment traps. This represents 7-12% of the total upward dissolved sulfide flux. Seasonal correspondence between sulfur and organic carbon fluxes, together with formation of particulate sulfides at the oxic-anoxic interface, are consistent with scavenging of sulfides at the interface during maximum production of settling organic aggregates, principally during the summer and autumn plankton blooms. Isotopic composition of particulate sulfide fluxes suggests that sulfide precipitates at the oxic-anoxic interface, where dissolved sulfide is isotopically heavier than dissolved sulfide below 180 m. No particulate sulfide fluxes have yet been measured which



resemble the isotopic composition of ambient dissolved sulfide at trap depths; sulfide precipitation deeper in the water column may be limited by availability of iron and/or polysulfides. Isotopically heavier particulate sulfides are also known from surface sediments, suggesting that sedimentary sulfides originate from metal sulfide fluxes forming at the oxic-anoxic interface and therefore reflect sulfur-cycling processes at the interface.

In Press: *Deep-Sea Research*, Black Sea volume, J. Murray, ed.

Supported by: NSF Grants OCE86-14462, OCE88-14363 and OCE88-00101.

WHOI Contribution No. 7302.

### **LITHOGENIC FLUXES TO THE DEEP ARABIAN SEA MEASURED BY SEDIMENT TRAPS**

*V. Ramaswamy, R. R. Nair, S. Manganini,  
B. Haake and V. Ittekkot*

Particle fluxes measured continuously for one year at three locations in the Arabian Sea using time-series sediment traps show that lithogenic sedimentation processes are strongly coupled to biological processes. The vertical flux of lithogenic matter is controlled by episodic production and fluxes of biogenic matter. Detailed clay mineral analyses carried out to study the seasonal variation in clay mineral fluxes, show that illite, and quartz are the dominant minerals in the traps at all three locations. Smectites generally range between 2 and 8%, but show higher fluxes of up to 25% in the central and eastern Arabian Sea during the SW monsoon period. It is seen that most of the river discharge is retained on the continental shelf and less than 5% of the annual input of lithogenic material to the Arabian Sea is deposited in the deeper part as hemipelagic sediments.

Supported by: NSF Grant OCE88-14228.

WHOI Contribution No. 7373.

**DEPARTMENT OF PHYSICAL OCEANOGRAPHY**

**James Luyten, Chairman**

**PHYSICAL OCEANOGRAPHY**



## OCEAN CIRCULATION & LOW FREQUENCY VARIABILITY

### EVIDENCE FOR BAROTROPIC WAVE RADIATION FROM THE GULF STREAM

*Amy S. Bower and Nelson G. Hogg*

Highly energetic velocity fluctuations associated with topographic Rossby waves have frequently been observed over the continental slope and rise off the US east coast. It has been suggested that the energy source for these waves could be eastward propagating Gulf Stream meanders, which can couple to the westward propagating Rossby waves if the meander shape is time-dependent. In this study, a historical archive of all available current meter data from the western North Atlantic has been examined for evidence of energy radiation from the Gulf Stream via barotropic/topographic Rossby waves. Horizontal maps of abyssal ( $> 2000$  m) eddy kinetic energy and Reynolds stress were constructed for four frequency bands. The maps are compared qualitatively with similar maps generated from a stochastic wave radiation model.

The eddy energy maps have many interesting features but bear little resemblance to the model-generated maps. This is most likely due to the oversimplified basin geometry used in the model. Observed energy levels reach maximum migrates northwestward to a location over the rise and slope south of New England at higher frequencies. Energy levels may be enhanced here due to refraction of Rossby waves emanating from the Gulf Stream.

The Reynolds stress maps show strong evidence of radiating waves north of the Gulf Stream over a large geographical area and at all frequencies considered. The velocity components are found to be statistically coherent and  $180^\circ$  out of phase at many locations when viewed in a coordinate system aligned with the local ambient potential vorticity gradient. Since we expect that energy is radiated symmetrically from the Gulf Stream, radiated waves are most likely present south of the stream as well. However, their presence is not apparent in the observations, perhaps due to the dominance of other eddy-generating mechanisms there such as baroclinic instability of the recirculation.

Supported by: NSF Grant OCE86-08258 and ONR Contracts N00014-85-C-0001, NR083-004.

WHOI Contribution No. 7587.

## MEASUREMENT OF THE FLOW THROUGH THE STRAIT OF GIBRALTAR

*Harry L. Bryden and R. Dale Pillsbury*

As part of the Gibraltar Experiment, eight subsurface moorings equipped with twenty-eight current meters were installed in the Strait of Gibraltar from October 1985 to April 1986. Another four moorings with fifteen current meters were installed from May 1986 to October 1986. Velocity, temperature, pressure and conductivity were measured at half-hourly intervals. Processing of these measurements and some initial results on the two-layer exchange between the Atlantic and Mediterranean through the Strait of Gibraltar are described in this paper.

Published in: *Advances in Water Resources*,  
13(2):64-69, November, 1989.

Supported by: ONR Contracts N00014-84-C-0218,  
NR083-102, N00014-85-C-0001 and NR083-004.

WHOI Contribution No. 7555.

### OCEAN HEAT TRANSPORT ACROSS 24°N IN THE PACIFIC

*Harry L. Bryden, Dean H. Roemmich, and  
John A. Church*

Ocean heat transport across  $24^\circ\text{N}$  in the North Pacific is estimated to be  $0.76 \times 10^{15}$  W northward from the 1985 transpacific hydrographic section. This northward heat transport is due half to a zonally averaged, vertical meridional circulation cell and half to a horizontal circulation cell. The vertical meridional cell is a shallow one, in which the northward Ekman transport of warm surface waters returns southward only slightly deeper and colder, all within the upper 700 m of the water column. In terms of its meridional heat transport, the horizontal circulation cell is also shallow with effectively all of its northward heat transport in the upper 700 m of the water column. Previous estimates of North Pacific heat transport at subtropical latitudes had ranged between  $1.14 \times 10^{15}$  W southward. The error in this new direct estimate of Pacific heat transport is approximately  $0.3 \times 10^{15}$  W. In addition, it is suggested that the annual variation in poleward heat transport across  $24^\circ\text{N}$  in the Pacific is of order  $0.2 \times 10^{15}$  W, as long as the deep circulation below 1000 m exhibits little variation in water mass transport. Together, the Pacific and Atlantic transoceanic sections essentially close off the global ocean north of  $24^\circ\text{N}$  so that the total ocean heat transport across  $24^\circ\text{N}$  is estimated to be  $2.0 \times 10^{15}$  W northward. This ocean heat transport is larger

than the northward atmospheric energy transport across  $24^{\circ}\text{N}$  of  $1.7 \times 10^{15}$  W. The ocean and atmosphere together transport  $3.7 \times 10^{15}$  W of heat across  $24^{\circ}\text{N}$ , which is in reasonable agreement with classic values of  $4.0 \times 10^{15}$  W derived from consideration of the earth's radiation budget but which is markedly less than the  $5.3 \times 10^{15}$  W required by recent satellite radiation budget determinations.

In Press: *Deep-Sea Research*.

Supported by: NSF Grant OCE85-04125.

WHOI Contribution No. 6570.

## THE GIBRALTAR STRAIT AND ITS ROLE IN THE DYNAMICS OF THE MEDITERRANEAN SEA

*Julio Candela*

The Strait of Gibraltar is the only dynamically relevant communication of the Mediterranean Sea with a large ocean basin, the North Atlantic. Although quite constrictive, important water exchanges occur through it over a broad frequency range.

With respect to the tides, considering the Mediterranean as a long zonal channel closed at both ends indicates that the principal tidal signal observed in its interior is astronomically forced. However, the tidal wave incoming from the Atlantic, although strongly reflected ( $\approx 94\%$ ) at the entrance to the Strait, has about 10% integrated contribution to the observed tide within the sea. In the Strait most of the tidal flow ( $\approx 92\%$ ) is barotropic, but a clear baroclinic tide is discernible from observations. The correlation between tidal currents and depth variations of the interface (separating Atlantic and Mediterranean waters) at Gibraltar's main sill represents up to 1/3 of the mean transport in each layer.

At subinertial frequencies, periods from days to a few months, the Strait restricts the meteorologically forced flows modifying the simple isostatic response of sea level to atmospheric pressure within the sea. A simple analytical model, consisting of two basins (the Western and Eastern Mediterranean) and two straits (Gibraltar and Sicily), indicates that the atmospheric pressure field over the sea accounts for 65% of the barotropic subinertial flows at Gibraltar, 68% of sea level variability in the western basin but only 41% of that in the eastern basin. These results are obtained by applying a linear friction coefficient to the limit the barotropic flows at both straits, Gibraltar and Sicily.

The long-term (seasonal to interannual) two-layered baroclinic exchange through the Strait has historically been related to the integrated

effects of the mass and salt balances in the sea. Recent works, based on the hydraulic behavior of the two-layer flow in from the Atlantic and out of the Mediterranean, allow speculation on the possible forcing and control mechanisms for this exchange, as well as their repercussions on the circulation and water characteristics within the sea. However, the true dynamical role played by time-dependent processes on these exchange flows remains a subject of debate and intense research.

In Press: *Dynamics of Atmospheres and Oceans*.

Supported by: Postdoctoral Scholarship.

WHOI Contribution No. 7477.

## EVIDENCE OF INTERNAL SWASH ASSOCIATED WITH SULU SEA SOLITARY WAVES?

*David C. Chapman, Graham S. Giese,  
Margaret Goud Collins, Rolu Encarnacion, and  
Gil Jacinto*

Vertical temperature profiles were measured near the shelf edge off the coast of Palawan Island, Philippines, during the passage of several "rip bands" of choppy surface waves. Such rip bands are commonly associated with internal waves. Coincident with the passage of one of the rip bands, the temperature near the bottom decreased by  $2.5^{\circ}\text{C}$  within 1.4 minutes, becoming colder than any water on the shelf. Furthermore, the apparent depth of our CTD decreased by about 8 m despite the fact that the "line-out" was held fixed. We interpret these limited data, along with a sea-level record, as evidence of internal swash created by breaking internal solitary waves which are generated by tidal flow over a shallow bank in the southeastern Sulu Sea (described by Apel *et al.*, 1985, *Journal of Physical Oceanography*, 15, 1625-1651).

In Press: *Continental Shelf Research*.

Supported by: NSF Grants OCE89-23065, INT88-16481 and WHOI Independent Study Award.

WHOI Contribution No. 7482.

## THE STRUCTURE OF THE KUROSHIO SOUTHWEST OF KYUSHU PART I: COMPARISON OF WINTER AND SUMMER HYDROGRAPHIC OBSERVATION IN THE KUROSHIO AND ADJACENT EAST CHINA SEA DURING 1986

*C. S. Chen, R. C. Beardsley, and R. Limeburner*

Two regional hydrographic surveys conducted in January and July 1986 aboard the

R/V *Thompson* and *Washington* illustrate the seasonal change in the water properties from winter to summer in the East China Sea and adjacent Kuroshio. In January, Kuroshio water was separated from the vertically well-mixed coastal water over the shelf by a strong front located near the shelf break. Evidence of horizontal mixing between the Kuroshio and coastal water extended far past the shelf break over the Kuroshio region near the surface, and in turn, Kuroshio water intruded onto the shelf near the bottom. Mixing between the Kuroshio and coastal water was found over much of the mid and outer shelf and upper slope, spanning a cross-stream distance of 75 km. Thus, the seasonal freshening and increased vertical stratification within the East China Sea contributed directly to the summer increase in fresh water transport in the upper Kuroshio. In addition, evidence of deep vertical mixing within the Kuroshio itself was found near 32.0°N, 128.2°E, most likely due to internal tidal mixing over the slope.

Supported by: NSF Grants OCE85-01366,  
OCE87-16937.

WHOI Contribution No. 7344.

### THE STRUCTURE OF THE KUROSHIO SOUTHWEST OF KYUSHU VELOCITY, TRANSPORT AND POTENTIAL VORTICITY FIELDS

*C. S. Chen, R. C. Beardsley, and R. Limeburner*

A triangular CTD/ADCP survey was made across the Kuroshio southwest of Kyushu aboard the R/V *Thompson* during January 1986. Due to relatively poor navigation data, a simple averaging technique has been used to convert the ADCP data taken between CTD station pairs into an average absolute velocity normal to the station pair with a maximum error varying from about  $\pm 5\text{ cm/s}$  to less than  $\pm 0.1\text{ cm/s}$  depending on the type of navigation data available. The average ADCP velocity at 60 m (or 10 m over the shelf) was then used as the reference velocity to calculate the absolute geostrophic velocity through the sides of the study triangle. The results show that the ADCP velocity shear was in reasonably good agreement with the geostrophic shear in the Kuroshio. The Kuroshio entered the study triangle as a coherent current, and then split around a tall seamount into two branches as it left the area. The volume transport of the Kuroshio southwest of Kyushu in January 1986 was  $30.3 \pm 2.0\text{ Sv}$ , and the advective heat transport was  $27.6 \pm 1.8 \times 10^{14}\text{ W}$ . These values are similar to those reported for the Gulf Stream in the Florida Strait, and a roughly linear correlation exists between heat and volume

transports in both regions. Mass conservation within the study triangle allowed construction of a streamfunction, which showed the presence of several mesoscale eddies to the north and northwest of the core of the Kuroshio. Potential vorticity estimated from the absolute geostrophic velocity field was conserved along streamlines on potential density surfaces except perhaps near a seamount where curvature vorticity must be considered, and the path of the Kuroshio could be traced by the core of maximum potential vorticity. Finally, the Kuroshio was potentially unstable as it flowed along the continental margin in the Okinawa Trough because the gradient of potential vorticity on potential density surfaces changed sign across the Kuroshio. This helps explain the mesoscale frontal and eddy features observed in the cyclonic side of the Kuroshio in the East China Sea.

Supported by: NSF Grants OCE85-01366,  
OCE86-16937.

WHOI Contribution No. 7368.

### WATER DISCHARGED FROM THE GULF STREAM NORTH OF CAPE HATTERAS

*James C. Churchill and Peter C. Cornillon*

Satellite radiometer-derived sea surface temperature images together with moored instrument and hydrographic survey data indicate that water ejected from the Gulf Stream often occupies the upper 200 m of the water column over the continental slope between Cape Hatteras and Hudson Canyon. At times this water resembles the energetic Gulf Stream frontal eddies commonly seen to the south of Cape Hatteras. However, many of the observed parcels of this water differ markedly from frontal eddies and Gulf Stream warm-core rings, and so appear to form a class of discharged Gulf Stream water different from any previously reported. These parcels generally cover a broad area (compared with frontal eddies), contain relatively weak currents (generally  $< 40\text{ cm s}^{-1}$  at 100 m), and are remarkably long lived (often remaining identifiable for more than two months). Salinity anomaly distributions indicate that, despite their persistence, these water masses contain intrusions of and mix with surrounding lower salinity water, particularly in the upper 50 m. Continuity of various tracers along  $\sigma_\theta$  surfaces indicate that the discharged Gulf Stream water observed near the sea surface originated within the nutrient-bearing stratum of the Gulf Stream having upwelled hundreds of meters along density surfaces. It enhances nutrient concentrations over the continental slope, markedly at the base of the euphotic zone but marginally within the center of

the zone. By contrast, this water does not carry unusually large kinetic energy densities into the slope region, but apparently gives up a good deal of kinetic energy before leaving the Gulf Stream. The mechanism responsible for this kinetic energy reduction is presently unknown, although some evidence indicates that spatial energy transfer through the action of eddy pressure work may be largely responsible.

Supported by: NSF Grant OCE88-12778, ONR Contract N00014-87-K-0235 and The Department of Energy under Contract # DE-ACO2-79EV10005.

WHOI Contribution No. 7553.

### ENERGETICS OF THE KUROSHIO EXTENSION AT 35°N, 152°E

*Melinda M. Hall*

A simplistic interpretation of eddy heat fluxes from a two year current meter mooring deployment in the Kuroshio Extension leads to the conclusion that the eddy field is decaying at 152°E, contradicting observations from the surface to 300 m that indicate the region to be one of steady or growing eddy energy. Thus, a simplified version of the method used by Hall (1989b) to construct the velocity field of the current from the moored data has been used to examine the baroclinic and barotropic energy conversions in the cyclonic and anti-cyclonic portions of the current, for both geographic and "stream" coordinates. Although the error bars are large, in stream coordinates significant conversions of mean to eddy potential energy occur on the anti-cyclonic side of the current at both 350 and 625 dbars, with smaller average conversions of eddy to mean energy over the cold portion. Barotropic conversions in this coordinate system are small, but qualitatively the calculated Reynolds stresses agree with previous observations showing that  $\partial(u'v')/\partial y < 0$  across the current, so that on average they converge mean momentum. For geographical coordinates, integrated energy balances still suggest overall decay of eddy energy, though not as strong as that found in the "simplistic" interpretation. Reynolds stresses are much stronger than for stream coordinates, and are still convergent, resulting in relatively large apparent conversions of eddy to mean kinetic energy in this coordinate system. Comparison with a similar energetic analysis by Rossby in the Gulf Stream at 73°W shows that: 1) The effects of going from geographical to stream coordinates are similar for the two currents; and 2) at locations that are geographically comparable for the two currents, very different energetic regimes prevail. Dynamical differences are also reflected in

the vertical velocity structure. It is hypothesized that external factors, such as the nature of the underlying deep flow, may influence the western boundary current systems in the two oceans in an important way.

In Press: *Journal of Physical Oceanography*.

Supported by: NSF Grant OCE87-10929.

WHOI Contribution No. 7360.

### MODELING THE GEOSTROPHIC ADJUSTMENT AND SPREADING OF WATERS FORMED BY DEEP CONVECTION

*A. J. Hermann and W. B. Owens*

The rate and the manner in which newly formed patches of dense oceanic waters may sink and spread is examined as a function of patch size and buoyancy input. The mass of dense fluid resulting from a rapid deep convective process comprises a large reservoir of potential energy, which may be carried away by two different means, broadly classed here as "radiative" (near-inertial waves) vs. "advective" (baroclinic instability). Both numerical and analytical methods are employed to investigate the relative amounts of potential energy and to the far field by either class of motion. We also consider the possible interactions between the radiative and advective motions for strong buoyancy forcing.

In Press: *Deep Convection and Deep Water Formation*, J.-C. Gascard and P.-C. Chu, eds. Elsevier Oceanography Series.

Supported by: ONR Contract N00014-86-K-0751.

WHOI Contribution No. 7549.

### MOORING MOTION CORRECTIONS REVISITED

*Nelson G. Hogg*

Several schemes are offered for the correction of temperature and velocity in the thermocline for mooring motion. They require measurements from at least two instruments spanning the thermocline and assume that the temporal variation of temperature (a proxy for density) results primarily from the vertical displacement of a fixed profile whose only degree of freedom is its pressure offset. Using two instruments in the thermocline from a mooring (the "GUSTO" mooring) in the Gulf Stream the procedure is tested against a third on the same mooring.

In Press: *Journal of Atmospheric and Oceanic Technology*.

Supported by: NSF Grant OCE86-08258 and ONR  
Contracts N00014-85-C-0001, NR083-004.

WHOI Contribution No. 7534.

### **A SIMPLE ONE-LAYER MODEL DRIVEN BY COMBINED WIND AND BUOYANCY FLUX**

*Rui Xin Huang*

A one-moving-layer model driven by combined wind and buoyancy flux is studied. The vertically integrated mass flux is determined by the wind stress, and the density distribution is determined by the air-sea interaction. The model highlights the physics of combining wind and buoyancy forcing in the simplest possible way. The model demonstrates the basic idea that satellite altimetry and scatterometry data can be used in reconstructing the oceanic general circulation.

In Press: *Dynamics of Atmospheres and Oceans*.

Supported by: NSF Grant OCE88-08076.

WHOI Contribution No. 7316.

### **THE THREE-DIMENSIONAL STRUCTURE OF WIND-DRIVEN GYRES; VENTILATION AND SUBDUCTION**

*Rui Xin Huang*

Theories of the three-dimensional structure of wind-driven gyres have been developed during the past decade. Potential vorticity homogenization of the unventilated thermocline and potential vorticity conservation of the ventilated thermocline have been proposed and tested against observations and numerical experiments. Models with continuous stratification, including a mixed layer of horizontally varying density and depth, have also been formulated; they reproduce a three-dimensional structure of the wind-driven circulation in the upper ocean. These theories have been extended in many directions. First, buoyancy forcing is included in the models by parameterizing it in terms of interfacial mass flux. Second, the connection with the western boundary current, the recirculations, the equatorial undercurrents, and the cross-gyre communication have been further studied. Tracer studies have provided new information about ventilation processes in the oceans.

In Press: *Reviews of Geophysics*.

Supported by: NSF Grant OCE88-08076 and ONR  
Contract N00014-90-J-1518.

WHOI Contribution No. 7590.

### **CONVECTIVE FLOW PATTERNS IN AN 8-BOX CUBE DRIVEN BY COMBINED WIND-STRESS, THERMAL AND SALINE FORCING**

*Rui Xin Huang and Henry M. Stommel*

We explore the circulation in an 8-box cube produced by combined wind-stress, surface heat exchange and precipitation/evaporation, mapping out the structure of the vertical velocity patterns, the existence of multiple steady states and the nature of bifurcations between them that occur as the precipitation/evaporation and amplitude of wind-stress are varied. With choice of parameters appropriate for the North Atlantic the model predicts a single stable state, circulating in the thermal sense (sinking at the pole) — and that this can be driven smoothly to a reversed saline sense (sinking at the equator), without catastrophe, by increasing the precipitation/evaporation rate beyond three times the present day value.

Supported by: NSF Grants OCE88-08076,  
OCE89-13128 and ONR Contract  
N00014-90-J-1518.

WHOI Contribution No. 7605.

### **MULTIPLE EQUILIBRIUM STATES IN COMBINED THERMAL AND SALINE CIRCULATION**

*Rui Xin Huang, James Luyten, and  
Henry M. Stommel*

Several box models are formulated, which are driven by a combination of thermal and saline forcings. Due to the physically different boundary conditions on temperature and salinity, the models' solution appear in multiple states. Each state is relatively stable to small perturbation and the system remains in the same state as the parameters change gradually. Bifurcation, both continuous transfer and catastrophe, appear as the parameters reach some critical values. Catastrophe can also be brought about by finite perturbations to the systems. The models' behavior may shed light on the catastrophic changes that occurred in the earth's history.

Supported by: WHOI Independent Study Award,  
NSF Grants OCE88-8076, OCE89-13128 and  
ONR Contracts N00014-90-J-1425,  
N00014-90-J-1518 and N00014-90-J-1508.

WHOI Contribution No. 7502.



## FLOW OF DEEP AND BOTTOM WATERS IN THE PACIFIC AT 10°N

*Gregory C. Johnson and John M. Toole*

Flow of Lower Circumpolar Water and North Pacific Deep Water is described in the Pacific at 10°N primarily using a recent trans-Pacific CTD/O<sub>2</sub> section. Water-mass properties are used to define boundaries at potential isotherms for these two water masses. In turn, zero-velocity surfaces are set at potential isotherms in each ocean basin along 10°N using the water-mass properties and the thermal wind field. These surfaces are then applied to estimate transport. Net northward transport of Lower Circumpolar Water is estimated at  $5.8 \times 10^6 \text{ m}^3 \text{ s}^{-1}$  in the East Mariana Basin and  $8.1 \times 10^6 \text{ m}^3 \text{ s}^{-1}$  in the Central Pacific Basin, while a small northward flow of  $0.4 \times 10^6 \text{ m}^3 \text{ s}^{-1}$  through the Yap trench into the Philippines Basin is inferred. In the Northeast Pacific Basin a southward transport of  $-4.7 \times 10^6 \text{ m}^3 \text{ s}^{-1}$  over the western flank of the East Pacific Rise is estimated. There is no Lower Circumpolar Water in the Guatemala Basin, thus the net transport of Lower Circumpolar Water across 10°N in the Pacific is estimated to be  $9.6 \times 10^6 \text{ m}^3 \text{ s}^{-1}$  northward. A net southward transport of  $-2.6 \times 10^6 \text{ m}^3 \text{ s}^{-1}$  of North Pacific Deep Water is estimated across this latitude, with the main feature being a southward transport of  $-3.6 \times 10^6 \text{ m}^3 \text{ s}^{-1}$  over the western flank of the East Pacific Rise in the Northeast Pacific Basin. Recent repeated hydrographic measurements in the Western Pacific are used to confirm the transport estimates for the two westernmost basins.

Supported by: NSF Grant OCE88-16910, ONR Contract N00014-89-J-1076 and NOAA Grant NA85AA-D-AC117.

WHOI Contribution No. 7608.

## FLOW OF BOTTOM WATER IN THE SOMALI BASIN

*Gregory C. Johnson, Bruce A. Warren, and Donald B. Olson*

Repeat CTD surveys by the R.R.S Charles Darwin in the Somali Basin at the height of subsequent northeast and southwest monsoons show only small differences in the circulation of the bottom water. About  $4 \times 10^6 \text{ m}^3 \text{ s}^{-1}$  moves north along the continental rise of Africa below a zero-velocity surface at the potential isotherm 1.2°C in a deep western-boundary current near 3°S. Cross-equatorial sections suggest that this flow turns eastward near the equator. North of the equator a large mass of cold water is found in the

interior, east of the Chain Ridge. The presence of this feature reinforces the evidence that the deep western-boundary current observed south of the equator turns east at the equator and feeds the interior circulation in the northern part of the basin from the equator, and not from the boundary. The deep circulation observed in the Somali Basin is roughly consistent with a flat-bottom uniform upwelling Stommel-Arons calculation with realistic basin geometry, source location and uniform upwelling. However, the model results indicate that the boundary current crosses the equator, whereas the observational analysis suggests that it turns eastward there.

In Press: *Deep-Sea Research*.

Supported by: ONR Contracts N00014-89-J-1076, N00014-87-K-0001 and NSF Grants OCE88-00135, OCE85-13825 and an ONR Fellowship.

WHOI Contribution No. 7396.

## A DEEP BOUNDARY CURRENT IN THE ARABIAN BASIN

*Gregory C. Johnson, Bruce A. Warren, and Donald B. Olson*

Recently collected CTD data are supplemented by historical Nansen bottle data to examine the circulation of bottom water in the Arabian Basin. A deep western-boundary current is observed flowing southeastward below a mid-depth zero-velocity surface along the Carlsberg Ridge. A zero-velocity surface at potential isotherm 1.7°C is chosen on the basis of water-mass properties. However, the origin of the bottom water in the Arabian Basin cannot be determined in a like manner. The bottom water could enter from the Somali Basin through the Owen Fracture Zone, or from the Central Indian Basin through passages in the Chagos-Laccadive Ridge south of the equator. Application of the Stommel-Arons framework for deep-circulation dynamics to the basin suggests that the bottom water is supplied primarily through the Owen Fracture Zone.

In Press: *Deep-Sea Research*.

Supported by: ONR Contracts N00014-89-J-1076, N00014-87-K-0001 and NSF Grants OCE88-00135, OCE85-13825 and an ONR Fellowship.

WHOI Contribution No. 7382.

## REVIEW OF U. S. CONTRIBUTIONS TO WARM-CORE RINGS

*Terrence M. Joyce*

Warm-core rings have been the subject of intense scrutiny in recent years. In fact, most of the detailed studies of rings have transpired since Richardson (1983) wrote his review of the literature for the Gulf Stream. Thus, this IUGG Quadrennial review of U.S. research will attempt to bring the reader up to date on the recent results since Richardson's summary for the Gulf Stream including some of the recent work by U.S. investigators in the Agulhas and Gulf of Mexico.

In Press: *Quadrennial Report to the IUGG*.

Supported by: NSF Grant OCE89-9908.

WHOI Contribution No. 7562.

## THE MEANDERING GULF STREAM AS SEEN BY THE GEOSAT ALTIMETER: SURFACE TRANSPORT, POSITION AND VELOCITY VARIANCE FROM 73° TO 46° W

*Kathryn A. Kelly*

The surface geostrophic velocity field for the Gulf Stream region was analyzed for the position, structure and surface transport of the Gulf Stream for 2.5 years of the Geosat altimeter Exact Repeat Mission. Synthetic data using a Gaussian velocity profile were generated and fit to the sea surface residual heights to create a synthetic mean sea surface height field and profiles of absolute geostrophic currents. Most of cross-track velocity variance was due to the meandering of the Gulf Stream, rather than to rings or complicated velocity profiles, which suggested that the simple model parameters are an efficient description of the Gulf Stream fluctuations. An analysis of the model parameters and the actual geostrophic velocity profiles revealed two different flow regimes for the Gulf Stream connected by a narrow transition region coincident with the New England Seamount Chain. The upstream region was characterized by relatively straight Gulf Stream paths, longer Eulerian time scales and eastward propagating meanders. The downstream region had more meanders, no consistent propagation direction and shorter Eulerian time scales. A 25% reduction in surface transport occurred in the transition region, with a corresponding reduction in current speed and no change in Gulf Stream width. A significant anomaly in surface transport near 69°W suggested the existence of small-scale recirculation gyres there. The highest-variance

empirical orthogonal functions of position and surface transport were significantly correlated, with larger surface transports leading more northerly positions by a month.

In Press: *Journal of Geophysical Research*.

Supported by: NASA Contract NAGW-1666.

WHOI Contribution No. 7355.

## THE GEOID AND MEAN SEA SURFACE HEIGHT ALONG THE GEOSAT SUBTRACK FROM BERMUDA TO CAPE COD

*Kathryn A. Kelly, Terrence M. Joyce,  
David M. Schubert, and Michael J. Caruso*

Measurements of near-surface velocity and concurrent sea level along a ascending Geosat subtrack were used to estimate the Earth's gravitational geoid and the mean absolute sea surface height. Velocity measurements were made on three traverses of the subtrack within 10 days, using an acoustic Doppler current profiler (ADCP). A small bias was removed by considering a mass balance for two pairs of triangles for which XBT measurements were also made. The resulting sea surface height was corrected for the cyclostrophic term to obtain the absolute sea surface height relative to the geoid. To take advantage of the reduction in mesoscale errors by temporal averaging, the alongtrack geoid estimate was computed as the difference between the mean sea level from the Geosat Exact Repeat Mission and an estimate of the mean sea surface height, rather than as the difference between instantaneous profiles of sea level and sea surface height. The mean sea surface height was estimated as the difference between the instantaneous sea surface height from ADCP and the Geosat residual sea level, and mesoscale errors were reduced by low-pass filtering the result. The geoid estimate differed from a gravimetric geoid by 0.24 m rms after removing a large-scale term, which was primarily due to the mean orbit error for Geosat. In three regions south of the mean Gulf Stream location, the discrepancies between the two geoids were not within the expected errors. An estimate of the mean sea surface height along the track agreed with an independent estimate of the mean sea surface height from Geosat, obtained by modeling the Gulf Stream as a Gaussian jet, within about 0.053 m, which was well within the expected errors in the estimates.

In Press: *Journal of Geophysical Research*.

Supported by: NASA Contract NAGW-1666 and NSF Grant OCE88-17698.

WHOI Contribution No. 7547.

## CAN REFLECTED EXTRA-EQUATORIAL ROSSBY WAVES DRIVE ENSO?

*William S. Kessler*

The possibility that the evolution of the ENSO phenomenon is determined by the reflection of extra-equatorial Rossby waves from the western boundary into the equatorial waveguide has been a subject of recent debate. Observations and some wind-driven models suggest an apparent continuity of off-equatorial signals and subsequent waveguide anomalies. On the other hand, coupled model results show that ENSO-like behavior can be simulated with no involvement of the extra-equatorial regions. Linear equatorial wave theory shows that significant reflection can only occur within about  $8^\circ$  of the equator, with a sharp fall-off in the reflectivity poleward of this latitude. Although the amplitude of the thermocline anomalies associated with observed ENSO-forced extra-equatorial Rossby waves can be large, it is the net zonal transport of these waves which is crucial to the reflectivity, and this net transport decreases rapidly as Rossby waves occur farther from the equator. If the zonal geostrophic flows associated with observed extra-equatorial signals do exert an influence on the equatorial waveguide, it must be through a mechanism other than simple boundary reflection.

Supported by: NSF Grants OCE88-16910 and OCE90-12508.

WHOI Contribution No. 7436.

## ASPIRATION OF DEEP WATERS THROUGH STRAITS

*Thomas H. Kinder and Harry L. Bryden*

In 1973 Stommel, Bryden and Mangelsdorf conjectured that high speed shallow flow in the Strait of Gibraltar is capable of sucking deep Mediterranean Water from the adjacent Alboran Sea directly up and over the sill into the Atlantic Ocean. This mechanism, which we call Bernoulli aspiration, has since been demonstrated in laboratory models, and the direct outflow has been confirmed by field experiment. Laboratory modeling, numerical experiment, and field measurement also have shown that the upstream path of the outflowing deep water is constrained by the combination of rotation and topography to form a narrow boundary current against the African coast. Data that was recently acquired during the Gibraltar Experiment (1985-1986) is used to describe the direct outflow of deep water and its distribution upstream of the sill.

We hypothesize that the uplift and direct outflow of deep water from the Mediterranean Sea through the Strait of Gibraltar is a mechanism which may be important in other strait and semi-enclosed sea systems. A key diagnostic for such flows is the upstream intensification of the deep flow as it approaches the sill.

Published in: *The Physical Oceanography of Sea Straits*. L. J. Pratt, ed. Kluwer Academic Publishers, Dordrecht, :295-319, 1990.

Supported by: ONR Contract N00014-87-K-0007.

## RECENT PROGRESS IN STRAIT DYNAMICS

*Thomas H. Kinder and Harry L. Bryden*

A major change in the understanding of the dynamics of flow through straits has occurred over the last few years with the development of two-layer hydraulic control models and their application to new observations in the Strait of Gibraltar. Observations of the flow through the Strait of Gibraltar indicate that there are at least two locations of critical flow where the Froude number equals one, at the sill and at the narrowest section of the Strait, as required by hydraulic theory for maximal exchange through the Strait. Predictions of the inflow and outflow transports and the salinity difference between them from hydraulic theory are in remarkable agreement with the recent observations. The physical configuration of the Strait of Gibraltar does indeed appear to control the amount of exchange between the Mediterranean and Atlantic Basins.

New observational techniques utilized in the Gibraltar Experiment have dramatically portrayed the physical processes operating in the two-layer exchange. Acoustic backscatter and Doppler current profiling have characterized hydraulic jumps and mixing, bore formation and propagation of internal solitary wave packets as no conventional measurements have done before. Time series current and, most importantly, salinity measurements on moorings have led to quantitative estimates of the inflow and outflow transports far superior to historical estimates and, furthermore, tidal oscillations contribute nearly half of the total transport. Microstructure measurements have allowed regions of intense mixing in the Strait to be identified and the amount of mixing to be quantified. Finally the first conclusive evidence of the direct aspiration of deep water up over a sill has been found in nearly all time series CTD stations at the Gibraltar sill.

In this progress report and review, the new hydraulic control theory and the recent Gibraltar observations are discussed in some detail. Next,

the effects of the Gibraltar flows on the circulation of the adjoining Mediterranean and Atlantic are described. A brief review of work in straits other than Gibraltar is presented. Then, models of the generation and propagation of large amplitude internal waves resulting from the interaction of tidal currents with a sill are reviewed and compared with the observed characteristics of waves in the Strait of Gibraltar. Finally, a list of important problems is presented with particular emphasis on the need to develop a fully time-dependent hydraulic theory for the two-layer exchange through a narrow and shallow strait.

In Press: *Reviews of Geophysics*.

Supported by: ONR Contract N00014-89-J-1085.

WHOI Contribution No. 7596.

### **OBSERVATIONS OF THE MINDANAO CURRENT DURING THE WESTERN EQUATORIAL PACIFIC OCEAN CIRCULATION STUDY (WEPOCS)**

*Roger Lukas, Eric Firing, Peter Hacker,  
Philip L. Richardson, Curtis A. Collins,  
Rana Fine, and Richard Gammon*

The WEPOCS III expedition was conducted from 18 June through 31 July 1988 in the far western equatorial Pacific Ocean to observe the low-latitude western boundary circulation there, with emphasis on the Mindanao Current. This survey provides the first quasi-synoptic current measurements which resolve all of the important upper-ocean currents in the western tropical Pacific and which includes an array of Lagrangian drifters with sufficient density to describe the surface circulation over the entire region. Observations were made of the temperature, salinity, dissolved oxygen, and current profiles with depth; of water mass properties including transient tracers; and of evolving surface flows with Lagrangian drifters. This paper provides a summary of the measurements and a preliminary description of the results.

The Mindanao Current was found to be a narrow, southward-flowing current along the eastward side of the southern Philippine islands, extending from 14°N to the south end of Mindanao near 6°N, where it then separates from the coast and penetrates into the Celebes Sea. The current strengthens to the south and is narrowest at 10°N. Direct current measurements reveal transports in the upper 300 M increasing from 10 Sv to 22 Sv between 10°N and 5°N. A portion of the Mindanao Current appears to recurve cyclonically in the Celebes Sea to feed the North Equatorial Countercurrent, merging with waters from the South Equatorial Current and the New Guinea

Coastal Undercurrent. Another portion of the Mindanao Current appears to flow directly into the NECC. The turning of the currents into the NECC is associated with the quasi-permanent Mindanao and Halmahera eddies.

Supported by: NSF Grants OCE87-16509 and OCE87-16510.

WHOI Contribution No. 7371.

### **A COMPARISON OF SHIP DRIFT, DRIFTING BUOY AND CURRENT METER MOORING VELOCITIES IN THE PACIFIC SOUTH EQUATORIAL CURRENT**

*M. J. McPhaden, D. V. Hansen, and  
P. L. Richardson*

In this note we compare mean seasonal cycles of zonal and meridional velocity in the Pacific South Equatorial Current based on current meter mooring data, drifting buoy data, and ship drift data. Monthly averages of ship drift and drifting buoy data were computed over 2° latitude by 10° longitude rectangles centered at the positions of multi-year current meter moorings near 0°, 110°W and 0°, 140°W. All three representations of the flow field show the basic character of the annual mean and its variations, provided that the sampling characteristics associated with each measurement technique are taken into account. In particular we find that more than 15 days of drifter data (regardless of year) are required on a 2° latitude by 10° longitude basis to produce monthly mean estimates that agree with moored estimates to within about 5–10 cm s<sup>-1</sup> rms. We also infer that windage effects climatological monthly mean ship drift velocities, although uncertainties in the data limit a precise determination of the windage magnitude. An upper bound appears to be about 3% of the surface wind speed, though the actual effect of windage may be considerably smaller.

Supported by: NSF Grant OCE87-16509.

WHOI Contribution No. 7367.

### **A STATISTICAL DESCRIPTION OF THE MEAN CIRCULATION AND EDDY VARIABILITY IN THE NORTHWESTERN ATLANTIC USING SOFAR FLOATS**

*W. Brechner Owens*

Velocity data obtained from trajectories of SOFAR floats launched as part of several experiments carried out in the Northwest Atlantic

during the last two decades are used to give a statistical description of the mean Gulf Stream and its recirculation. The distribution of eddy variability in the region is also presented. A mean Gulf Stream which bifurcates between 55° and 45°W to feed the North Atlantic Current and a southern recirculation can be clearly identified. A weak interior Sverdrup flow is also suggested. The spatial distribution of eddy variability is consistent with previous descriptions, showing a maximum near the Gulf Stream.

In Press: *Progress in Oceanography*.

Supported by: NSF Grants OCE81-09145, OCE76-11726, OCE86-00055, OCE78-18662, OCE89-16082 and ONR Contracts N00014-82-C-0019, N00014-89-J-1184 and N00014-86-K-0751.

WHOI Contribution No. 7516.

## THE LINK BETWEEN WESTERN BOUNDARY CURRENTS AND THE EQUATORIAL UNDERCURRENT

*Joseph Pedlosky*

A constant potential vorticity model is used to investigate the relation between the properties of an equatorward-directed western boundary current and the formation of the Equatorial Undercurrent in the western equatorial oceans.

It is shown that the value of the Bernoulli function at the equator, undetermined in earlier purely inertial EUC models, is fixed by the bifurcation latitude of the western boundary current which feeds the EUC. This is an additional example of the non-local forcing of the EUC subtropical gyre.

The constant potential vorticity model yields reasonable values for the initial EUC core velocities for a bifurcation latitude on the order 6° from the equator.

In Press: *Journal of Physical Oceanography*.

Supported by: NSF Grant ATM89-03890.

WHOI Contribution No. 7535.

## THE NONLINEAR DYNAMICS OF SLIGHTLY SUPERCRITICAL BAROCLINIC JETS

*J. Pedlosky and P. Klein*

The nonlinear dynamics of a slightly unstable baroclinic wave is studied for a two-layer f-plane system in which the basic flow is strongly sheared in the horizontal direction. The basic flow is purely baroclinic, i.e., equal to and opposite in

each layer. In addition, the basic flow vanishes on the channel walls containing the flow. Weakly nonlinear theory predicts that for small supercriticality, the basic wave eigenfunction has the same horizontal structure as the basic flow although it is vertically barotropic. Moreover, weakly nonlinear theory predicts growth of the wave amplitudes which is unrestrained by wave-mean flow interaction. This prediction is verified by direct numerical calculation. The numerical calculations further reveal the manner by which the wave eventually equilibrates. The strongly growing wave cascades energy to higher zonal harmonics. These harmonics alter the meridional structure of the fundamental which allows wave-mean flow interaction to operate, leading finally to equilibration. If the cascade to higher zonal wavenumbers is artificially blocked by truncating the numerical model to a single zonal wavenumber, equilibration requires artificially, the annihilation of the basic shear.

In Press: *Journal of Atmospheric Sciences*.

Supported by: NSF Grant ATM89-03890.

WHOI Contribution No. 7551.

## THE ROLE OF FINITE MIXED-LAYER THICKNESS IN THE STRUCTURE OF THE VENTILATED THERMOCLINE

*Joseph Pedlosky and Paul Robbins*

A model of the ventilated thermocline consisting of three adiabatic layers surmounted by a mixed layer of finite thickness is presented. The mixed-layer depth and density increase continuously northward, and these attributes of the mixed layer are specified. The effect of the mixed layer on the thermocline circulation is explicitly calculated.

The mixed-layer thickness and its variation play a significant role in shifting the trajectories of the streamlines westward. The shadow zones enlarge more rapidly south of the outcrop lines. The finite mixed-layer depth and its increase northward produce shadow zones in each of the adiabatic layers of the thermocline.

The augmentation of the ventilation rate, i.e., the rate which fluid enters the thermocline from the mixed layer in excess of the Ekman pumping is directly proportional to the northward gradient of the mixed-layer potential vorticity. The enhancement is greatest in regions where the circulation is surface-intensified, i.e., above the eastern shadow zones.

In Press: *Journal of Physical Oceanography*.

Supported by: NSF Grant ATM89-03890.

WHOI Contribution No. 7585.

## RADIATION-INDUCED BAROCLINIC INSTABILITY

*J. Pedlosky and R. M. Samelson*

The baroclinic instability of a broad zonal flow on the  $\beta$ -plane is studied in the case in which the  $\beta$ -effect renders the flow stable except within a narrow gradient in the lower of the model's two layers. An exact solution of the problem and simple asymptotic representations of that solution demonstrate that the flow is destabilized by the radiation of Rossby waves into the locally stable far field. The radiation-induced instability persists for all values of the ratio of the width of the locally supercritical region divided by the deformation radius. Even for small values of this ratio, an infinite number of radiating meridional modes are found. The largest growth rate occurs for the gravest mode.

The instability has relatively strong growth rates when the potential vorticity is uniform in the far field. We speculate that locally supercritical zones embedded in otherwise homogenized zones of uniform potential vorticity can act as efficient sources of radiated eddy energy.

In Press: *Geophysical Astrophysical Fluid Dynamics*.

Supported by: NSF Grant OCE89-16463.

WHOI Contribution No. 7408.

## SPACE-TIME VARIABILITY OF THE DEEP WESTERN BOUNDARY CURRENT OXYGEN CORE: MEANDERING AND VARIABILITY

*Robert S. Pickart*

Twelve historical CTD/oxygen sections between the Grand Banks and Cape Hatteras, occupied over the time period 1981-1985, are analyzed to investigate the variability of the Deep Western Boundary Current (DWBC) property core. The sections are transformed into a bottom depth versus height above the bottom coordinate system, then interpolated onto a regular grid in order to facilitate an inter-section comparison. The average sections show a high oxygen core near 3200 m depth,  $\theta = 2.2$  C which corresponds to a region of upward sloping isotherms against the boundary, inshore of the deep Gulf Stream. As the DWBC progresses towards Cape Hatteras it shoals significantly and becomes less dense as a result of mixing with surrounding fluid along its path. There is, however, much scatter about this general alongstream trend and large density fluctuations are correlated with changes in bottom depth and cross-sectional area of the DWBC core. This

variability is most likely the downstream response to changes in the overflow source waters of the DWBC. Some of the DWBC appears to get recirculated with the deep Gulf Stream near Cape Hatteras (where the two currents cross each other), forming a weaker offshore oxygen core.

Supported by: NSF Grant OCE90-09464 and ONR Contract N00014-87-K-0235.

WHOI Contribution No. 7603.

## SHALLOW AND DEEP COMPONENTS OF THE NORTH ATLANTIC DEEP WESTERN BOUNDARY CURRENT

*Robert S. Pickart*

A set of four hydrographic sections across the North Atlantic deep western boundary current from 55°W to 70°W is analyzed to distinguish the property features of the current's different water mass components. For each property a composite vertical profile versus potential temperature is constructed using all stations within the boundary current as well as anomaly profile relative to a composite of interior stations. The deepest component of the boundary current is the Norwegian-Greenland overflow water (2-3°C) which is characterized most readily by a core of low potential vorticity. The shallowest component of the boundary current (4-5°C) is revealed by a core of high tritium, CFC's and low salinity anomaly, but it has no corresponding oxygen signal because of its proximity to the pronounced oxygen minimum layer. A careful analysis of the shallow water mass reveals that it is not dense enough to be formed in the central Labrador Sea even during warm winters. Rather, based on historical hydrography the area of formation is the southern Labrador Sea inshore of the North Atlantic current where surface layer salinities are particularly low. A simple scale analysis shows that lateral mixing with the adjacent North Atlantic current can increase the salinity of this component to the values observed in the mid-latitude data set.

Supported by: NSF Grant OCE90-09464 and ONR Contract N00014-87-K-0235.

WHOI Contribution No. 7495.

## THE PHYSICAL OCEANOGRAPHY OF SEA STRAITS

*L. J. Pratt*

In July, 1989, a group of scientists gathered in Les Arcs, France to discuss the physical oceanography of sea straits. The five-day meeting was sponsored by the North Atlantic Treaty

Organization (NATO) and the United States Office of Naval Research (ONR). The purpose was to assess the present state of scientific knowledge with respect to strait and sill flow and to identify important and tractable problems for consideration in the near future. This volume is a compilation of the scientific work presented and the discussions held at Les Arcs.

Published in: *The Physical Oceanography of Sea Straits*. L. J. Pratt, ed. Kluwer Academic Publishers, Dordrecht, 587 pages, 1990.

Supported by: NATO Contract 18/71388 and ONR Contract N00014-89-J-1182.

WHOI Contribution No. 7470.

## GESTROPHIC VS. CRITICAL CONTROL IN STRAITS

Lawrence J. Pratt

The concept of geostrophic control of a steady flow by a sea strait, first established by Garrett and Toulany (1982), has been the subject of numerous debates and investigations [Garrett, 1983; Toulany and Garrett, 1984; Garrett and Majaess, 1984; Whitehead, 1986; Rocha and Clarke, 1987 and Wright, 1987]. Despite this attention, doubt and confusion continue to exist concerning the basic concept and its formal range of validity. For example, it is not known whether the formulas of rotating hydraulics (e.g., Whitehead *et al.*, 1974 or Gill, 1977) reduce to those of geostrophic control in any limit, or whether geostrophic control provides bounds on the transports predicted by hydraulic theory.

In this note it is argued that the steady flows described by existing, deductive hydraulic theories are not geostrophically controlled in any limit, nor does the transport relation given by geostrophic control occurs when advective effects (which are essential to the behavior of hydraulically-driven flow) are overwhelmed by time-dependence. This restriction places lower bounds on the values that the characteristic frequency  $\omega$  of motion can take. At the same time geostrophic control theory assumes time-dependent effects to be *weak* in the sense that ( $\omega \ll f$ , where  $f$  is the Coriolis parameter). Thus time-dependence must be weak, but not too weak.

In Press: *Journal of Physical Oceanography*.

Supported by: ONR Contract N00014-89-J-1182 and NSF Grant OCE89-16446.

WHOI Contribution No. 7517.

## A SEARCH FOR MEDDIES IN HISTORICAL DATA

P. L. Richardson, M. S. McCartney, and C. Maillard

A search was made using historical hydrographic data from the eastern North Atlantic to find measurements of very salty layers between 700–1300 m that could be observations of the warm, salty lenses known as Meddies (Mediterranean Water eddies). Twenty-five stations were found out of a total of 13,551 with positive salinity anomalies of at least 0.4 ‰, about half that of a strong Meddy in the Canary Basin. These possible Meddy observations were combined with additional reported Meddy observations to show that Meddies generally lie in an oval whose long axis extends 3000 km southwestward from the coast of Portugal. Five possible Meddy observations were found north of this region, near 44°N, where Meddies have never been reported.

Supported by: NSF Grants OCE86-00055 and OCE88-22826.

WHOI Contribution No. 7309.

## CURRENTS FORCED BY STOCHASTIC WINDS WITH MERIDIONALLY-VARYING AMPLITUDE

R. M. Samelson and B. Shroyer

Motivated by discrepancies between observations and previous theory, we construct and analyze a stochastically-forced model of wind-driven current fluctuations that includes the observed northward intensification of wind stress curl, a feature absent from a previous model. The model is linear, barotropic, and quasi-geostrophic, and is bounded meridionally by absorbing walls. The northward wind intensification causes a northward bias in the coherence of wind stress curl and currents that is similar to that observed. An unanticipated secondary maximum occurs northeast of the mooring in the low frequency (37-day period) meridional velocity coherence predictions. Corrected predictions from a previous model are also presented.

Supported by: NSF Grant OCE89-16463.

WHOI Contribution No. 7583.

## SPECTRAL TIME SCALES FOR MID-LATITUDE EDDIES

*William J. Schmitz, Jr. and James R. Luyten*

A few hundred current meter records of roughly one to two years' duration are now available from diverse locations in the world's oceans, primarily the North Atlantic. The shape of the spectrum for low frequency ocean current fluctuations is shown to have a geographical distribution related to the general ocean circulation. In the offshore segment of the Gulf Stream and Kuroshio Extension systems along with their recirculations, and near the Agulhas Current as well, normalized frequency distributions of eddy kinetic energy tend to be comparatively depth-independent and peaked at the mesoscale. However, in the immediate vicinity of current axes or fronts, spectral shapes may become "red" in the thermocline, as a result of meandering of a baroclinic jet across mooring sites.

Normalized frequency distributions of eddy kinetic energy from some areas distant from strong currents but perhaps near weaker upper-ocean fronts tend to be baroclinic and not peaked at the mesoscale in the thermocline, rather they are "red" there, although peaked at the mesoscale at abyssal depths. There are also low energy regions where spectral shapes tend to be red and comparatively independent of depth. In some areas, frequency distributions are relatively energetic or peaked at periods of order days, normally at depth near bottom relief.

In Press: *Journal of Marine Research*, 49(1), 1991.

Supported by: ONR Contracts N00014-76-C-0197, NR083-400, N00014-84-C-0134 and NR083-400.

WHOI Contribution No. 7389.

## DIURNAL CYCLES OF CURRENT, TEMPERATURE, AND TURBULENT DISSIPATION IN A MODEL OF THE EQUATORIAL UPPER OCEAN

*Rebecca R. Schudlich and James F. Price*

We have used a simple, one-dimensional model to simulate the diurnal cycle of the equatorial upper ocean. The model is initialized with the stratification and shear of the Equatorial Undercurrent (EUC), and is driven with heating and wind stress. A surface mixed layer is determined by bulk stability requirements, and entrainment is simulated in a transition layer below the mixed layer by requiring that the gradient Richardson number be greater than  $1/4$ . A principal result is that the nighttime phase of

the diurnal cycle is strongly affected by the EUC, resulting in deep mixing and large dissipation at night consistent with observations of the equatorial upper ocean during TROPIC HEAT.

The daytime (heating) phase of the simulated diurnal cycle is very similar to that seen at mid-latitudes. Solar heating produces a stably stratified surface layer roughly 10 m thick within which there is little,  $O(1 \times 10^{-8} \text{ W kg}^{-1})$ , turbulent dissipation. For the typical range of conditions at the equator, diurnal warming of the sea surface is  $0.2\text{--}0.5^\circ\text{C}$ , and the diurnal variation of surface current (diurnal jet) is  $0.1\text{--}0.2 \text{ m s}^{-1}$ , consistent with observations.

The nighttime (cooling) phase of the simulated diurnal cycle is quite different from that seen at mid-latitudes. As nighttime cooling removes the warm, stable surface layer, the wind stress can work directly against the shear of the EUC. This produces a transition layer that can reach to 80 m depth, or nearly to the core of the EUC, within which the turbulent dissipation is quite large,  $O(2 \times 10^{-7} \text{ W kg}^{-1})$ . Thus, the simulated dissipation has a diurnal range of about one order of magnitude, as observed in TROPIC HEAT, though the diurnal cycle of stratification and current that accompany it are fairly modest.

Supported by: ONR Contract N00014-89-J-1053.

WHOI Contribution No. 7548.

## BOTTOM WATER CIRCULATION IN THE WESTERN NORTH ATLANTIC

*Kevin G. Speer and Michael S. McCartney*

Antarctic Bottom Water flows into the western North Atlantic across the equator, shifting from the western side to the eastern side of the trough formed by the Mid Atlantic Ridge as it continues north. This is puzzling because such large-scale motion is thought to be controlled by dynamics which disallows an eastern boundary current. Previous explanations involve a (necessarily small-scale) density current which changes sides because of the change in sign of rotation across the equator, or a topographic effect which changes the sign of the effective mean vorticity gradient and thus requires an eastern boundary current. Here an alternative explanation for the overall structure of bottom flow is given.

A source of mass to a thin bottom layer is assumed to upwell uniformly across its interface into a lighter layer at rest. A simple formula for the magnitude of the upwelling and thickness of the layer is derived which depends, for fixed geometry, on the source strength to the bottom layer. For a strong enough source the bottom layer thickness is zero along a grounding curve,



separating the bottom water from the western boundary and confining it to the east. A band of recirculating interior flow occurs, supplied by an isolated northern and western boundary current. Similar structures appear to exist in the Antarctic Bottom Water of the western North Atlantic.

Supported by: NSF Grant OCE86-14486.

WHOI Contribution No. 7563.

## TRANS-PACIFIC SECTIONS AT 47°N AND 152°W: DISTRIBUTION OF PROPERTIES

*Lynne D. Talley, Terrence M. Joyce, and  
Roland A. DeSzoeko*

Three CTD/hydrographic sections with closely-spaced stations were occupied between May 1984, and May 1987, primarily in the subpolar North Pacific. Vertical sections of CTD quantities, oxygen and nutrients are presented. Upper water properties suggest that the Subarctic Front is located south of the subtropical/subpolar gyre boundary at 152°W that there is leakage of North Pacific Intermediate Water from the subtropical to the subpolar gyre in the eastern Pacific, and verify the poleward shift of the subtropical gyre center with depth. At intermediate depths (1000-2000 m), a separation between the western and eastern parts of the subpolar gyre is found at 180° along 47°N. Abyssal waters are oldest in the Northeast, with primary sources indicated at the western boundary and north of the Hawaiian Ridge. Properties and geostrophic velocity from detailed crossings of the boundary trenches suggest that flow in the bottom of the Kuril-Kamchatka Trench at the western boundary at 42°N and 47°N is northward. Very narrow boundary layers at intermediate depths are revealed in silica, as well as in the dynamical properties, at both the western and northern boundaries, and probably reflect southward and westward flow.

In Press: *Deep-Sea Research*.

Supported by: NSF Grants OCE84-16211,  
OCE87-40379, OCE86-58120, OCE84-16197,  
OCE83-16930 and ONR Contract  
N00014-84-C-0218.

WHOI Contribution No. 7353.

## DEEP CURRENTS IN THE ARABIAN SEA IN 1987

*Bruce A. Warren and Gregory C. Johnson*

New features of the deep circulation in the Arabian Sea were revealed by four sections of deep

CTD-O<sub>2</sub> stations occupied by the R.R.S. *Charles Darwin* late in 1986 and early in 1987, during the northeast monsoon, and repeated during the succeeding southwest monsoon. The most prominent elements in the bottom-water layer were (a) a northward flowing, western-boundary current of volume transport about  $4 \times 10^6 \text{ m}^3 \text{ s}^{-1}$  in the southern Somali Basin, which appeared to turn eastward at the equator and supply water to the northern Somali Basin from along the equator; and (b) a southeastward flowing boundary current along the northeastern flank of the Carlsberg Ridge in the Arabian Basin, which demonstrated that the bottom water of the Arabian Basin enters mainly from the Somali Basin through the Owen Fracture Zone, rather than from the Central Indian Basin. The strength of the boundary current in the Somali Basin implies an unusually large upward velocity at the top of the bottom water, about  $12 \times 10^{-5} \text{ cm s}^{-1}$ .

Mapping of water properties in the deep-water layer above the bottom water during successive monsoons was undertaken because three earlier surveys had shown differing horizontal distributions there, and had thus raised the possibility of a monsoonal reversal of the circulation, paralleling that in the near-surface water. However, the patterns of variation in the salinity and oxygen fields were essentially the same on the two *Darwin* cruises, suggesting a broad southwestward flow in the deep-water layer of the Somali Basin during both monsoons. We propose that this pattern was not forced by the monsoons but reflected mainly the mean circulation of the deep water as driven by the upwelling of the bottom water from below; that that pattern might be enhanced during the northeast monsoon if the wind-forcing penetrates into the deep water; and that a moderately strong southwest monsoon (in contrast to the extraordinarily weak monsoon of 1987) would be required to disrupt this distribution of water properties.

In Press: *Deep-Sea Research*.

Supported by: NSF Grant OCE86-14497, ONR  
Contracts N00014-89-J-1076,  
N00014-87-C-0001, NR083-004 and a Graduate  
Fellowship.

WHOI Contribution No. 7607.

## SUPPRESSION OF DEEP OXYGEN CONCENTRATIONS BY DRAKE PASSAGE

*Bruce A. Warren*

By establishing a zone free of topographic barriers, Drake Passage denies any net meridional geostrophic flow across the zone on isopycnal

surfaces in the approximate interval of potential-density anomaly  $\sigma_\theta = 27.5 - 27.8 \text{ mg/cm}^3$ . It thus prevents the convective processes that occur in the Southern Ocean south of the zone from renewing water to the north of it in this density range by mean flow. Inasmuch as this interval coincides roughly with that of the oxygen-poor layers found at mid-depths in the South Indian and South Pacific Oceans, the Drake Passage constraint seems to contribute significantly to the suppression of oxygen concentrations in those layers.

Published in: *Deep-Sea Research*, 37(12A):1899-1907, 1990.

Supported by: NSF Grant OCE86-07913.

WHOI Contribution No. 7312.

### **FASINEX, A STUDY OF AIR-SEA INTERACTION IN A REGION OF STRONG OCEANIC GRADIENTS**

*Robert A. Weller*

From 1984 to 1986 the cooperative Frontal Air-Sea Interaction Experiment (FASINEX) was conducted in the subtropical convergence zone southwest of Bermuda. The overall objective of the experiment was to study air-sea interaction on 1 to 100 km horizontal scales in a region of the open ocean characterized by strong horizontal gradients in upper ocean and sea surface properties. Ocean fronts provided large spatial gradients in sea surface temperature and also strong jet-like flows in upper ocean. The motivation for and detailed objectives of FASINEX are reviewed. Then, the components of the field program are summarized. Finally, selected results are presented in order to provide an overview of the outcome of FASINEX.

In Press: *Journal of Geophysical Research*.

Supported by: ONR Contract N00014-84-C-0134.

WHOI Contribution No. 7417.

### **RIDING THE CREST: A TALE OF TWO WAVE EXPERIMENTS**

*R. A. Weller, M. A. Donelan, M. G. Briscoe and N. E. Huang*

This paper gives a general overview of two ocean wave experiments. The experimental goals of the Surface Wave Processes Program (SWAPP) and of the Surface Wave Dynamics Experiment (SWADE) are quite different but complementary. In general terms SWAPP is focused on local processes: principally wave breaking, upper mixed layer dynamics and microwave and acoustic

signatures of wave breaking. SWADE, on the other hand, is concerned primarily with the evolution of the directional wave spectrum in both time and space, improved understanding of wind forcing and wave dissipation, the effect of waves on the air-sea coupling mechanisms and the radar response of the surface. Both programs acknowledge that wave dissipation is the weakest link in our understanding of wave evolution on the ocean. SWAPP takes a closer look at wave dissipation processes directly, while SWADE, with the use of fully non-linear (3rd generation) wave models and carefully measured wind forcing, provides an opportunity to study the effect of dissipation on spectral evolution. Both programs involve many research platforms festooned with instruments and large teams of scientists and engineers gathering and analyzing huge data sets. The success of SWAPP and SWADE will be measured in the degree to which the results can be integrated into a far more complete picture than we have had heretofore of interfacial physics, wave evolution and mixed layer dynamics.

Published in: *Bulletin of American Meteorological Society*, 72(2):163-183, 1991.

Supported by: ONR Contracts NR083-400, N00014-88-J-1028, N00014-84-C-0134.

WHOI Contribution No. 7380.

### **FORCED OCEAN RESPONSE DURING THE FRONTAL AIR-SEA INTERACTION EXPERIMENT (FASINEX)**

*R. A. Weller, D. L. Rudnick, C. C. Eriksen, K. L. Polzin, N. S. Oakey, J. M. Toole, R. W. Schmitt, and R. T. Pollard*

Prior to the field work done as part of the Frontal Air Sea Interaction Experiment (FASINEX), it was anticipated that the strong gradients in the upper ocean associated with ocean fronts would spatially modulate the response of the ocean to local atmospheric forcing. For five months, measurements of near-surface meteorology and upper ocean variability were made from an array of moorings. During this period a number of fronts passed through the experiment site. The moored meteorological and current meter data are used to examine the response of the upper ocean to atmospheric forcing at sub-inertial and near-inertial frequencies. At low frequencies both an Ekman-like frictionally-driven component in the mixed layer and a more deeply penetrating component thought to be forced by Ekman pumping were found. Strong near-inertial response was found in the mixed layer. The near-inertial motion showed considerable spatial variability in

the seasonal thermocline. Data about fine- and microscale variability in the upper ocean was obtained by profiling instruments deployed along cross-frontal sections during one month of the experiment. These data are used to examine the temporal variability of the small scale velocity field and its relation to atmospheric events and to determine whether or not the front and spatial variations in the near-inertial internal wave field associated with the front led to spatial variability at small scales.

In Press: *Journal of Geophysical Research*.

Supported by: NSF Grant OCE85-15336 and ONR Contracts N00014-89-J-1073, N00014-87-K-0007, N00014-84-C-0134, NR083-400 and N00014-89-J-1621.

WHOI Contribution No. 7490.

## ON THE TRANSPORT OF FRESH WATER BY THE OCEANS

*Susan Wijffels, Harry Bryden, Raymond Schmitt and Anders Stigebrandt*

The global distribution of freshwater transport in the ocean is presented, based on an integration point at Bering Strait, which connects the Pacific and Atlantic Oceans via the Arctic Ocean. Through Bering Strait,  $0.8 \times 10^6 \text{ m}^3 \text{ s}^{-1}$  of relatively fresh, 32.5 p.s.u., water flows from the Pacific into the Arctic Ocean (Coachman and Aagaard, 1988). Baumgartner and Reichel's (1975) tabulation of the net gain of freshwater by the ocean in  $5^\circ$  latitude intervals is then integrated from the reference location at Bering Strait to yield the meridional freshwater transport in each ocean. Freshwater transport in the Pacific is directed northward at nearly all latitudes. In the Atlantic, the freshwater transport is directed southward at all latitudes with a small southward freshwater transport out of the Atlantic across  $35^\circ\text{S}$ . Salt transport, which must be considered jointly with the freshwater transport, is northward throughout the Pacific and southward throughout the Atlantic (in the same direction as the freshwater flux) and is equal to the salt transport through Bering Strait. The circulation around Australia associated with the poorly known Pacific-Indian throughflow modifies the above scenario only in the South Pacific and Indian Oceans. A moderate choice for the throughflow indicates that it dominates the absolute meridional fluxes of freshwater and salt in these oceans.

Supported by: NSF Grants OCE87-13060 and OCE87-16910.

WHOI Contribution No. 7554.

## THEORETICAL AND LABORATORY MODELS

### CHAOS IN A MODEL OF FORCED QUASI-GEOSTROPHIC FLOW OVER TOPOGRAPHY: AN APPLICATION OF MELNIKOV'S METHOD

*J. S. Allen, R. M. Samelson, and P. A. Newberger*

We demonstrate the existence of a chaotic invariant set of solutions of an idealized model for wind forced quasigeostrophic flow over a continental margin with variable topography. The model (originally formulated to investigate mean flow generation by topographic wave drag) has bottom topography that slopes linearly offshore and varies sinusoidally alongshore. The alongshore topographic scales are taken to be short compared to the cross-shelf scale, allowing Hart's (1979) quasi-two-dimensional approximation, and the governing equations reduce to a nonautonomous system of three coupled nonlinear ordinary differential equations. For weak (constant plus time-periodic) forcing and weak friction, we apply a recent extension (Wiggins and Holmes, 1987) of the method of Melnikov (1963) to test for the existence of transverse homoclinic orbits in the model. The inviscid unforced equations have two constants of motion, corresponding to energy  $E$  and enstrophy  $M$ , and reduce to a one-degree-of-freedom Hamiltonian system which, for a range of values of the constant  $G = E - M$ , has a pair of homoclinic orbits to a hyperbolic saddle point. Weak forcing and friction cause slow variations in  $G$ , but for a range of parameter values one saddle point is shown to persist as a hyperbolic periodic orbit and Melnikov's method may be applied to study the perturbations of the associated homoclinic orbits. In the absence of time-periodic forcing, the hyperbolic periodic orbit reduces to the unstable fixed point that occurs with steady forcing and friction. The method yields analytical expressions for the parameter values for which sets of chaotic solutions exist for sufficiently weak time-dependent forcing and friction. The prediction of the perturbation analysis are verified numerically with computations of Poincaré sections for solutions in the stable and unstable manifolds of the hyperbolic periodic orbit and with computations of solutions for general initial-value problems. In the presence of constant positive wind stress  $\tau_0$  (equatorward on eastern ocean boundaries), chaotic solutions exist when the ratio of the oscillatory wind stress  $\tau_1$  to the bottom friction parameter  $r$  is above a critical value that depends on  $\tau_0/r$  and the bottom topographic height. The analysis complements a previous study of this model (Samselson and Allen, 1987), in which

chaotic solutions were observed numerically for weak near-resonant forcing and weak-friction.

In Press: *Journal of Fluid Mechanics*.

Supported by: NSF Grants OCE86-20403, OCE89-16463 and ONR Contracts N00014-84-C-0134, NR083-400 and N00014-90-3-1050.

WHOI Contribution No. 7343.

## THE INTERACTION OF AN EDDY WITH AN UNSTABLE JET

*George I. Bell and Larry J. Pratt*

Interactions between an unstable jet and eddy are explored using a jet with piecewise constant potential vorticity and eddy represented by a point vortex. A linear theory is developed for the case where the jet is nearly zonal and the eddy is far away in the sense that the velocity at the jet induced by the eddy is small compared with the maximum jet velocity. The calculations are extended into the nonlinear domain by the method of contour dynamics. Specific examples of barotropic and equivalent barotropic jets are discussed, with particular attention to processes leading to eddy propagation.

In the barotropic case, long range eddy-jet interactions are dominated by the instability, which breaks the jet up into eddies downstream from the forcing eddy. For a forcing eddy south of an unperturbed eastward flowing jet, the initial eddy propagation tendency is SW for cyclones and NE for anticyclones. In the equivalent barotropic case, the fact that long waves in the jet are neutrally stable modifies the interaction considerably. Although the jet instability is triggered by the eddy, the instability may be advected downstream rapidly enough that it does not affect the eddy. A long wavelength, steady lee wave may develop downstream from the forcing eddy, and this results in a propagation of the eddy in the opposite direction from the barotropic case (NE for cyclones, SW for anticyclones).

Supported by: NSF Grant OCE89-16446, ONR Contract N00014-89-J-1182 and a Postdoctoral Fellowship.

WHOI Contribution No. 7591.

## A REVIEW OF ROTATING HYDRAULICS

*K. M. Borenäs and L. J. Pratt*

The concepts of hydraulics of rotating-channel flow are presented. The review includes work on uniform as well as nonuniform potential vorticity

flow. A unified formalism is used when discussing the various contributions to the field. Rotating hydraulics jumps and bores are also considered.

In Press: *The Physical Oceanography of Sea Straits*. L. J. Pratt, ed. NATO ASI Series, Kluwer Dordrecht, :321-341, 1990.

Supported by: ONR Contract N00014-89-K-1182 and Swedish Natural Science Research Council under Contract # R-RA 9811-300 and NATO Contract 18/71388.

WHOI Contribution No. 7469.

## EXPERIMENTS ON BAROCLINIC VORTEX SHEDDING FROM HYDROTHERMAL PLUMES

*Karl R. Helfrich and Thomas B. Battisti*

Laboratory experiments have been conducted to examine the effects of rotation on the structure and stability of hydrothermal plumes. It is shown that the plume forces a baroclinic vortex consisting of an anticyclonic eddy at the neutral buoyancy level and cyclonic circulation in the ambient fluid around the rising plume. These features agree qualitatively with Speer's (1989) model. However, the experiments show that this state is unstable leading to the breakup of the plume and the unsteady generation of baroclinic vorticities (hetons) that propagate away from the source. Two nearby plumes interact repulsively for separations  $\gtrsim NZ_s/f$ , where  $N$  is the buoyancy frequency,  $f$  is the Coriolis frequency and  $Z_s$  is the height of the spreading level. It is suggested that oceanic hydrothermal plumes may shed isolated baroclinic vortices which are capable of retaining anomalous properties (temperature, salinity,  $^3\text{He}$  etc.) over large distances.

Supported by: WHOI Mellon Award.

WHOI Contribution No. 7438.

## REVIEW OF DISPERSIVE AND RESONANT EFFECTS IN INTERNAL WAVE PROPAGATION

*K. R. Helfrich and W. K. Melville*

Theories and models for the generation, propagation and dissipation of long, nonlinear internal waves are reviewed. The roles of dispersive and resonant effects are then discussed in the context of transcritical flow through channels. Recent work on the resonant generation of upstream advancing solitary waves is reviewed. It is shown that these waves (which include non-hydrostatic effects) may be important in the

time-dependent hydraulic control problem. The instability of non-linear Kelvin waves in a rotating channel is also discussed and it is shown that this instability may be responsible for observations of wave-front curvature. These processes may be significant in resolving the dynamics of sea straits.

Published in: *The Physical Oceanography of Sea Straits*. L. J. Pratt, ed. NATO ASI Series, Kluwer Academic Publishers, Dordrecht, :391-420, 1990.

Supported by: NSF Grant OCE89-02671.

## CURRENT RESEARCH PROBLEMS

*Lawrence J. Pratt and Karl R. Helfrich*

Below is a list of research problems and questions that the participants of the NATO/ONR meeting on the physical oceanography of sea straits put forward towards the end of the meeting. The suggestions were made in response to the question "What problem would you personally like to see solved within the next 5-10 years?" As the reader will see, there is a great deal of interest in the hydraulics of time-dependent strait and sill flows. Related issues include internal bore propagation, rectification, and the applicability of hydraulic control concepts. Other major topics of interest include the determination of maximal *vs.* submaximal exchange, the prediction of interfacial mixing and its consequences, and a host of issues related to flow with multiple density layers or continuous stratification. The following is not a comprehensive list of important issues but rather a statement of personal interests.

Published in: *The Physical Oceanography of Sea Straits*, L. J. Pratt ed. NATO ASI Series, Kluwer Academic Publishers, Dordrecht, :577-580, 1990.

Supported by: NATO Contract 18/71388.

WHOI Contribution No. 7468.

## HYDRAULICS OF ROTATING STRAIT AND SILL FLOWS

*L. J. Pratt and P. A. Lundberg*

The area of rotating hydraulics (defined as comprising field, laboratory, and theoretical studies) has expanded rapidly. The aim of the present review is to present a broad outline of subsequent developments as they have evolved over the past years and to identify current gaps in our knowledge.

Supported by: WHOI Independent Study Award and Swedish Natural Resource Council under Contract # G-GU-4768.

WHOI Contribution No. 7435.

## LINEAR AND NONLINEAR BAROTROPIC INSTABILITY OF GEOSTROPHIC SHEAR LAYERS

*L. J. Pratt and J. Pedlosky*

The linear, weakly nonlinear and strongly nonlinear evolution of unstable waves in a geostrophic shear layer is examined. In all cases, the growth of initially small amplitude waves in the periodic domain causes the shear layer to break up into a series of eddies or pools. Pooling tends to be associated with waves having a significant varicose structure. Although the linear instability sets the scale for the pooling, the wave growth and evolution at moderate and large amplitudes is due entirely to nonlinear dynamics. Weakly nonlinear theory provides a catastrophe time  $t_c$  at which the wave amplitude is predicted to become infinite. This time gives a reasonable estimate of the time observed for pools to detach in numerical experiments with marginally unstable and rapidly growing waves.

Published in: *Journal of Fluid Mechanics*, 91:49-76.

Supported by: NSF Grant OCE87-00601 and ONR Contract N00014-89-J-1182.

WHOI Contribution No. 7446.

## SEPARATION OF A BOUNDARY JET IN A ROTATING FLUID

*Melvin E. Stern and J. A. Whitehead*

A semi-infinite jet flows along a vertical wall in a rotating fluid, with the nose of the intrusion approaching a corner where the wall turns through an obtuse angle  $\theta + 180^\circ$ . The jet separates at the corner and flows into the interior if  $\theta$  exceeds a critical  $\theta_c$ , otherwise part of the jet continues around the corner and flows along the downstream segment of the wall. The separation criterion is computed using an inviscid and piecewise-uniform-vorticity model, with  $s$  denoting the ratio of the maximum 'offshore' to 'inshore' vorticity. The separation effect is demonstrated by a laboratory experiment in which a two-dimensional jet flows along the wall from a source. Average velocities are used to estimate  $s$ , and to make semi-quantitative comparisons of experimental and theoretical  $\theta_c$ . This suggests that the separation mechanism is independent of local viscous forces, although the cumulative effect of lateral eddy stresses in the jet is important in establishing the value of  $s$  immediately upstream from the corner. We suggest that our barotropic separation mechanism is relevant to mesoscale oceanic coastal currents.

Published in: *Journal of Fluid Mechanics*, 217:41–69, 1990.

Supported by: NSF Grant OCE86–14842 and partial support from ONR is acknowledged.

## MAGMA WAVES AND DIAPYRIC DYNAMICS

*J. A. Whitehead and Karl R. Helfrich*

The roots of magma sources lie at great depths where melt first begins to form. As the melt collects it must ultimately rise by either one (or both) of two distinct mechanisms: by bulk diapirism, where an entire partially melted mass buoyantly rises, or by porous flow (either around the periphery of grains in slightly melted material or through veins, cracks etc.). This paper focuses principally on the first of these mechanisms. We will close the paper with some discussion of certain similarities between the first and second mechanisms.

In the early stages, a layer of material with either enhanced melt or a higher temperature will tend to develop a lower density and also a lower viscosity than the surrounding regions. Such a layer is prone to develop fluid dynamic instabilities. Both observations of laboratory experiments and theory show that a relatively thin and horizontal plane of unstable material progresses through the following stages: The first stage is a Rayleigh-Taylor instability, in which disturbances of one specific wavelength grow most rapidly. If  $\xi$  is the ratio of the viscosity of the ambient material to the viscosity of the melt-enhanced or hot layer, fastest growth is usually for wavelength of order  $\xi^{1/3}$ , though in some cases  $\xi^{1/6}$  also holds. In the second stage, the distortion of the interface is large, and it is found experimentally that the fluid moves out of the thick layer as cylindrical columns surrounded by relatively broad regions of descending material. In the third stage, fully matured structures are formed with the development of a rim-syncline and pronounced syncline overhang. Eventually the original material will ascend as a spherical pocket of fluid trailed by a conduit. The presence of rigid horizontal surfaces below the layer does not change this result. If the original body has a form closer to a horizontal cylindrical tube the wavelength can be considerably shorter—of the order of the radius of the tube. For a continuous melt source, the first fluid to rise forms spherical pockets. A trailing conduit transports upwelling material through steady Poiseuille flow in which the stress of the low viscosity fluid balances the buoyancy force.

Theory and laboratory experiment show that the walls of these conduits support solitary waves. Among other interesting properties, these waves

behave nearly like solitons (solitary waves that are conserved upon collision with any other waves). In laboratory experiments, wave characteristics (shape, amplitude and speed) are very nearly conserved after collision with another wave. There has been a slight tendency for the large wave to increase in amplitude and the small wave to decrease. The phase speed of both interacting waves decreased by  $< 4\%$ . Measurement of phase shifts has compared well with direct numerical calculations using the full conduit equations. Korteweg-deVries (KdV) equations, formally valid for small amplitudes, gave poor quantitative results. It is also shown theoretically that these waves have closed streamlines in a frame moving with the wave. Hence they directly transport unmixed material upward. Calculations indicate that material in these parcels will be far less contaminated by diffusion from the surroundings than material in ordinary pipe flow. Thus such waves might convey material with little mixing from thousands of kilometers inside the earth to the brittle region tens of kilometers beneath the surface.

In magma chambers, conduits of one type of magma rising through another type of magma are also a possibility. When the Reynolds number  $4\sqrt{(g'Q^3)/\nu}$  is large for either fluid ( $g'$  is the buoyancy difference between the two magmas,  $Q$  is the volume flux, and  $\nu$  is the kinematic viscosity), flow in the conduit is 'turbulent'. The 'turbulence' is accompanied by severe axisymmetric or meander types of distortion of the conduit walls, and there can be extensive mixing between the two magmas. When the flow is non turbulent, and especially when there are solitary waves, there may be almost no mixing between the two magmas.

The flow and nonlinear waves in conduits are analogous to flow and waves in the compaction problem and share similar governing equations. It does not appear, however, that compaction waves have closed streamlines.

In Press: *Magma Transport and Storage*, M. P. Ryan ed. John Wiley and Sons, New York, :53–76, 1990.

Supported by: NSF Grant EAR87–08033.

## EXPERIMENTAL OBSERVATIONS OF BAROCLINIC EDDIES ON A SLOPING BOTTOM

*John A. Whitehead,  
Melvin E. Stern, Glenn R. Flierl, and Barry A.  
Klinger*

Baroclinic eddies in a rotating box with a sloping bottom were produced by squirting dense salt water up the sloping bottom and along the

"eastern" wall. The jet stagnated in shallow water and was ejected normal to the wall. For certain parameters (volume flux of jet, etc.), a coherent lens of dense bottom water formed and propagated west with an overlying cyclonic vortex. The circulation in the bottom lens, on the other hand, was relatively weak. No such eddy forms when the depth of fresh water is relatively deep, and a regime diagram is given for the formation of the coherent eddies. Thus a relatively simple structure emerges despite the complexity of the generating process. The pressure field determined from density measurements is discussed in terms of an integral theorem for coherent eddies, and the westward propagation is also related to previous theories. Several other techniques for generating such eddies are discussed.

Published in: *Journal of Geophysical Research*, 95(C6):9585-9610, 1990.

Supported by: NSF Grants OCE84-16100, OCE87-14842 and ONR Contracts N00014-87-K-0007 and NR083-004.

WHOI Contribution No. 7054.

# **INSTABILITY OF FLOW WITH TEMPERATURE - DEPENDENT VISCOSITY: A MODEL OF MAGMA DYNAMICS**

*J. A. Whitehead and Karl R. Helfrich*

In material whose viscosity is very temperature dependent, flow from a chamber through a cooled slot can develop a fingering instability or time dependent behavior, depending on the elastic properties of the chamber, the viscosity temperature relationship, and the geometry of the slot. A laboratory experiment is described where syrup flows from a reservoir through a tube immersed in a chilled bath to an exit hole at constant pressure. Flow is either steady, or periodic, depending on the temperature of the bath and the flow rate into the reservoir. A theory indicates that the transition from steady to periodic flow depends on nonlinearities in the steady state relation between pressure and flow rate and a general stability criterion is advanced. Parameters governing the oscillation period are determined. Theory also indicates that flow through a slot would develop finger-like instabilities under certain conditions. Qualitative laboratory experiments with paraffin spreading over a cold plate reveal the fingering.

Supported by: NSF Grants EAR87-08033 and EAR89-16857.

WHOI Contribution No. 7431.

## **COASTAL CIRCULATION & DYNAMICS**

### **COASTAL OCEAN PROCESSES (COOP): RESULTS OF AN INTERDISCIPLINARY WORKSHOP**

*Kenneth H. Brink, John M. Bane, Thomas M. Church, Christopher W. Fairall, Gerald L. Geernaert, Donn S. Gorsline, Robert T. Guza, Douglas E. Hammond, George A. Knauer, Christopher S. Martens, John D. Milliman, Charles A. Nittrouer, Charles H. Peterson, David P. Rogers, Michael R. Roman, and James A. Yoder*

A new interdisciplinary scientific effort, CoOP (Coastal Ocean Processes), is now being formulated to study basic scientific questions in the coastal ocean. Biological, Chemical, Geological and Physical Oceanography are represented as well as Marine Meteorology. CoOP is responding to the numerous important research opportunities presented by the coastal ocean and to the need for a holistic, fully interdisciplinary approach. The specific goal of CoOP is

to obtain a new level of quantitative understanding of the transports, transformations and fates of biogeochemically important matter over the continental margins.

The approach envisioned for CoOP calls for several process-oriented studies to be selected by the importance of the process and for the ability to study it in relative isolation. Plans call for pilot funding to start in late 1991. In order to give some definition to the CoOP effort, the first large-scale meeting was held July 9-11, 1990. Results, in the form of ideas for a pilot field effort, are summarized by a sequence of short reports presented in section III.

Published in: *Coastal Ocean Processes (CoOP): Results of an Interdisciplinary Workshop*. Report of the Coastal Processes Workshop, July 9-11, 1990, University of California, San Diego. Prepared by the CoOP Interim Steering Committee.

Supported by: NSF Grant OCE90-15613.

WHOI Contribution No. 7584.

## FORMATION AND MAINTENANCE OF SHELFBREAK FRONTS IN AN UNSTRATIFIED FLOW

*Glen Gawarkiewicz and David C. Chapman*

A depth-averaged model with no density variations was used by Chapman (1986, *J. Phys. Oceanogr.*, 1273-1279) to describe the formation of a passive tracer front at a shelfbreak. We examine the relevance of this frontogenesis mechanism to cases which allow vertical variations by considering the three-dimensional structure of a passive tracer front with explicit finite vertical mixing and bottom boundary layer dynamics. A three-dimensional primitive-equation numerical model is configured in a channel with a continental shelf, slope, and abyssal plain running the length of the channel. A vertically and horizontally uniform inflow is imposed over the shelf, with a large horizontal velocity shear near the shelfbreak. In the primitive-equation model, the offshore flow is concentrated in the bottom boundary layer while the alongshelf flow distribution is similar to the depth-averaged case; the presence of the bottom topography maintains a strong horizontal shear near the shelfbreak above the bottom boundary layer. This velocity shear causes a smooth passive tracer distribution imposed at the inflow boundary to develop strong cross-shelf gradients near the shelfbreak (i.e., a passive tracer front) within a rather short downstream distance, as in the depth-averaged model. Neutrally buoyant Lagrangian particles initialized above the bottom boundary layer are rapidly advected along the shelf with little cross-shelf motion. However, particles initialized within the bottom boundary layer move quickly offshore toward the shelfbreak and beyond while being advected alongshelf relatively slowly. The shelfbreak does *not* act as a barrier to the offshore transport of neutrally buoyant particles despite the presence of the passive tracer front. The result is a continuous net offshore transport from the shelf to the deep ocean due to the effects of bottom friction.

Supported by: NSF Grant OCE88-16015.

WHOI Contribution No. 7595.

## EVIDENCE OF A CRITICAL RICHARDSON NUMBER IN MOORED MEASUREMENTS DURING THE UPWELLING SEASON OFF NORTHERN CALIFORNIA

*Pijush K. Kundu and Robert C. Beardsley*

Evidence is found for a cut-off gradient Richardson number of  $Ri \approx 0.25$  in the moored

measurements of temperature and current obtained during the second Coastal Ocean Dynamics Experiment (CODE-2), conducted off northern California during the upwelling season of March-August, 1982. The cut-off at  $Ri \approx 0.25$  was noticed even when the instruments were separated by depth intervals as large as 40 m, or when the time series (having a sampling interval of 7.5 min) were averaged over an hour. During several strong wind events which tend to increase the mean shear,  $Ri \approx 0.25$  occurred in the main thermocline beneath the surface mixed layer over the shelf. On the other hand, several instances were found when a low  $Ri$  was not directly related to any wind event, suggesting that superposition of various waves can locally generate unstable conditions. The deeper water over the shelf and slope was generally stable with  $Ri > 0.25$ .

These results suggest that in coastal areas with strong currents, the intensification of mean vertical shear seems to be very important in bringing about Kelvin-Helmholtz-type instabilities, as compared to the open ocean without strong currents where superposition of internal waves is believed to be primarily responsible for causing the instabilities. Because the density structure almost everywhere in the ocean is in the form of steps, and because the overall Richardson number across vertical scales as large as 20 m are frequently near critical, it follows that appreciably thick regions in the ocean frequently remain on the brink of Kelvin-Helmholtz instability, even though the actual mixing may take place within thin interfaces between relatively homogeneous layers. A small increase of the overall shear then greatly increases the frequency of billow events and vertical mixing, and a small decrease of the overall shear greatly decreases such activity. It is suggested that in numerical circulation models the Richardson number be constantly checked and vertical mixing be used to maintain the Richardson number above a minimum value of 0.25.

In Press: *Journal of Geophysical Research.*

Supported by: NSF Grants OCE87-09705 and OCE88-16937.

WHOI Contribution No. 7597.

## THE BOTTOM BOUNDARY LAYER OVER THE NORTHERN CALIFORNIA SHELF

*Steve J. Lentz and John H. Trowbridge*

Moored temperature and shipboard CTD observations from the Northern California coastal upwelling region reveal variable bottom mixed-layer heights which are typically 5 - 15 m, but occasionally exceed 50 m. Observations from



Oregon, northern California, and Peru, indicate that in coastal upwelling regions, maximum bottom mixed layer heights tend to increase with water depth over the shelf, but rarely exceed half the water depth. Over the northern California shelf the bottom mixed-layer height is shown to depend on the stratification, the current magnitude, and the current direction. The dependence on current direction tends to dominate the response, with thicker bottom mixed layers during poleward flows and thinner bottom mixed layers during equatorward flows. This asymmetric response to poleward and equatorward currents is consistent with the model results of Weatherly and Martin [1978] and Trowbridge and Lentz [1990] which indicate that the asymmetric response is due to the up or down slope Ekman transport of buoyancy along the bottom.

Supported by: ONR Contract N00014-89-J-1074.

WHOI Contribution No. 7445.

### **INSTRUMENTATION & EXPERIMENTAL METHODOLOGY**

#### **TESTS OF LONG-RANGE OCEAN DATA TELEMETRY USING FREQUENCY-AGILE HF PACKET-SWITCHING PROTOCOLS**

*David A. Brooks and Melbourne G. Briscoe*

We describe experiences with two prototype telemetry systems developed for potential use with moored or drifting ocean instruments. The systems transfer data and commands between remote and base stations using direct high-frequency (HF) ionospheric radio propagation ("shortwave" radio) without intervening relay stations or satellites. The strategy exploits recent developments in digital packet-switching technology, which is readily available and can be inexpensively applied to oceanic problems. The potential advantages of packet methods over satellite methods include low cost and autonomy; the HF packet telemetry also provides a two-way link for remote control of the oceanic instrument or device and data rates of typically 1-10 bit/s, averaged over several days. Coverage is effectively global, but intermittent. Disadvantages mostly result from the interference and skip zones that characterize HF propagation. The tests described here took place near the time of a sunspot minimum; the utility of HF packet telemetry will be greatly increased during the early 1990s, when the current sunspot cycle is near its maximum.

Supported by: NSF Grant OCE87-00396 and ONR Contract N00014-86-K-0751.

WHOI Contribution No. 7568.

### **OCEAN FRONTAL VARIABILITY IN FASINEX**

*Charles C. Eriksen, Robert A. Weller,  
Daniel L. Rudnick, R. T. Pollard, and  
Lloyd A. Regier*

Oceanographic observations during the Frontal Air Sea Interaction Experiment (FASINEX) in the Sargasso Sea indicate that upper ocean fronts in the subtropical convergence zone are strongly surface intensified coherent flow structures which have a preferred orientation and translation speed. Fronts grow as they propagate in this region such that currents roughly double in strength in a time that they translate by twice their width. While currents are dominated by geostrophic momentum balance, the Rossby number of these flows can reach a few tenths. Mixed layer water from the cold side of fronts appears to subduct under warm side near surface waters, since isolated lenses of water with cold side temperature and salinity characteristics are found embedded in the seasonal thermocline on the warm side of fronts. Although plausible vertical speeds were observed, no actual rates of subduction could be estimated. Typical frontal widths, temperature contrasts; horizontal currents, vertical shears, vertical currents and translation speeds of fronts in the region studied are 20 km, 1°C, 0.5 m/s  $0.0005\text{ s}^{-1}$ , 0.0005 m/s and 0.2 m/s, respectively.

In Press: *Journal of Geophysical Research.*

Supported by: ONR Contract N00014-84-C-0134.

WHOI Contribution No. 7447.

### **AN INTELLIGENT CHILLED MIRROR HUMIDITY INSTRUMENT, D10IQ**

*David S. Hosom, James F. Price, Clifford Winget,  
Sumner Weisman, and Donald P. Doucet*

An intelligent, chilled mirror humidity instrument has been designed for use on buoys and ships. Our design goal is that the instrument make high quality dew point temperature measurements for a period of up to one year from an unattended platform, while consuming as little power as possible.

The instrument uses a General Eastern Dew-10 chilled mirror sensor, and is controlled by an onboard digital processor which is programmable in BASIC. Nominal system accuracy is 0.3°C and a measure of data quality is provided to indicate possible drift in calibration. Communications to an external logger is provided by an RS 232-compatible interface. The housing is made of PVC and is approximately 76 cm long

by 11.5 cm in diameter; the complete instrument weight is 28 kg. Energy consumption is typically 800 J per measurement; standby power consumption is 0.05 W.

A series of dock side tests have been carried out to evaluate the long-term accuracy and reliability of the D10IQ. As a standard, we use an EG&E 200M Dewtrak chilled mirror instrument which is cleaned manually at frequent intervals. We find that the mean difference between the D10IQ and EG&E 200M is roughly  $0.7^{\circ}\text{C}$ , and that the standard deviation of the difference is about  $0.7^{\circ}\text{C}$ . These errors are close to the design goal of  $0.5^{\circ}$  (assuming that the EG&G 200M is "correct"), but in the future we hope to reduce the bias by a better calibration procedure, and reduce the random error by refining the control algorithm of the D10IQ.

In Press: *Journal of Atmospheric and Oceanic Technology*.

Supported by: NSF Grant OCE87-09614 and ONR Contract N00014-84-0134.

WHOI Contribution No. 7439.

### ERROR IN MEASUREMENTS OF INCOMING SHORTWAVE RADIATION MADE FROM SHIPS AND BUOYS

*M. A. MacWhorter and R. A. Weller*

Errors in shortwave solar radiation measurements resulting from mean tilts and rocking motions as well as response time of the sensors are determined experimentally. The magnitude of the mean tilt error, as suggested by Katsaros and DeVault (1986), can be large and lead to errors in daily-averaged incoming shortwave radiation in excess of  $10 \text{ W}\cdot\text{m}^{-2}$ . Mean errors due to rocking motions and time response errors are less severe. The spatial distribution of the diffuse component of the radiation and the motion of the platform must both be known to attempt to correct for this error. An algorithm to perform this correction was derived, yet is only sufficiently accurate when the time response of the pyranometer is significantly smaller than the period of the rocking motion. Gimballing the sensors may be a more practical method of error reduction.

Published in: *Journal of Atmospheric and Oceanic Technology*, 8(1):108-117, 1991.

Supported by: NSF Grant OCE87-09614.

WHOI Contribution No. 7322.

### AN INDEX OF REFRACTION ALGORITHM FOR SEAWATER OVER TEMPERATURE, PRESSURE, SALINITY, DENSITY, AND WAVELENGTH

*R. C. Millard and G. Seaver*

A 27-term index of refraction algorithm for pure and sea waters has been developed using four experimental data sets of differing accuracies. They cover the range 500 to 700 nm in wavelength, 0 to  $30^{\circ}\text{C}$  in temperature, 0 to 40 psu in salinity, and 0 to 11,000 decibars in pressure. The index of refraction algorithm has an accuracy that varies from 0.4 ppm for pure water at atmospheric pressure to 80 ppm at high pressures, but preserves the accuracy of each original data set. This algorithm is a significant improvement over existing descriptions as it is in analytical form with a better and more carefully defined accuracy. A salinometer algorithm with the same uncertainty has been created by numerically inverting the index algorithm using the Newton-Raphson method.

The 27-term index algorithm was used to generate a pseudo-data set at the sodium D wavelength (589.26 nm) from which a 6-term densitometer algorithm was constructed. The densitometer algorithm also produces salinity as an intermediate step in the salinity inversion. The densitometer residuals have a standard deviation of  $0.049 \text{ kg}\cdot\text{m}^{-3}$  which is not accurate enough for most oceanographic applications. However, the densitometer algorithm was used to explore the sensitivity of density from this technique to temperature and pressure uncertainties. To achieve a deep ocean densitometer of  $0.001 \text{ kg}\cdot\text{m}^{-3}$  accuracy would require the index of refraction to have an accuracy of 0.3 ppm, the temperature an accuracy of  $0.01^{\circ}\text{C}$  and the pressure to 1 decibar.

Our assessment of the currently available index of refraction measurements finds that only the data for fresh water at atmospheric pressure produce an algorithm satisfactory for oceanographic use (density to 0.4 ppm). The data base for the algorithm at higher pressures and various salinities requires an order of magnitude or better improvement in index measurement accuracy before the resultant density accuracy will be comparable to the currently available oceanographic algorithm.

Published in: *Deep-Sea Research*, 37(12):1909-1926, 1990.

Supported by: NSF Grant ISI86-00918.

WHOI Contribution No. 7342.

## HIGH-SPEED, REAL-TIME DATA ACQUISITION FOR VECTOR MEASURING CURRENT METERS

*Melora M. Park, Robin C. Singer,  
Albert J. Plueddemann, and Robert A. Weller*

Recent observations indicate that rapidly varying, small-scale velocity structures in the upper ocean may be important in the heat and momentum balances near the air-sea interface. Observation of small-scale velocity structure in the upper ocean requires high-speed sampling to resolve rapidly varying flows and to reduce aliasing from surface wave orbital velocities. Since these flows may be temporally transient and vary over short spatial scales, obtaining and displaying the data in real-time are critical to implementing proper sampling strategy. This paper describes an integrated hardware and software approach used to provide real-time data acquisition and display of Vector Measuring Current Meter (VMCM) data at high sample rates (2 sec) along with supporting data from other instruments at somewhat slower rates. The hardware component consists of a new circuit board for the VMCM that captures the VMCM data output, stores it, and re-transmits it at high speed in response to a request from the data acquisition computer. The data acquisition software runs on a Masscomp 5600 computer under the UNIX operating system. A central control program provides timing information to several software processes that handle serial data acquisition, display, and storage for one or more instruments. Deployed as part of the Surface Waves Processes Program (SWAPP) experiment, the integrated data acquisition system successfully collected, processed, stored and displayed data from 19 VMCMs and 4 other instruments over a 22 day period in February and March of 1990.

Supported by: ONR Contracts N00014-84-C-0134 and NR083-400.

WHOI Contribution No. 7550.

## BIASING OF THE COVARIANCE-BASED SPECTRAL MEAN ESTIMATOR IN THE PRESENCE OF BAND-LIMITED NOISE

*Albert J. Plueddemann and Robert Pinkel*

Estimation of spectral mean frequency (spectral first moment) by the covariance technique is considered for a signal process contaminated by band limited, additive noise. It is shown that the covariance-based spectral mean estimator is biased for low signal-to-noise ratios if the noise bandwidth is not large compared to the signal bandwidth. The bias is towards the mean frequency of the

noise spectrum, typically equivalent to the center of the frequency band passed by the receiver. This noise-biasing is potentially important in the processing of Doppler data from radars, sodars and sonars operating in a pulse-to-pulse incoherent mode. Biasing of the mean frequency estimator can be easily corrected if measurements of the noise covariance are available. In the absence of noise measurements, correction for biasing can still be accomplished by estimating the signal and noise bandwidths and introducing simple models for the signal and noise covariance functions. This technique allows estimation of noise covariance from measurements of signal-plus-noise covariance at more than one time lag. In addition, the models provide a means of predicting potential biasing problems in a generalized Doppler system.

Published in: *Journal of Atmospheric and Oceanic Technology*, 8:172-178.

Supported by: ONR Contract N00014-79-C-0472.

## THE MOTION OF A SOLID SPHERE IN AN OSCILLATING FLOW: AN EVALUATION OF REMOTELY-SENSED DOPPLER VELOCITY ESTIMATES IN THE SEA

*David A. Siegel and Albert J. Plueddemann*

Several popular techniques employed to remotely sense oceanic velocity fields utilize the Doppler shifts of backscattered radiation (such as, sound or light) from suspended particles to estimate fluid velocities. Implicit in this use is the assumption that the motion of the particles and the fluid parcels about them is identical. Here, a simple dynamical model of a solid sphere in a unidirectional oscillating flow is used to evaluate the effects of differential particle motion on remotely sensed Doppler velocity estimates. The analysis shows that particles move with the fluid driving their motion if their density is equal to the fluid's density or if the oscillation frequency ( $\omega$ ) is less than a critical frequency ( $\omega_c \equiv 0.1 v/a^2$ ; where  $v$  is the kinematic viscosity of the fluid and  $a$  is the particle radius). For oscillation frequencies greater than  $\omega_c$ , the amplitude of the frequency response function between the particle and flow diverges significantly from unity. Particle motion will be amplified for particles less dense than the fluid and reduced for relatively heavy particles. The motions of particles and the fluid may have significant phase differences as well. Critical frequencies are estimated for some common oceanic particles enabling the performance of several Doppler velocity measurement techniques to be evaluated. The present results indicate that for some oceanographic applications the Doppler sensing of

fluid velocities using particulate backscatter may be limited by the inability of the particles to follow the fluid motion. The important implication is that a greater emphasis should be placed on the characterization of the materials that are producing the backscattered radiation signals.

Supported by: ONR Contract N00014-89-J-1683.

WHOI Contribution No. 7354.

## MISCELLANEOUS

### GEOLOGY OF THE SOLITARIO, TRANS-PECOS TEXAS

*Charles E. Corry, Eugene Herrin,  
Fred W. McDowell, and Kenneth A. Phillips*

The Solitario displays geologic features that span virtually the entire regional history of Trans-Pecos Texas since Cambrian time. The visible structure (cover) is the eroded remnant of the roof of a rapidly symmetric late Eocene (38 Ma) laccolith. Erosion of the laccolith roof has exposed a remarkably complete stratigraphic section. The rock record begins with Upper Cambrian Dagger Flat Sandstone. Deposition of Upper Cambrian sand and shale in a shallow sea gave way during Ordovician to deposition of black shales interbedded with some sea gave way during Ordovician to deposition of black shales interbedded with some sand and black chert, reflecting more restricted circulation. About 1 km of sediments, from the craton to the north and northwest, accumulated in the Ouachita Trough during Late Cambrian and Ordovician time. The area was elevated and slightly tilted, but not significantly deformed, by the Llanorian Orogeny during Silurian time. Silurian rocks are missing, and the Lower Devonian-Mississippian Caballos Novaculite rests uncomfortably on the Upper Ordovician Maravillas Formation. More than 1.4 km of flysch, from a source to the southeast, forms the Mississippian-Pennsylvanian Tesnus Formation. No Paleozoic rocks younger than Early Pennsylvanian (Morrowan Series) have been found. The measured thickness of Paleozoic rocks in the Solitario is approximately 2.6 km and represents a time span of 240 m.y., with a single break of  $\approx$  Ma during Silurian, one of the longest depositional records known.

The Paleozoic rocks presently found in the Solitario are allochthonous and were intensely deformed during the Ouachita Orogeny. The orogeny affected the Solitario area from Middle Pennsylvanian (Desmoinesian) until Early Permian middle Wolfcampian). Transport of the allochthon during the Ouachita Orogeny was at least tens of

kilometers from the southeast. Deformation was primarily by folding, with the development of nappes, S-folds, boudinage structures, and local and regional thrust faults evident in the exposed Paleozoic rocks.

After the Ouachita Orogeny, the Solitario area remained positive from Early Permian (middle Wolfcampian) on the structural block known as the Tascotal Uplift that formed the southern margin of the Permian sea. Throughout early Mesozoic, the area remained elevated on the West Texas-Coahuila Platform, and was extensively eroded as part of the Wichita paleoplain. In Early Cretaceous (late Aptian), the area was covered by a shallow sea, and 1.2 km of carbonates were deposited. These rocks are now magnificently exposed in cross section in the shutups that cut the rim of the Solitario dome. The Cretaceous rocks are correlative with carbonate units founds to the east and south in the Gulf Coast area.

At the end of the Cretaceous (Gulfian), the area was elevated once again as the Laramide Orogeny migrated eastward. Regionally, the Solitario lies on a large structural block that is defined by gravity data as a remnant of the Tascotal Uplift. The block appears to have responded to Laramide compression by uplift and rigid-body rotation without undergoing extensive internal deformation. Deformation associated with the Laramide Orogeny had no discernible effect on the later emplacement of the Solitario laccolith. Within the mapped area, Laramide compression is, at most, presently evident only as sparse stylolites in the Cretaceous rim rocks. Mid-Eocene basal conglomerate of only as sparse stylolites in the Cretaceous rim rocks. Mid-Eocene basal conglomerate of the Devils Graveyard Formation, shed Laramide folds to the west, is found in Fresno Canyon, and is the only Tertiary rock that predates the formation of the Solitario dome.

The oldest reliably dated igneous rock in the Solitario is a  $37.5 \pm 0.8$  Ma rhyolite sill. The sill intruded the base of the Cretaceous section immediately prior to the formation of the Solitario dome. The dome was formed by intrusion of  $\approx 100$  km<sup>3</sup> of silicic magma that formed the present granite laccolith shortly after the emplacement of the rim sill. The structural relief of the dome is 1.6 km, and the roof underwent 400 m of radial extension from the center. A crestral graben formed during doming, and the graben block collapsed less than 1 Ma after formation of the dome, foundering and rotating down to the south after the roof was deeply eroded. The foundering of the crestral graben block was probably contemporaneous with the emplacement of a granite intrusion on the eastern side of the collapsed block and formation of a small caldera south of the crestral graben block.

The series of intrusive and extrusive volcanic rocks found within the dome includes 14 mappable

rock types, with a wide range of compositions. The Solitario igneous suite was emplaced over a total time span of 11 Ma; silicic igneous activity was probably limited to the first 3 Ma of this time. Younger, more mafic rocks have vents within the Solitario dome, and are thus included within the suite, but appear to be genetically and temporally related to the Bofecillos volcanic center, immediately west of the dome.

The oldest units of the central basin-filling Needle Peak Tuff were deposited in late Eocene within 1 Ma after the dome was formed. The roof of the dome was therefore eroded to virtually its present level by the end of the Eocene. The emplacement of the Needle Peak Tuff is associated, at least in part, with the collapse of a small caldera in the south part of the central basin. Volcaniclastic rocks accumulated in surrounding areas during the Oligocene and early Miocene, particularly those erupted from the Bofecillos western flank of the dome. These volcanic units eventually lapped high onto the eroded rim of the dome, but did not spill over into the central basin.

From early Miocene until the Quaternary, the area was an elevated plain, with the streams at or near their base level. There is no evidence in the map area for significant erosion or deposition from early Miocene until the Pleistocene, when the Rio Grande began actively downcutting its bed to the south. The base level of all local streams was lowered as a result. The map area is presently being rapidly eroded, and the late Eocene topography has been partially resurrected.

In Press: *GSA Special Paper 250*.

WHOI Contribution No. 7592.

#### **ANDREW F. BUNKER: PIONEERING IN AIR-SEA INTERACTION RESEARCH 1946-79**

*Carl A. Friehe and Henry M. Stommel*

Andrew F. Bunker was a research scientist at the Woods Hole Oceanographic Institution for over 30 years until his death in 1979. He was interested in the energy exchanges between the atmosphere and ocean and devised techniques for their measurement from aircraft. He participated in many of the major oceanic field experiments of the 1960's and 1970's with Woods Hole research aircraft. His work in air-sea interaction culminated in a climatological atlas of air-sea fluxes for the Atlantic Ocean. We document here his career and scientific work in his memory.

Published in: *Bulletin of the American Meteorological Society*, 72(1):44-49, 1991.

Supported by: NSF Grant OCE89-13128.

WHOI Contribution No. 7403.

## **TECHNICAL REPORTS**

### **ALTIMETER PROCESSING TOOLS FOR ANALYZING MESOSCALE OCEAN FEATURES**

*Michael J. Caruso, Ziv Sirkes, Pierre J. Flament,  
and M. K. Baker*

Satellite altimeters provide many opportunities for oceanographers to supplement their research with a valuable new data set. The recent GEOSAT exact repeat mission is the first of several altimeter missions proposed during the next decade. To utilize this new data, a software package was developed at the Woods Hole Oceanographic Institution and the University of Hawaii to facilitate the extraction of useful information from the NODC distributed GEOSAT data tapes. This software package was written with portability and modularity in mind. It should be possible to use this package with little or no modifications on data from future altimeters. The code was written in C and tested on Sun workstations and is oriented toward UNIX operating systems. However, since standard code was used, the programs should port easily to other computer systems. The modularity of the code should enable users to create additional programs. Additional programs designed to handle collocated water vapor corrections are also included for comparison.

Supported by: ONR Contract N00014-86-K-0751.

WHOI Technical Report 90-45.

### **HYDROGRAPHIC OBSERVATIONS FROM THE US/PRC COOPERATIVE PROGRAM IN THE WESTERN EQUATORIAL PACIFIC OCEAN: CRUISES 1-4**

*M. Cook, L. Mangum, R. Millard, G. LaMontagne,  
S. Pu, J. Toole, Z. Wang, K. Yang, and L. Zhao*

In support of the Tropical Oceans and Global Atmosphere (TOGA) program, investigators from Woods Hole Oceanographic Institution (WHOI), NOAA Pacific Marine Environmental Laboratory and the State Oceanic Administration (SOA) from both Qingdao (First Institute) and Guangzhou (South China Sea Branch) conducted hydrographic observations aboard the Chinese research vessels *Xiang Yang Hong 5* and *Xiang Yang Hong 14* in the western equatorial Pacific. The objective of this component of the TOGA program was to document the water mass property distributions of the western equatorial Pacific Ocean and describe the oceanic velocity field. The four cruises

summarized here were conducted during the period November 1985 to June 1988 and are the first half of an eight cruise repeated survey of the region scheduled to be completed in spring 1990. Conductivity-Temperature-Depth-Oxygen (CTD/O<sub>2</sub>) stations were collected to a minimum cast depth of 2500 m or the bottom when shallower. The cruises reoccupied the same stations to provide temporal information. Summarized listings of CTD/O<sub>2</sub> data together with selected physical properties of sea water for these cruises are provided here, as well as a description of the hardware used and an explanation of the data reduction techniques employed.

Supported by: NOAA Grant NA85AA-D-AC117.

WHOI Technical Report 90-07.

### IMPROVED METEOROLOGICAL MEASUREMENTS FROM BUOYS AND SHIPS (IMET): PRELIMINARY COMPARISON OF HUMIDITY SENSORS

*Gennaro H. Crescenti, Richard E. Payne, and Robert A. Weller*

Humidity sensors using various principals of operation are evaluated for the potential use at sea on buoys and ships. Thin film capacitive polymer sensors include the Vaisala Humicap HMP-14U (with WHOI electronics), Hy-CAL Engineering Ultra-H (also with WHOI electronics), the new Vaisala HMP-35A, and the Rotronic MP-100F. Impedance sensors include the Thunder Scientific PC-2101, PHys-Chem PCRC-11, and the General Eastern 850. The Hygrometrix 8503A is the only organically based cellulose crystallite sensor evaluated. Chilled mirror dew sensors include the EG&G 200M Dewtrak, which was used as a comparative standard, the General Eastern Dew-10 and the WHOI D101Q Intelligent Dew Point Sensor. The IR-200 infrared optical hygrometer from Ophir is also included in this study. The performance of the EG&G 200M Dewtrak was quite disappointing. Errors of up to 2.5 degrees C in air temperature were observed due to inadequate shielding from solar radiation.

Supported by: NSF Grant OCE87-09614.

WHOI Technical Report 90-18.

### THE SEADATA PROGRAM

*Thomas W. Danforth*

Current meter and meteorological instrument data are typically stored in the instrument on

cassette tapes. Seadata, described in this report, is a PC version of the original CARP program (CAssette Reading Program) which transferred the data and prepared it for further processing. Also described are two programs which provide byte swapping which is necessary to use the PC data on a VAX/VMS computer. Some changes to the CARP format have been made and are documented here.

Supported by: ONR Contract N00014-84-C-0134 and USGS Contract 14-08-0001-A0245.

WHOI Technical Report 90-44.

### REPORT ON R.V. AKADEMIK VERNADSKY CRUISE 39, STAGE IV JUNE 17 - JULY 19, 1989

*Nick P. Fofonoff, Ellen Levy, A. James Kettle, and Richard C. Navitsky*

Participation by U.S. personnel on Cruise 39, Leg IV (June 17 - July 17, 1989) of the Marine Hydrophysical Institute's research vessel *Akademik Vernadsky* provided valuable information, documented in the present report, for planning future cooperative projects with Soviet oceanographers. Detailed descriptions are given of the ship, its scientific laboratories, computers and on-board instrumentation. Planning and operating procedures are described and examples of given of daily work plans, seminars, menus and social activities. Personal accounts by the U.S. participants are also included. Many of the shipboard activities were recorded on VHS video cassettes. The oceanographic data collected in the Gulf Stream survey region during Leg IV are documented in the report. Copies of data sets were provided to the U.S. participants in exchange for U.S. data from the region during the survey period.

Supported by: Vetelsen Award, Education Office of WHOI, and Dr. William B. Richardson Summer Fellowship provided by Alden Products Company.

WHOI Technical Report 90-12.

### AUTOMATED OXYGEN TITRATION AND SALINITY DETERMINATION

*George P. Knapp, M. C. Stalcup, and R. J. Stanley*

This report describes a newly developed automated Winkler titration system for dissolved oxygen in seawater which is presently in use at the Woods Hole Oceanographic Institution. This amperometric, calculated endpoint system was compared with two different automated and one

manual Winkler method during a recent cruise. The four different methods agreed to within about 0.04 ml/1 and the accuracy is about 0.02 ml/1. A technique to automatically acquire conductivity ratio measurements and calculate salinity using a Guildline Autosol Salinometer is also described.

Supported by: NSF Grant OCE88-22542.

WHOI Technical Report 90-35.

### **MOORED CURRENT METER, AVHRR, CTD, AND DRIFTER DATA FROM THE AGULHAS CURRENT AND RETROFLEXION REGION (1985-1987) VOLUME XLII**

*J. Luyten, A. Spencer, S. Tarbell, K. Luetkemeyer,  
P. Flament, J. Toole, M. Francis, and S. Bennett*

Data are presented from an experiment designed to explore the spatial and temporal structure of the Agulhas Current and Retroflexion by direct means. Included are the current meter results from 10 moorings in the Retroflexion region, CTD stations occupied on the deployment cruise in 1985, data from satellite tracked (ARGOS) freely drifting surface buoys and numerous images of the sea surface temperature.

In addition, this report includes a floppy disk on which can be found the one-day average currents, the path of the Agulhas Current, CTD stations in "Live Atlas" format, SST frontal analyses (Chassignet and Olson, personal communication) as well as programs written in QuickBASIC which allow one to access and display these observations. The programs are stored in ASCII and can be run under the Microsoft QuickBasic (Version 4.0 or higher). Instructions for running the programs can be found in a file entitled "read.me" on the disk.

Supported by: ONR Contracts N00014-84-C-0134,  
N00014-85-C-0001 and N00014-87-K-0007.

WHOI Technical Report 90-30.

### **US/PRC CTD INTERCALIBRATION REPORT 1986-1990**

*R. C. Millard,  
B. J. Lake, N. L. Brown, J. M. Toole, D. Schaaf,  
K. Yang, H. Yu, and L. Zhao*

A series of laboratory intercalibrations of a CTD system were undertaken between 1986 and 1990 as part of cooperative research program between the United States (US) and People's Republic of China (PRC). A comparison of US and PRC calibration facility standards is carried out

using a NBIS/EG&G Marine Instruments Mark IIIB CTD system as a "quasi-transfer standard". When compared with the quoted accuracy of the calibration facilities, pressure was found to be more accurate and temperature was about as accurate as stated. The conductivity standard differences between facilities are difficult to assess because of the CTD conductivity sensor drift.

Supported by: NOAA Grant NA85AA-D-AC117.

WHOI Technical Report 90-53.

### **AN EXPLORATION OF THE NORTH ATLANTIC CURRENT AND ITS RECIRCULATION IN THE NEWFOUNDLAND BASIN USING SOFAR FLOATS**

*W. Brechner Owens and Marguerite E. Zemanovic*

Trajectories and time series of velocity, temperature, and pressure are presented for 13 neutrally-buoyant, acoustically tracked (SOFAR) floats that were launched in May and June, 1986 in the Newfoundland Basin by the Woods Hole Oceanographic Institution SOFAR float operations group. The deployment of these floats and the array of Autonomous Listening Stations (ALS's) used to track the floats was designed to investigate the North Atlantic Current and its possible recirculation. Although there were a number of technical difficulties which reduced the data return for this experiment, we have obtained a total of nearly 12 years of float data for the region at three depths, nominally 700, 1200, and 2000 m.

The data obtained from two deployments of ALS's covering nearly three years, are presented in this report. Of particular note is the strong eddy variability at 700 m depth that is comparable to those found in the Gulf Stream Extension and the entrainment of 2000 m depth floats into the deep western boundary current.

Supported by: ONR Contracts N00014-82-C-0019,  
N00014-84-C-0278, and ONR Grant  
N00014-89-J-1184.

WHOI Technical Report 90-32.

### **SURFACE DRIFTER MEASUREMENTS IN THE WESTERN EQUATORIAL PACIFIC OCEAN CIRCULATION STUDY (WEPOCS III)**

*Christine M. Wooding, Philip L. Richardson, and  
Curtis A. Collins*

Forty freely drifting drogued buoys were tracked by satellite in the western tropical Pacific

from June 1988 to January 1, 1990, as part of the Western Pacific Ocean Circulation Study (WEPOCS III). The data consist of buoy trajectories and sea surface temperature and velocity along trajectories. The main results presented here are the collection of figures which show trajectories and time series data in the South Equatorial Current, the North Equatorial Countercurrent, the Mindanao Current, and the North Equatorial Current. One striking result is that we obtained the first quasi-synoptic map of surface velocity in this region that shows the major currents and their interconnections.

Supported by: NSF Grant OCE87-16509.

WHOI Technical Report 90-37.

### **SOFAR FLOAT MEDITERRANEAN OUTFLOW EXPERIMENT SUMMARY AND DATA FROM 1986 - 1988**

*Marguerite E. Zemanovic, Philip L. Richardson,  
and James F. Price*

In October, 1984, the Woods Hole Oceanographic Institution SOFAR float group began a three and a half year field program to measure the velocity field of the Mediterranean water in the eastern North Atlantic. The principal scientific goal was to learn how the Mediterranean salt tongue is produced by the general circulation and the eddy diffusion of the Canary Basin. Thirty-two floats were launched at depths near 1100 m: 14 in a cluster centered on 32 degrees N, 24 degrees W, with nearest neighbors at 20 km spacing, 10 at much wider spacing to explore regional variations of first order flow statistics, and 8 in different Meddies (Mediterranean water eddies) in collaboration with investigators from Scripps Institution of Oceanography and the University of Rhode Island.

The floats were launched in 1984 and 1985, and tracked with U.S. and French ALSs (moored listening stations) from October 1984 to June 1988. This report includes a summary of the whole three and a half year experiment, the final year and a half of data processed from the third ALS setting (October 1986-June 1988), and the first deep sea test of Bobber EB014 in the eastern subtropical North Atlantic (May 1986-May 1988). Approximately 60 years of float trajectories were produced during the three and a half years of the experiment.

Supported by: NSF Grants OCE82-14066,  
OCE85-17375, OCE86-00055 and  
OCE88-22826.

WHOI Technical Report 90-01.





**MARINE POLICY CENTER**  
**James M. Broadus III, Director**

**MARINE POLICY CENTER**



## MULTIPLE USE PLANNING FOR COASTAL AND MARINE PROTECTED AREAS IN THE CARIBBEAN

*M. Tundi Agardy*

Coastal and marine areas in the Caribbean region provide food, transportation, recreation, and energy resources to increasing numbers of people each year. As demands for these resources rise, the potential for user conflicts is radically heightened. Competition for resources then becomes more intense as resources become more scarce, causing the use of coastal resources to move to non-sustainable levels. As a result, traditional uses of coastal resources are often displaced by profitable but non-conservative technologies which preclude effective, comprehensive, and long-term management. In addition, the unregulated or mismanaged use of fragile tropical coastal ecosystems can continue to undermine the ecological health of the environment, degrading the very resource base on which local economies depend. These situations can be avoided or counteracted by instigating proactive multiple use planning in which all users can be accommodated in a sustainable way.

One important component of multiple use planning is the establishment of protected areas which conserve critical resources or processes without precluding economic growth. In the Caribbean, marine and coastal protected areas are common, but their effectiveness is often questionable. This paper focuses on several types of coastal and marine protected areas in the Caribbean region, which vary in objectives or in implementation. Planning for tourism as well as resource use by locals is an integral part of these protected areas. The spectrum of effective Caribbean coastal protected areas runs from large, relatively well-financed extensions of terrestrial national parks, as demonstrated in the Virgin Islands Biosphere Reserve, to very small grass roots efforts like the Saba Marine Park. Other good examples fall somewhere in between, and all have important lessons for coastal planners.

In Press: *Ocean and Shoreline Management*.

Supported by: The Pew Charitable Trusts and the Marine Policy Center.

WHOI Contribution No. 7479.

## PACIFIC SEA TURTLES UNDER THREAT

*M. Tundi Agardy*

By now just about everyone has heard about the plight of Atlantic sea turtles: leatherbacks

stranded on New England beaches, Gulf of Mexico loggerheads drowning in shrimp nets, Kemps ridley turtles with hurricane-ravaged nesting beaches, and Cayman Island green turtles being ranched for European gourmet turtle soup. But we rarely hear about the sea turtles of the Pacific, which are also in dire straits.

Published in: *Oceanus*, 32(4):80-81, 1990.

Supported by: The Pew Charitable Trusts and the Marine Policy Center.

## WATER MASSES AND SEABIRD DISTRIBUTIONS IN THE SOUTHERN CHUKCHI SEA: THE 1988 JOINT SOVIET-AMERICAN EXPEDITION OF THE AKADEMIK KOROLEV

*Jonathan M. Andrew and J. Christopher Haney*

Seabirds were censused during ship-board CTD surveys in the Chukchi Sea during the 1988 joint Soviet-American cruise of the AKADEMIK KOROLEV. Seabird distributions were compared to three water masses (Siberian Coastal, mixed Bering Shelf-Anadyr, and Alaska Coastal) oriented across the southern Chukchi continental shelf. Eighteen species were recorded: 14 in Siberian Coastal, 16 in Bering Shelf-Anadyr, and 8 in Alaska Coastal waters. Total abundances of all species (mostly Short-tailed Shearwaters, *Puffinus tenuirostris*) in Siberian Coastal Water were 4 and 13 times greater, respectively, than total abundances in mixed Bering Shelf-Anadyr and Alaska Coastal waters. Differential occurrences of seabirds among the three water masses were a function of: 1) specific oceanographic and other environmental conditions that favored feeding, 2) geographic adjacency of water masses to the nearest population source, and 3) linear distance from breeding colonies.

In Press: *Marine Pollution Bulletin Special Monograph*.

Supported by: The U.S.-U.S.S.R. Joint Committee on Environmental Protection under bilateral activity 02.07-2101, U.S. Fish and Wildlife Service, The John D. and Catherine T. MacArthur Foundation, Marine Policy Center and The Pew Charitable Trusts.

WHOI Contribution No. 7324.

## THE SOVIET MARITIME ARCTIC

*Lawson W. Brigham*

This volume offers a multidisciplinary examination of the historical record and current

developments surrounding Soviet activities in their maritime arctic regions. These regions are home for more than 1 million people, hold immense potential as a source of hydrocarbon and mineral resources, serve as patrol area for nuclear submarines and remain one the few pristine natural environments remaining on earth. The Russian presence in the Arctic dates back some 500 years. Soviet (and Russian) progress in exploring and developing maritime arctic regions has outpaced that of the other arctic states. The primary contribution of this book is to provide information on the current status of Soviet scientific and technical progress in adapting to the demands of their maritime Arctic. Authors from five arctic rim nations, including the Soviet Union, are represented, from the fields of marine transportation, environmental affairs, oceanography, geology, history, law, philosophy and strategic studies.

In Press: *The Soviet Maritime Arctic*. By Lawson W. Brigham. Belhaven Press, United Kingdom.

Supported by: The John D. and Catherine T. MacArthur Foundation and the Marine Policy Center.

WHOI Contribution No. 7604.

## NONFUEL MINERALS

*James M. Broadus and Porter Hoagland III*

The methods of managing nonfuel minerals are one emerging issue of OCS management. Many nonfuel minerals from the OCS are forecast to become important economically, although there is only minor administrative experience and little organizational structure in place. This chapter surveys the existing institutions, the potential resources, and the emerging issues in the management of OCS nonfuel minerals.

Published in: *Managing the Outer Continental Shelf Lands: Oceans of Controversy*. By R. Scott Farrow. Taylor and Francis, New York, :119-134, 1990.

Supported by: Department of Commerce, NOAA, National Sea Grant College Program, Grant No. NA86-AA-D-SG090, Woods Hole Oceanographic Institution Sea Grant Project Nos. R/S-9 and R/S-18 and the Marine Policy Center.

## USING DYNAMIC OPTIMIZATION FOR INTEGRATED ENVIRONMENTAL MANAGEMENT: AN APPLICATION TO SOLVENT WASTE DISPOSAL

*Mark E. Eiswerth*

The choice of disposal strategy for a residuals

stream often determines the environmental medium into which the pollution is released. In turn, choice of medium may influence both the kinds of adverse effects that the pollution will have and the timing of those effects as well. As an illustration of the way in which these factors may be taken into account in integrated environmental management, this paper demonstrates the application of a dynamic optimization model to the problem of allocating a pollutant between two different disposal methods. The alternatives examined are incineration and land disposal for metal-bearing solvent waste.

Supported by: The Pew Charitable Trusts; Marine Policy Center; Sloan Foundation and Computer Science Center, University of Maryland.

WHOI Contribution No. 7533.

## ALLOCATING CONSERVATION EXPENDITURES ACROSS HABITATS: ACCOUNTING FOR INTER-SPECIES GENETIC DISTINCTIVENESS

*Mark E. Eiswerth and J. Christopher Haney*

During recent attempts to discuss biological diversity, economists have drawn upon the tools and techniques of mainstream resource economics to estimate the values of species. This leads to a tendency to focus on the importance of species in isolation to one another and on the numbers of species (species diversity) in natural areas. This approach stands quite at odds with the ongoing efforts of natural scientists to define and analyze different types of diversity among species and natural systems (e.g. genetic diversity and ecological diversity). Rather than address the explicit valuation of individual species or of biological diversity, we show how potential guidelines for the allocation of conservation expenditures among habitats might be changed by consideration of the "genetic distinctiveness" of species, in addition to solely the numbers of species, inhabiting those habitats. We use recent estimates of inter-species genetic distances originating from DNA-DNA hybridization as an example of the kind of weighted information that could prove useful in conservation planning. As an illustration, we examine crane habitats in Africa and Asia.

Supported by: The Pew Charitable Trusts and the Marine Policy Center.

WHOI Contribution No. 7531.

**MANAGING THE OUTER  
CONTINENTAL SHELF LANDS:  
OCEANS OF CONTROVERSY**

*R. Scott Farrow, James M. Broadus,  
Thomas A. Grigalunas, Porter Hoagland III,  
and James J. Opaluch*

The three parts of this book describe, analyze, and predict policy issues for the management of the Outer Continental Shelf (OCS). Each part reflects the view that good policy analysis and good policy require both knowledge about institutions and skill in analysis. Analysis without institutional context is like a language without people – it can exist but it is seldom useful – whereas institutions unaffected by analysis are prey to being blindsided by the future.

Published in: *Managing the Outer Continental Shelf Lands: Oceans of Controversy*. By R. Scott Farrow. Taylor and Francis, New York, 168 pp., 1990.

Supported by: Marine Policy Center, The Pew Charitable Trusts, U.S. Department of Urban and Public Affairs at Carnegie Mellon University, Department of Commerce, NOAA, National Sea Grant College Program, the University of Rhode Island, and the Environment and Policy Institute of the East-West Center.

**DEVELOPING A NATIONAL MARINE  
ELECTRONICS AGENDA:  
PROCEEDINGS OF THE MARINE  
INSTRUMENTATION PANEL MEETING,  
SEPTEMBER 12-14, 1989**

*Arthur G. Gaines and Kristina L. C. Lindborg*

Thirteen short papers address aspects of competitiveness in the marine electronics instrumentation industry. Topics include activity and status of government initiatives in Japan and Europe to promote this industry; and the possible role of federal-state collaboration in the U.S. Papers address technology transfer between research institutions and the commercial sector; the role of "strategic alliances" in this process; and the "dual-use" concept in effective technology development and commercialization. Other papers address electronic technology applications in specific marine areas, such as the use and implications of the COMSAT mobile satellite communication infrastructure; electronic charts and safety of tanker operations; and instrumentation applications in aquaculture and environmental monitoring.

Supported by: NOAA through a grant to the Massachusetts Centers of Excellence Corporation, grant No. NA87-AA-D-M00037.

WHOI Technical Report 90-52.

**INFLUENCE OF PYCNOCLINE  
TOPOGRAPHY AND WATER COLUMN  
STRUCTURE ON MARINE  
DISTRIBUTIONS OF ALCIDS (CLASS  
AVES: FAMILY ALCIDAE) IN ANADYR  
STRAIT, NORTHERN BERING SEA,  
ALASKA**

*J. Christopher Haney*

Systematic ship-board surveys simultaneously recorded seabird abundances and resolved coarse-scale (3-10 km) horizontal and fine-scale (1-10 m) vertical variability in water column structure and bathymetry for portions of the coastal zone in Anadyr Strait near western St. Lawrence Island, northern Bering Sea, Alaska, during August and September 1987. Three plankton-feeding alcids, least (*Aethia pusilla*), crested (*A. cristatella*), and parakeet auklets (*Cyclorhynchus psittacula*), each exhibited distinct associations for different pycnocline characteristics. Least auklets were more abundant in mixed water, but they also occurred within stratified water where the pycnocline and upper-mixed layer were shallow ( $\leq 8$  m) and thin ( $\leq 10$  m), respectively. Low body mass (85 g), high buoyancy, and relatively poor diving ability may have restricted this auklet to areas where water column strata nearly intersected the surface, or to areas where strata were absent altogether due to strong vertical mixing. Crested and parakeet auklets, larger-bodied (ca. 260 g) planktivores with presumably greater diving ability, were more abundant in stratified water, and both species exhibited less specific affinities for water column characteristics at intermediate and shallow levels. All three auklets avoided locations with strong pycnocline gradients ( $\geq 0.22 \sigma_t$  units  $m^{-1}$ ), a crude index of the strong, subsurface shear in water velocities characteristic of this region. Auklet distributions in Anadyr Strait thus tended to correspond with: 1) strata accessibility as estimated from relationships between body mass and relative diving ability, 2) possible avoidance of strong subsurface water motions, and 3) habits and distributions of plankton prey. In contrast, large-bodied ( $> 450$  g) alcids [i.e., common (*Uria aalge*) and thick-billed murre (*U. lomvia*), pigeon guillemots (*Cephus columba*), tufted (*Fratercula cirrhata*), and horned puffins (*F. corniculata*) feeding on fish or benthic invertebrates] showed no consistent relationships to either the pycnocline or upper-mixed layers. All large alcids were more common in stratified than in vertically-mixed waters, but differences in abundance between mixing regimes were small or equivocal. The only measured variable with which all large alcids were associated was total water column depth: murre,

puffins, and guillemots each used areas with shallow sea floors and avoided areas with deeper sea floors. Failure of large alcids to discriminate among foraging areas in Anadyr Strait as a function of pycnocline topography and strength may be attributed to: 1) greater reliance on large active, non-pycnocline-associated pelagic and benthic prey, 2) higher body mass, lower buoyancy, and greater diving ability, or 3) foraging over a uniquely shallow continental shelf where all vertical strata, including the sea floor, were potentially accessible from the ocean surface.

In Press: *Marine Biology*.

Supported by: Department of the Interior: Minerals Management Service and U.S. Fish and Wildlife Service, Marine Policy Center, and The Pew Charitable Trusts.

WHOI Contribution No. 7559.

# **VARIABILITY IN DISTRIBUTIONS OF NORTHERN FULMARS (*FULMARUS GLACIALIS*) AND SHORT-TAILED SHEARWATERS (*PUFFINUS TENUIROSTRIS*) IN THE SOUTHERN CHUKCHI SEA**

*J. Christopher Haney and J. M. Andrew*

Bi-directional surveys of seabirds were conducted simultaneously with synoptic oceanographic measurements during a joint Soviet-American study of the southern Chukchi Sea. During late summer 1988, Short-tailed Shearwaters (*Puffinus tenuirostris*) and Northern Fulmars (*Fulmarus glacialis*) exhibited greater variability in abundance along (parallel to) than across (perpendicular to) the Chukchi shelf. This variability corresponded to across-shelf orientations of three distinct water masses equi-distant from both species' entry point into the Chukchi Sea via Bering Strait. Fulmars were 17 and 13 times, and shearwaters were 50 and 500 times, more abundant in Siberian Coastal Water (SCW) than in Bering Shelf-Anadyr (BSAW) and Alaska Coastal waters (ACW), respectively. Within SCW, numbers of both procellariiform species: 1) were lower near the transition with BSAW and at greater distances from Bering Strait, and 2) were highest over a baroclinically-stable pycnocline located 5-10 m below (and within probable diving range of) the ocean surface. Seabird affinities for water masses can be more clearly differentiated if environmental conditions are equally accessible to the birds, and if there are few intercorrelated environmental variables present during study comparisons.

Supported by: The U.S.-U.S.S.R. Joint Committee on Environmental Protection under bilateral activity 02.07-2101, U.S. Fish and Wildlife

Service, The John D. and Catherine T. MacArthur Foundation, Marine Policy Center, and The Pew Charitable Trusts.

WHOI Contribution No. 7667.

# **ANALYZING QUANTITATIVE RELATIONSHIPS BETWEEN SEABIRDS AND MARINE RESOURCE PATCHES**

*J. Christopher Haney and Andrew R. Solow*

In this review of marine birds, we evaluate the general designs and statistical analyses of distributional studies that rely upon line transect sampling. The following topics are critiqued: 1) use of seabird abundances measured from line transects as criterion variables, 2) rationales behind choice of environmental predictor variables, and 3) detecting relationships between criterion and predictor variables. We explain how apparent contradictions among marine studies have arisen, how "noisy" count data occurs, and how study designs from marine investigations can be improved. We also draw attention to a forgotten dimension important to the analysis of marine distributional data (the scale of seabird ambits), and advocate clear identification and careful separation of biological and statistical hypothesis-testing. We conclude by recommending study designs that reconcile the hybrid environments seabirds occupy (terrestrial, aerial, marine) as well as recommending use of analytical tools, including inferential statistics, which are robust to and efficient for this reconciliation.

In Press: *Current Ornithology*, D. M. Power, ed. Volume 9, Plenum Press, New York, 1991.

Supported by: NOAA Outer Continental Shelf Environmental Assessment Program, Minerals Management Service, U.S. Fish and Wildlife Service, Burleigh-Stoddard Fund, University of Georgia, Skidaway Institute of Oceanography, NSF grant OCE81-10707, Marine Policy Center, and The Pew Charitable Trusts.

WHOI Contribution No. 7235.

# **SOME INITIAL EFFECTS OF HURRICANE HUGO ON ENDANGERED AND ENDEMIC SPECIES OF WEST INDIAN BIRDS**

*J. Christopher Haney, Joseph M. Wunderle, Jr.,  
Wayne J. Arendt*

Hurricane Hugo, a Category 4 hurricane with sustained winds of 140-150 miles per hour and gusts over 180, passed directly over or near Puerto Rico, Montserrat, Guadeloupe, and Dominica.

Each island harbors endangered, threatened, or otherwise vulnerable species of endemic forest birds: the Puerto Rican Parrot (*Amazona vitata*), Yellow-shouldered Blackbird (*Agelaius xanthomus*), Puerto Rican Plain Pigeon (*Columba inornata wetmorei*), Montserrat Oriole (*Icterus oberi*), Guadeloupe Woodpecker (*Melanerpes herminieri*), Imperial (*Amazona imperialis*) and Red-necked parrots (*Amazona arausiaca*). We report on Hurricane Hugo's initial impacts to and immediate consequences for these West Indian birds following the storm's landfalls during mid-September 1989 in the eastern Caribbean. We summarize damage to each island, contrast Hurricane Hugo's impacts on birds with other historical hurricanes, and briefly evaluate these catastrophic events with respect to future conservation strategies for island birds inhabiting coastal forest habitats.

In Press: *American Birds*.

Supported by: The Pew Charitable Trusts, Marine Policy Center, and Department of Commerce, NOAA, National Sea Grant College Program, Grant No. NA86-AA-D-SG090, Woods Hole Oceanographic Institution Sea Grant Project No. R/M-22-PD.

WHOI Contribution No. 7450.

## COASTAL ZONE MANAGEMENT IN SOUTH KOREA

*Seoung-Yong Hong*

The physical characteristics of South Korea have had a profound impact on the uses of the coastal zone that have, in turn, been determined by and reinforced the nation's economic development strategy. While coastal zone management in many developed economies is more heavily oriented toward environmental protection and the resolution of user conflicts, policies for coastal zone management in South Korea have emphasized the role of coastal space and other resources for economic development and industrial needs. Increasing demand for land reclamation to provide ever-increasing industrial sites and human settlements, traditional and future needs of the fishery, and concern for the environment have led to a vast array of competition and, finally, often to conflicts. The basic pattern of coastal zone use in South Korea has changed from the lineal expanse of coastal zone to integrated coastal uses. An increased number of critical coastal zone issues and interactions were reflected in the creation of new governance that dealt with coastal zone resources and environment.

In Press: *Coastal Management*.

Supported by: Marine Policy Center, Korea Ocean Research and Development Institute (KORDI), and the Korea Science and Engineering Foundation.

WHOI Contribution No. 7437.

## ANTARCTIC TREATY DIPLOMACY: PROBLEMS, PROSPECTS AND POLICY IMPLICATIONS

*Christopher C. Joyner*

Major international developments affected the progress of Antarctic diplomacy during 1989. For one, the regime that had been painstakingly negotiated to regulate Antarctic mineral activities was scuttled by two of the very governments that had worked in good faith for six years to attain its promulgation. Second, there was the Fifteenth Antarctic Treaty Consultative Party Meeting that convened in Paris in October to consider several factors relating to future environmental protection in Antarctica. Also holding direct policy relevance for the Antarctic was the Eighth Meeting of the Commission of the Convention for the Conservation of Antarctic Living Marine Resources, which met in Hobart, Tasmania, in November to deliberate and set conservation measures in the Southern Ocean.

This study examines these developments in order to assess how their legal, political and policy implications affect the course of diplomacy governing activities in the Antarctic. At the outset, it is important to realize that the Antarctic region, which covers one-tenth of the earth's surface, is administered by a special series of international agreements. This arrangement of treaties, known as the Antarctic Treaty System, supplies the main conduits through which Antarctic diplomacy is channeled and policy for the region is formulated and set.

Published in: *Diplomatic Record 1989-1990*, David D. Newsom, ed. Westview Press, :155-180, 1990.

Supported by: George Washington University and the Marine Policy Center.

WHOI Contribution No. 7395.

## ANTARCTICA AND THE INDIAN OCEAN STATES: THE INTERPLAY OF LAW, INTERESTS, AND GEOPOLITICS

*Christopher C. Joyner*

The Indian Ocean littoral states represent a microcosm of the Group of 77 members that began to dabble in Antarctic politics during the 1980s and used the United Nations General Assembly as



their main forum. The economic interests and legal priorities of these developing countries have come into conflict with the Antarctic Treaty System, the legal arrangement of largely non-Indian Ocean states that has evolved for administering the region. Recent developments in Antarctic affairs may exacerbate the tensions in the frozen south: the "Malaysian initiative" to extend the notion of "common heritage of mankind" to the Antarctic; the impending 1991 date and the possible convening of an Antarctic Treaty review conference; and the apparent collapse of the 1988 Antarctic mineral resource treaty because of the opposition of France and Australia – these circumstances may complicate the Antarctic legal situation and make future scientific cooperation and peaceful uses only of the region more difficult. If a minerals regime is eventually put in place, the critical test will come in the protection and conservation of the fragile Antarctic environment. As population pressures mount, Indian Ocean littoral states are likely to perceive greater economic opportunities in the Antarctic. The key to realizing benefits for all interested states from future activities in the Antarctic is stability of the management regime, a quality commendably supplied for 30 years by the Antarctic Treaty System.

Published in: *Ocean Development and International Law*, 21:41-70, 1990.

Supported by: The Pew Charitable Trusts and the Marine Policy Center.

WHOI Contribution No. 6538.

## GEOPOLITICS AND ANTARCTICA

*Christopher C. Joyner*

Antarctica is synonymous with geopolitics. The continent is the coldest, highest, driest, windiest, most remote and least hospitable place on earth. For most of human history, the frozen south has remained beyond the concern of most peoples and governments. Within the past decade, however, international interest in Antarctica has heightened appreciably, largely due to geopolitical considerations.

This chapter has three principal purposes. First, it sets out the contemporary character of the legal regime that governs and coordinates geopolitical priorities among States active in the Antarctic. Second, the study examines two prominent themes that dominate contemporary geopolitics in the region: (a) the maintenance of international security through treaty-based nonmilitarization of the Antarctic; and (b) the increasingly prominent role of natural resources in Antarctic affairs, both among States active in

Antarctic affairs and for the international community at large. A third purpose is to assess how geopolitical factors could complicate the Antarctic situation, not only by posing threats to the fragile ecosystem but also by unraveling international cooperation. From this analysis, some conclusions affecting Antarctica's place in the future world order then will be distilled for critical reflection.

In Press: *Antarctica and World Order*, Richard Falk, ed. 1991.

Supported by: Marine Policy Center and The George Washington University.

WHOI Contribution No. 7337.

## CRAMRA: THE UGLY DUCKLING OF THE ANTARCTIC TREATY SYSTEM?

*Christopher C. Joyner*

Nearly everyone knows the children's story of Hans Christian Andersen about the ugly duckling. This paper examines the ugly duckling thesis as applied to the 1988 Wellington Convention on the Regulation of Antarctic Mineral Resource Activities (CRAMRA). In mid-1990 the Wellington Convention became the object of considerable international scorn and criticism for both what it would and would not purport to do. CRAMRA has in effect been branded the ugly duckling of the Antarctic Treaty System (ATS), criticized by many, loved by some and ignored by few. This study aims to weigh the political, legal and environmental costs and benefits of putting the Wellington Convention into force, with a view toward determining how this now-sullied instrument might be permitted someday to evolve into a beautiful regulatory swan for the Antarctic Treaty System.

In Press: *Proceedings, The Antarctic Treaty System in World Politics*, 21-23 May, 1990.

Supported by: The Pew Charitable Trusts and the Marine Policy Center.

WHOI Contribution No. 7426.

## MARITIME ZONES IN THE SOUTHERN OCEAN: PROBLEMS CONCERNING THE CORRESPONDENCE OF NATURAL AND LEGAL MARITIME ZONES

*Christopher C. Joyner*

A significant body of international law drafted simultaneously but separately for the Antarctic Treaty system (ATS) and the law of the sea affects the Southern Ocean. Although this ocean is

characterized by several distinct geophysical zones, it is not easy to secure a consensus regarding an appropriate northern boundary. The law of the sea defines a series of maritime jurisdictional zones, whose application to Antarctica is hindered by the region's continuing uncertain legal status. Nevertheless, the Antarctic relevance of the law of the sea raises a number of interesting questions, while highlighting the fact that legal zones in Antarctica have often developed without taking full account of geographical criteria. An understanding of geographical and other factors facilitates an improved understanding of the need for new legal approaches designed to regulate Antarctic activities in a more equitable and effective manner.

Published in: *Applied Geography*, 10:307-325, 1990.

Supported by: George Washington University and the Marine Policy Center.

WHOI Contribution No. 7393.

### **PLASTIC POLLUTION IN THE MARINE ENVIRONMENT: TOWARDS AN INTERNATIONAL SOLUTION**

*Christopher C. Joyner and Scot Frew*

This article seeks to confirm the proposition that an international legal norm prohibiting pollution of the marine environment by plastic debris is operative today as a constraint on international conduct. The basis for this assertion rests in the development of contemporary positive international law, i.e., in the multiplicity of international treaties and conventions that have been recently promulgated and in the broad reach of State support for banning plastic pollution that has evolved over the past two decades.

In Press: *Ocean Development and International Law*.

Supported by: The George Washington University.

WHOI Contribution No. 7577.

### **KEY PROBLEMS IN THE MANAGEMENT OF SPORTS FISHERIES**

*Yoshiaki Kaoru*

This article discusses issues associated with valuation of sports fishing activities for marine resource management. Since management decisions have effects on marine resource quality and activity levels of different groups of resource users, careful benefit-cost evaluation of alternative management plans is essential to implement an efficient management system. Three important issues for measuring sports fishing benefits are

discussed: (1) aspects of fishing experience enjoyed by recreationists, (2) congestion, and (3) recreational inputs purchased for fishing participation. The household production function framework is discussed as a plausible approach to incorporate a variety of recreational inputs for describing sports fishing demand. Throughout the article, data deficiency is emphasized. Individual microlevel data about recreationists' socioeconomic characteristics and expenditures as well as fishing site quality variables are necessary to improve the sports fishing valuation task.

Published in: *Ocean Development and International Law*, 21:317-333, 1990.

Supported by: The Pew Charitable Trusts and the Marine Policy Center.

WHOI Contribution No. 7458.

### **"BLACK MAYONNAISE" AND MARINE RECREATION: METHODOLOGICAL ISSUES IN VALUING A CLEANUP**

*Yoshiaki Kaoru and V. Kerry Smith*

There has been substantial increase in the use of random utility models (RUM) to estimate the values people would place on reducing marine pollution. This paper identifies and evaluates the importance of four methodological issues that arise in using the RUM framework for estimating the effects of estuarine quality on the choice of recreation sites and the benefits from reducing pollution. The issues include: (a) specifying the set of alternatives to be indicated in the choice set; (b) evaluating how the definition of what constitutes an elemental alternative affects the plausibility of the independence of irrelevant alternatives; (c) examining the effects of the definition of alternatives for benefit measures; and (d) evaluating the implications of multiple pollutants for describing the factors influencing people's recreation site choices.

The analysis describes each problem in analytical terms and examines its effects using a survey of sport fishermen's decisions in using the Albemarle-Pamlico Estuary in North Carolina.

Supported by: Dept. of Commerce, NOAA, National Sea Grant College Program, Grant No. NA86AA-D-SG046, University of North Carolina Sea Grant Project No. R/MRD-9; The Pew Charitable Trusts and the Marine Policy Center.

WHOI Contribution No. 7560.

## **GONE FISHING, BE BACK LATER: ENDING AND RESUMING RESEARCH AMONG FISHERMEN**

*Ilene M. Kaplan*

This chapter addresses issues related to ending and resuming longitudinal research on fishermen and problems associated with fieldwork conducted in fishing communities. The lifestyles and work habits of fishermen are more complex phenomena than common-sense imagery of the sea suggests. Methodological issues discussed include: establishing a work identity, gaining the trust of people in fishing communities, and maintaining objectivity.

In Press: *Experiencing Fieldwork: Qualitative Research in the Social Sciences*. W. Shaffir and R. Stebbins, eds. Sage Publications, California.

Supported by: Union College/Dana Fellowships and the Marine Policy Center.

WHOI Contribution No. 7289.

## **TOURISM IN THE GALÁPAGOS ISLANDS: THE DILEMMA OF CONSERVATION**

*Richard A. Kenchington*

The Galápagos Archipelago is an area of very special significance to ecologists. Its unique flora and fauna, rugged scenery, and historical connections with Charles Darwin, make it a place of environmental pilgrimage. Management of tourism has involved a policy which requires most visitors to be accommodated on boats, places strict controls on the sites which can be visited, and requires tourists to be accompanied by highly-trained Naturalist Guides. The policy precludes development of any substantial island-based tourist infrastructure.

The recent increase in visitors has resulted in the rapid and little-coordinated development of small hotels and guest houses. There has been considerable economic benefit to the local population, which was previously largely dependent on a finite fish-stock or the public sector for employment. However, there have been recent calls for tourism to be rejected as a vehicle for economic development of the Galápagos, and for the controls of existing policies to be retained. Nevertheless, it is clear that local tourism is now an established and increasingly important socio-economic factor.

This paper summarizes the issues indicated in its title and points to the need for a new policy which addresses ecological and economic factors

while calling for re-establishment of the beneficial symbiosis between tourism and conservation that was effective in the development of the initial Galápagos tourism management policy.

Published in: *Environmental Conservation*, 16(3):227-232, 1989.

Supported by: Heritage Division of UNESCO and the Tinker Foundation through a grant to the Marine Policy Center.

WHOI Contribution No. 7292.

## **DIABLOTIN (*PTERODROMA HASITATA*): BIOGRAPHY OF AN ENDANGERED PROCELLARIIFORM**

*David S. Lee and J. Christopher Haney*

The Black-capped Petrel (*Pterodroma hasitata*) is the only extant gadfly petrel known to breed in the wider West Indies region. Now seriously threatened or endangered, current breeding populations occur on only two, possibly three, of the six historically documented breeding islands. Breeding populations on the large islands of Hispaniola (Dominican Republic and Haiti) and Cuba are small, fragmented, and currently believed to be declining, although the exact sizes, locations, and detailed chronologies of all petrel breeding colonies remain poorly-studied. Nesting sites are limited to open-canopy highland forest on or near cliff faces, but in the past the species may have used open sites maintained by fires, hurricanes, earthquakes, and volcanism. In addition to direct exploitation by colonists in previous centuries and recent declines in breeding habitat due to deforestation, introduced predators (mongoose, feral cats, dogs, pigs, and opossums) may have played a role in the species' decline. Presently, there is insufficient information available for ascertaining the taxonomic status, number of races and populations, morphological variation, and genetic differentiation of Black-capped Petrels. Unlike the majority of currently-threatened seabird species, considerably more is known about the petrel's marine ecology than its breeding biology. The Gulf Stream current is a principal factor influencing the marine distribution of Black-capped Petrels, and the primary foraging range of the species is the offshore zones of the southeastern United States between Cape Canaveral, Florida and Cape Hatteras, North Carolina. Populations at sea are at risk from anticipated exploration and development of offshore oil and gas resources, and Black-capped Petrels tested off North Carolina have the highest mercury concentrations of any species in that region. As conservation recommendations, we suggest that 1) this species be formally designated

endangered by the U.S. Fish and Wildlife Service, 2) genetic studies be initiated so that both the taxonomic and population status of the species can be determined, 3) one or more long-term monitoring sites at breeding colonies be designated, 4) satellite imagery be used to ascertain the amount of suitable breeding habitat remaining in Caribbean mountain forests, and 5) remote sensing methods (e.g., bioacoustic tomography) be developed for counting breeding populations of this secretive, nocturnal species.

Supported by: Burleigh-Stoddard Fund, Sheldon Fund, University of Georgia, Skidaway Institute of Oceanography, NSF grants OCE81-10707 and OCE81-17761, the Marine Policy Center and The Pew Charitable Trusts.

WHOI Contribution No. 7666.

### **GUIDING THE OCEAN SEARCH PROCESS: APPLYING PUBLIC LAND EXPERIENCE TO THE DESIGN OF LEASING AND PERMITTING SYSTEMS FOR OCEAN MINING AND OCEAN SHIPWRECKS**

*Robert H. Nelson*

The federal administration of the Mining Law of 1872 and of the Mineral Leasing Act of 1920 offers a wealth of experience on the public lands that should be taken into account in managing ocean resources that are similarly under government control. The government has faced a conflict between policy goals because the earlier assurance of development rights stimulates exploration but also makes it more difficult to assure environmental protection. Greater public expenditures for planning and advance information gathering may reduce such conflicts but are limited in their extent by economic considerations. This article analyzes past government attempts to deal with such issues in leasing offshore and onshore oil, and gas, coal, and in the administration of the "hardrock" claim and patent system. The article suggests alternative ways of sequencing the acquisition of minerals and environmental information in the design of future systems for managing ocean resources.

Published in: *Ocean Development and International Law*, 20:577-600, 1989.

Supported by: Marine Policy Center.

### **THE DETECTION OF GREENHOUSE WARMING**

*Andrew R. Solow*

Global climate is influenced by atmospheric composition. Atmospheric composition is changing, largely as a result of human activities associated with the economic maintenance of a growing population. Unfortunately, insufficient understanding of climate processes and their interactions precludes all but the crudest predictions of the timing, nature, and magnitude of the expected climatic response.

The detection of a climatic response to changes in atmospheric composition – what has come to be called the detection of climate change – is not a prerequisite for concern about the occurrence of such a response in the future. However, such a detection would be important scientifically, to say nothing of its implications for policy.

Efforts to detect climate change are very much in their infancy. A small number of approaches have been proposed and applied. It is probably fair to say that no serious attempt to detect a climatic response to changes in atmospheric composition has been successful. This is not to say that this response has not occurred, only that the problem is a difficult one and requires a detailed scientific understanding of global climate and a considerable amount of high quality climatological data.

In this paper, some of the broad issues in detecting climate change are discussed.

In Press: *Proceedings, World Meteorological Organization*.

Supported by: The Pew Charitable Trusts.

WHOI Contribution No. 7472.

### **AN EXPLORATORY ANALYSIS OF THE OCCURRENCE OF EXPLOSIVE VOLCANISM IN THE NORTHERN HEMISPHERE, 1851-1985**

*Andrew R. Solow*

Studies of regional climate following volcanic eruptions suggest that explosive volcanism exerts a short-term cooling effect. To understand the effects of explosive volcanism on historic temperatures, it is necessary to identify changes through time in the frequency of explosive eruptions. This paper presents an exploratory analysis of a record of explosive eruptions in the Northern Hemisphere over the period 1851-1985. This record is modelled as a non-stationary Poisson process and the intensity function is estimated by kernel smoothing. Approximate

confidence bands are constructed and diagnostics for checking the Poisson assumption are described. A comparison with a record of Northern hemisphere temperatures indicates that part of the variability in temperature can be explained by variations in explosive volcanic activity.

In Press: *Journal of the American Statistical Association*.

Supported by: The Pew Charitable Trusts and the Marine Policy Center.

WHOI Contribution No. 7391.

### **A METHOD OF APPROXIMATE MULTIVARIATE NORMAL ORTHANT PROBABILITIES**

*Andrew R. Solow*

A simple method for approximating multivariate normal orthant probabilities is presented. The method is based on decomposing the orthant probability into a product of conditional probabilities and approximating the terms in the product using a linear model. Some results are given showing that the method works well.

Published in: *Journal of Statistical Computation and Simulation*, 37:225-229, 1990.

Supported by: The Pew Charitable Trusts and the Marine Policy Center.

WHOI Contribution No. 7425.

### **THE NONPARAMETRIC ANALYSIS OF POINT PROCESS DATA: THE FREEZING HISTORY OF LAKE KONSTANZ**

*Andrew R. Solow*

Climate records sometimes have the form of point processes (i.e., observations of the times of occurrence of a specified type of event). A central problem in the analysis of point process data is the estimation of the rate function, defined as the expected number of events occurring in a time interval of unit length. This paper describes some simple nonparametric methods for estimating the rate function and for assessing its statistical significance. The methods are applied to the freezing history of Lake Konstanz.

In Press: *Journal of Climate*.

Supported by: The Pew Charitable Trusts and the Marine Policy Center.

WHOI Contribution No. 7461.

### **A NOTE ON THE STATISTICAL PROPERTIES OF ANIMAL LOCATIONS**

*Andrew R. Solow*

A statistical model of the successive locations of an animal in the plane induces a statistical model of the relative positions of successive locations. A common locational model is that the Cartesian coordinates of successive locations in the plane are independent bivariate normal random variables. This note gives the statistical properties of the direction and length of the vector joining successive locations.

Published in: *Journal of Mathematical Biology*, 29(2):189-193, 1990.

Supported by: Penzance Foundation Fund.

WHOI Contribution No. 7443.

### **A RANDOMIZATION TEST FOR MISCLASSIFICATION PROBABILITY IN DISCRIMINANT ANALYSIS**

*Andrew R. Solow*

Discriminant analysis is often used in ecological research to test for differences between two groups of individuals. A randomization procedure is described for assessing the significance of the estimated misclassification probability in such an application. The test is applied to an analysis of genetic differences between two geographically distinct subpopulations of leatherback turtles.

Published in: *Ecology*, 71(6):2379-2382, 1990.

Supported by: The Pew Charitable Trusts and the Marine Policy Center.

WHOI Contribution No. 7336.

### **TESTING FOR DENSITY DEPENDENCE: A CAUTIONARY NOTE**

*Andrew R. Solow*

The robustness and sensitivity of a test for density dependence in an animal population against departures from the assumed null and alternative model is assessed via simulation. The test is shown to be non-robust and insensitive to departures from the assumed models.

Published in: *Oecologia*, 83:47-49, 1990.

Supported by: The Pew Charitable Trusts and the Marine Policy Center.

WHOI Contribution No. 7362.

## DECISION-MAKING AND THE VALUE OF INFORMATION UNDER UNCERTAINTY

*Andrew R. Solow and James M. Broadus*

An approach to decision-making and the value of information under uncertainty is presented. This approach is based on Bayesian decision theory. The approach is developed in the context of an actual case study concerning responding to uncertain future sea level at Long Beach Island, New Jersey.

In Press: *Environment and Emerging Development Issues*, P. Dasgupta and K-G. Maler eds. Oxford University Press.

Supported by: World Institute for Development Economics Research, United Nations University and The Pew Charitable Trusts.

WHOI Contribution No. 7650.

## GLOBAL WARMING: QUO VADIS?

*Andrew R. Solow and James M. Broadus*

Global warming is with us, and there is an urgent need for the world community to confront it. This, at least, is the popular conception garnered from the media and from a sheaf of conference reports. The same sources tell us that international relations and international law must be totally reorganized to deal with this impending threat.

This paper outlines the current state of knowledge about global warming and concludes that the fears of the world community have very little foundation in scientific fact.

Published in: *The Fletcher Forum of World Affairs*, 14(2):262-269, 1990.

Supported by: The Pew Charitable Trusts and the Marine Policy Center.

WHOI Contribution No. 7738.

## DETECTING CLUSTER IN A HETEROGENEOUS COMMUNITY SAMPLED BY QUADRATS

*Andrew R. Solow, Woolcott Smith and J. Frederick Grassle*

A diagnostic procedure is described for detecting cluster in the spatial distribution of a heterogeneous community sampled by quadrats. The procedure is based on a comparison of the estimated species-area curve with its distribution under a completely random distribution of individuals. The results of a small simulation

experiment are described and the procedure is applied to two actual data sets.

In Press: *Biometrics*.

Supported by: The Pew Charitable Trusts and the Marine Policy Center.

WHOI Contribution No. 7476.

## ON SAMPLE SIZE, STATISTICAL POWER, AND THE DETECTION OF DENSITY DEPENDENCE

*Andrew R. Solow and John H. Steele*

In reviewing the results of Stiling (1988) on the detection of density dependence in insect populations, Hassell, Latto & May (1989) observed that density dependence is more commonly detected in large samples. We interpret this observation in terms of the statistical power of the test used to detect density dependence.

Using simple models, we show that even for moderately strong density dependence, it is necessary to observe up to thirty generations before density dependence can be rejected with high probability.

Published in: *Journal of Animal Ecology*, 59:1073-1076, 1990.

Supported by: The Pew Charitable Trusts and the Marine Policy Center.

WHOI Contribution No. 7358.

## MARINE INSTRUMENTS: USER'S VIEWPOINTS

*Glenn Woodsum and Hauke Kite-Powell*

Survey results from a 1988 study of marine instrumentation user groups revealed some good news for both instrument makers and users. Designed to provide insights into current and future instrument use and purchase decisions, the survey also revealed some significant challenges and interesting opportunities for firms serving the marine instrument market.

The survey was conducted by Florida State University's Center for Aquatic Research and is part of Woods Hole Oceanographic Institution's "National Marine Electronics Agenda" program organized by WHOI's Marine Policy Center.

Published in: *Sea Technology*, 31(1):5758, 1990.

Supported by: NOAA through a grant to the Massachusetts Centers of Excellence Corporation, grant No. NA87-AA-D-M00037.



**COASTAL RESEARCH CENTER**

**David G. Aubrey, Director**

**COASTAL RESEARCH CENTER**





## **TIDAL VELOCITY ASYMMETRIES AND BEDLOAD TRANSPORT IN SHALLOW EMBAYMENTS**

*Virginia A. Fry and David G. Aubrey*

Tidal circulation can cause a net transport of sediment when the tidal velocity is asymmetric about a zero mean (flood or ebb dominant) and the sediment transport rate is related nonlinearly to velocity. The relationship between tidal elevation velocity is elucidated here to permit determination from tide gauge data and sediment transport relations whether tidal asymmetry needs to be considered as a mechanism for net sediment transport in the shallow water, nonlinear system is derived through the continuity equation and shown to be significantly different than the linear relation. Finite difference numerical solutions of the one-dimensional, shallow water nonlinear equations are compared to the continuity relation and are in agreement especially toward the landward end of the channel. Tide gauge data collected at the landward end of the embayment are most useful for predicting velocity asymmetries throughout a major portion of the embayment channel.

The ratio of flood-to-ebb bedload transport and its relation to an asymmetric tidal elevation has been determined for both the linear relation between elevation and velocity and nonlinear relation. Results show that the ratio of flood-to-ebb bedload transport as calculated from the nonlinear relation between elevation and velocity is similar to the flood-to-ebb ratio calculated from the linear relation because of offsetting effects.

Published in: *Estuarine, Coastal and Shelf Science*, 30:453-473, 1990.

Supported by: NOAA National Sea Grant College Program Office NA86-AA-D-SG090; WHOI Sea Grant Project Number R/M-16-PD; USAE WES, CERC, Inlet Channel Work No. 31716; WHOI Education Office; and WHOI CRC.

WHOI Contribution No. 7212.

## **POTENTIAL IMPACTS OF CONTEMPORARY CHANGING CLIMATE ON SOUTH ASIAN SEAS STATES**

*F. J. Gable and D. G. Aubrey*

Assumes that, because global change is inevitable, the South Asian seas region should begin the appropriate research and planning studies to set forth a reasoned response to global change, for implementation when scientific evidence for global change is more quantitative.

Similarities and differences of national settings must be identified now to form the basis for local response strategies.

Published in: *Environmental Management*, 14(1):33-46, 1990.

Supported by: Richard King Mellon Foundation  
WHOI Contribution No. 7179.

## **POTENTIAL IMPACTS OF CONTEMPORARY CHANGING CLIMATE ON CARIBBEAN COASTLINES**

*Frank J. Gable and David G. Aubrey*

The threat of man-induced global change on the nations of the wider Caribbean region varies from place-to-place because of differences in exposure to storms, differences in local tectonics and subsidence, and variations in land-use practices. Because of the large number of nations involved, many having only subsistence budgets, and the cost of deriving independently a comprehensive response to global change, the similarities and differences between national settings must be identified soon. These comparisons will form the basis for local response strategies; the common elements between nations provide a basis for responses similar to those other nations, whereas the differences mandate local adaptation. That the Caribbean will be impacted by climate change is certain: its environment, land uses, and economies are dictated in large part by this marine influence. Accompanying global change will be changes in sea level, differences in storm climate, and altered precipitation patterns; science cannot define today what form these changes will take. Because global change is inevitable although its magnitude, timing, and geographic distribution are unknown the wider Caribbean should begin the appropriate research and planning studies to set forth a response to global change, for implementation when scientific evidence for global change is more quantitative.

Published in: *Ocean and Shoreline Management*, 13(1):35-67, 1990.

Supported by: Richard King Mellon Foundation  
WHOI Contribution No. 6965.

## **GLOBAL CLIMATIC ISSUES IN THE COASTAL WIDER CARIBBEAN REGION**

*Frank J. Gable, J. H. Gentile and D. G. Aubrey*

Some of the most pronounced warming during the 1980's was observed in the lower latitudes,

including the wider Caribbean, which is considered one of the regions most vulnerable to the perturbations and uncertainties of environmental change. Important potential impacts to the natural and human environments are identified that are associated with sea-level rise and the increased frequency, intensity and seasonality of tropical storms.

Published in: *Environmental Conservation*,  
17(1):51-60, 1990.

Supported by: Richard King Mellon Foundation  
WHOI Contribution No. 7180.

### **ESTIMATING THE VALUE OF BEACH RECREATION FROM PROPERTY VALUES: AN EXPLORATION WITH COMPARISONS TO NOURISHMENT COSTS**

*Steven F. Edwards and Frank J. Gable*

This paper explores how the economic value of recreation at local public beaches can be estimated from nearby property values. The negative effect of distance from the nearest public beach on coastal property values was used to reveal recreational value. Estimates of recreational value were also compared to the costs of beach nourishment that were calculated from a simulation of beach erosion caused in part by increases in relative sea level. Although a complete benefit-cost analysis was beyond the scope of this inquiry, the results suggest that potential losses of recreational value by only local users could establish the efficiency of beach nourishment projects.

In Press: *Ocean and Shoreline Management*, 15(1).

Supported by: NOAA and Richard King Mellon  
Foundation

WHOI Contribution No. 6967.

### **GLOBAL ENVIRONMENTAL CHANGE ISSUES IN THE WESTERN INDIAN OCEAN REGION**

*Frank J. Gable, David G. Aubrey and  
John H. Gentile*

In the context of this study, the important consequences of climate warming are: 1) the potential impacts associated with rising sea level due to thermal expansion of the oceans; 2) melting of land-based ice sheets and glaciers; 3) the increased frequency, intensity, and seasonality of tropical storms and the monsoon season; and 4) changes in local land-use practices.

The purpose of this paper is to place into a regional context for the Western Indian Ocean region the problems arising from changes in global climate and their cumulative effects upon the environment. Specifically, this paper focuses on the potential for impacts in the coastal zone, where the indirect pressures of climate change and anthropogenic forcings (e.g. pollution, dredging, coral mining) and policy (land use, coastal zone) collide.

In Press: *Geoforum*, 22(3).

Supported by: WHOI Sea Grant Program and  
Andrew W. Mellon Foundation

WHOI Contribution No. 7370.

### **CONTEMPORARY CLIMATE CHANGE AND ITS RELATED EFFECTS ON GLOBAL SHORELINES**

*Frank Gable*

Public, governmental, and scientific interest in global warming and the ancillary effect of rising sea level seem to be rising faster than sea level itself. Numerous national and international scientific committees have looked into this problem, and in the past several years newspapers and popular magazines also have displayed increased interest. Government-sponsored legislation, particularly in the United States, has been introduced dealing with global change as well.

Rapid coastal inundation is predicted for many parts of the world within the next 10 to 100 years, when in fact the present rate of relative sea-level rise is probably only about 1.5 mm/yr. With a possible large amount of sea-level rise resulting from projected greenhouse-related climatic warming, many coastal areas of the world may suffer increasing adverse effects. This paper identifies some of these areas reportedly experiencing erosion, perhaps due to a local rise in sea level.

Published in: *Proceedings of Coastal Zone '89*,  
ASCE, New York, NY, Vol. 2:1370-1383, 1989.

Supported by: Richard King Mellon Foundation.

WHOI Contribution No. 6966.

### **POTENTIAL COASTAL EFFECTS OF CLIMATE CHANGE IN THE CARIBBEAN**

*F. J. Gable and D. G. Aubrey*

Changes in climate are the norm when one studies the history of the earth. Examples of these changes include the glacial epochs and more recent

and largest contemporary climatic variation of the El Niño/Southern Oscillation. Many paleoclimatic records illustrate the results of natural variability.

Good reliable long-term data and selected *in situ* quantitative analyses would allow the research community to better understand and forecast the potential coastal effects of climate change on Caribbean shorelines. The uncertainty of contemporary climate conditions warrants the need for more study.

Published in: *Proceedings of the Second North American Conference on Preparing for Climate Change: A Cooperative Approach*. J. C. Topping, ed. The Climate Institute, Washington, DC, :417-421, 1989.

Supported by: Richard King Mellon Foundation and WHOI CRC.

WHOI Contribution No. 6964.

## **CHANGING INFRASTRUCTURE OF AN URBAN WATERFRONT: THE SOUTH BOSTON FLATS 1863-1920**

*Frank Gable*

The onset of the Industrial Revolution in the early nineteenth century gave prominence to the northeastern United States. Massachusetts, with its flourishing mills and inundation of immigrant labor was the most intensively organized state in the region. It was primarily through the port of Boston that this region secured its raw materials and distributed its products.

This paper examines waterfront changes in the South Boston Flats from its initial phase of development around 1863, up to 1920 when the Port of Boston became one of the three most important ports in total foreign commerce.

Published in: *Proceedings of the Eleventh International Coastal Society Conference - Ports and Harbors: Our Link to the Water*, Boston, Massachusetts, October 22-26, 1988. L. R. King, ed. :68-76, 1990.

Supported by: Richard King Mellon Foundation.

WHOI Contribution No. 6922.

## **CARIBBEAN COASTAL AND MARINE TOURISM - COPING WITH CLIMATE CHANGE AND ITS ASSOCIATED EFFECTS**

*F. Gable*

Coastal and marine tourism in many parts of the Caribbean is a significant source of revenue and tourism is the leading economic sector as a whole. On the Caribbean islands effectively all tourism

development has occurred in the coastal areas, where the beaches are the principal attraction.

Relatively few of the most intensively developed resorts have beaches broader than about 30 meters at high tide, and qualitative assessments show that most of the world's sandy shorelines are in retreat. This situation is likely to get worse, in part, because ocean level rise, a possible ancillary effect of climate change, has risen by about 15 cm (1/2 foot) during the past century. Both the increasing warming (about 0.5°C past 100 years), possibly due in part, to the build up of anthropogenic trace gases in the atmosphere, and the increasing level of the seas are projected by computer modelers to increase over the next several decades. With this prognosis, several shore areas of the Caribbean may suffer increasing adverse effects, both to the environment and to the economy.

In Press: *Proceedings of 1990 Congress on Coastal and Marine Tourism (May 25-31, 1990, Honolulu Hawaii)*, Honolulu, May 23-29, 1990. Marc L. Miller and Jan Auyong, eds. National Coastal Resource Research and Development Institute, Newport, Oregon, Vol. 1:248-258, 1990.

Supported by: WHOI Sea Grant Program and Andrew W. Mellon Foundation.

WHOI Contribution No. 7369.

## **RECENT GLOBAL SEA LEVELS AND LAND LEVELS**

*David G. Aubrey and K. O. Emery*

Tide gauge records from around the world ambiguously document the rise and fall of relative sea levels during the past century. Analysis of these records, nonuniformly distributed in time and space, reveals that land levels as well as ocean levels are changing, making difficult the estimation of sea-level change alone. Because most tide gauges are concentrated in the northern hemisphere instead of the southern hemisphere (where most ocean area is located), tide-gauge data reflect major continental motions due to glacio-isostasy and neo-tectonism, suppressing and masking the signal from eustatic sea-level change.

Estimation of the magnitude of sea-level change is important for many reasons, including interpretation of possible effects of global climate change resulting from carbon dioxide and other trace-gas loading of the atmosphere. Proper interpretation of past sea-level changes is required to calibrate and assess global climate models and observations of past climate change. The oceanic lag to atmospheric temperature change can be determined from study of tide-gauge records and

other records of relative sea levels only if the land level changes are separated from sea-level changes.

Published in: *Climate and Sea Level Change: Observations, Projections and Implications*. R.A. Warrick and T.M.L. Wigley, eds. Proceedings Climate Change Workshop, Norwich, U.K., Cambridge University Press, NY, 1990.

Supported by: National Science Foundation, Grant OCE-8501 174; WHOI Coastal Research Center; and U.S. Department of Commerce, National Oceanic and Atmospheric Administration of Sea Grant under Grant No. NA 83-AA-D-00049(RB-54).

## TECHNICAL REPORTS

### ATLANTIC SHELF SAND RIDGE STUDY: PHYSICAL OCEANOGRAPHY AND SEDIMENT DYNAMICS DATA REPORT

*Paul Dragos and David G. Aubrey*

This report describes and presents the hydrodynamic measurements made during the Atlantic Shelf Sand Ridge Study at and near Peahala Ridge, offshore of Long Beach Island, New Jersey, in Spring 1985. The intent of this phase of the study was to examine the physical oceanographic and fluid mechanical processes in the vicinity of Peahala Ridge, one of the large shore-oblique sand ridges common in the area, and from this to identify those processes responsible for sand transport near the ridge with particular reference to its generation, maintenance and migration. The field measurement program was carried out from March to May 1985 by scientists and staff of the Woods Hole Oceanographic Institution. It included measurements of currents, temperature, waves, pressure and near-bed velocity profiles. This phase was part of a larger oil industry study that included extensive geological and geophysical measurements of Peahala Ridge and other ridge-and-swale areas of the mid-Atlantic continental shelf.

Supported by: Cities Service Oil and Gas Corporation and WHOI Coastal Research Center.

WHOI Technical Report 90-11.

### SEDIMENTATION STUDY ENVIRONMENTAL MONITORING AND OPERATIONS GUIDANCE SYSTEM (EMOGS) KINGS BAY, GEORGIA AND FLORIDA PHASE III - FY 1989

*David G. Aubrey, Thomas R. McSherry and  
Wayne D. Spencer*

Repeated side-scan sonar and multi-frequency bathymetric surveys, accompanied by accurate, high resolution, and repeatable navigation, were conducted in the vicinity of a tidal inlet to define the length and time scales associated with bedforms and channel shoaling in a structured tidal inlet. The study site, St. Mary's entrance channel along the Georgia/Florida border, has a dredged channel approximately 46-52 feet in depth, bordered by a large ebb tidal delta. The tidal inlet serves Cumberland Sound, Kings Bay, and associated waterways, providing a large discharge of water from the inlet that creates bedforms and channel shoaling, given the abundance of sand-sized sediment in the vicinity. The jettied inlet produces flows that are predominantly tidally-driven, whereas farther offshore the driving forces consist predominantly of waves and storm-generated flows. In the channel reaches between these two areas, combined wave/steady flows are present, creating a myriad of scales of bedforms and shoaling patterns. This study was designed to elucidate the time and space scales of these variable bedforms and shoaling patterns, emphasizing the difference in these scales between the three different flow regimes. The results provide an important data base for quantifying shoaling processes and mechanisms in tidal inlet channels.

During phase III six bathymetric and side scan sonar surveys were accomplished. Not all data acquired during these surveys are directly comparable inside the channel. Dredging activity during the year created major changes to the channel, making comparison of differences in channel bathymetry ambiguous. Similarly, comparison of channel bedforms was difficult because many of the forms were not fully developed following dredging. Comparisons of bedforms in areas outside and adjacent to the channel over different surveys is less ambiguous.

Phase III data indicate the following tentative conclusions:

a) Changes in bathymetry occur within and outside the channel on various time and space scales.

b) Bedforms of various scales occur in and outside of the channel. Within the channel, bedforms occur commonly, having heights of 2-3 feet and possibly higher. Outside the channel,

bedforms (shoals) reach more than 10 feet higher than the ambient delta depths.

c) Shoaling appears largest along the north margin of the channel.

d) Shoals on the ebb tidal delta move to the south, towards the dredged channel.

e) Hotspots where sedimentation rates appear highest are concentrated on the ebb-tidal delta, just outside and inside the jetties. A sedimentation monitoring program emphasizing periodic hotspot surveys from a surface vessel is suggested to guarantee adequate information about channel depths for the EMOGS program.

Supported by: National Oceanic Atmospheric  
Administration under Sea Grant No.  
NA860A-D- SG090.

WHOI Technical Report 90-34.

## GEODETIC FIXING OF TIDE GAUGE BENCH MARKS

*William E. Carter, David G. Aubrey,  
Trevor Baker, Claude Boucher,  
Christian LeProvost, David Pugh, W. R. Peltier,  
Mark Zumberge, Richard H. Rapp,  
Robert E. Schutz, K. O. Emery and  
David B. Endfield*

This is organized in two sections. This first section states the terms of reference established for the geodetic committee by the President of the Commission on Mean Sea Level and tides [Pugh, private communication, 1988]. The second section lists the 5 primary technical conclusions reached by the committee.

More detailed discussions of the geodetic techniques, references, and supporting documentation are presented in the main body of the report.

### Terms of Reference

The terms of reference established for the geodetic committee were:

1. To identify the oceanographic and geophysical requirements for fixing Tide Gauge Bench Marks (TGBM's) in an absolute terrestrial coordinate system.

2. To evaluate the technology available for fixing TGBM's.

3. To make recommendations to the MSLT commission of a strategy for coordinated global fixing of TGBM's and for making the results centrally available.

### Technical Conclusions

The primary technical conclusions reached by the geodetic committee are:

1. All gauges to be used to monitor sea level must have local network of several (6 to 10) bench marks that are resurveyed by spirit leveling or

Global Positioning System (GPS) at least once each year.

2. Tide Gauges should be organized into regional networks and the relative positions of the gauges within each network should be determined frequently, preferable at least once per year, GPS surveys designed to achieve sub-centimeter accuracy.

3. The regional sea level networks should be organized around the primary stations of the International Earth Rotation Service (IERS) Terrestrial Reference Frame. This is the only terrestrial reference frame of sufficient accuracy for monitoring global sea level change.

4. Absolute gravity measurements should be made at all of the IERS primary stations, near as many of the individual tide gauges as possible (with highest priority being given to island tide gauges), and in regions of glacial rebound and tectonic activity. The measurements should be repeated on appropriate time scales to detect secular changes in gravity of 1 to 3  $\mu$ gals per year (equivalent to vertical crustal motion of 0.3 to 1 cm per year).

5. A center, preferably the PSMSL, should be designated to collect, archive, and distribute the geodetic information for each of the TGBM's, absolute gravity stations established for monitoring global sea level, and the tide gauge time series.

Supported by: International Associations for Physical  
Sciences of the Ocean, National Oceanic and  
Atmospheric Administration and WHOI Sea  
Grant Program.

WHOI Technical Report 89-31.

## DEVELOPMENT, CHARACTERISTICS, AND EFFECTS OF THE NEW CHATHAM HARBOR INLET

*Graham S. Giese, David G. Aubrey and  
James T. Liu*

A new tidal inlet into Chatham Harbor, Massachusetts, has developed from a bench in the barrier beach, Nauset Beach, that forms the outer shoreline of southeastern Cape Cod. Increased tidal range and wave energy resulting from the new inlet produced acute coastal erosion and channel shoaling within Chatham Harbor, with significant impacts on the fishing and boating industries, and on private and public property and interests. Study results are consistent with the hypothesis that the Nauset-Monomoy barrier beach system undergoes a long-term cycle of geomorphological change, and that a new cycle was initiated with the formation of this new inlet. Based on this new understanding, future changes in the system can be foreseen and provided to coastal resource managers.

Supported by: Commonwealth of Massachusetts,  
Department of Environmental Management,  
Division of Waterways; the Town of Chatham,  
WHOI Sea Grant Program; Massachusetts Office  
of Coastal Zone Management; U.S. Army Corps  
of Engineers (New England Division and Coastal  
Engineering Research Center); Town of Orleans;  
and Friends of Pleasant Bay.

*WHOI Technical Report* 89-19.

## **GRADUATE STUDENTS**

Abstracts of papers of theses submitted in 1990 by graduate students of the Woods Hole Oceanographic Institution Doctoral Degree Program and the Woods Hole Oceanographic Institution/Massachusetts Institute of Technology Joint Program in Oceanography/Oceanographic Engineering. Other papers authored or coauthored by graduate students are included in the departmental sections.





PHYSIOLOGICAL STUDIES OF  
PHOTOTROPHY AND  
HETEROTROPHY IN TWO ALGAE  
WITH CONTRASTING NUTRITIONAL  
CHARACTERISTICS, *PYRENUMONAS*  
*SALINA* (CRYPTOPHYCEAE) AND  
*POTERIOOCHROMONAS*  
*MALHAMENSIS* (CHRYSTOPHYCEAE)

Alan J. Lewitus

The ability of algae to take up dissolved organic compounds is well-documented for cultured and field populations yet the physiological mechanisms controlling this behavior are largely unknown. The effects of dissolved organic compound additions on the growth and photosynthetic apparatus were examined in two nanophytoplankton with contrasting nutritional characteristics, *Pyrenomonas salina* (Cryptophyceae) and *Poterioochromonas malhamensis* (Chrysophyceae). Although both species are capable of chemoheterotrophic nutrition, great differences were found in the relative contribution of heterotrophy to their overall nutrition and the physiological response of their photosynthetic systems to changes in nutritional mode. These differences indicate that the physiological mechanisms involved in integrating autotrophic and heterotrophic nutrition and the environmental control of this integration are distinct in these species.

In comparison to other facultatively heterotrophic algae, *P. malhamensis* is exceptional in the dominant contribution of heterotrophy to its overall nutrition. Growth could be significantly enhanced by organic substrate additions to *P. malhamensis* at all light intensities and the growth rate on flucose in the dark was equal to the maximum growth rate on glucose in the light. In addition, when organic substrates were available to the alga, chlorophyll *a* cell<sup>-1</sup> was reduced and the extent of this reduction varied with the type of organic substrate. These results support the hypothesis that chloroplast development in *P. malhamensis* is catabolite-sensitive. The inhibitory effect of organic substrates on chlorophyll production by *P. malhamensis* was only transitory; i.e., after the initial decline in chlorophyll *a* cell<sup>-1</sup>, chlorophyll production increased and the organic substrate uptake rate cell<sup>-1</sup> decreased despite the persistence of a relatively high substrate concentration in the culture medium. These results suggest that the accumulation of substance(s) excreted by *P. malhamensis* conditioned the culture medium and led to a relief of the inhibitory effect of organic substrates on chlorophyll production by the alga.

*P. salina* is typical of most facultatively

heterotrophic algae in culture in that phototrophic growth can be enhanced by organic enrichment only at light intensities limiting for photoautotrophic growth. Contrary to *P. malhamensis*, the effect of organic compounds on the growth rate of *P. salina* was critically light intensity-dependent under all organic substrate concentrations used in this study. In addition, whereas in *P. malhamensis* the addition of organic substrates repressed chloroplast development, only selected elements of the photosynthetic system were inhibited by organic substrate additions to *P. salina*, and the uptake rate of inorganic carbon was not affected. These results indicate that these algae have contrasting metabolic strategies for integrating autotrophic and heterotrophic nutrition for growth. When organic substrates are available to *P. malhamensis*, the synthesis of the photosynthetic apparatus is repressed and growth and maintenance requirements are met by the catabolism of organic substrates. In contrast, given a sufficient light supply, maximal growth rates can be obtained photoautotrophically by *P. salina*, but organic substrates can be used to augment the carbon, energy, and/or reductant supply when photosynthetic rates are light-limited.

The physiological response of *P. salina*'s photosynthetic system to changes in environmental conditions was further examined by testing two hypotheses. The first hypothesis was that *P. salina* responds to nitrogen deprivation by mobilizing phycoerythrin in order to help sustain cellular nitrogen requirements. In response to nitrogen depletion from the culture medium, the phycoerythrin content of *P. salina* cells decreased prior to any changes in growth rate, cell volume, or cellular concentrations of chlorophyll *a*, carbon, or nitrogen. These results support the hypothesis and suggest that, in addition to its light-harvesting role, phycoerythrin may serve as an important endogenous nitrogen source for this cryptophyte. The second hypothesis was that glycerol uptake selectively inhibits the synthesis of photosynthetic components involved in light-harvesting. Glycerol addition to *P. salina* cultures grown at a limiting light intensity reduced the cell phycoerythrin content, phycoerythrin to chlorophyll *a* ratio, thylakoid width, degree of thylakoid packing, number of thylakoids cell<sup>-1</sup>, and size of photosystem II complexes. These properties were reduced to a similar extent by increasing the light intensity for growth. These results strongly support the hypothesis and indicate that enhancement of heterotrophic potential occurs at the expense of light-harvesting ability in glycerol-grown *P. salina*.

Thesis Supervisor: Dr. David A. Caron,  
WHOI.

Supported by: OVF Grant 25/85.10, NSF Grants  
BSR-8620443 and BSR-8919447.

## ANALYSIS AND DISTRIBUTION OF INTEGRINS IN CHICKEN EMBRYOS

*Lisa Andrea Urry*

Integrins of the  $\beta_1$  class in chicken were characterized biochemically and immunologically, and related to their human counterparts. This group of proteins, initially believed to comprise three bands on SDS-PAGE gels, was shown to include at least six proteins and probably more. Immunoprecipitation experiments demonstrated the electrophoretic pattern to reflect a collection of heterodimers with a common  $\beta_1$  subunit and at least four different  $\alpha$  subunits, rather than a heterotrimeric or multimeric complex.

Polyclonal antisera were generated against bands from the  $\alpha$  subunit regions of gels. Although these antisera are not specific for single  $\alpha$  subunit, they could prove useful for future cloning of further chicken  $\alpha$  subunits by screening of expression libraries. Polyclonal antisera against peptides from the putative cytoplasmic domains of human and chicken  $\alpha$  subunits were generated or obtained from other laboratories. These reagents were used in conjunction with polyclonal antisera to isolated human  $\alpha$  subunits in order to identify the chicken integrin subunits  $\alpha_3$ ,  $\alpha_4$ ,  $\alpha_5$ , and, tentatively,  $\alpha_1$ . The human heterodimers  $\alpha_3\beta_1$ ,  $\alpha_4\beta_1$ , and  $\alpha_5\beta_1$  are known to bind to fibronectin; a related chicken heterodimer,  $\alpha_{5-1}\beta_1$ , was shown by affinity chromatography to perform the same function.

The expression of  $\alpha_3$ ,  $\alpha_4$ ,  $\alpha_5$ , and  $\beta_1$  in developing chicken embryos was analyzed by Western blotting. The  $\alpha_3$  subunit is expressed at 2-5x higher amount per unit protein at embryonic day 2 compared with day 11. The other subunits are expressed at constant levels.

The patterns of localization of  $\beta_1$ ,  $\alpha_5$ , and  $\alpha_3$  on cells in culture was explored using immunofluorescence labelling experiments.  $\beta_1$  was observed in focal contacts, along stress fibers, and intercellularly between chicken embryonic lens cells (an epithelial cell type).  $\alpha_5$  was present in a similar pattern, in focal contacts and along stress fibers. However, in some focal contacts,  $\beta_1$  was present while  $\alpha_5$  was absent, suggesting that different  $\alpha$  subunits in association with  $\beta_1$  might perform distinct functions in conjunction with subtly different cytoskeletal elements.  $\alpha_5$  was also shown to be distributed intercellularly in "bridges" between human EJ cells (an epithelial bladder carcinoma cell line). Intercellular localization of integrin subunits has since been demonstrated by other researchers. The function performed by integrins in these regions is not fully understood at present.

The  $\alpha_3$  subunit was never observed in focal contacts, under a wide variety of conditions. On

human EJ cells, this subunit was clearly shown to be distributed diffusely all over the surfaces of a subset of cells. A wounding experiment was performed to investigate a possible role for  $\alpha_3\beta_1$  in cell migration. Although the  $\alpha_3$  subunit did not appear to become concentrated in the leading edges of migratory cells, it remains possible that  $\alpha_3\beta_1$  is involved in cell adhesion to the substrate during migration. Because of their different patterns of localization on fibronectin,  $\alpha_3\beta_1$  and  $\alpha_5\beta_1$  probably perform distinct cellular functions when associated with this ligand.  $\alpha_3\beta_1$  may also be capable of binding other ligands or mixtures of ligands which have not yet been identified.

Monoclonal antibodies were generated against integrin subunits. One antibody recognized a doublet in the band 2 region of purified integrins on Western blots, but did not stain cells or embryos in immunofluorescence experiments. Two antibodies were tentatively shown to be directed against actin or an actin-associated protein and an extracellular matrix molecule. Two other antibodies could not be demonstrated biochemically to recognize integrin subunits, but their patterns of localization on cells in culture are clearly related to that of integrin  $\beta_1$ .

The distribution of  $\alpha_4$  protein in chicken embryos was analyzed by immunofluorescence staining of 2-1/2-day embryos with a polyclonal antiserum to human  $\alpha_4$ . Intense fluorescence was observed in regions where epithelial sheets were bending, suggesting that  $\alpha_4\beta_1$  might play a role in such morphogenetic events.  $\alpha_4$  mRNA had been shown previously to be localized in cells which were proposed to be neural crest cells based on their location in the embryo. The identity of these cells was confirmed by staining with the neural crest cell marker HNK-1. However,  $\alpha_4$  protein was not detected on these cells nor in several of their derivatives analyzed at later time points. Extensive control experiments confirmed that observed immunofluorescence pattern was due to antibodies in the anti-human  $\alpha_4$  antiserum which could be affinity purified on chicken  $\alpha_4$ . The basis for the discrepancy between the most striking aspects of the patterns seen for  $\alpha_4$  protein and mRNA is not understood and will require generation of more reagents for a satisfactory resolution.

Further experiments extending the results of the current project are necessary to address the functions of integrins during development. Chicken embryos are an excellent system to use for such studies, since there are many developmental events in which integrins are likely to play a role where the relevant cells can be explanted and cultured in vitro. We envision that our extensive characterization of these proteins and preliminary data on their distribution will have laid the groundwork for future research on the role integrins play in the interaction between cells and

their environment in vivo.

Thesis Supervisor: Dr. Richard Hynes, MIT.

Supported by: Ida M. Green Fellowship and National Institutes of Health Grant NIH RO1 Ca17007.

## DINOFLAGELLATE BLOOMS AND PHYSICAL SYSTEMS IN THE GULF OF MAINE

Peter John Selwyn Franks

Numerous studies have shown dinoflagellate blooms to be closely related to density discontinuities and fronts in the ocean. The spatial and temporal patterns of the dinoflagellate population depend on the predominant mode of physical forcing, and its scales of variability. The present study combined field sampling of hydrographic and biological variables to examine the relationship of dinoflagellate population distributions to physical factors along the southwestern coast of the Gulf of Maine.

A bloom of *Ceratium longipes* occurred along this coast during the month of June, 1987. A simple model which coupled alongisopycnal diffusion with the logistic growth equation suggested that the cells had a growth rate of about  $0.1 \text{ d}^{-1}$ , and had reached a steady horizontal across-shelf distribution within about 10 d. Further variations in population density appeared to be related to fluctuations of light with periods of  $\sim 10 \text{ d}$ . To our knowledge, this was the first use of this simple diffusion model as a diagnostic tool for quantifying parameters describing the growth and movement of a specific phytoplankton population.

Blooms of a toxic dinoflagellate, *Alexandrium tamarense* have been nearly annual features along the coasts of southern Maine, New Hampshire and Massachusetts since 1972; however the mechanisms controlling the distribution of cells and concomitant shellfish toxicity and relatively poorly understood. Analysis of field data gathered from April to September, 1987-1989, showed that in two years when toxicity was detected in the southern part of this region, *A. tamarense* cells were apparently transported into the study area between Portsmouth and Cape Ann, Massachusetts, in a coastally trapped buoyant plume. This plume appears to have been formed off Maine by the outflow from the Androscoggin and Kennebec Rivers. Flow rates of these rivers, hydrographic sections, and satellite images suggest that the plume had a duration of about a month, and extended alongshore for several hundred kilometers. The distribution of cells followed the position of the plume as it was influenced by wind and topography. Thus when winds were downwelling-favourable, cells were moved alongshore to the south, and were held to the

coast; when winds were upwelling-favourable, the plume sometimes separated from the coast, advecting the cells offshore.

The alongshore advection of toxic cells within a coastally trapped buoyant plume can explain the temporal and spatial patterns of shellfish toxicity along the coast. The general observation of a north-to-south temporal trend of toxicity is consistent with the southward advection of the plume. In 1987 when no plume was present, *Alexandrium tamarense* cells were scarce, and no toxicity was recorded at the southern stations. A hypothesis was formulated explaining the development and spread of toxic dinoflagellate blooms in this region. This plume-advection hypothesis included: source *A. tamarense* populations in the north, possibly associated with the Androscoggin and Kennebec estuaries; a relationship between toxicity patterns and river flow volume and timing of flow peaks; and a relationship between wind stresses and the distribution of low salinity water and cells.

Predictions of the plume-advection hypothesis were tested with historical records of shellfish toxicity, wind speed and direction, and river flow. The predictions tested included the north-south progression of toxic outbreaks, the occurrence of a peak in river flow prior to the PSP events, the relationship of transit time of PSP toxicity along the coast with river flow volume, and the influence of surface wind stress on the timing and location of shellfish toxicity. All the predictions tested were supported by the historical records. In addition it was found that the plume-advection hypothesis explains many details of the timing and spread of shellfish toxicity, including the sporadic nature of toxic outbreaks south of Massachusetts Bay, and the apparently rare occurrence of toxicity well offshore on Nantucket Shoals and Georges Bank.

Thesis Supervisor: Dr. Donald M. Anderson, WHOI.

Supported by: Office of Naval Research and the Woods Hole Oceanographic Institutions Sea Grant Program. ONR Contract N00014-87-K-0007, ONR Grant N00014-89-J-111 and Sea Grant NA86AA-D-SG090.

## ESTIMATION AND CORRECTION OF GEOMETRIC DISTORTIONS IN SIDE-SCAN SONAR IMAGES

Daniel Tavora De Queiroz Cobra

This thesis introduces a new procedure for the enhancement of acoustic images of the bottom of the sea produced by side-scan sonars. Specifically, it addresses the problem of estimating and correcting geometric distortions frequently observed in such images as a consequence of

motion instabilities of the sonar array. This procedure estimates the geometric distortions from the image itself, without requiring any navigational or attitude measurements. A mathematical model for the distortions is derived from the geometry of the problem, and is applied to estimates of the local degree of geometric distortion obtained by cross-correlating segments of adjacent lines of the image. The model parameters are then recursively estimated through deterministic least-squares estimation. An alternative approach based on adaptive Kalman filtering is also proposed, providing a natural framework in which a priori information about the array dynamics may be easily incorporated. The estimates of the parameters of the distortion model are used to rectify the image, and may also be used for estimating the attitude parameters of the array. A simulation is employed to evaluate the effectiveness of this technique and examples of its application to high-resolution side-scan sonar images are provided.

Thesis Supervisor: Dr. Alan V. Oppenheim,  
MIT.

Supported by: DARPA (monitored by ONR) Grant  
No. N00014-89-J-148, NSF Grant No. MIP  
87-14969.

## STOCHASTIC MODELING OF SEAFLOOR MORPHOLOGY

*John Anson Goff*

At scale lengths less than 100 km or so, statistical descriptions of seafloor morphology can be usefully employed to characterize processes which form and reshape abyssal hills, including ridge crest volcanism, off-axis tectonics and volcanism, mass wasting, sedimentation, and post-depositional transport. The objectives of this thesis are threefold: (1) to identify stochastic parameterizations of small-scale topography that are geologically useful, (2) to implement procedures for estimating these parameters from multibeam and side-scan sonar surveys that take into account the finite precision, resolution, and sampling of real data sets, and (3) to apply these techniques to the study of marine geological problems.

The seafloor is initially modeled as a stationary, zero-mean, Gaussian random field completely specified by its two-point covariance function. An anisotropic two-point covariance function is introduced that has five free parameters describing the amplitude, orientation, characterization width and length, and Hausdorff (fractal) dimension of seafloor topography. The general forward problem is then formulated relating this model to the statistics of an ideal multibeam echo sounder, in particular the

along-track autocovariance functions of individual beams and the cross-covariance functions between beams of arbitrary separation. Using these second moments as data functionals, we then pose the inverse problem of estimating the seafloor parameters from realistic, noisy data sets with finite sampling and beamwidth, and we solve this inverse problem by an iterative, linearized, least squares method.

Resolution of this algorithm is tested against ship variables such as length of data, the orientation of ship track with respect to topographic grain, and the beamwidth. This analysis is conducted by inverting sets of synthetic data with known statistics. The mean and standard deviation of the inverted parameters can be directly compared with the input parameters and the standard errors output from the inversion. The experiments conducted in this study show that the rms seafloor height can be estimated to within ~15% and anisotropic orientation to within ~5° (for a strong lineation) using very short track lengths (down to 3 characteristic lengths, or ~10 to 100 km), and characteristic lengths of seafloor topography can be estimated to within ~25% using fairly short track lengths (down to 5 or 6 characteristic lengths, or 10's of km to ~200 km). The number of characteristic lengths sampled by a ship track, and hence the accuracy of the estimation, is maximized when the ship track runs perpendicular to abyssal hill lineation.

Using the assumed beamwidth, the measured noise valued, and the seafloor parameters recovered from the inversion, Sea Beam "synthetics" are generated whose statistical character can be directly compared with raw Sea Beam data. However, these comparisons are spatially limited in the athwartship direction. A recent SeaMARC II survey along the flanks and crest of the East Pacific Rise between 10° and 15°N included sufficient off-axis topography to permit a comparison of a complete 2-D synthetic topographic field with a region of abyssal-hill terrain that has close to 100% data coverage. Synthetic data is compared to both Sea Beam swaths and SeaMARC II survey data. These comparisons generally indicate that we are successful in characterizing the second order properties of the seafloor. They also indicate the directions we will need to take to improve our modeling, including generalization of the second-order model and characterization of higher moments.

The inversion procedure is applied to a data set of 64 near-ridge Sea Beam swaths to characterize near ridge abyssal hill morphology and its relationship to ridge properties. Much of the data (27 swaths) comes from cruises to the Pacific-Cocos spreading section of the East Pacific Rise between 9° and 15°N. These data provide very

good abyssal hill coverage of this well-mapped and studied ridge section and form the basis of a regional analysis of the correlation between ridge morphology and stochastic abyssal hill parameters. This regional analysis suggests a strong relationship between magma supply and the character of abyssal hills. We also have data from near the Rivera (9) and Nazca (7) spreading sections of the East Pacific Rise, the Mid-Atlantic Ridge (18), and the Indian-African Ridge (3). Though spotty, this constitutes a good initial data set for the analysis of correlations among covariance parameters and between parameters and ridge characteristics, especially spreading rate. A working hypothesis contends 1) that the maximum size of abyssal hills is related to the lithosphere's ability to elastically support the load, 2) that fissuring and horst and graben formation dominate abyssal hill formation at fast spreading ridges, and 3) that volcanic edifice formation, modified by faulting driven by lithospheric necking, dominates abyssal hill formation at slow spreading ridges.

To quantify abyssal hill characteristics such as vertical and lateral asymmetry and "peakiness" we must appeal to higher statistical moments than order two. A mathematical framework is introduced for the study of higher moments of a topographic field. This framework is built upon the concept that lower-order moments provide the groundwork for studying the higher-order moments. A simple 1-D parameterized model is proposed for moments up to order 4. This model includes two parameters for the third moment, describing vertical and lateral asymmetries, and one for the fourth moment, which describes the peakiness of topography. Initial methods are developed for estimating these parameters from bathymetric profiles. Results from the near ridge data set are presented and interpreted with regard to abyssal hill forming processes.

Thesis Supervisor: Dr. Thomas H. Jordan,  
MIT.

Supported by: Office of Naval Research through the  
Massachusetts Institute of Technology.

## COMPARATIVE DESIGN, MODELING, AND CONTROL ANALYSIS OF ROBOTIC TRANSMISSIONS

*Hagen Schempf*

Transmission dynamics are shown to dominate the stability and performance of impedance- and torque controlled rotary electro-mechanical systems. The experimental analysis focuses on planetary, cycloidal, harmonic and cable reducers, but excludes direct-drive, pneumatic, hydraulic and friction drives. Neither sensors nor actuators

with better resolution nor increased dynamic range can circumvent reduced stability and performance limitations unless certain hardware criteria can be met. Simple transmission models are proposed to model such effects as (1) transmission stiffness, (2) soft-zones and wind-up, (3) backlash and lost motion, and (4) stiction, friction and viscous losses. These models are experimentally verified using six different transmission types most commonly used in robot designs. Simple lumped-parameter linear/nonlinear models are shown to predict stability margins and bandwidths at these margins fairly closely. Simple nonlinear lumped-and fixed-parameter models were unable to properly predict time responses when the torque signals were of low-frequency and amplitude, underscoring the complexity in modeling the transmission-internal stick-slip phenomena.

The clear distinction between speed reducers and torque multipliers is theoretically and experimentally explored. The issue of actuator and sensor colocation is shown to be extremely important in predicting the reduced bandwidth and stability of torque-controlled actuator-transmission-load systems. Stiffening transmission behaviors are shown to be of a conditionally stabilizing nature, while also reducing the dynamic range of impedance- and torque-servoed systems. System damping, whether active or passive, as well as low-pass filtering motor-controller signals, are shown to dramatically increase stability without having any effect on increasing system bandwidth. Transmission soft-zones are proven to reduce the stability margins of colocated impedance controlled electro-mechanical systems. None of the standard controller structures explored here were able to noticeably increase the system bandwidth of the open-loop system, without reducing the overall system performance.

The different transmissions are tested for system nonidealities and generalizations drawn on the stability and performance margins of impedance and torque-servoed geared, cycloidal, planetary, and cable reducers in hard contact with the environment. Experimental results are furnished which underscore the validity and limitations of the theoretical modeling approach and comparative transmission analysis, while highlighting the importance of different physical system parameters necessary for proper transmission design.

Thesis Supervisor: Dr. Dana Yoerger, WHOI.

Supported by: ONR N00014-86-C-0038, NRL  
N00014-88-K-2022.

# TRACE ELEMENT GEOCHEMISTRY OF OCEANIC PERIDOTITES AND SILICATE MELT INCLUSIONS: IMPLICATIONS FOR MANTLE AND OCEAN RIDGE MAGMAGENESIS

*Kevin Todd Michael Johnson*

The mantle melting process is fundamental to basalt genesis and crustal accretion at mid-ocean ridges. It is believed that melts ascend more rapidly than the surrounding mantle, implying a process similar to fractional melting may be occurring, but geochemical evidence for this has been lacking. Furthermore, crustal accretion is thought to be episodic at slow spreading ridges, but sampling programs that can test this temporal variability are virtually nonexistent. This dissertation examines the trace element compositions of abyssal peridotites and discusses how they preserve details of the melting process that are not recognizable in mid-ocean ridge basalts. The results support fractional melting as the dominant melting process in the sub-ridge upper mantle. Evidence is also presented supporting non-steady state mantle melting at the Atlantis II Fracture Zone cutting the very slow spreading Southwest Indian Ridge.

Trace element compositions of peridotite clinopyroxenes from fracture zones along the American-Antarctic and Southwest Indian Ridges vary as a function of proximity to hotspots. The results presented in Chapter 2 are consistent with higher degrees of melting and greater incompatible element depletion in the upper mantle near hotspots. All peridotites studied are consistent with being residues of fractional melting and inconsistent with batch melting. Some samples recovered near hotspots appear to have begun melting in the garnet stability field, deeper than samples recovered away from hotspots. Most samples show pronounced negative Zr and Ti anomalies, which increase with increasing incompatible element depletion (increased melting), on extended rare earth (spider) diagrams.

The results of Chapter 2 indicated the importance of accurately knowing trace element partition coefficients between clinopyroxene and liquid. It was found that existing partitioning studies report either rare earth elements, Ti, or Zr, but not all elements together. Thus, there is ambiguity about relative partition coefficients for these elements. Accurate knowledge of partitioning is important in understanding the formation of negative Zr and Ti anomalies observed in peridotite clinopyroxenes as well as in constructing realistic melting models for peridotites. To that end, Chapter 3 reports the results of a clinopyroxene/basaltic liquid trace element

partitioning study carried out on natural dredged basalts and experimental charges of mid-ocean ridge basalts. It was found that there are small negative anomalies in the partition coefficients of Zr and Ti relative to adjacently plotted rare earth elements on spider diagrams.

Fractional melting implies that small parcels of refractory (e.g., high  $Mg/[Mg+Fe]$ ), incompatible element depleted melts must exist somewhere in the ascending body of melt. Since mixing, wall rock reaction, and fractional crystallization probably alter the compositions of silicate melts extensively on their way from source to surface, representatives of these refractory fractional melts will rarely be erupted as flows on the seafloor. However, some refractory silicate melt inclusions possess compositional characteristics akin to those expected in fractional melts, i.e. low incompatible element concentrations and fractionated trace element ratios. Chapter 4 is a study of refractory melt inclusions from a variety of tectonic settings. The inclusions were obtained from Dr. A.V. Sobolev of the Vernadsky Institute of Geochemistry, Soviet Academy of Sciences, Moscow. They are not ideally suited for studying mid-ocean ridge processes, as only a few of the inclusions are from this environment, but in general, the inclusions show more refractory, incompatible element depleted compositions than their host lavas. Furthermore, the suite of inclusions in different mineral phases contained in a single N-type mid-ocean ridge basalt show variable trace element characteristics indicating unrelated sources for some inclusions. The results of the study do not strongly endorse the fractional melting hypothesis, but some support is suggesting by trace element depletions and fractionations warranting a more thorough study of a suite of inclusions.

Finally, the along-ridge major and trace element variability in peridotites observed previously and in Chapter 2 is compared to the variability found in a single fracture zone. The high sampling density at the Atlantis II Fracture Zone on the Southwest Indian Ridge, coupled with its great distance from a hotspot make it a good subject for a baseline study. It was found that the compositional variability observed in peridotites from the Atlantis II Fracture Zone covers nearly the whole range of compositions found along the American-Antarctic and Southwest Indian Ridges in Chapter 2. However, there are systematics to this wide range, suggesting different processes may control the depletions. On the eastern side of the transform, a compositional gradient is observed from the center of the eastern wall to the northern ridge-transform intersection. Peridotites on this side have become gradually more depleted in incompatible elements and modal clinopyroxene over at least the last 10-11 million years. Samples

form the western side of the transform are, in general, more depleted than those from the eastern side and show some indication of a compositional gradient as well, although sampling is less dense. Basalts from the western side are clearly different in iron composition and degree of rare earth element fractionation. These differences are consistent with higher pressure, higher degrees of melting producing lavas on the western side. It is believed that the long wavelength chemical variations corresponding to hotspot proximity described in Chapter 2 result from regional thermal conditions in the upper mantle imposed, in large part, by the hotspots. On the other hand, the short wavelength variability on a fracture zone or spreading cell scale may result from episodic mantle upwelling and magma production due to non-steady accretion at very slow spreading ridges.

Thesis Supervisor: Dr. Henry J.B. Dick,  
WHOI.

Supported by: NSF-DPP-8720002,  
NSF-OCE-8416634.

# **DETECTION AND CHARACTERIZATION OF DEEP WATER WAVE BREAKING USING MODERATE INCIDENCE ANGLE MICROWAVE BACKSCATTER FROM THE SEA SURFACE**

*Andrew Thomas Jessup*

The importance of wave breaking in both microwave remote sensing and air-sea interaction has led to this investigation of the utility of a Ku-Band CW Doppler scatterometer to detect and characterize wave breaking in the open ocean. Field and laboratory measurements by previous authors of microwave backscatter from sharp-crested and breaking waves have shown that these events can exhibit characteristic signatures in moderate incidence angle measurements of the radar cross-section (RCS) and Doppler spectrum. Specifically, breaking events have been associated with polarization independent sea spikes in the RCS accompanied by increased mean frequency and bandwidth of Doppler spectrum.

Simultaneous microwave, video, and environmental measurements were made during the SAXON experiment off Chesapeake Bay in the fall of 1988. The scatterometer was pointed upwind with an incidence angle of 45 degrees and an illumination area small compared to the wavelength of the dominant surface waves. An autocovariance estimation technique was used to produce time series of the RCS, mean Doppler frequency, and Doppler spectral bandwidth in real-time.

The joint statistics of the microwave quantities indicative of breaking are used to investigate detection schemes for breaking events identified from the video recordings. The most successful scheme is based on thresholds in both the RCS and the Doppler bandwidth determined from joint distributions for breaking and non-breaking waves. Microwave events consisting of a sea spike in the RCS accompanied by a large bandwidth are associated with the steep forward face of waves in the early stages of breaking. The location of the illumination area with respect to the phase of the breaking wave, the stage of breaking development, and the organization of an individual crest with respect to the antenna look-direction all influence the detectability of a breaking event occurring in the vicinity of the radar spot. Since sea spikes tend to occur on the forward face of waves in the process of breaking, the whitecap associated with a given sea spike may occur after the crest of the wave responsible for the sea spike has passed the center of the illumination area. Approximately 70% of the waves which produce whitecaps within a distance of 5m of the bore sight location are successfully identified by a threshold-based detection scheme utilizing both RCS and bandwidth information.

The sea spike statistics are investigated as functions of wave field parameters and friction velocity  $u^*$ . For VV and HH polarization, the frequency of sea spike occurrence and the sea spike contribution to the mean RCS show an approximately cubic dependence on  $u^*$ , which is consistent with theoretical modelling and various measures of whitecap coverage. The data also suggest that the average RCS of an individual sea spike is not dependent on  $u^*$ . At high friction velocities ( $u^* \approx 40-50 \text{ cm s}^{-1}$ ), the contribution of sea spikes to the mean RCS is in the range of 5-10% for VV and 10-20% for HH. The wind speed dependence of the percentage of crests producing sea spikes is comparable to that of the fraction of breaking crests reported by previous authors. The percentage of wave crests producing sea spikes is found to vary approximately as  $(Re^*)^{1.5}$ , where  $Re^*$  is a Reynolds number based on  $u^*$  and the dominant surface wavelength. This result agrees with measurements of the degree of wave breaking by previous authors and is shown to be consistent with a cubic dependence on  $u^*$ . Models for the probability of wave breaking as a function of moments of the wave height spectrum are compared to our results. The Doppler frequency and bandwidth measurements are also used to inquire into the kinematics of the breaking process.

Thesis Supervisor: Dr. Ken Melville, MIT.

Supported by: ONR: N00014-86-K-0325, MIT Sloan  
Basic Research Fund, NASA: NAGW-1272, NSF:  
8614889-OCE.



## REFINEMENT AND APPLICATION OF A NEW PALEOTEMPERATURE ESTIMATION TECHNIQUE

Elisabeth Lynn Sikes

A recently developed technique for determining past sea surface temperatures (SST), based on an analysis of the unsaturation ratio of long chain  $C_{37}$  methyl alkenones ( $U_{37}^k$ ) produced by *Prymnesiophyceae* phytoplankton, has been applied to late Quaternary sediment cores. Previous studies have shown that the  $U_{37}^k$  ratio of these alkenones is linearly proportional to the sea-water temperature in which the plankton grow, both in culture and water column samples. Furthermore, a reasonable correlation has been found between open ocean paleo-SST estimates based on  $U_{37}^k$  values and those derived from  $\delta^{18}O$ , for the period spanning approximately the last 100,000 years (Brassell, 1986b). These results indicate this technique has potential for determining paleo-SST from analysis of alkenones extracted from marine sediments. In order to apply the  $U_{37}^k$  method quantitatively, it is necessary to calibrate the method for sediment samples, and to assess how well the alkenones maintain their temperature signal under some common conditions of sediment deposition and sample handling. It is also necessary to determine the method's usefulness downcore, that is, back in time, by comparing it to established methods.

This study examined the effect on  $U_{37}^k$  of conditions that cause dissolution of carbonates in the sediment, and methods of storage and sample handling. These are two problems that must be resolved before the method can be applied rigorously and quantitatively to sediments for paleotemperature estimations. A comparison of duplicate samples collected and stored frozen versus those stored at room temperature for up to four years showed no resolvable differences in  $U_{37}^k$ . Laboratory experiments of carbonate dissolution indicated there is no effect on  $U_{37}^k$  values under the acidic conditions that dissolve carbonates. Initial field results support this, but indicate more studies are necessary. The  $U_{37}^k$  "thermometer" was calibrated by analyzing  $U_{37}^k$  in coretops from widely varying open ocean sites. Sediment values of  $U_{37}^k$  reflected overlying SST for the appropriate season of the phytoplankton bloom, which for this study was assumed to be summer in high latitudes. These results fall on the same regression line for culture and water column samples derived by Prah and Wakeham (1987), indicating that their equation ( $U_{37}^k = 0.033 T + 0.043$ ) is suitable for use in converting  $U_{37}^k$  values in sediments to overlying SST for the season of coccolith bloom. Using this calibration for sediments, the  $U_{37}^k$

paleotemperature method can be quantitatively applied down core to open ocean sediments.

In the Equatorial Atlantic,  $U_{37}^k$  temperature estimates were compared to those obtained from  $\delta^{18}O$  of the planktonic foraminifer *Globigerinoides sacculifer*, and planktonic foraminiferal assemblages for the last glacial cycle. The alkenone method showed  $\sim 1.56^\circ C$  cooling at the last glacial maximum. This is about half the decrease shown by both the isotopic method ( $\sim 3.40^\circ C$ ) and foraminiferal assemblages ( $\sim 3.75^\circ C$ ), implying that, if  $U_{37}^k$  estimates are correct, SST in the equatorial Atlantic was only reduced slightly in the last glaciation.

In the Northeast Atlantic,  $U_{37}^k$  temperature estimates show a profile downcore which is similar to the estimates from foram assemblages but with a constant offset toward warmer values throughout the core.  $U_{37}^k$  SST estimates are substantially warmer than foraminiferal estimates at all times, which may indicate inaccuracy in  $U_{37}^k$  temperature at this site.  $U_{37}^k$  indicates a SST of  $12^\circ C$  for the late glacial and  $18^\circ C$  for the Recent, whereas assemblages give estimates of  $9^\circ C$  and  $13^\circ C$ , respectively. At 12,700 yrs BP, the  $U_{37}^k$  and foram assemblage methods indicate a  $2^\circ C$  warming. A temperature change of  $2^\circ C$  can account for only  $0.44\text{‰}$  of the observed  $1.2\text{‰}$   $\delta^{18}O$  signal, indicating that the additional  $0.8\text{‰}$  change in  $\delta^{18}O$  must result from changes in surface salinity most likely due to a meltwater lid.  $U_{37}^k$  estimates show the major temperature shift from glacial to interglacial temperature occurred at about 9,000 yrs BP disagreeing with assemblage data which shows the shift of Holocene values at about 12,700 yrs BP. If  $U_{37}^k$  temperature estimates are accurate, this disagreement may reflect differing habitats of flora and fauna under the unusual sea surface conditions in this area during the deglaciation.

Thesis Supervisor: Dr. Lloyd D. Keigwin,  
WHOI.

Supported by: National Science Foundation and the  
Woods Hole Oceanographic Institution's Ocean  
Ventures Fund.

## THE LIFE CYCLE OF THE CENTRIC DIATOM *THALASSIOSIRA WEISSFLOGII*: CONTROL OF GAMETOGENESIS AND CELL SIZE

Elisabeth Virginia Armbrust

The predominant mode of reproduction in all unicellular algae is via asexual reproduction. In diatoms, the physical constraints of the cell wall, or frustule, during these mitotic divisions generally result in a decrease in the average cell size of a population over successive generations. The most common manner of breaking this trend of

diminishing cell size is through sexual reproduction; meiosis replaces mitosis and the resulting male and female gametes fuse to create a zygote or auxospore which then develops outside the confines of the frustule and forms a postauxospore cell many times larger than either parent. It is traditionally believed that these newly created large cells are unable to undergo sexual reproduction; theoretically, only cells at the lower end of the size spectrum possess this capability. However, most of the studies concerning diatom life cycles are descriptive and in reality very little is known about what determines if and when a cell will undergo gametogenesis and subsequent zygote formation. The motivation behind this research was a desire to understand more about this "decision making" process in centric diatoms.

Using flow cytometric techniques, I showed that the marine centric diatom, *Thalassiosira weissflogii*, can be induced to undergo spermatogenesis by exposing cells maintained at saturating intensities of continuous light to either dim light or darkness. From zero to over ninety percent of a population can differentiate into male gametes depending upon both the induction trigger and the population examined, regardless of cell size. Through the use of populations representing distinct cell cycle distributions, it was shown that responsiveness to an induction trigger is a function of cell cycle stage; cells in early G<sub>1</sub> are not yet committed to complete the mitotic cycle and can be induced to form male gametes, whereas cells further along in their cell cycle are unresponsive to these same cues.

*T. weissflogii* can also undergo sexual reproduction under constant environmental conditions as often as every 120 generations. In the absence of any external induction signals, the ability of a cell to undergo gametogenesis and subsequent auxospore formation is linked with the attainment of an appropriate cell size. However, this permissive size range can vary between isolates and within a given isolate over time. Moreover, the size of the postauxospore cells created during these sexual events is also extremely variable; absolute cell size predicts very little about the future conduct of a cell. The unpredictable behavior of these cultures is hypothesized to result from the fact that the genetic composition of a diatom population changes over time. Since diatoms are diploid, each round of sexual reproduction creates genetic diversity, thus enabling the characteristics of a population to undergo frequent transformations.

Thesis Supervisor: Prof. Sallie W. Chisholm, MIT.

Supported by: Office of Naval Research and the National Science Foundation through the Massachusetts Institute of Technology.

## EVOLUTION OF GAUSSIAN VORTICES IN VERTICAL SHEAR ON THE BETA PLANE

James D. McLaren

Numerical integration of a two layer quasigeostrophic fluid on the beta plane was carried out to test the effect of vertically sheared background flow on the behaviour of isolated mesoscale vortices. In uniform zonal shear, the zonal response was found to be in the direction of the of the upper layer flow, while the meridional response was very weak for oceanographically relevant parameters.

Several analytic and numerical estimates of translation rates are presented. The singular limit of infinite lower layer was found to approximate the zonal motion of the two layer case adequately, but not so for the more highly wave-dependent meridional motion. Techniques incorporating azimuthal dipole fields were somewhat more promising in this regard, but it appears that transient effects of the radiating wavefield cannot be ignored.

Analysis of the continuity equation in the reference frame of the moving vortex indicated that, in stable shear, the radial vertical velocity field and the horizontal mass flux tended to flatten the interface near the vortex center. The latter effect possibly indicates the importance of vertical shear in horizontally separating the wavefield between the two layers. In unstable shear, the sense of vertical motion is reversed and the interface tends to contract.

Thesis Supervisor: Dr. Glenn R. Flierl, MIT.

Supported by: Massachusetts Institute of Technology.

## VARIATIONS IN STRUCTURE AND TECTONICS ALONG THE MID-ATLANTIC RIDGE, 23°N AND 26°N

Laura Sau Lin Kong

The variation in the depth and width of the median valley along the Mid-Atlantic Ridge (MAR) suggests that the formation of ocean crust at slow spreading centers is not a simple two-dimensional process in which crustal accretion occurs uniformly both along the ridge axis and with time. Rather, it has been proposed that the ridge axis can be divided into a number of distinct segments or spreading cells. This thesis investigates the segmentation model by studying the variability in the structure and tectonics within spreading cells at 23°N and 26°N along the MAR. The results support the segmentation model in which accretion varies along the ridge, evolving

as independent spreading cells or segments, with different portions of the ridge system being in different stages of volcanic and tectonic evolution.

Chapter 2 presents an overview of morphologic and tectonic variations along a 100km-length of the MAR south of the Kane Fracture Zone (MARK area). Sea MARC I side scan sonar data and multi-beam Sea Beam bathymetry are used to document the distribution of crustal magmatism and extensional tectonism near 23°N. The data indicate a complex median valley composed by two distinct *en echelon* spreading cells which overlap in a discordant zone that lacks a well-developed rift valley or neovolcanic zone. The northern cell, immediately south of the fracture zone, is dominated by a large constructional volcanic ridge and is associated with active high-temperature hydrothermal activity. In contrast, the southern cell is characterized by a NNE-trending band of small fissured and faulted volcanos that are built upon relatively old, fissured and sediment-covered lavas; this cell is inferred to be in a predominantly extensional phase with only small, isolated volcanic eruptions. Despite the complexity of the MARK area, volcanic and tectonic activity appears to be confined to the 10-17 km wide inner rift valley. Small-offset normal faulting along near-vertical planes begins within a few kilometers of the ridge axis and appears to be largely completed by the time the crust moves out of the median valley. Mass-wasting and gullying of scarp faces, and sedimentation which buries low-relief seafloor features, are the major geological processes occurring outside the rift valley.

In chapters 3 and 4, the microearthquake characteristics and P wave velocity structure beneath the median valley of the Mid-Atlantic Ridge near 26°N are studied. This ridge segment is characterized by a large high-temperature hydrothermal field situated within the inner floor at the along-axis high. Chapter 3 explores the tectonic variations within the crust as evidenced from the distribution and source mechanisms of microearthquakes observed by a network of seven ocean bottom hydrophones and two ocean bottom seismometers over a three week period in 1985. Hypocenters were determined for 189 earthquakes, with good resolution of focal depth obtained for 105 events. Almost all events occurred at depths between 3 and 7 km beneath the seafloor, with earthquakes occurring at shallower depths beneath the along-axis high (<4 km). The distribution of hypocenters and the diversity of faulting associated with earthquakes beneath the inner floor and walls suggests a spatially variable tectonic state for the ridge segment at 26°N. These variations are presumably a signature of lateral heterogeneity in the depth region over which brittle failure occurs, and are a consequence of along-axis changes in the thermal structure and state of stress.

We suggest that at present the hydrothermal activity and deposition of massive sulfides is being sustained by heat generated by a recent magmatic intrusion. A consequence of this scenario is that thermal stresses play a dominant role in controlling the distribution of earthquakes and nature of faulting. Such a hypothesis is consistent with an apparent lack of seismicity beneath the hydrothermal field, the location of hypocenters around the low velocity zone (Chapter 4), attenuation of P wave energy to instruments atop the high (Chapter 4), the higher b-values associated with the along-axis high region, and the occurrence of high-angle (or very low angle) normal faulting and reverse faulting, as well as the variability in nodal plane orientations, associated with inner floor events beneath the along-axis high and the volcano.

In Chapter 4, we report results from the explosive refraction line and from the tomographic inversion of P wave travel time residuals for seismic velocity structure in the vicinity of the hydrothermal field. The two-dimensional along-axis P wave structure beneath the inner floor indicates that young oceanic crust cannot be adequately characterized by a simple, laterally homogeneous velocity structure, but that one-dimensional structures are at least locally valid (at 5-10 km length scales). The shallowmost crust (upper 1-2 km) beneath an axial volcano and the along-axis high is characterized by significantly higher velocities (by more than 1 km/s) than are associated with the upper crust in the deepest portions of the median valley. The variation is inferred to be a consequence of more recent magmatic and volcanic activity in the along-axis high region, as compared with the along-axis deep where tectonic fissuring has created a highly porous crust characterized by lower seafloor velocities. The crust beneath the along-axis deep appears to be typical of normal young oceanic crust, with a mantle velocity of 8.25 km/s observed at 5 km depth.

A low velocity zone centered beneath the along-axis high and extending under an axial volcano is imaged from 3 to 5 km depth (7.2 km/s to 6.0 km/s); the velocity decrease is required to satisfy the travel time residual data and to explain the severe attenuation in compressional wave energy to instruments atop the along-axis high. The presence of an active high-temperature hydrothermal field atop the along-axis high, together with the observations of lower P wave velocities, the absence of microearthquake activity greater than 4 km in depth, and the propagation of S waves through the crust beneath the volcano and along-axis high (Chapter 3), suggest that the volume corresponds to a region of hot rock with no seismically-resolvable pockets of partial melt. The shallow velocity gradients describing the low

velocity volume ( $<0.6 \text{ s}^{-1}$ ) appear to be a common characteristic of inferred zones of magmatic intrusion on the MAR. Comparison of the depth to the velocity inversion with the depths determined in other seismic studies at locally high regions along the MAR, the Juan de Fuca Ridge, and the East Pacific Rise reveals a correlation between lid thickness and spreading rate, suggesting that the amount of magma available at each location is spatially variable, or that the differences in lid thickness are describing the temporal evolution of magmatic intrusions beneath mid-ocean ridges.

In Chapter 5, the first direct measurement of upper mantle P- and S- wave delay times beneath an oceanic spreading center is presented. Two independent estimates of the epicenters and origin times are made for each of two earthquakes in a 1985 earthquake swarm near  $25^{\circ}50'N$  on the Mid-Atlantic Ridge using local and teleseismic arrival time data. Comparison indicates a 14-20 km northward bias in the epicenters teleseismically located using a *Herrin*[1968] Earth model. The bias is due to departures of the actual velocity structure from that implicit in the travel time tables used for the locations, combined with unbalanced station distribution. The comparison of origin times for the best-located event, after correction for the epicentral bias and for an oceanic crustal thickness, shows there to be only slightly lower velocities than a *Herrin*[1968] upper mantle; the P-wave delay is  $+0.3 \pm 0.9 \text{ s}$  ( $+0.2 \pm 0.9 \text{ s}$  relative to the isotropic Preliminary Earth Reference Model (PREM) and the *Jeffreys-Bullen*[1940] (JB) travel time tables, respectively). The lack of a resolvable P-wave delay suggests that the *Herrin*[1968] model is a good approximation to the average upper mantle velocity beneath this segment of the MAR.

Measurement of the S-wave delay for the same MAR swarm event shows there to be a positive delay ( $+3.1 \pm 2.0 \text{ s}$ ), or larger travel times and slower velocities compared to the JB S-wave tables ( $+3.9 \pm 2.0 \text{ s}$  relative to the isotropic PREM S-wave model). In contrast to the larger P-wave delays found in other MAR studies, the lack of a significant seismic anomaly near  $26^{\circ}N$  indicates that sizeable regions of low velocity material do not presently exist in the upper few hundred kilometers of mantle beneath this section of the ridge. This evidence argues for substantial along-axis variations in the active upwelling of mantle material along the slowly-spreading Mid-Atlantic Ridge. In order to explain the observation of a smaller than expected P wave delay in a region where the S delay suggests significant temperature anomalies (low velocities), we propose a model for mantle upwelling in which the decrease in travel time is due to an anisotropic P wave structure (fast direction vertical); the anisotropy results from the reorientation of olivine crystals parallel to

the ascending flow and balances the travel time delay due to a region of low velocities.

Thesis Supervisor: Dr. G. Michael Purdy,  
WHOI.

Supported by: NSF EAR 8407798.

## THE GEOCHEMISTRY OF BERYLLIUM ISOTOPES: APPLICATIONS IN GEOCHRONOMETRY

*Erik Thorson Brown*

The cosmogenic radioisotope beryllium-10 (half-life = 1.5 Myr) has been determined in suites of samples from tropical river systems and from areas of the oceans influenced by input from the continents, and also within the mineral lattices of quartz grains from Antarctic moraines. These data have been used to investigate the geochemistry of  $^{10}\text{Be}$  and apply that knowledge to development of geochronometric techniques. Beryllium-10 is primarily produced by neutron-induced spallation of  $^{14}\text{N}$  and  $^{16}\text{O}$  in the atmosphere; its flux to the Earth's surface at low latitude was examined through measurements in tropical rainfall. Distributions of  $^{10}\text{Be}$  and  $^9\text{Be}$  (the stable isotope) in dissolved and particulate phases in tropical rivers were used, in conjunction with major ion data, to delineate the geochemical cycle of Be in these river systems. Fluxes of Be isotopes from the continents were examined in oceanic regions strongly affected by atmospheric aerosols or by rivers. These results indicate that aeolian aerosols play a major role in delivering  $^9\text{Be}$  to the oceans. Low levels of  $^{10}\text{Be}$  and  $^{26}\text{Al}$  (another cosmogenic radioisotope; half-life = 0.705 Myr) are produced by cosmic ray-induced spallation reactions *in situ* within mineral lattices of surficial rocks, and may be used to quantify surface exposure ages. The present work applies *in situ* cosmogenic production to the examination of the deposition history of moraines of varying ages in Antarctica. It also yields estimates of  $^{10}\text{Be}$  and  $^{26}\text{Al}$  production rates:  $6.4^{+1.5}_{-1.5} \text{ at/g yr}$  and  $42^{+6}_{-20} \text{ at/g yr}$  at sea level and high geomagnetic latitude. The associated  $^{26}\text{Al}:^{10}\text{Be}$  production ratio is  $6.5 \pm 1.3$ .

Work in the Orinoco and Amazon Basins defines the major factors which affect riverine Be distributions. These include the concentration of  $^9\text{Be}$  in the rocks of the drainage, and partitioning of both isotopes between the dissolved phase and particle surfaces. These effects were examined individually in basins where a single process dominates. The extent of adsorption, quantified through the use of distribution coefficients ( $K_D$ ), was shown to be affected by the pH (which determines surface properties of particles and the speciation of Be) and also by weathering intensity. At high pH, where Be is present primarily as

hydroxy-complexes,  $K_D$  increases. Similarly, calculated  $K_D$ s are highest in rivers which drain regions where weathering has resulted in significant formation of clay minerals, which are involved in cation adsorption and exchange processes. In regions of more complete weathering, where clay minerals are broken down,  $K_D$ s are lower. The passage of  $^{10}\text{Be}$  through tropical river drainage basins is strongly influenced by interaction with particle surfaces, both within soils and in the rivers themselves. However, when the soil profiles within a region become saturated with respect to  $^{10}\text{Be}$ , rivers draining that region carry out as much dissolved  $^{10}\text{Be}$  as enters in rainwater.

Results from the estuaries of the Amazon and the Ganges-Brahmaputra are consistent with earlier finding that there is significant removal of Be at low salinities. The present work supports earlier estimates of  $\sim 150$  pM for the average freshwater  $^9\text{Be}$  endmember (corrected for estuarine removal), corresponding to an annual flux of  $5 \times 10^6$  mol/yr. As estimate of  $\sim 250$  at/g is made for the corrected  $^{10}\text{Be}$  freshwater endmember, implying that only about 1% of  $^{10}\text{Be}$  delivered to continents reaches the oceans in dissolved form. In contrast, the riverine particulate flux is large, on the order of the atmospheric flux, but this material is retained in coastal sediments.

The influence of atmospheric aerosols, in this case Saharan dust, on the Be isotope distribution in seawater was examined through analysis of samples from the Mediterranean Sea and its inflow and outflow. Based on water column profiles of  $^{10}\text{Be}$  and  $^9\text{Be}$ , it appears that interaction between particles and seawater involves both dissolution and adsorption of Be. A budget for the Mediterranean suggests on the order of 0.2 ppm of  $^9\text{Be}$  is dissolved from aeolian particles during interaction with seawater. This represents  $\sim 10\%$  of the total Be in aeolian material, assuming that they have average crustal Be concentrations. Applying this result to global estimates of aeolian fluxes suggests that  $1 \times 10^7$  to  $3 \times 10^7$  mol/yr of  $^9\text{Be}$  are delivered to the oceans by this mechanism, significantly higher than the riverine flux. Comparable values were obtained using an ocean box model to balance the Be isotope budgets.

A suite of *in situ* produced cosmogenic isotopes ( $^{26}\text{Al}$ ,  $^{10}\text{Be}$  from the present work combined with the  $^3\text{He}$  data of Brook and Kurz) were used for examining glacial history and also for refining our understanding of exposure age dating. Samples were taken in Arena Valley, Antarctica from sandstone boulders perched on moraine ridges associated with various periods of glacial expansion. The general concordance among these three isotopes, and the agreement with glaciological evidence, establish the utility of this method in examining exposure ages on 50 kyr to 3 Myr timescales. Nevertheless, variations from the

expected production ratios indicate that there are several complicating factors. These include: contamination by meteoric  $^{10}\text{Be}$ , the presence of  $^3\text{He}$  at the initiation of exposure (either from an earlier exposure to cosmic rays or from inherited primordial  $^3\text{He}$ ), production of these isotopes by mechanisms other than neutron spallation reactions, and geological uncertainties associated with the individual exposure histories of each boulder. Measurement of a suite of isotopes provides insight into these processes, since each additional isotope adds new and unique information to constrain the history of the samples.

Thesis Supervisor: Dr. John M. Edmond, WHOI.

Supported by: Massachusetts Institute of Technology.

## INTER-ANNUAL VARIABILITY OF ACOUSTIC RAY TRAVEL TIMES IN THE NORTHEAST PACIFIC

*John Alan Furgerson*

An acoustic tomography experiment consisting of a source near Hawaii and seven receivers along the west coast of North America was conducted from November 1987 to May 1988 and from February 1989 to July 1989. In this thesis, the acoustic ray travel times are analyzed in order to investigate inter-annual basin-scale thermal variability. These thermal fluctuations may help detect any greenhouse warming and greater understanding of them will increase knowledge of ocean-atmospheric interactions which affect weather and climate. A discussion of the program for finding the travel times is included along with a comparison of two methods of measuring travel times.

Thesis Supervisor: Dr. John L. Spiesberger, WHOI.

Supported by: United States Navy.

## OBSERVATIONS OF OCEAN FLUCTUATIONS BETWEEN 15 AND 23 HOUR PERIODS IN THE PACIFIC

*Wayne Richard Blanding*

Pulse-like acoustic signals are transmitted from an acoustic source near Oahu to seven receivers off the west coast of the United States for 124-day period in 1988. Acoustic travel-time oscillations are observed in the received signal at periods between 15 and 23 hours, which are caused by barotropic (or first or second mode barclinic) fluctuations in the ocean. It is shown that these fluctuations cannot be local processes isolated to

either the source or to the receivers. It is further shown that resonant barotropic gravity wave modes (Platzman et al., 1981) are not consistent with the data. The cause of these fluctuations remains unresolved, but the data and other oceanographic measurements put many constraints on the process causing these fluctuations.

Thesis Supervisor: Dr. John L. Spiesberger,  
WHOI.

Supported by: United States Navy.

### **A BEAM PATTERN DESIGN PROCEDURE FOR MULTIDIMENSIONAL SONAR ARRAYS EMPLOYING MINIMUM VARIANCE BEAMFORMING**

*Randall George Richards*

This paper develops a beam pattern design procedure for general multidimensional irregular sonar arrays that incorporates the not well understood effects of array geometry into the design process. The procedure is implemented by generating a "penalty function" in a spectral covariance function form. Processing the penalty function causes beam pattern high sidelobes to be penalized and the main lobe to be emphasized. This is accomplished by forming the penalty function in terms of an isotropic noise field of specified strength modified with a finite sector of low coherent energy and stabilized with incoherent sensor noise. By inputting the penalty function into a minimum variance beamformer, the beam pattern and aperture weights are calculated based on the given array geometry. The beamformer used is Capon's Maximum Likelihood Method. The array used to test the procedure is located on a sixty degree sector of a cylindrical surface. The procedure is implemented by two different methods, each with some desirable characteristics. One method suppresses sidelobes directly by the placement of nulls. The other method suppresses sidelobes indirectly by the enhancement of the main lobe the anti-nulls. Both methods are evaluated in terms of sensitivity factor which constrains the maximum white noise array gain. Results show that both methods result in sidelobe levels that range from 20 to 35 dB lower compared to a conventional beam pattern with uniform aperture weighting and that the design procedure is applicable to beam patterns steered to both true broadside and to off-broadside directions.

Thesis Supervisor: Dr. Arthur B. Baggeroer,  
MIT.

Supported by: United States Navy.

### **THE DISTRIBUTION OF WAVE HEIGHTS AND PERIODS FOR SEAS WITH UNIMODAL AND BIMODAL POWER DENSITY SPECTRA**

*Matthew Michael Sharpe*

Observed distributions of wave heights and periods taken from one year of surface wave monitoring near Martha's Vineyard and compared to distributions based on narrow-band theory. The joint distributions of wave heights and periods and the marginal height distributions are examined. The observed significant wave heights and the heights and periods of the extreme waves are also studied.

Seas are classified by the shapes of their power density spectra. Spectra with a single peak are designated as unimodal and spectra with two peaks as bimodal. Seas are further classified by spectral width, a function of the three lowest spectral moments.

The joint distributions of wave heights and periods from seas with narrow spectral widths take the general shape predicted by narrow-band theory and the statistics of extreme waves for these seas are well described. As spectral width increases, agreement between the theoretical and observed distributions diminishes and the significant wave heights and statistics of extreme waves show increasing variability. Bimodal seas with wide-banded spectra are found to have larger significant and extreme wave heights and shorter extreme wave periods than unimodal seas of the same width.

Thesis Supervisor: Dr. Hand C. Graber,  
WHOI.

Supported by: United States Navy.

### **BASIN-SCALE TIDAL MEASUREMENTS USING ACOUSTIC TOMOGRAPHY**

*Robert Hugh Headrick*

Travel-times of acoustic signals were measured between a bottom-mounted source near Oahu and four bottom-mounted receivers located near Washington, Oregon, and California in 1988 and 1989. This paper discusses the observed tidal signals. At three out of four receivers, observed travel times at  $M2$  and  $S2$  periods agree with predictions from barotropic tide models to within  $\pm 30^\circ$  in phase and a factor of 1.6 in amplitude. The discrepancy at the fourth receiver can be removed by including predicted effects of phase-locked baroclinic tides generated by seamounts.

Our estimates of barotropic  $M2$  tidal dissipation by seamounts vary between  $2 \times 10^{18}$

$\text{ergs}^{-1}$ . The variation by two orders of magnitude is due to uncertainties in the numbers and sizes of seamounts. The larger dissipation ( $1 \times 10^{18} \text{ ergs}^{-1}$ ) is the same order as previous estimates and amounts to 4% of the total dissipation at  $M2$ .

Thesis Supervisor: Dr. John L. Spiesberger, WHOI.

Supported by: United States Navy.

## OBSERVATION AND INVERSION OF SEISMO-ACOUSTIC WAVES IN A COMPLEX ARCTIC ICE ENVIRONMENT

*Bruce Edward Miller*

The propagation of low frequency seismo-acoustic waves in the Arctic Ocean ice canopy is examined through the analysis of hydrophone and geophone data sets collected in 1987 at an ice camp designated PRUDEX in the Beaufort Sea.

Study of the geophone time series generated by under-ice explosive detonations reveals not only the expected longitudinal and flexural waves in the ice plate, but also an unexpected horizontally-polarized transverse (SH) wave arriving at a higher amplitude than the other wave types. The travel paths of all three observed wave types are found to be refracted in the horizontal plane along a line coincident with a known ridge separating the ice canopy locally into two distinct half-plates, the first of thin first year ice and the second of thicker multi-year ice. The origin of the SH wave appears to be near the detonation and not associated with the interaction of longitudinal, flexural or waterborne waves with the ridge line. The need to determine the exact location of each detonation from the received time series highlights the dramatic superiority of geophones over hydrophones in this application, as does the ability to detect the anomalous SH waves and the refracted ray paths, neither of which are visible in the hydrophone data.

Inversion of the geophone data sets for the low frequency elastic parameters of the ice is conducted initially by treating the ice as a single homogeneous isotropic plate to demonstrate the power of SAFARI numerical modeling in this application. A modified stationary phase approach is then used to extend SAFARI modeling to invert the data sets for the elastic parameters of the two ice half-plates simultaneously. The compressional/shear bulk wave speeds estimated in the half-plates, 3500/1750 m/s in the multi-year ice and 3000/1590 m/s in the new ice, are comparable to previously obtained values; however, the compressional/shear attenuation values in the two half-plates, 1.0/2.99 dB/ $\lambda$  and 1.0/2.67 dB/ $\lambda$ ,

respectively, are somewhat greater than previously measured values and four times greater than estimates extrapolated from high frequency data.

Thesis Supervisor: Dr. Henrik Schmidt, MIT.

Supported by: Massachusetts Institute of Technology.

## RELATIVE SEA-LEVEL VARIATIONS REVEALED BY TIDE-GAUGE RECORDS OF LONG DURATION

*Anthony James Withnell*

Trends in mean relative sea-level and patterns of occurrence of extreme sea levels are analyzed separately in the two parts of this thesis.

In Part 1, twenty-eight of the world's longest tide-gauge records are examined for clues to the uncertain balance among factors contributing to relative sea-level (RSL) fluctuations. Obtaining these clues requires a description of the data in terms of component functions, whether chosen for their special properties (regression analysis) or empirically determined (EOF analysis). Part 1 describes a regression model that allows for gradual changes of the RSL trend and for sudden changes in the level to which tide-gauge measurements are referred (gauge zero); also describes is an EOF analysis procedure that offers certain advantages in the handling of missing observations. Although the rate of RSL rise exhibits significant gradual change over 60- to 120-year analysis intervals at many stations, no support is found for the idea of a gradual *global* acceleration of RSL rise. Results that seem to show RSL rise accelerating globally over the last century can be attributed instead to the changing geographical distribution of tide-gauge observations. Regional and local controls, which include vertical crustal movements and changes due to oceanographic or meteorological effects, must be responsible for the accelerations documented at many stations, and are dominant in controlling shorter-term departures from the RSL trend too. Preliminary results of EOF analysis reveal regionally coherent fluctuations of annual mean RSL in the Baltic Sea with r.m.s. amplitudes as large as 70 mm. Globally coherent fluctuations have smaller r.m.s. amplitudes: a tentative upper limit is 20mm.

In Part 2, 40 years of hourly sea-level records from two stations on the mid-Atlantic coast of the U.S. are used in a compilation of monthly 'surge'-level exceedance counts. 'Surge' level is defined as observed sea level minus predicted tide level. The results are compared with previously published storm counts, and the annual cycle of 'surge'-level exceedance frequency is found to lead that of storm frequency by nearly two months. It is recommended that further work aimed at modelling 'surge'-level exceedances should include:

(i) recognition that the tide record includes meteorological/oceanographic as well as astronomical components, especially at the frequency of the solar annual tide, and (ii) quantification of the relative importance of tide and surge in the timing of extreme sea-level occurrences at different times and places.

Thesis Supervisor: Dr. David G. Aubry,  
WHOI.

Supported by: United States Geological Survey and  
National Oceanic Atmospheric Administration  
Office of Sea Grant.

## MARINE BACTERIA AS A SOURCE OF DISSOLVED FLUORESCENCE IN THE OCEAN

*Paula G. Coble*

The hypothesis that marine bacteria produce sufficient quantities of highly fluorescent compounds to permit mapping of their distribution in low oxygen oceanic waters using fluorescence profiling has been investigated. Individual fluorescent compounds produced by natural seawater isolates in the laboratory include flavins, which are produced in sufficient quantities to explain *in situ* concentration in the ocean. Maxima in riboflavin concentrations were found at the depth of the oxic/anoxic interface in both the Black Sea and the Cariaco Trench, coincident with maxima in other indicators of elevated microbial biomass, including bacteriochlorophyll *a* concentration and electron transport system (ETS) activities.

In the Black Sea, simultaneous, continuous profiles of fluorescence due to dissolved organic matter (DOM) (Ex/Em = 355/500), flavins (Ex/Em = 445/525) and chlorophyll (Ex/Em = 445/>660) from 0 to 300 m show DOM and flavin fluorescence increase with depth. Sharp increases were observed at density boundaries. Local maxima in flavin fluorescence were found in the zone of denitrification. A secondary maximum in chlorophyll fluorescence was due to bacteriochlorophyll *a* form *Chlorobium* and was associated with maxima in beam attenuation coefficient and electron transport system (ETS) activity.

High performance liquid chromatography (HPLC) analysis of individual dissolved fluorescent compounds (DFCs) in samples from both the Black Sea and the Cariaco Trench showed 15-20 peaks superimposed on a high background of unresolved material. The compositional patterns displayed remarkable similarity at the two sites. Individual components identified included several flavin compounds. There are good agreement between estimates of dissolved fluorescence as

measured by both HPLC analysis and *in situ* fluorescence profiling.

Overall, results indicate that important information regarding the source and nature of marine DOM can be obtained using the combined approach of fluorescence spectroscopy and individual compound analysis.

Thesis Supervisor: Dr. Robert B. Gagosian,  
WHOI.

Supported by: National Science Foundation.

## FORAMINIFERAL AND CORALLINE BARIUM AS PALEOCEANOGRAPHIC TRACERS

*David W. Lea*

The distribution of Ba in the ocean is similar to the refractory components, silica and alkalinity. Therefore reconstructions of Ba in ancient water masses can be used to probe the circulation and chemistry of past oceans. Paleo-Ba distributions are recovered from the aragonite skeletons of corals and the calcite shells of planktonic and benthic foraminifera, since Ba substitutes for Ca in the lattice of these biogenic phases. The shell or coral material is treated with a rigorous cleaning procedure to remove spurious Ba associated with residual sedimentary phases. The Ba/Ca ratio of the purified foraminiferal calcite or coralline aragonite is quantified by a combination of isotope dilution flow injection on an ICP-MS for Ba and flame atomic absorption for Ca.

A quarter-annual record of coralline Ba recovered from a cored sample of *Pavona clavus* from the Galapagos Islands demonstrates that variability in Ba can be related to temporal variability in upwelling of source waters to the surface ocean. Ba/Ca ratios vary between about 4 and 5  $\mu\text{mol/mol}$ , with the highest values associated with bands formed during periods of cold sea surface temperatures. Upwelling in the equatorial Pacific transports cold, Ba-rich upper thermocline waters to the surface ocean, causing the coincidence between Ba and sea surface temperature. Depression of the thermocline during El Nino/Southern Oscillation (ENSO) events results in the coincidence of negative Ba anomalies with the positive temperature anomalies characteristic of ENSO events. Sr/Ca ratios in the same coral record vary between about 9.2 and 9.8  $\text{mmol/mol}$ , presumably in response to a temperature effect on Sr incorporation. Similarities between Ba and Sr records in the coral suggest that the Ba/Ca ratio of corals may be partially controlled by a temperature effect.

Planktonic foraminifera *Globigerinoides sacculifera*, *ruber*, *conglobatus*, *Orbulina* spp. and *Neoglobobulimina dutertrei* from the Panama



Basin, North Atlantic, and Mediterranean have Ba/Ca ratios between 0.6 and 1.0  $\mu\text{mol/mol}$ . Variation in foraminiferal Ba contents between the three basins is consistent with the trend in surface seawater Ba. The distribution coefficient for Ba incorporation in these 5 species is  $0.19 \pm 0.05$ . Records of planktonic-Ba reaching back to the end of the last glacial period do not reveal any large change in the Ba concentration of North-West Atlantic and Eastern Equatorial Pacific surface waters. *Globorotalia* have Ba/Ca ratios as high as 10  $\mu\text{mol/mol}$ ; these anomalously high Ba contents are inconsistent with coprecipitation of Ba in the shell. High Ba contents of *Globorotalia* could result from diatom-rich food sources, since precipitation of barite in marine biogenic particulate matter is apparently associated with diatom frustules.

The Ba/Ca ratios of the benthic foraminifera *Cibicides* and *Uvigerina*, recovered from sedimentary core-tops range from 2 to 5  $\mu\text{mol/mol}$ ; ratios can be directly related to local bottom water Ba. The calculated benthic distribution coefficient is  $0.37 \pm 0.06$ . Ba/Ca of benthic foraminifera recovered from glacial sections (15-25 kyr) of cores from the Atlantic indicates that waters deeper than 2900 m had ~30-60% higher Ba. These changes are consistent with previously observed nutrient shifts based on foraminiferal Cd and  $\delta^{13}\text{C}$ . Increases in Atlantic deep water nutrient contents can be explained by reduction in NADW formation during the last glacial maximum (LGM). Ba/Ca of benthic foraminifera from the glacial sections of intermediate depth Atlantic cores are equal or lower to Holocene values. This Ba evidence argues against the Mediterranean as a gently increased source to Atlantic intermediate waters during the LGM, since the Mediterranean is enriched in Ba today and apparently remained enriched during the LGM. Deep waters of the Glacial Pacific were about 25% lower in Ba (~3000 m). The Ba content of waters of the deep Atlantic, Antarctic and Pacific were similar at the last glacial maximum.

The main difference between LGM foraminiferal Ba and Cd distributions is that Cd remains significantly lower in the deep Atlantic relative to the Pacific. A simple seven-box ocean model is used to explore several scenarios for reconciling LGM Ba and Cd distributions. While the changed distribution of both tracers suggests diminishment in the flux of nutrient depleted waters to the deep Atlantic during the LGM, increased Atlantic upwelling rates and consequently enhanced Ba-particle fluxes can account for the lack of Ba fractionation between the deep Atlantic and Pacific. The model suggests that Ba can be transferred efficiently to the deep Atlantic by enhanced upwelling because the vast majority of the Ba is regenerated in the deep Atlantic box.

A 212 kyr record of benthic foraminiferal Ba

has been recovered from CHN82 Sta24 Core4PC at 3427m water depth in the North-West Atlantic. Ba/Ca ranges from a low of about 2  $\mu\text{mol/mol}$  during interglacial periods to a high of 4  $\mu\text{mol/mol}$  during glacial periods. These variations are consistent with reduced NADW formation during glacial periods. Variability in benthic Ba is not strictly linked to a glacial-interglacial pattern. Spectral analysis of the Ba time series indicates dominance of the 23 kyr period of procession of the earth's axis. Since power at the precessional frequencies is far greater in the Ba time series than in the time series of Cd and carbon isotopes from the same core. Ba variations apparently record a second process distinct from variations in the flux of nutrient depleted water to the side of the core. One possible explanation for this second mechanism might be the increase in Atlantic upwelling and the consequently enhanced particulate Ba fluxes suggested to explain the observed differences in Ba and Cd at the LGM.

Thesis Supervisor: Dr. Edward A. Boyle, MIT.

Supported by: NSF Grant OCE 8710168.

## SHIPBOARD AND SATELLITE OBSERVATIONS OF UPPER OCEAN VELOCITY AND TRANSPORT VARIABILITY IN THE GULF STREAM

David Michael Schubert, Jr.

Acoustic doppler velocities are combined with velocity profiles generated from XBT measurements to produce estimates of the flow field between Bermuda and the eastern coast of the United States. Repeated shipboard measurements along an ascending GEOSAT subtrack between Bermuda and Cape Cod allow study of rapid Gulf Stream Variability along the track, and comparison of sea surface and velocity measurements with those computed from the GEOSAT altimeter. The shipboard data were taken during two separate cruises on the R/V Oceanus in April and December, 1989. Using mass conservation constraints and inverse techniques, the transport across the Cape Cod-Bermuda track has been balanced with transport across additional ship tracks between Bermuda and Cape Hatteras, and between Bermuda and Nova Scotia. The shipboard results show evidence of a rapid barotropic mode which caused changed in transport along the Cape Cod-Bermuda track on the order of 8 Sverdrups in a week period. Comparisons of sea surface velocity and dynamics height determined from the ship's data with measurements made from the GEOSAT altimeter showed a consistent picture of the Gulf Stream location and were also consistent in showing smaller scale variations in flow. The dynamics height difference across the Gulf Stream

was approximately 10% higher for the GEOSAT measurements than for the shipboard measurements, which is within the expected errors of the analysis techniques.

Thesis Supervisor: Dr. Terrence M. Joyce, WHOI.

Supported by: United States Navy.

## SEDIMENTARY LIPIDS AS INDICATORS OF DEPOSITIONAL CONDITIONS IN THE COASTAL PERUVIAN UPWELLING REGIME

Mark A. McCaffrey

This thesis assesses the utility of various sedimentary lipids as indicators of short-term changes in depositional conditions and sedimentary organic matter sources in the coastal upwelling regime off of Peru. A variety of lipids (n-alkanes, n-alkanols,  $C_{37}$  alkenones, hopanoids, keto-ols, lycopane, phytol, stenols, stanols, sterenes, and tetrahymanol) were quantified in Peru margin sediments from both the oxygen minimum zone (OMZ) and several near-shore locations. I discuss the utility of the lipid profiles, the alkenone- $U_{37}^k$  "paleothermometer", the n-alkane CPI, and several stanol/stenol ratios as indicators of short-term changes in depositional conditions. This work also provides the first assessment of the influence of *Thioploca*, a genus of sulfur-oxidizing bacteria, on organic compound distributions in upwelling regime sediments.

The potential of the alkenone- $U_{37}^k$  as a sedimentary marker for El Nino/Southern Oscillation (ENSO) events was assessed by comparing the historical ENSO record with detailed  $U_{37}^k$  profiles for  $^{210}\text{Pb}$ -dated cores from the OMZ. Sediments from the center of the OMZ sectioned at intervals  $\leq$  the yearly sedimentation rate have the greatest potential for holding a  $U_{37}^k$  record of El Nino events. The  $U_{37}^k$  signals of individual EL Nino events were substantially attenuated in the sediments examined, and periods of frequent ENSO activity (e.g., 1870-1891) were more readily identified than isolated ENSO events in periods of less frequent ENSO activity. Detailed depth profiles of the  $C_{37}$  alkenones in a core, SC3, from  $\approx 15^\circ\text{S}$  collected nine years apart are consistent with the use of these compounds for "molecular stratigraphy."

The utility of sedimentary hydrocarbons and alcohols as indicators of short-term changes in depositional conditions was determined in core SC3 by (1) a multivariate factor analysis of the lipid data and (2) a consideration of individual source-specific biomarkers. In this core, profiles of odd-carbon-number n-alkanes ( $C_{25}$ - $C_{33}$ ) and

even-carbon number n-alkanols ( $C_{24}$ - $C_{28}$ ) reflect changes in the input of terrigenous sediment relative to marine sediment during deposition, as indicated by the correlations between these lipids and inorganic indicators of terrigenous clastic debris. The n-alkane carbon preference index (CPI) provides a less-sensitive record of fluctuations in the terrestrial input than the concentration profiles of the individual n-alkanes and n-alkanols, and these lipids are *not* well-correlated with the historical El Nino record. The similarity of all the stanol profiles measured and the lack of concordance between these profiles and inorganic indicators of terrigenous input suggest that fluctuations in the abundance of higher plant stanols are obscured by the larger marine contribution of these compounds. Similarities between the profiles of total organic carbon (TOC) and cholestanol/cholesterol are consistent with stanol hydrogenation being influenced by the sediment redox conditions.

Profiles of sterols and sterol alteration products illustrate that the rapid downcore decreases in sterol concentrations do not simply represent conversion of sterols into other steroidal compounds, but must also involve steroid degradation and possibly formation of non-solvent-extractable steroids. In OMZ sediments, the ratio [cholesterol + cholesterol alteration products] substantially increases from 0-4 cm, but at deeper depths, there is no systematic change in the ratio. This suggests that if there is a progressive conversion of cholesterol to these degradation products below 4 cm, then it is obscured by an equally rapid removal of these compounds from the sediments. Stenol profiles in surface sediments suggest a range of degradation rates for these compounds. Differential remineralization of steroids can cause the relative steroid abundances in ancient sediments to bear little resemblance to the relative abundances of the sterols from which these compounds were derived. This limits the use of steroids as indicators of the *relative importance* of the original organic matter inputs. However, important quantitative statements can be made concerning the depositional environment, based on the presence, rather than relative abundance, of certain steroids derived from specific sources.

In SC3, the downcore increase in burial time (100 cm  $\approx$  310 years b.p.) and the downcore changes in sediment chemistry did not result in accumulation of cholesterol alteration products from more advanced portions of the alteration pathways than are achieved in the 0-1 cm interval. The absence of cholest-4-ene, cholest-5-ene and cholestane suggests that cholestadiene reduction to cholestenes and cholestene reduction to cholestane do not begin to occur over the time scale and under the sedimentary conditions encountered in

the surface 100 cm of Peru margin OMZ sediments.

Although the hopanoids found in the Peru sediments can be related relatively easily to compounds found in ancient sediments and oils, these hopanoids are not as useful as steroids for reconstruction of organic matter sources and paleoenvironmental conditions. This is because the bacterially-derived precursors of these compounds are generally not specific to any particular type of bacteria.

This thesis provides the first assessment of the influence of *Thioploca* on organic compound distributions in upwelling regime sediments.

*Thioploca*, a genus of colorless, sulfur-oxidizing, filamentous bacteria, constitutes as much as 80% of the biomass in surface sediments from the OMZ. Since marine species of *Thioploca* have been found only in dysaerobic surface sediments of upwelling regimes, biomarkers for this organism may be useful in identifying similar depositional conditions in the sedimentary record. *Thioploca* (dry) was found to be  $\approx 3.8\text{--}4.1$  wt% lipid. Three fatty acids, hopanoids and hydrocarbons were conspicuously absent from the *Thioploca*. This organism was found to contain cyclolaudenol, a  $C_{31}$  sterol with an unusual structure; diagenetic alteration products of this sterol may serve as markers for *Thioploca* input to sedimentary organic matter, and hence as markers for paleo-upwelling depositional environments in the sedimentary record. No quantitatively significant alteration products of cyclolaudenol were identified in the Peru surface sediments.

*Thioploca* was found to be 9-10 dry wt% protein, and the THAA composition of the *Thioploca* contained no unusual amino acids that might serve as *Thioploca* markers. The *Thioploca* THAA composition was similar to surface sediments from core SC3 (0-1 cm), but differed significantly from the THAA composition of surface sediments (0-3 cm) from the Peru margin analyzed in a previous study.

Thesis Supervisors: Dr. John Farrington, Dr. Daniel Repeta, WHOI.

Supported by: National Science Foundation and the Woods Hole Oceanographic Institution's Ocean Ventures Fund.

## THE NUTRITIONAL ROLE OF ENDOSYMBIOTIC BACTERIA IN ANIMAL-BACTERIA SYMBIOSES: *SOLEMYA VELUM*, A CASE STUDY

Noellette Mary Conway

The trophic interactions occurring between endosymbiotic bacteria and the host in animal-bacteria symbioses were investigated using the endosymbiont-containing protobranch clam,

*Solemya velum*, as a general model. C, N, and S stable isotope compositions were investigated in tissues of *S. velum*; C and N isotope values were also examined in an enriched bacterial fraction, separated from intact gills by differential centrifugation. The bacterial fraction and host tissues had similar  $\delta^{13}\text{C}$  values which were different to those of organisms utilizing a phytoplankton-based food chain. The  $\delta^{15}\text{N}$  values of both *S. velum* and the endosymbiont fraction were comparable and considerably lower than those of bivalve controls that do not harbor endosymbionts. The  $\delta^{34}\text{S}$  values of *S. velum* were very negative and suggest that use of biogenically produced  $\text{H}_2\text{S}$  as a S source. The  $\delta^{13}\text{C}$  and  $\delta^{15}\text{N}$  isotope ratios of *S. velum* suggest that the endosymbiotic bacteria may provide almost 100% of the hosts C and N budgets.

The lipid composition of most organisms is related to dietary intake. Consequently, a detailed analysis of the lipid composition of *S. velum* was undertaken to verify the nutritional importance of the symbiotic bacteria. The  $\delta^{13}\text{C}$  ratios of the lipids were also measured in order to determine potential carbon sources for the lipids of *S. velum*. The lipids of *S. velum* were characterized by large amounts of 18:1 $\omega$ 7 (*cis*-vaccenic acid, a lipid found in many species of bacteria), 16:0, 16:1 $\omega$ 7 and low concentrations of the highly unsaturated fatty acids characteristic of most marine bivalves. The predominant sterol found in *S. velum* was cholesterol. The *cis*-vaccine acid found in *S. velum* is almost certainly symbiont-derived and could serve as a biomarker for symbiont-lipid incorporation by the animal host. The high concentrations of *cis*-vaccenic acid in the tissues of *S. velum* suggest an important role for the endosymbionts in the lipid metabolism of this bivalve. In addition, the presence of *cis*-vaccenic acid in all major lipid classes of *S. velum* demonstrates both incorporation and utilization of this fatty acid. The reduced amounts of polyunsaturated fatty acids found in *S. velum*, along the absence of sterols of plant origin, provide further evidence to suggest that this symbiosis relies on endosymbiont chemoautotrophy to fulfill the majority of its nutritional requirements. The  $\delta^{13}\text{C}$  ratios of the fatty acids and sterols of *S. velum* were very negative and similar to the values found for the fatty acids of *Thiomicrospira crunogena*, a sulfur-oxidizing bacterium, suggesting that the lipids of *S. velum* are either derived directly from the endosymbionts or are synthesized using carbon derived from the endosymbionts.

The stable isotope and lipid composition profiles of *S. velum* were very similar to those of *Solemya borealis*, a newly discovered symbiosis, and *Inanidrillus leukodermatus*, a symbiotic annelid. This demonstrates the usefulness of stable isotopes and lipid composition studies in the

analysis and characterization of these types of symbioses. In particular, both techniques are valuable as initial screening tools for the presence of symbiotic sulfur-oxidizing bacteria.

In order to further characterize differences between *S. velum* and typical marine bivalves, total and free amino acids were determined for *S. velum*, and *Mya arenaria*. Both the relative and absolute amounts of free amino acids differed significantly between the two species. In *S. velum*, the absolute concentrations of the sulfur amino acid taurine were greater than the total free amino acid concentrations typically found in bivalves. The possible roles for taurine as a sink for oxidized sulfur compounds in the *Solemya velum* symbiosis was examined. Preliminary experiments suggest that taurine levels increase in the presence of reduced sulfur compounds; this demonstrates a possible link between sulfur-oxidation and taurine synthesis in this symbiosis.

Thesis Supervisor: Dr. Judith McDowell-Capuzzo, WHOI.

Supported by: Ocean Ventures Fund, National Oceanic Atmospheric Administration Office of Sea Grant, Woods Hole Oceanographic Institution Coastal Research Center, and the Environmental Protection Agency



## Index

- Agardy, M. Tundi ..... MPC-1  
 Allen, J. S. .... PO-16  
 Allsup, Geoff ..... AOEPE-8  
 Altabet, M. A. .... B-14  
 Andersen, E. S. .... GG-3  
 Anderson, Donald M. .... B-6  
 Andrew, Jonathan M. .... MPC-1,4  
 Arendt, Wayne J. .... MPC-4  
 Armbrust, Elizabeth V. .... B-14;GS-8  
 Arnone, Robert A. .... B-12  
 Arthur, Michael A. .... GG-15  
 Atema, Jelle ..... B-1  
 Aubrey, David G. .... CRC-1,2,3,4,5  
 Aubry, Marie-Pierre ..... GG-1,5,11  
 Auzende, Jean-Marie ..... GG-5  
 Backman, Jan ..... GG-14  
 Backus, Richard H. .... B-4  
 Bacon, Michael P. .... C-10,11  
 Baker, M. K. .... PO-26  
 Baker, Trevor ..... CRC-5  
 Ball, L. A. .... C-15  
 Bane, John M. .... PO-20  
 Battisti, Thomas B. .... PO-17  
 Bazylnski, Dennis A. .... B-11,19  
 Beardsley, Robert C. .... PO-2,3,21  
 Beier, J. A. .... GG-14  
 Belastock, R. A. .... C-10  
 Bell, George I. .... PO-17  
 Bennett, S. .... PO-28  
 Berggren, William A. .... GG-5,10,11,12  
 Berteaux, Henri O. .... AOEPE-1,8  
 Bhaud, Yvonne ..... B-11  
 Blanding, Wayne R. .... GS-12  
 Blough, Neil ..... C-6,7,8,14  
 Borenäs, K. M. .... PO-17  
 Boucher, Claude ..... CRC-5  
 Bower, Amy S. .... PO-1  
 Bowin, Carl ..... GG-2  
 Bowlin, James B. .... AOEPE-16  
 Bradley, Albert M. .... AOEPE-15,17  
 Bradshaw, Alvin L. .... C-12  
 Brewer, Peter G. .... C-12  
 Brigham, Lawson W. .... MPC-1  
 Brink, Kenneth H. .... PO-20  
 Briscoe, Melbourne G. .... AOEPE-17;PO-15,22  
 Broadus, James M. .... MPC-2,3,11  
 Brooks, David A. .... PO-22  
 Brown, Erik T. .... GS-11  
 Brown, N. L. .... PO-28  
 Bryden, Harry ..... PO-1,8,16  
 Buckland-Nicks, J. .... B-16  
 Buesseler, Ken O. .... C-9,10  
 Bullister, John L. .... C-12  
 Burczynski, Janusz ..... B-8,22  
 Burgess, J. J. .... AOEPE-2  
 Burggraf, Siegfried ..... B-1  
 Burns, Daniel R. .... GG-5,6  
 Bushong, Paul J. .... AOEPE-13  
 Butenko, G. .... GG-3  
 Butman, Cheryl Ann ..... AOEPE-12;B-13  
 Cabrera, R. .... AOEPE-6  
 Caffee, Marc W. .... C-3  
 Candela, Julio ..... PO-2  
 Capuzzo, Judith McDowell ..... B-3,20,22  
 Cardone, Vincent J. .... AOEPE-10  
 Caron, David A. .... B-1,21  
 Carter, William E. .... CRC-5  
 Caruso, Michael J. .... PO-7,26  
 Casso, Susan A. .... C-9  
 Caswell, Hal ..... B-1,2,15,17,18  
 Catipovic, Josko A. .... AOEPE-4,6,9,10  
 Chapman, David C. .... PO-2,21  
 Chen, C. S. .... PO-2,3  
 Cheng, C. H. .... GG-6  
 Chia, F.-S. .... B-16  
 Chisholm, Sallie W. .... B-14,15  
 Chu, Dezhang ..... AOEPE-12  
 Church, John A. .... PO-1  
 Church, Thomas M. .... PO-20  
 Churchill, James C. .... PO-3  
 Cisne, John L. .... GG-15  
 Clay, C. S. .... AOEPE-18  
 Coble, Paula G. .... C-6;GS-15  
 Cobra, Daniel T.D.Q. .... GS-3  
 Cohen, Joel E. .... B-2  
 Collins, Curtis A. .... PO-9,28  
 Collins, Margaret Goud ..... PO-2  
 Colman, Steven M. .... GG-13  
 Conway, Noelle M. .... B-3,7;GS-18  
 Cook, M. .... PO-26  
 Cooke, John G. .... AOEPE-2  
 Cornillon, Peter C. .... PO-3  
 Corry, Charles E. .... PO-25  
 Craddock, James E. .... B-4,19  
 Crescenti, Gennaro H. .... PO-27  
 Cullen, James L. .... GG-14  
 Curry, William B. .... GG-9,14  
 Daher, Mary Ann ..... B-4  
 Danforth, Thomas W. .... PO-27  
 Davis, Linda H. .... B-20  
 Dean, Walter E. .... GG-15  
 DeLong, Edward F. .... B-4,5  
 DeSzoeko, Roland A. .... PO-14  
 Deuser, Werner G. .... C-1  
 Dickinson, Wayne H. .... C-5  
 Dickson, Andrew G. .... B-9  
 DiPerna, Daniel T. .... AOEPE-15  
 DiPietro, David M. .... AOEPE-18  
 Distel, D. L. .... B-5  
 Dister, B. .... C-14  
 Donelan, Mark A. .... AOEPE-10;PO-15  
 Doney, Scott C. .... C-12  
 Doucet, Donald P. .... PO-22  
 Dougherty, Martin E. .... GG-8  
 Dragos, Paul ..... CRC-4  
 Druffel, Ellen R. M. .... C-6,10,13;GG-1

DuBois, D. L. .... GG-7  
 Duester, Alan R. .... AOEPE-15  
 Dunlap, Paul V. .... B-5  
 Dusenberry, J. A. .... B-14  
 Edwards, Steven F. .... CRC-2  
 Ehrendorfer, Thomas .... GG-11  
 Eiswerth, Mark E. .... MPC-2  
 Emeis, Kay-Christian .... C-7  
 Emery, K. O. .... CRC-3,5;GG-10  
 Encarnacion, Rolu .... PO-2  
 Endfield, David B. .... CRC-5  
 Eriksen, Charles C. .... PO-14,22  
 Fabry, Victoria J. .... C-1,4  
 Fairall, Christopher W. .... PO-20  
 Farrar, Harry IV .... C-3  
 Farrington, John W. .... C-3  
 Farrow, R. Scott .... MPC-3  
 Feder, Meir .... AOEPE-10,11,13  
 Fine, Rana .... PO-9  
 Firing, Eric .... PO-9  
 Fisher, Nicholas S. .... GG-14  
 Flament, Pierre J. .... PO-26,28  
 Flierl, Glenn R. .... PO-19  
 Fofonoff, Nick P. .... PO-27  
 Forester, Richard M. .... GG-13  
 Forman, Steven L. .... GG-3  
 Foster, David S. .... GG-13  
 Francis, M. .... PO-28  
 Francois, Roger .... C-10,11  
 Frankel, R. B. .... B-19  
 Franks, Peter J. S. .... B-6;GS-3  
 Freitag, Lee E. .... AOEPE-1,6  
 Frew, Scot .... MPC-7  
 Friehe, Carl A. .... PO-26  
 Frisk, George V. .... AOEPE-4,6  
 Fry, Brian .... GG-15  
 Fry, Virginia A. .... CRC-1  
 Frye, Daniel .... AOEPE-4  
 Furgerson, John A. .... GS-12  
 Gable, Frank J. .... CRC-1,2,3  
 Gagosian, Robert B. .... C-4,6  
 Gaines, Arthur G. .... MPC-3  
 Gammon, Richard .... PO-9  
 Garcia, Michael O. .... C-1  
 Gastrock, G. .... B-7  
 Gawarkiewicz, Glen .... PO-21  
 Geernaert, Gerald L. .... PO-20  
 Gentile, John H. .... B-22;CRC-1,2  
 Gerhardt, Greg A. .... B-1  
 Geyer, W. Rockwell .... AOEPE-7,11  
 Giere, O. .... B-7  
 Giese, Graham S. .... CRC-5;PO-2  
 Goetz, Frederick E. .... B-7  
 Goff, John A. .... GS-4  
 Goldsborough, Robert G. .... AOEPE-1  
 Goldsmith, R. .... GG-7  
 Gordon, R. L. .... AOEPE-6  
 Gorsline, Donn S. .... PO-20  
 Goyet, Catherine .... C-12  
 Graber, Hans C. .... AOEPE-10

Gradstein, F. M. .... GG-12  
 Grassle, J. Frederick .... MPC-11  
 Gray, E. S. .... B-7  
 Green, Sarah A. .... C-6,7  
 Greenberg, E. P. .... B-5  
 Greene, Charles H. .... AOEPE-14;B-8,22  
 Grigalunas, Thomas A. .... MPC-3  
 Grosenbaugh, Mark A. .... AOEPE-2,9,13,14  
 Gross, Thomas F. .... AOEPE-18  
 Guza, Robert T. .... PO-20  
 Haake, B. .... GG-16  
 Hacker, Peter .... PO-9  
 Hacker, S. .... B-8  
 Hahn, Mark E. .... B-9,19  
 Hale, Robert C. .... B-21  
 Hall, Melinda M. .... PO-4  
 Hammond, Douglas E. .... PO-20  
 Haney, J. Christopher .... MPC-1,2,3,4,8  
 Hanley, Q. .... C-15  
 Hansen, D. V. .... PO-9  
 Hartel, Karsten E. .... B-19  
 Hay, Bernward J. .... GG-15  
 Headrick, Robert H. .... AOEPE-13;GS-13  
 Helfrich, Karl R. .... PO-17,18,19,20  
 Hennet, R. J.-C. .... C-1,2  
 Hermann, A. J. .... PO-4  
 Herrin, Eugene .... PO-25  
 Herzog, Michel .... B-11  
 Hinton, Alan .... AOEPE-1,8  
 Ho, P. S. .... C-7  
 Hoagland, Porter III, .... MPC-2,3  
 Hoffman, Nathan J. .... C-3  
 Hogg, Nelson G. .... PO-1,4  
 Holland, Heinrich D. .... B-9  
 Hong, Seoung-Yong .... MPC-5  
 Honjo, Susumu .... GG-14,15  
 Hosom, David S. .... AOEPE-1;PO-22  
 Hover, Franz S. .... AOEPE-9,13  
 Howarth, Robert W. .... GG-15  
 Howes, Brian L. .... B-10,18  
 Howitt, Cinthia S. .... AOEPE-16  
 Huang, N. E. .... PO-15  
 Huang, Rui Xin .... PO-5  
 Hudson, G. Bryant .... C-3  
 Huggett, Robert J. .... B-21  
 Hunt, John M. .... C-1,2,8  
 Irish, James D. .... AOEPE-15  
 Ittekkot, V. .... GG-15,16  
 Jacinto, Gil .... PO-2  
 Jannasch, Holger W. .... B-1,7,9,10,11,17,19  
 Jech, J. Michael .... AOEPE-18  
 Jenkins, W. J. .... C-5,11  
 Jenter, Harry L. .... AOEPE-15  
 Jessup, Andrew T. .... GS-7  
 John, A. Meredith .... B-2  
 Johnson, Gregory C. .... PO-6,14  
 Johnson, Kevin T. M. .... GS-6  
 Jones, Glenn A. .... GG-3,13  
 Jones, Russell H. .... C-3  
 Joyce, Terrence M. .... PO-7,14

|                               |               |  |             |
|-------------------------------|---------------|--|-------------|
| Joyner, Christopher C. ....   | MPC-5,6,7     | Lundberg, P. A. ....                   | PO-18       |
| Jørgensen, Bo Barker ....     | B-10          | Lupton, John ....                      | C-3         |
| Kaminski, M. A. ....          | GG-11,12      | Luyten, James ....                     | PO-5,13,28  |
| Kammer, David P. ....         | C-2           | Lynch, James F. ....                   | AOPE-4      |
| Kaoru, Yoshiaki ....          | MPC-7         | Mackensen, Andreas ....                | GG-12       |
| Kaplan, Ilene M. ....         | MPC-8         | MacWhorter, M. A. ....                 | PO-23       |
| Keho, Timothy H. ....         | GG-8          | Madin, Laurence P. ....                | B-1,8,12,16 |
| Keigwin, L. D. ....           | GG-3          | Madsen, Ole Secher ....                | AOPE-15     |
| Keller, Mary Ruth ....        | AOPE-2        | Magnuson, J. J. ....                   | AOPE-18     |
| Keller, William C. ....       | AOPE-2        | Maillard, C. ....                      | PO-12       |
| Kelly, Kathryn A. ....        | PO-7          | Mammaloukas-Frangoulis, Vassilios .... | GG-5        |
| Kenchington, Richard A. ....  | MPC-8         | Manganini, S. ....                     | GG-16       |
| Kessler, William S. ....      | PO-8          | Mangum, L. ....                        | PO-26       |
| Kettle, A. James ....         | PO-27         | Mann, S. ....                          | B-19        |
| Kieber, David J. ....         | C-8,14        | Marquis, Judith K. ....                | B-11        |
| Kinder, Thomas H. ....        | PO-8          | Martens, Christopher S. ....           | PO-20       |
| King, Linda L. ....           | C-10          | Martin, W. R. ....                     | C-12        |
| Kitchell, Judith P. ....      | B-11          | Martini, Marinna A. ....               | AOPE-15     |
| Kite-Powell, Hauke ....       | MPC-11        | McCaffrey, Mark A. ....                | C-3;GS-17   |
| Klein, P. ....                | PO-10         | McCartney, Michael S. ....             | PO-12,13    |
| Klinger, Barry A. ....        | PO-19         | McClatchie, Sam ....                   | AOPE-14     |
| Klinkhammer, Gary P. ....     | GG-1          | McCorkle, Daniel C. ....               | GG-1        |
| Kloepper-Sams, Pamela J. .... | B-11          | McDowell, Fred W. ....                 | PO-25       |
| Knap, Anthony A. ....         | B-12          | McLaren, James D. ....                 | GS-9        |
| Knapp, George P. ....         | PO-27         | McNichol, Ann P. ....                  | C-13;GG-1   |
| Knauer, George A. ....        | B-12;PO-20    | McPhaden, M. J. ....                   | PO-9        |
| Koelsch, Donald E. ....       | AOPE-1        | McSherry, Thomas R. ....               | CRC-4       |
| Kong, Laura S. L. ....        | GG-2;GS-9     | Melville, W. K. ....                   | PO-17       |
| Krogstad, H. E. ....          | AOPE-6        | Merriam, J. Stevens ....               | AOPE-1      |
| Kundu, Pijush K. ....         | PO-21         | Metzger, Kurt ....                     | AOPE-5,6,16 |
| Kunze, Eric ....              | AOPE-17       | Miangping, Zheng ....                  | B-9         |
| Kurz, Mark D. ....            | C-1,2,3,5     | Michaels, Ann E. ....                  | B-20        |
| Kuzirian, A. M. ....          | B-17          | Micinski, E. ....                      | C-14        |
| Lagabirelle, Yves ....        | GG-5          | Millard, R. C. ....                    | PO-23,26,28 |
| Lake, B. J. ....              | PO-28         | Miller, Bruce E. ....                  | GS-14       |
| LaMontagne, G. ....           | PO-26         | Miller, V. W. ....                     | C-4         |
| Lea, David W. ....            | GS-15         | Milliman, John D. ....                 | PO-20       |
| Lee, Cindy ....               | C-13;GG-1     | Miyamoto, Robert T. ....               | B-8         |
| Lee, David S. ....            | MPC-8         | Moffett, James W. ....                 | C-11,14     |
| Lee, John ....                | B-13          | Monosson, Emily ....                   | B-13        |
| Lehman, S. J. ....            | GG-3          | Moore, Paul A. ....                    | B-1         |
| Lenaers, Guy ....             | B-11          | Morgan, J. Phipps ....                 | GG-7        |
| Lentz, Steve J. ....          | AOPE-11;PO-21 | Morrey, John R. ....                   | C-3         |
| LeProvost, Christian ....     | CRC-5         | Muenow, David W. ....                  | C-1         |
| Levy, Ellen ....              | PO-27         | Mullineaux, Lauren S. ....             | B-13        |
| Lewan, M. D. ....             | C-2           | Nair, R. R. ....                       | GG-15,16    |
| Lewistus, Alan J. ....        | GS-1          | Navitsky, Richard C. ....              | PO-27       |
| Light, R. D. ....             | C-4           | Neff, Eric D. ....                     | GG-15       |
| Limeburner, R. ....           | PO-2,3        | Nelson, Robert H. ....                 | MPC-9       |
| Lin, J. ....                  | GG-7          | Newberger, P. A. ....                  | PO-16       |
| Lindborg, Kristina L. C. .... | MPC-3         | Nicholson, Jo Ann M. ....              | GG-15       |
| Little, Sarah A. ....         | GG-7          | Nicolaus, Barbara ....                 | B-1         |
| Liu, James T. ....            | CRC-5         | Nittrouer, Charles A. ....             | PO-20       |
| Livingston, Hugh D. ....      | C-9           | Nochur, Saraswathy V. ....             | B-11        |
| Lohmann, G. P. ....           | GG-9,13       | O'Kane, Dennis J. ....                 | B-15        |
| Lohrenz, Steven E. ....       | B-12          | Oakey, N. S. ....                      | PO-14       |
| Lohrmann, A. ....             | AOPE-6        | Oliver, Brian M. ....                  | C-3         |
| Lovely, D. R. ....            | B-19          | Olson, Donald B. ....                  | PO-6        |
| Luetkemeyer, K. ....          | PO-28         | Olson, L. O. ....                      | C-4         |
| Lukas, Roger ....             | PO-9          | Olson, Robert J. ....                  | B-14,15     |



|                               |                       |
|-------------------------------|-----------------------|
| Opaluch, James J. ....        | MPC-3                 |
| Oppenheim, Alan V. ....       | AOPE-11               |
| Østmø, S-R ....               | GG-3                  |
| Owens, W. Brechner ....       | PO-4,9,28             |
| Park, Melora M. ....          | PO-24                 |
| Pascual, Mercedes ....        | B-15                  |
| Pawlik, Joseph R. ....        | AOPE-12               |
| Payne, Richard E. ....        | PO-27                 |
| Peal, Kenneth R. ....         | AOPE-7                |
| Pedlosky, Joseph ....         | PO-10,11,18           |
| Peltier, W. R. ....           | CRC-5                 |
| Peltzer, Edward T. ....       | C-4                   |
| Peterson, Charles H. ....     | PO-20                 |
| Phelps, H. L. ....            | B-22                  |
| Phillips, Kenneth A. ....     | PO-25                 |
| Pickart, Robert S. ....       | PO-11                 |
| Pillsbury, R. Dale ....       | PO-1                  |
| Pilskaln, C. H. ....          | GG-14                 |
| Pinkel, Robert ....           | PO-24                 |
| Plant, William J. ....        | AOPE-2,3              |
| Plueddemann, Albert J. ....   | PO-24                 |
| Pollard, R. T. ....           | PO-14,22              |
| Polzin, K. L. ....            | PO-14                 |
| Porta, Dave ....              | AOPE-4                |
| Prada, Kenneth E. ....        | AOPE-1,7              |
| Prasher, Douglas C. ....      | B-13,15,16            |
| Pratt, Lawrence J. ....       | PO-11,12,17,18        |
| Price, James F. ....          | PO-13,22,29           |
| Prindle, Bryce ....           | AOPE-8                |
| Pu, S. ....                   | PO-26                 |
| Pugh, David ....              | CRC-5                 |
| Purcell, Jennifer E. ....     | B-16                  |
| Purdy, G. Michael ....        | GG-2,3,4,7,8          |
| Putman, Susan S. ....         | AOPE-8                |
| Putt, Mary ....               | B-20                  |
| Rajan, Subramaniam D. ....    | AOPE-4,6,16           |
| Ramaswamy, V. ....            | GG-15,16              |
| Rapp, Richard H. ....         | CRC-5                 |
| Raventos, Jose ....           | B-17,18               |
| Recchia, Cheri A. ....        | B-21                  |
| Regier, Lloyd A. ....         | PO-22                 |
| Rein, Charles R. ....         | B-12                  |
| Reiter, Edmund C. ....        | GG-8                  |
| Repeta, Daniel J. ....        | C-3,9                 |
| Richards, Randall G. ....     | GS-13                 |
| Richardson, Philip L. ....    | PO-9,12,22,28,29      |
| Robbins, Paul ....            | PO-10                 |
| Roemmich, Dean H. ....        | PO-1                  |
| Rogers, David P. ....         | PO-20                 |
| Roman, Michael R. ....        | PO-20                 |
| Rudnick, Daniel L. ....       | PO-14,22              |
| Ruiz, Brian V. ....           | C-3                   |
| Saint-Hilaire, Danielle ....  | B-11                  |
| Samelson, R. M. ....          | PO-11,12,16           |
| Santala, Markku J. ....       | AOPE-9                |
| Sayles, F. L. ....            | C-5,12                |
| Schaaf, André ....            | GG-5                  |
| Schaaf, D. ....               | PO-28                 |
| Scheltema, Amelie H. ....     | B-16,17               |
| Scheltema, R. S. ....         | B-17                  |
| Schempf, Hagen ....           | AOPE-18;GS-5          |
| Schlegel, Hans G. ....        | B-17                  |
| Schmidt, C. ....              | B-7                   |
| Schmitt, Raymond ....         | PO-14,16              |
| Schmitz, William J., Jr. .... | PO-13                 |
| Schneider, D. L. ....         | C-13                  |
| Scholin, Christopher ....     | B-11                  |
| Schouten, Hans ....           | GG-3,7                |
| Schubert, David M. Jr. ....   | GS-16;PO-7            |
| Schudlich, Rebecca R. ....    | PO-13                 |
| Schutz, Robert E. ....        | CRC-5                 |
| Schweitzer, Peter N. ....     | GG-13                 |
| Scott, J. H. ....             | GG-9                  |
| Scott, K. J. ....             | B-22                  |
| Seaver, G. ....               | PO-23                 |
| Sempéré, Jean-Christophe .... | GG-3,7                |
| Shah, Jyotsna ....            | B-5                   |
| Shalvi, Ofir ....             | AOPE-3                |
| Sharpe, Matthew M. ....       | GS-13                 |
| Shaw, Peter R. ....           | GG-4,8                |
| Sholkovitz, Edward R. ....    | C-3,13                |
| Shrayer, B. ....              | PO-12                 |
| Sicre, Marie-Alexandrine .... | C-4                   |
| Siegel, David A. ....         | PO-24                 |
| Signell, Richard P. ....      | AOPE-7,11             |
| Sikes, C. Steven ....         | C-4                   |
| Sikes, Elisabeth L. ....      | GS-8                  |
| Silva, Juan F. ....           | B-17,18               |
| Simpson, Daniel J. ....       | C-7,9                 |
| Singer, Robin C. ....         | PO-24                 |
| Sirkes, Ziv ....              | PO-26                 |
| Slotine, Jean-Jacques E. .... | AOPE-2                |
| Smith, Craig L. ....          | B-21                  |
| Smith, David G. ....          | B-19                  |
| Smith, Deborah K. ....        | GG-4,8                |
| Smith, George I. ....         | B-9                   |
| Smith, Richard L. ....        | B-10,18               |
| Smith, V. Kerry ....          | MPC-7                 |
| Smith, Woolcott ....          | MPC-11                |
| Smolowitz, R. M. ....         | B-19                  |
| Smoot, N. Christian ....      | GG-4                  |
| Solomon, Sean C. ....         | GG-2,4                |
| Solow, Andrew R. ....         | MPC-4,9,10,11         |
| Sparks, N. H. C. ....         | B-19                  |
| Speer, Kevin G. ....          | PO-13                 |
| Spencer, A. ....              | PO-28                 |
| Spencer, Wayne D. ....        | CRC-4                 |
| Spiesberger, John L. ....     | AOPE-5,6,13,16        |
| Stalcup, M. C. ....           | PO-27                 |
| Stanley, R. J. ....           | PO-27                 |
| Stanton, Timothy K. ....      | AOPE-12,14,15,18;B-22 |
| Starczak, Victoria R. ....    | AOPE-12               |
| Steele, John H. ....          | MPC-11                |
| Stegeman, John J. ....        | B-7,9,11,13,19,21     |
| Stephen, Ralph A. ....        | AOPE-1;GG-8           |
| Stern, Melvin E. ....         | PO-18,19              |
| Stetter, Karl. O. ....        | B-1                   |
| Stewart, W. Kenneth ....      | AOPE-3,12             |
| Stigebrandt, Anders ....      | PO-16                 |
| Stoecker, Diane K. ....       | B-20                  |

Stolzenbach, Keith D. ....GG-7  
 Stommel, Henry M. ....PO-5,26  
 Suman, Daniel O. ....C-10  
 Swanberg, Neil R. ....B-21  
 Swift, Stephen A. ....GG-8  
 Talley, Lynne D. ....PO-14  
 Tarbell, S. ....PO-28  
 Taylor, Craig D. ....B-12  
 Terray, E. A. ....AOPE-6  
 Thompson, D. ....GG-6  
 Tiping, Ding ....B-9  
 Tivey, M. K. ....C-4  
 Toksöz, M. Nafi ....GG-8  
 Toole, John M. ....PO-6,14,26,28  
 Toomey, Douglas R. ....GG-4,5  
 Trevisan, Maria Cristina ....B-18  
 Triantafyllou, Michael S. ....AOPE-2,13,9,14  
 Trowbridge, John H. ....AOPE-3,11,16;PO-21  
 Trull, T. W. ....C-5  
 Tscherkassky, M. ....B-17  
 Tucholke, Brian E. ....GG-4  
 Tyack, Peter L. ....B-21  
 Uchupi, Elazar ....GG-10  
 Urry, Lisa A. ....GS-2  
 van Veen, A. ....C-3  
 Van Veld, Peter A. ....B-21  
 Villaret, Catherine ....AOPE-16  
 Von Herzen, R. P. ....GG-9  
 Wacker, John F. ....C-3  
 Wakeham, Stuart G. ....GG-14  
 Walden, Barrie B. ....AOPE-7,17  
 Wang, Z. ....PO-26  
 Warner, K. A. ....B-22  
 Warren, Bruce A. ....PO-6,14  
 Waterbury, J. B. ....B-5  
 Weinberg, James R. ....B-22  
 Weinstein, Ehud ....AOPE-3,11  
 Weisman, Sumner ....PO-22  
 Weller, Robert A. ....PO-14,15,22,23,24,27  
 Westbrook, Donna J. ....B-21  
 Whelan, Jean K. ....C-7  
 Whitehead, J. A. ....PO-18,19,20  
 Wiebe, Peter H. ....AOPE-14;B-8,22  
 Wiesenburg, Denis A. ....B-12  
 Wijffels, Susan ....PO-16  
 Wilcock, William S. D. ....GG-4,5  
 Wilkens, R. H. ....GG-6  
 Williams, Albert J., III ....AOPE-9,17,18  
 Williams, Peter M. ....C-6  
 Winget, Clifford ....PO-22  
 Withnell, Anthony J. ....GS-14  
 Wong, Kuo-Chuin ....AOPE-3  
 Woodin, Bruce R. ....B-7,15,21  
 Wooding, Christine M. ....PO-28  
 Woodsum, Glenn ....MPC-11  
 Woodward, Bonnie ....B-13,15,16  
 Wunderle, Joseph M., Jr. ....MPC-4  
 Yang, K. ....PO-26,28  
 Yoder, James A. ....PO-20  
 Yoerger, Dana R. ....AOPE-2,13,17,18

Yu, H. ....PO-28  
 Zafiriou, O. C. ....C-11,14,15  
 Zawacki, Leon X. ....B-10  
 Zemanovic, Marguerite E. ....PO-28,29  
 Zettler, E. R. ....B-14,15  
 Zhao, L. ....PO-26,28  
 Zhou, G. ....C-7  
 Zumberge, Mark ....CRC-5



## DOCUMENT LIBRARY

January 17, 1990

### *Distribution List for Technical Report Exchange*

Attn: Stella Sanchez-Wade  
Documents Section  
Scripps Institution of Oceanography  
Library, Mail Code C-075C  
La Jolla, CA 92093

Hancock Library of Biology &  
Oceanography  
Alan Hancock Laboratory  
University of Southern California  
University Park  
Los Angeles, CA 90089-0371

Gifts & Exchanges  
Library  
Bedford Institute of Oceanography  
P.O. Box 1006  
Dartmouth, NS, B2Y 4A2, CANADA

Office of the International  
Ice Patrol  
c/o Coast Guard R & D Center  
Avery Point  
Groton, CT 06340

NOAA/EDIS Miami Library Center  
4301 Rickenbacker Causeway  
Miami, FL 33149

Library  
Skidaway Institute of Oceanography  
P.O. Box 13687  
Savannah, GA 31416

Institute of Geophysics  
University of Hawaii  
Library Room 252  
2525 Correa Road  
Honolulu, HI 96822

Marine Resources Information Center  
Building E38-320  
MIT  
Cambridge, MA 02139

Library  
Lamont-Doherty Geological  
Observatory  
Columbia University  
Palisades, NY 10964

Library  
Serials Department  
Oregon State University  
Corvallis, OR 97331

Pell Marine Science Library  
University of Rhode Island  
Narragansett Bay Campus  
Narragansett, RI 02882

Working Collection  
Texas A&M University  
Dept. of Oceanography  
College Station, TX 77843

Library  
Virginia Institute of Marine Science  
Gloucester Point, VA 23062

Fisheries-Oceanography Library  
151 Oceanography Teaching Bldg.  
University of Washington  
Seattle, WA 98195

Library  
R.S.M.A.S.  
University of Miami  
4600 Rickenbacker Causeway  
Miami, FL 33149

Maury Oceanographic Library  
Naval Oceanographic Office  
Bay St. Louis  
NSTL, MS 39522-5001

Marine Sciences Collection  
Mayaguez Campus Library  
University of Puerto Rico  
Mayaguez, Puerto Rico 00708

Library  
Institute of Oceanographic Sciences  
Deacon Laboratory  
Wormley, Godalming  
Surrey GU8 5UB  
UNITED KINGDOM

The Librarian  
CSIRO Marine Laboratories  
G.P.O. Box 1538  
Hobart, Tasmania  
AUSTRALIA 7001

Library  
Proudman Oceanographic Laboratory  
Bidston Observatory  
Birkenhead  
Merseyside L43 7 RA  
UNITED KINGDOM



|   |                                    |  |                                     |
|---|------------------------------------|--|-------------------------------------|
| <b>REPORT DOCUMENTATION<br/>PAGE</b>  | <b>1. REPORT NO.</b><br>WHOI-91-08 | <b>2.</b>  | <b>3. Recipient's Accession No.</b> |
| <b>4. Title and Subtitle</b><br>Abstracts of Manuscripts Submitted in 1990 for Publication  |                                    | <b>5. Report Date</b><br>May, 1991                                 |                                     |
|   |                                    | <b>6.</b>  |                                     |
| <b>7. Author(s) Editor:</b> Alora Paul  |                                    | <b>8. Performing Organization Rept. No.</b><br>WHOI-91-08          |                                     |
| <b>9. Performing Organization Name and Address</b><br><br>Woods Hole Oceanographic Institution<br>Woods Hole, Massachusetts 02543   |                                    | <b>10. Project/Task/Work Unit No.</b>                              |                                     |
|   |                                    | <b>11. Contract(C) or Grant(G) No.</b><br>(C)<br>(G)               |                                     |
| <b>12. Sponsoring Organization Name and Address</b>   |                                    | <b>13. Type of Report &amp; Period Covered</b><br>Technical Report |                                     |
|   |                                    | <b>14.</b>   |                                     |
| <b>15. Supplementary Notes</b><br>This report should be cited as: Woods Hole Oceanog. Inst. Tech. Rept., WHOI-91-08.  |                                    |  |                                     |
| <b>16. Abstract (Limit: 200 words)</b><br><br>This volume contains the abstracts of manuscripts submitted for publication during calendar year 1990 by the staff and students of the Woods Hole Oceanographic Institution. We identify the journal of those manuscripts which are in press or have been published. The volume is intended to be informative, but not a bibliography.<br>The abstracts are listed by title in the Table of Contents and are grouped into one of our five departments, Marine Policy Center, Coastal Research Center, or the student category. An author index is presented in the back to facilitate locating specific papers. |                                    |  |                                     |
| <b>17. Document Analysis</b> <b>a. Descriptors</b><br>abstracts<br>oceanography<br>ocean engineering<br><br><b>b. Identifiers/Open-Ended Terms</b><br><br><br><br><b>c. COSATI Field/Group</b>  |                                    |  |                                     |
| <b>18. Availability Statement</b><br><br>Approved for publication; distribution unlimited.  |                                    | <b>19. Security Class (This Report)</b>                            | <b>21. No. of Pages</b><br>202      |
|   |                                    | <b>20. Security Class (This Page)</b>                              | <b>22. Price</b>                    |

